CZECH TECHNICAL UNIVERSITY IN PRAGUE

Faculty of Civil Engineering

Department of Materials Engineering and Chemistry

Characterisation of Czech Modern Mosaic Mortars

DOCTORAL THESIS

Pavla Bauerová

Doctoral study programme: Civil Engineering

Branch of study: Physical and Materials Engineering

Doctoral thesis tutor: doc. Ing. Martin Keppert, Ph.D.

Consultant: doc. Ing. Zuzana Slížková, Ph.D.

Prague, 2023

CZECH TECHNICAL UNIVERSITY IN PRAGUE
Faculty of Civil Engineering
Thákurova 7, 166 29 Praha 6

DECLARATION

Ph.D. student's name: Pavla Bauerová

Title of the doctoral thesis: Characterisation of Czech Modern Mosaic Mortars

I hereby declare that this doctoral thesis is my own work and effort written under the guidance of the tutor doc. Ing. Martin Keppert, Ph.D.
All sources and other materials used have been quoted in the list of references.

The doctoral thesis was written in connection with research on the project: GAČR No. 18-13525S

In Prague on 20. 9. 2023

signature

ACKOWLEDGEMENT/ PODĚKOVÁNÍ

There are so many people who have supported me on my way to this thesis - I hope to mention them all. First of all, I would like to thank my mosaic holy trinity - my friend and mosaic guru Magda Kracík Štorkánová, who opened up completely new artistic and scientific horizons for me and showed me a real passion for mosaics. Secondly (as ladies go first) I would like to thank my consultant Zuzana Slížková for all her support, advice, experience, kindness and for accepting me at UTAM - this gave so many new impulses to my dying motivation. Finally, I would like to thank my supervisor Martin Keppert for his patience, trust, kindness, knowledge (I am tempted to write wisdom) and enormous help.

Speaking of UTAM, I must not forget to thank my nice colleagues - first of all my dear thermal analysis expert and my personal mentor, nutritionist and German conversation partner Dita Frankeová, then Míša Vondráčková and Pavla Náhůnková, Katka Kulawiecová for being such a great and kind and fast librarian, Jan Válek for the useful books he lent me, which I should now return, Veronika Koudelková for teaching me how to operate our MIRA (oh, and I should also thank the MIRA electron microscope for staying alive), Petr Kozlovcev for teaching me how to use light microscopes, and all colleagues for their support in my daily work. A very grateful and sincere thank you goes to Petra Mácová for her kindness and expertise in FTIR. A special thanks goes to our former colleague Cristiana Lara Nunes, whose passion for linseed oil in mortars opened the door to UTAM for me.

I also have great colleagues at the Institute of Physics! They have supported me all these years, they are always ready to help and discuss, even though mosaic mortars are not the centre of their universe... Thank you, Bohouš Rezek, Tonda Fejfar, Léďa (my boss Martin Ledinský and I can call him "Léďa!"), Štěpán Stehlík and Štěpán Potocký! If you had not said yes to my crazy idea of studying, I would never have made it. I also have to thank other colleagues for their help - namely Aleš Vlk, Raja Jackivová, Veronika Buňatová, Lucka Landová, Müller for the photos of Phannerer und für alles andere... I hope I have not forgotten anyone.

I would be very upset if I forgot to thank Malu Storch and her family, especially her mother, for providing me with samples of reference mosaic mortars from Austria. I would also like to thank Frau Natascha Mader and Herr Gernot Fussenegger for giving me the opportunity to search the archives of the Tiroler Glasmalerei company.

I would like to thank all the people who helped me with the analyses, namely Dr. Havelcová for the GC, Farkas Pintér for the polarising microscopy, Marek Pacák for the photogrammetry, which is still awaiting publication, Pavel Reitermann, Lenka Scheinherrová and prof. Milena Pavlíková from the CTU. Also to my former

colleagues from UCEEB - Zdenda Prošek, Petr Svora and Robert Jára. And all the teachers I met during my studies. Not only at the CTU.

I would also like to thank all my colleagues and friends from Art & Craft Mozaika. To name a few - Martin Hemelík and Veronika Vicherková for the papers, Dana Rohanová for future papers and to Zdeněk and Klaudie for their enthusiasm and mosaic hearts!

A special section - my best friends who have never stopped supporting me. Never. Thank you, Jíťo, Jíťo, Dašo, Zdeňko, Sylwie! My family, who never stopped supporting me. Never. Thank you so much!

Finally, I would like to thank all the artists and mosaicists whose works I had the honour to study. It was - and still is - extremely interesting. I hope you are not angry with me.

https://doi.org/10.14311/dis.fsv.2023.015

ABSTRACT

The main goal of this thesis was to characterise mosaic fixing mortars of 27 mosaics from the late 19th century to the late 20th century. The mortars were examined by SEM—EDS, XRD, light and light polarising microscopy, thermal analysis coupled with EGA-MS, FTIR and gas chromatography. The mosaics studied come from different mosaic workshops and periods but all of them relate to the present-day Czech Republic. Although the analysed set is small, some trends and preferences in the use of materials can be traced in the works of different workshops.

Portable sepulchral mosaics designed by Neuhauser/ Tiroler Glasmalerei workshop, the first mosaic studio operating in the Czech Lands, follow a traditional 16th century technology – bedding mortars based on lime binder + marble aggregates + high amount of linseed oil (up to almost 40%) as a plasticizer. In order to fix façade mosaics, the company applied hydraulic mortars made of lime, marble dust, random waste glass splinters and reactive ceramic aggregates (bricks, chamotte) or Portland cement based materials with carbonate aggregates. A mixture of lime and Portland cement appears to be a common binder of Josef Pfefferle´s mosaics.

The works by the first Czech local mosaicist Viktor Foerster consist of sand, early Portland cement or mixtures of Portland cement and lime and crushed bricks or gypsum. Foerster´s wife Marie used blended Portland cement with blast furnace slag grains to fix the vault mosaic of the Slavín crypt. The analysed bedding mortars from mosaics produced by other early 20th century mosaic workshops also document the on-going transition from traditional calcium carbonate aggregates and *cocciopesto* technique to the application of sand and Portland cement based mortars.

Portland cement was the main compound in the binders of the studied “socialistic” mosaics of the latter half of the 20th century. This work brought evidence of a common use of blended cements containing granulated blast furnace slag.

Linseed oil turned out to be an important compound of some late 19th/ early 20th century mortars. Therefore, a methodology of linseed oil content estimation in the historic mortars was proposed based of the three methods (TG coupled with EGA-MS and TOC). The approach based on EGA-MS (identification and analysis of *m/z* 95 signal corresponding to “oil-specific” $[C_7H_{11}]^+$ ion), developed on a set of model mortars and tested on authentic mosaic mortars´ samples, provided the most satisfactory results.

ABSTRAKT

Hlavním cílem této práce bylo charakterizovat fixační malty 27 mozaik z období od konce 19. do konce 20. století. Malty byly zkoumány pomocí SEM-EDS, XRD, světelné a světelně polarizační mikroskopie, termické analýzy spojené s EGA-MS, FTIR a plynové chromatografie. Studované mozaiky pocházejí z různých mozaikářských dílen a období, všechny se však vztahují k dnešní České republice. Přestože je analyzovaný soubor malý, lze v dílech různých dílen vysledovat rozdíly v technice a preferenci používaných materiálů.

Přenosné náhrobní mozaiky navržené dílnou Neuhauser/ Tiroler Glasmalerei, prvním mozaikářským ateliérem působícím v českých zemích, vycházejí z tradiční technologie vynalezené v 16. století - ložní malty na bázi vápenného pojiva + mramorové kamenivo + vysoké množství lněného oleje (až téměř 40 %) jako plastifikátoru. Pro fixaci fasádních mozaik firma používala hydraulické malty z vápna, mramorového prachu, odpadních skleněných střepů a reaktivního keramického kameniva (cihly, šamot) nebo materiály na bázi portlandského cementu s karbonátovým kamenivem. Směs vápna a portlandského cementu se jeví jako být běžné pojivo mozaik Josefa Pfefferleho.

Malty prvního českého mozaikáře Viktora Foerstera se skládají z písku, raného portlandského cementu nebo směsi portlandského cementu a vápna s drcenými cihlami nebo sádrou. Foersterova manželka Marie použila k fixaci mozaiky klenby krypty Slavína směsný portlandský cement s přídavkem vysokopecní strusky. Analyzované podkladové malty z mozaik vyrobených v jiných mozaikářských dílnách z počátku 20. století rovněž dokumentují probíhající přechod od tradičního kameniva z uhličitanu vápenatého a techniky *cocciopesto* k použití malt na bázi písku a portlandského cementu.

Portlandský cement tvoří hlavní složku pojiv studovaných "socialistických" mozaik druhé poloviny 20. století. Tato práce přinesla důkazy o běžném používání směsných cementů obsahujících granulovanou vysokopecní strusku.

Lněný olej se ukázal být důležitou složkou některých hmot z přelomu 19. a 20. století. Proto byla navržena metodika odhadu obsahu lněného oleje v historických maltách na základě tří metod (TG ve spojení s EGA-MS a TOC). Nejuspokojivější výsledky přinesl přístup založený na EGA-MS (identifikace a analýza signálu m/z 95 odpovídajícího "olejově specifickému" iontu $[C_7H_{11}]^+$), vyvinutý na souboru modelových malt a testovaný na autentických vzorcích mozaikových fixačních malt.

ABBREVIATIONS

Cement chemical nomenclature:

S – SiO_2

C – CaO

A – Al_2O_3

F – Fe_2O_3

H – H_2O

C_2S	dicalcium silicate (belite)
C_3S	tricalcium silicate (alite)
C_4AF	tetracalcium ferroaluminate (ferrite)
C_3A	tricalcium aluminate (aluminate)
C-S-H	calcium silicate hydrate
C-A-H	calcium aluminate hydrate

PHOTOS:

Unless otherwise stated, the photos were taken by the author of the thesis.

TABLE OF CONTENTS

1 INTRODUCTION 1
2 OBJECTIVES 2
3 MATERIALS USED FOR THE FIXATION OF MOSAIC MORTARS 3
3.1 Binders 4
3.1.1 Lime 4
3.1.2 Cocciopesto 7
3.1.3 Roman cement 7
3.1.4 Portland cement 8
3.1.5 Gypsum 11
3.2 Aggregates 11
3.3 Organic admixtures in mosaic mortars 11
3.4 Aging and degradation of mortars 12
4 DEVELOPMENT OF MOSAIC FIXING TECHNIQUE 15
4.1 Antiquity 16
4.1.1 Floor mosaics 16
4.1.2 Emblemata 18
4.2 Early Christian and Byzantine mosaics 18
4.3 Medieval mosaics 20
4.3.1 Last Judgment Mosaic at the Prague Castle 21
4.4 Early modern mosaics 22
4.5 Indirect method of setting and the 19th century revival of mosaic art 24
4.6 The 20th century – prefabrication and cement domination 26
4.6.1 Alternative methods of mosaic fixation 30
5 BRIEF HISTORY OF MOSAIC ART IN THE CZECH LANDS 31
5.1 The rising of mosaic art in the Czech Lands (1880s – 1918) 31
5.2 Mosaics in inter-war Czechoslovakia (1918-1938) 34
5.3 Mosaics under socialism (1948 – 1989) 35
5.4 After 1989 36
6 CHARACTERISATION OF AUTHENTIC MOSAIC MORTARS 38
6.1 Samples 38
6.2 Methods 44

6.2.1 SEM-EDS 44
6.2.2 Light microscopy (LM) 44
6.2.3 Polarised light microscopy (PLM) 44
6.2.4 Thermal analysis coupled with EGA mass spectroscopy 45
6.2.5 X-ray powder diffraction (XRD) 45
6.2.6 ATR-FTIR 45
6.2.7 Gas chromatography 46
6.2.8 TOC 46
6.2.9 Binder/ aggregate ratio assessment - HCl dissolution test 46
6.3 Results and discussion 47
6.3.1 Tirolean workshops – Neuhauser/Tiroler Glasmalerei and J. Pfefferle 47
6.3.1.1 Microstructure and chemical composition (LM, SEM-EDS) 47
6.3.1.2 Mineralogical composition (XRD) 53
6.3.1.3 Thermal analysis (TG/DTG-EGA) 56
6.3.1.4 Aggregates of Getzner and Krip bedding mortars 61
6.3.1.5 Organic compound identification (FTIR, GC) 66
6.3.1.6 Summary I – Tirolean workshops´ mosaics 71
6.3.2 Foerster´s workshop 72
6.3.2.1 Microstructure and chemical composition (SEM-EDS) 72
6.3.2.2 Mineralogical composition (XRD) 74
6.3.2.3 Thermal analysis 75
6.3.2.4 Comparison of analysed bedding mortars 78
6.3.2.5 Summary II – Foerster´s mosaic bedding mortars 81
6.3.3 Other early 20th century mosaics 82
6.3.3.1 Microstructure and chemical composition 82
6.3.3.2 Mineralogical composition 86
6.3.3.3 Thermal analysis 87
6.3.3.4 Summary III – Other early 20th century mosaics 88
6.3.4 Mosaics of the socialistic period 88
6.3.4.1 Microstructure and chemical composition 89
6.3.4.2 Mineralogical composition 95
6.3.4.3 Thermal analysis 96
6.3.4.4 Organic compound assessment (GC) 98

6.3.4.5 Summary IV – Mosaics of the socialistic period 99
7 MODEL MORTARS FOR THE ESTIMATION OF LINSEED OIL CONTENT .. 101
7.1 Materials 101
7.2 Methods 102
7.3 Results and discussion 103
7.3.1 Reference pure linseed oil 103
7.3.1.1 Thermal analysis (TG/DTA and EGA-MS) 103
7.3.1.2 FTIR spectroscopy 104
7.3.2 Model mortars 105
7.3.2.1 FTIR spectroscopy 105
7.3.2.2 XRD 107
7.3.2.3 SEM-EDS 109
7.3.2.4 Thermal analysis 110
7.3.2.5 Thermal analysis 113
7.3.2.6 EGA-MS 113
7.3.2.7 TOC 115
7.3.3 Evaluation of methods 116
7.4 Summary – Model samples 117
8 CONCLUSIONS 118
9 FUTURE PERSPECTIVES 120
REFERENCES 121

1 INTRODUCTION

Mosaics art is a very complex artistic discipline standing in between painting and plastic art. Yet mosaic monuments, especially those from modern times, still remain in the shadow of paintings, sculptures and architecture. So does an investigation of modern (i.e. late 19th century and younger) mosaics´ materials composition and durability. Apart from glass (or stone or ceramic) cubes – the so called *tesserae* – that actually make the main visual impression of a mosaic, fixing materials, i.e. cements or mortars, play an important role in the durability of these artworks.

Czech Republic can boast a living mosaic tradition which arose in the late 19th century. However, mosaics have been stained with a stigma of “communist art” as this technique was widely used in the architecture built during the socialistic era and – admittedly – some of them depicted propagandistic motifs. That is why the society put their hands off from them after 1989 (the breakdown of socialism), overlooking not just propaganda-free masterpieces of the past period but mosaics in general. During the last decade the perception of mosaics has been changing. Mosaics of the past are being recognized and several research projects have been carried out to monitor and evaluate them from mainly art historic point of view.

In the course of time the status of modern mosaics has shifted from contemporary artworks to historic monuments. Since they have not been considered “historic enough”, quite low attention has been drawn to their characterization and conservation. Thus little is known about their materials composition and degradation processes. Understanding these issues can bring a significant benefit to design proper conservation and restoration strategies.

2 OBJECTIVES

This PhD. project focused on the characterization of mosaics´ fixing mortars – inorganic binders in which stone, glass or ceramic *tesserae* (mosaic cubes) are fixed. The goal of the project is to study the composition and properties of modern mosaic mortars (late 19th and 20th century) using wide range of analytical methods (scanning electron microscopy, light microscopy, thermal analysis, x-ray diffraction and others). Special attention was drawn to the study of analytical determination of oil content as fatty substances turned out to be quite a frequent admixture in mosaic mortars. The characterization and experiments were performed on (a) historic samples from 27 authentic artworks and (b) model samples imitating authentic mosaic materials in which linseed oil had been identified. The aim of the experiment was to evaluate the possibilities and limitations of analytical methods conventionally used for the identification and quantification of organic admixtures (namely linseed oil) in mortars.

The main objectives of the project are:

- Characterization of collected late 19th and early 20th century mosaics´ inorganic fixing mortars – identification of binder and aggregates, identification of possible organic additives in order to determine the technology of mortars´ production.

- Tracing the development of mosaics´ fixing technique from the late 19th to late 20th century on a representative set of fixing mortars from mosaics situated mostly in the present-day Czech Republic.

- Identification of possible workshop-specific markers in fixing techniques between different mosaic workshops operating in the Czech Lands.

- Characterization of microstructure and engineering properties of linseed oil containing model mortars imitating the composition of authentic historic mosaic mortars.

- Improvement of analytical tools for oil content identification in historic mortars – testing the combination of conventional and easy-accessible analytical methods such as infrared spectroscopy, thermal analysis, gas chromatography and total organic carbon on a set of model samples with a variable oil concentration.

3 MATERIALS USED FOR THE FIXATION OF MOSAIC MORTARS

Mosaic tesserae have to be fixed to form a solid image. The most common way to do so is to use a mortar. The use of both traditional and modern inorganic materials can be expected in modern mosaic fixing mortars (i. e. mortar beds and grouts). Fig. 1 outlines the materials used in mosaic art since the Antiquity to this day. These materials, their compounds and the most serious issues concerning their durability will be briefly discussed in the following sections.

Mortar is a mixture of an inorganic binder, water and fine aggregates. Its properties depend on the chemical composition and quality of raw materials, the way of preparation (binder: aggregate ratio, amount of mixing water) and craftsmanship (e.g. the degree of compaction). Mortars´ properties can be modified by the presence of both inorganic and organic admixtures. The admixtures affect waterproofing, water-repellency, efflorescence control, air entrainment using plasticizers to enhance workability, retarding setting times etc.

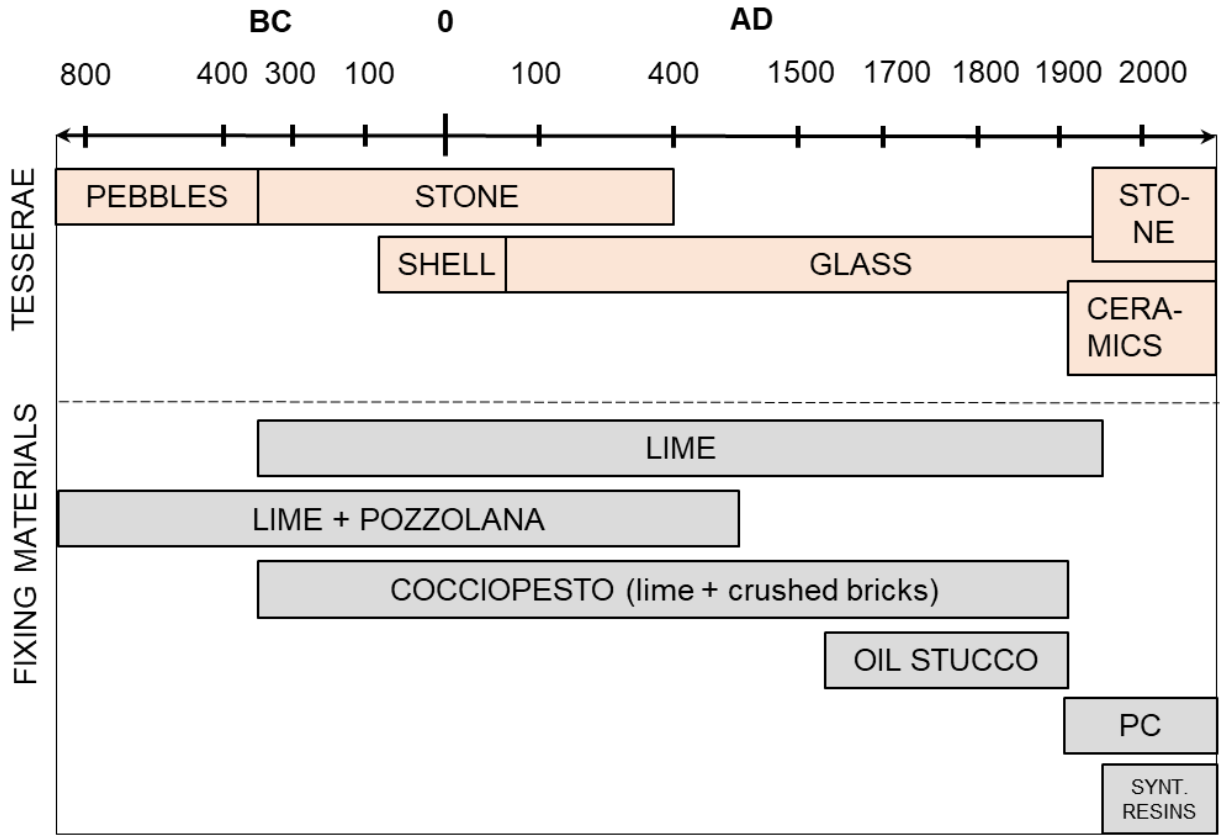

Figure 1. Materials commonly used for mosaic tesserae and mosaic mortars since the Antiquity to this day. PC – Portland cement.

3.1 Binders

The term binder refers to materials with adhesive and cohesive properties which make them capable of bonding mineral fragments in a coherent, solid mass [1]. The first phase of the solidification process is setting. In this stage, the liquid or mushy mixture loses its original workability and gradually acquires a character of a solid substance. In the subsequent hardening phase, the resulting solid gains a higher strength needed for specific construction applications [2].

Material scientists distinguish two basic groups of binders – **air hardening** (**non-hydraulic**) and **hydraulic**. Air-hardening (non-hydraulic) carbonate binders, such as air lime, harden slowly in air by reacting with carbon dioxide and moisture to form an insoluble carbonate. Hydraulic binders, such as natural hydraulic lime, Roman or Portland cement, set and harden by chemical interaction with water and are capable of doing so under water [1].

3.1.1 Lime

Air lime

Lime seems to have been intentionally calcined as early as the 6th millenium B.C. [3]. Some scholars [4] suggest, burning of limestones might have been a direct predecessor of pottery firing. Quick lime (CaO) is a product obtained by the calcination of calcium carbonate rich rocks (limestones, marbles, chalk) at approximately 900 °C. Its subsequent slaking, i.e. hydration, leads to the formation of slaked lime $Ca(OH)_2$.

In mosaic mortar beds the use of lime (mixed with pozzolanic rocks) was documented as early as pebble mosaics of ancient Greeks [5]. The use of lime in mosaic mortars is documented from the Antiquity to the early 20th century (see Section 4).

Air lime is a product obtained by the calcination of pure carbonate rocks with very low contents of reactive oxides, i.e. silica and alumina. The setting of air lime is based on the decrease of water content in a mortar by evaporation or its soaking by a porous material – e.g. bricks. The hardening of air lime is driven by the conversion of slaked lime $Ca(OH)_2$ to calcium carbonate $CaCO_3$

$$Ca(OH)_2 + CO_2 + nH_2O \rightarrow CaCO_3 + (n+1)\ H_2O \qquad (1)$$

The presence of water between reactants emphasizes the fact, carbonation takes place in a liquid phase – in a pore solution. In fact, water is not a reactant, just a medium for this process. The carbonation of air lime is quite slow, lasting minimum six months [6]. It depends on CO_2 concentration in air, relative humidity, temperature and last but not least on the degree of CO_2 penetration into the mortar. Arrizzi and Cultrone [7] found only 3-6% non-carbonated lime after two years of their experimental air lime mortars´

carbonation. However, in some inner parts of thick masonry structures´ joint mortars with a limited air CO_2 access, carbonation has not been completed even after centuries [8], [9].

According to valid ČSN EN 459-1 standard [10], air lime must content at least 70% CaO + MgO.

Lime with hydraulic properties (hydraulic lime)

Most of the rocks used for lime production contain a certain degree of siliceous or argillaceous impurities. *Natural hydraulic lime (NHL)* is a binder obtained by the calcination of limestones containing 10-25% of clay minerals at temperatures between 1100-1250 °C [11]. Clayey compounds provide reactive silica and alumina and also iron oxide, the sources of the binder´s hydraulicity. During calcination, these hydraulic oxides react with CaO from the decomposed calcium carbonate matrix to form hydraulic clinker phases, i.e. calcium silicates and aluminates. The most frequent calcium silicates aluminates in hydraulic lime are belite – C_2S, tricalcium aluminate – C_3A, tetracalcium aluminate – C_4AF and wollastonite – CS [12]. Callebaut et al. [13] find significant the presence of gehlenite C_2AS, a mineral that cannot be formed at temperatures higher than 1250 °C.

Chemically, mineralogically and also with its engineering properties, lime with hydraulic properties stands in between air lime and Portland cement. The presence of clinker phases makes it different from air lime. The ultimate dominance of belite C_2S over alite C_3S, the most common clinker phase in Portland cement, as well as a considerable amount of free lime (CaO and MgO) makes the difference between hydraulic lime and Portland cement [6], [14].

According to ČSN EN 459-1 standard [10], natural hydraulic lime is classified based on the free lime content (must be at least 15 wt%) and compressive strength.

Apart from NHL, the standard [10] differentiates two other types of lime with hydraulic properties – formulated lime and hydraulic lime. *Formulated (blended) lime* consists prevailingly of air lime or NHL and other hydraulic and/or pozzolanic admixtures. *Hydraulic lime* is made of lime and other compounds such as cement, blast furnace slag or fly ash.

However, hydraulic binders of historic mortars are difficult to be classified according to the present-day standards. Their production, as well as chemical composition was not so strictly controlled. That is why the term “hydraulic lime” often stands for the more general term “lime with hydraulic properties” in the literature.

The hydraulicity degree of lime and cement can be expressed by cementation index introduced by Eckel [15]. Cementation index is calculated according to the formula:

$$CI = \frac{2.8\,SiO_2 + 1.1\,Al_2O_3 + 0.7\,Fe_2O_3}{CaO + 1.4\,MgO}\ (wt\%) \qquad (2)$$

Eckel [15] sets an arbitrary limit for hydraulicity to CI = 0.3. He uses this index mostly to classify “natural cements”, i.e. strongly hydraulic binders whose CIs generally fall within the range 1-2 [15]. Böke et al. [16] use CI to categorize hydraulic limes into three groups:

- weekly hydraulic – CI = 0.3 – 0.5
- moderately hydraulic – CI = 0.5-0.7
- highly hydraulic – CI = 0.7-1.1

Setting and hardening of hydraulic lime takes place in two stages. At first, hydration of reactive clinker phases takes place. This leads to a relatively fast formation of a basic solid silicate network. Clinker phases react with water to form strong, water-insoluble hydrated products which adhere to aggregate grains. These substances, calcium silicate hydrates (C-S-H) and calcium aluminate hydrates (C-A-H) possess a very poor crystallinity and therefore are often referred to as gel. At the subsequent stage, carbonation of free lime takes place [14]. The presence of hydrated C-S-H and C-A-H phases brings about higher compressive strength of lime with hydrated properties compared to air lime.

Apart from different chemical composition (lower Ca/Si ratios in NHL compared to air lime), the two types of lime binder occurring in historic mortars can be distinguished in a microscope. Aged air lime is usually almost completely carbonated. Its microstructure is rather homogeneous with uniformly distributed newly formed calcite crystals (Fig. 2a). On the contrary, aged NHL mortar shows a significant inhomogeneity caused by Ca leaching and redistribution within the binder. Highly compacted carbonated areas rich in calcium alternate with siliceous, often completely decalcified matrix with secondary recrystallized $CaCO_3$ (“popcorn structure”) – Fig. 2b [11], [17].

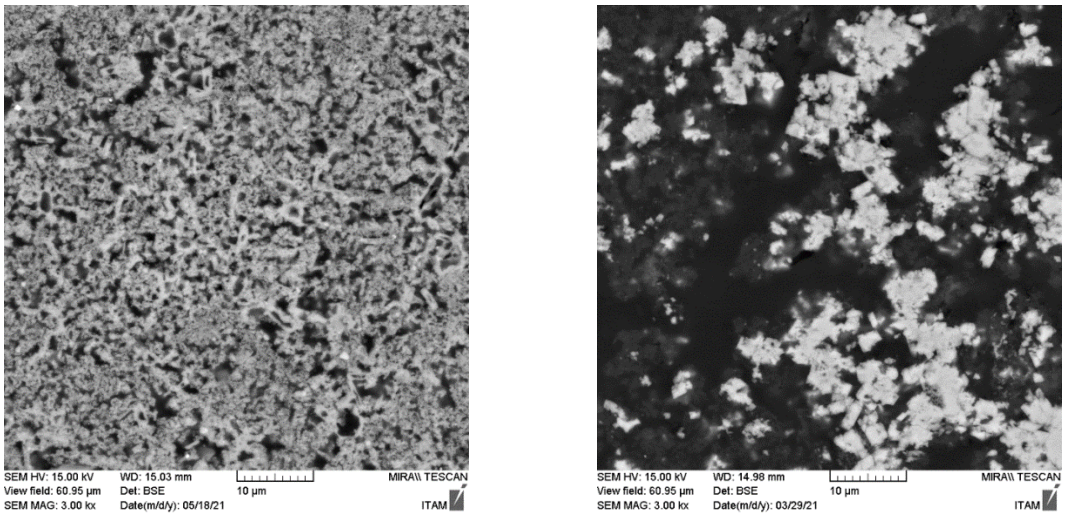

a) b)

Figure 2. Difference between homogeneous air lime binder (a) and inhomogeneous natural hydraulic lime binder with “popcorn-like” $CaCO_3$ crystals (light) and decalcified siliceous matrix (dark). SEM-BSE microphotographs. Courtesy of D. Frankeová **[11]**.

3.1.2 Cocciopesto

A *cocciopesto* mortar consists of lime binder, crushed brick (ceramic) shards or dust and other aggregates (typically sand). Bricks or ceramics represent an artificial pozzolanic material. Pozzolanic materials are latent hydraulic – they can react with lime in the presence of water to form hydrated C-S-H and C-A-H phases identical to those occurring in Portland cement [18] or hydraulic lime binder. Lime mortars "reinforced" with such hydrated pozzolanic reaction products show higher mechanical strength compared to air lime [19].

Silica and alumina containing clay minerals are the main components of the raw material used for brick or ceramics production. Clay gains a distinct pozzolanic activity when burnt at temperatures between 600 – 900 °C [18].

The hydrated gel forms dense reaction rims [9], [8], [20], [21]. However, in some cases the brick dust may retain water without developing hydration products as the growth of hydrated phases at the interface of the ceramic fragments requires suitable composition of the brick´s clay material, its adequate firing temperature, sufficient amount of moisture and enough time [21].

When evaluating the effectiveness of lime and brick aggregates´ pozzolanic reaction, one should have in mind, an absence of reaction rims in distinct brick grains is not a reliable indicator of the pozzolanic material´s inactivity. In fine brick grains, the reactive dehydroxylated clay, could have completely reacted with the surrounding lime and as a consequence, these fine grains disappear leaving only traces of intact brick compounds, such as iron oxide, quartz or mica, in the matrix [17].

Lime mortars with crushed bricks or ceramics were used as early as in the 3rd millennium BC [22] and became wide-spread especially in Roman and early Byzantine civil engineering [23], [24]. Since earliest times, ancient builders were aware of the strengthening effect of pozzolanic materials [25]. Therefore it is no surprise, *cocciopesto* mortars were recommended to be applied in mosaic floors as a part of a multilayer mortar system [26]. Such multilayer arrangement of floor mosaic mortar beds was documented in excavations dating back to 4th century BC, in later hellenistic and Roman mosaics as well as Byzantine mosaic works (see Section 4). In Western Europe, the ancient awareness of pozzolanic hydraulic binders´ benefits for structural mortars was almost forgotten during the Middle Ages [14] but the tradition of *cocciopesto* in mosaic mortars seems to have survived until early 20th century (see Section 4).

3.1.3 Roman cement

Despite a misleading name, the term "Roman cement" refers to a special group of European rapid-setting natural "cements" [27], i.e. in fact natural hydraulic lime, which first appeared on the market in the late 18th century in England [27]. In the first half of the 19th century Roman cement production spread to continental Europe. In Austrian

monarchy, the first factories for Roman cement were opened in 1840s. Mass Roman cement production commenced in the last third of the 19th century. In this period first Roman cement factories were founded in the Czech Lands [27]. The heyday of Roman cement production ended during the First World War when this binder was almost completely replaced by Portland cement [27].

Roman cement is produced by the calcination of clayey limestones containing 15-40% hydraulic oxides (SiO_2, Al_2O_3, Fe_2O_3) [27]. Rapid setting (within minutes), very low free lime content (3-7 wt %), good corrosion resistance and typical brownish-yellowish colour represent the most typical features of this binder [27], [28].

Chemical and mineralogical characteristics of Roman cement are similar to hydraulic lime and to some 19th century early Portland cements [29], [13]. Cementation indices of natural cements should fall within the interval 1.1-2 [15]. Phases identified in Roman cement mortars comprise belite (C_2S), the dominant crystalline phase of original Roman cements, portlandite (CH), wollastonite (CS), gehlenite C_2AS or rankinite (C_3S_2) [27], [30]. The presence of three types of residual Roman cement grains, the so-called phenograins, is a typical feature of Roman cement mortars´ microstructure. Phenograins reflect temperature variations inside a kiln during Roman cement´s calcination as they represent underburnt, optimally fired and overburnt Roman cement lumps [30].

To our knowledge, no Roman cement mortar has been reported to have been applied to mosaics. This can be explained by the extremely fast Roman cement´s setting which can cause complications in mosaic´s assembly. However, to verify this assumption, a much larger set of 19th and early 20th century mosaics should be investigated.

3.1.4 Portland cement

Despite its relatively young history compared to other binders discussed here, Portland cement (PC) is nowadays the most common hydraulic binder used in all branches of civil engineering. Limestone and clay, usually in form of a single rock, represent essential raw materials for Portland cement manufacture. When heated to incipient fusion (above 1450 °C), a carefully controlled mixture of the raw materials turns into clinker which is subsequently cooled down and ground to a fine powder. Additional compounds such as gypsum, a setting retarding agent, are mixed and ground with the clinker.

Chemically, Portland cement typically consists of 65 wt% CaO, 21 wt% SiO_2, 4.5 wt% Al_2O_3 and 3 wt% Fe_2O_3. Other minor oxides (< 2.5 wt%) include SO_3, MgO, Na_2O and K_2O

Portland cement clinker is made up of calcium silicates and aluminates. These compounds give Portland cement its hydraulic properties. The most import hydraulic clinker phases are listed in Table 1.

Table 1. The most abundant hydraulic phases in Portland cement clinker. After **[6]**.

Compound	Chemical Name	Abbreviation	Chemical formula	Percentage amount	Rate of reaction with water
Alite	Tricalcium silicate	C_3S	$3CaO{\cdot}SiO_2$	35-65	Medium
Belite	Dicalcium silicate	C_2S	$2CaO{\cdot}SiO_2$	15-40	Slow
Aluminate	Tricalcium aluminate	C_3A	$3CaO{\cdot}Al_2O_3$	0-15	Fast
Ferrite	Tetracalcium aluminoferrite	C_4AF	$4CaO{\cdot}Al_2O_3{\cdot}Fe_2O_3$	6-20	Medium

Calcium silicates alite and belite are the most abundant PC clinker phases. While belite C_2S occurs commonly also in hydraulic lime and Roman cement, the common presence of alite crystals C_3S is typical for PC clinker. The relative proportion of C_3S and C_2S affects the strength characteristics of Portland cement. A bigger percentage of C_3S accounts for faster gain in strength during setting. On the contrary, belite-rich PC show higher later-age strength [6]. Throughout history, the proportion of C_3S in cement has steadily increased while the rate of C_2S has decreased (Tab. 2). Present-day PC (CEM I) typically contains around 60% C_3S and 16% C_2S but PC manufactured in 1890 had only 30 % C_3S and 36 % C_2S [6].

Table 2. The development of alite to belite proportion in Portland cement **[6]**.

Year	Alite C_3S (wt%)	Belite C_2S (wt%)
1890	30	36
1935	55	23
2000	60	16

Similarly to hydraulic lime and Roman cement, reactions of clinker phases with moisture in the presence of carbon dioxide represent the principle of PC´s setting. Hydration of cement is a very complex process. Simplified, it can be summarized by the following equations [11]:

C_2S and $C_3S \rightarrow$ *C-S-H* (hydrated calcium silicate) + CH (calcium hydroxide) (3)

C_3A and $C_4AF \rightarrow$ C-A(F)-H (hydrated calcium aluminates and ferrites) (4)

C-S-H phase is nearly amorphous or poorly crystalline and has the properties of a rigid gel. The composition of C-S-H gel varies according to initial raw materials and hydration conditions. Based on Ca/Si ratio two types of C-S-H gel can be distinguished – C-S-H type I (Ca/Si < 1.5), structurally corresponding to tobermorite, and C-S-H type II (Ca/Si > 1.5) having a more ordered or jennite-like structure [31]. The Ca/Si ratio significantly changes during the aging and carbonation of cement. Initially, the Ca/Si ratio decreases. As the reaction with CO_2 or CO_3^{2-} ions proceeds, C-S-H gel disappears and transforms gradually to hydrous silica [31].

To retard the setting, gypsum has been being added to PC clinker since 1890 [32]. The hydration of alite in the presence of gypsum leads to the formation of a thin ettringite layer on the surface of cement grains. Ettringite crystals prevent water from an immediate reaction with clinker minerals and thus retard the start of setting by hours. Subsequently, ettringite further reacts with unconsumed C_3A to the so called monosulphate [14].

The present-day ČSN EN 197-1 ed. 2 defines 5 main types of common cement [33] Apart from CEM I Portland cement containing 95% of clinker and maximum 5% minor constituents, other types of cements consist of PC clinker and more than 5% other constituents such as blastfurnace slag, silica fume, natural pozzolana or pulverized fuel ash.

The technology of PC production has been developing over the last 200 years. Up to 1890s, early PC materials were heterogeneous materials containing mostly belite crystals, alite being developed in much smaller amount. This was due to limited temperature inside traditional shaft or ring kilns and slow cooling of clinker [23], [29]. The most important technological breakthrough came around the turn of the 20th century with the adoption of rotary kilns and the implementation of clinker coolers into the Portland cement production process. However, new technological inventions spread slowly over the European continent. In the 1900s the dominant share of Central European PC production still came from shaft kilns and ring kilns [29]. In the Czech Lands, the first rotary kilns were installed in 1908 in Čížkovice and Králův Dvůr cement plants followed by Maloměřice and Štramberk in 1911 [34].

All these technological inventions reflect in the chemistry and microstructure of early 20th century cements. Materials of this period stand in between the 19th century protocements and present-day ordinary Portland cement. Alite C_3S dominates over C_2S, residual fuel particles are missing, interstitial aluminate and ferrite particles are finer compared to 19th century materials, indicating faster cooling. On the other hand, compared to ordinary Portland cement, early 20th century materials are still coarser and the crystal grain sizes of the flux aluminate and ferrite phases indicate the use of simple clinker coolers [29].

3.1.5 Gypsum

Gypsum does not belong to binders traditionally used for mosaic mortars. Gypsum and gypsum-lime mortars are prone to moisture. Moreover, their application can cause serious damage of mosaic glass [35]. However, gypsum-containing binder has been identified in some modern mosaic fixing materials [35], [36].

The most common raw material for gypsum binders is gypsum, i.e. calcium sulphate dihydrate $CaSO_4 \cdot 2H_2O$. During calcination up to 160 °C, calcium sulphate dihydrate loses its crystalline water and turns to calcium sulphate hemihydrate $CaSO_4 \cdot ½H_2O$. Setting of gypsum is based on the rehydration of the calcined product. When calcium sulphate hemihydrate is mixed with water, an exothermic chemical reaction takes place, and the hemihydrate is converted back to less soluble solid calcium sulphate dihydrate:

$$CaSO_4 \cdot ½H_2O + 1½H_2O \rightarrow CaSO_4 \cdot 2H_2O \qquad (5)$$

Mechanical properties of hardened gypsum depend on its moisture content. Dry gypsum has a 2-3x stronger mechanical strength than wet gypsum [14].

When mixed with lime, gypsum sets faster. A solid microstructure made of gypsum crystals with interstitial calcium hydroxide particles is formed. Calcium hydroxide subsequently carbonates to calcite [14].

In general, gypsum mortars are better to be applied in interiors. Neither gypsum nor gypsum-lime plasters should get in contact with hydraulic binders. When moisture is present, ettringite or thaumasite crystals can develop. Their crystallization is accompanied by volume expansion possibly leading to a mortar´s cracking [14].

3.2 Aggregates

The addition of aggregates to binder pastes can reduce volume changes during hardening and thus limit shrinkage effects. They also increase the overall volume of the mortar [23]. The aggregates of mosaic mortars are usually rather fine-grained (< 1 mm). Siliceous sand and or crushed carbonate rocks were identified as the most common aggregates in modern mosaic mortars [36]–[39]. The use of sand as well as crushed limestones or marble dust was recommended as early as by Vitruvius [26] for ancient mosaic floors (see Section 4.1.1)

3.3 Organic admixtures in mosaic mortars

Organic compounds have been added to inorganic binders since the time of the first ancient civilizations in order to improve their mechanical workability, mechanical properties and durability. Various organic additives have been used – namely fats (both plant and animal), proteins (animal glue, egg proteins, casein of curdled milk),

saccharides and polysaccharides (sugar, various gums and sizes) or more complex substances such as animal blood [40], [41].

Organic compounds of different nature seem to have been quite a frequent part of mosaic mortars. The aim was to provide a better adhesion of mosaic tesserae, water repellency and longer plasticity of the mortar bed. In the Byzantine-style mosaics, straw fibres were added to mosaic mortars to enhance their fracture toughness and flexural strength [42], [43]. Byzantines also used bitumen, tar or resins as water-proofing agents to impregnate the underlying wall prior to the application of mosaic mortars [44].

In a 16th century treatise, two-step preparation of a “glue” consisting of bran, boiled barley, elm bark, malva and flax is described [45]. This sticky liquid was exclusively designed for mosaic mortar beds. It was mixed with lime instead of common mixing water. Supposedly, boiled barley and malva provided polysaccharides (mucilage). Similarly to other polysaccharides such as commercially available gum guar derivative hydroxypropyl guaran [46], they might have served as viscosity modifiers providing a larger water-retention capacity and a delay of setting time. Elm bark is a source of tannin which consumes Ca^{2+} ions during the formation of calcium-chelate complex [47] and thus can retard carbonation.

Egg proteins have been identified by Stulik [48] in medieval mosaic mortars of the 14th century Last Judgement mosaic at the Prague Castle. Allen [43] reports the identification of egg white albumen from St. Mark basilica in Venice.

The use of various fats is quite frequently mentioned in the literature. Vitruvius recommends to impregnate completed exterior floor mosaics by olive oil to provide frost-resistance [26]. The use of hog´s lard is mentioned in some medieval treatises [45]. The most common fatty substance added to mosaic mortars as late as the turn of 19th/ 20th century [37] is linseed oil (see Section 4.4).

In the 20th century synthetic polymer suspensions based on poly vinyl acetate were recommended to be added to cement-based mosaic mortars [49].

3.4 Aging and degradation of mortars

Carbonation in the presence of moisture plays a crucial role in the ageing of all carbonatic binders (Fig. 3). In case of air lime, this reaction (Equation 1) is directly responsible for the mortars´ hardening. Aged air lime mortars have homogeneous matrix consisting of fine $CaCO_3$ crystals. Typical shrinkage cracks developed due to setting and water evaporation can be observed [50]. On the other hand, aged hydraulic binders are inhomogeneous as a result of the binder´s segregation to calcium enriched areas with $CaCO_3$ crystals and decalcified silica-rich matrix [51], [52]. “Popcorn structure”, i.e. newly formed calcium carbonate crystals surrounded by amorphous silica (Fig. 2), also indicate the decomposition of hydrated C-S-H phases as a result of carbonation and water circulation through the binder´s pore system [17]. Unhydrated

clinker residues often undergo decalcification but their crystal shape remains unaffected.

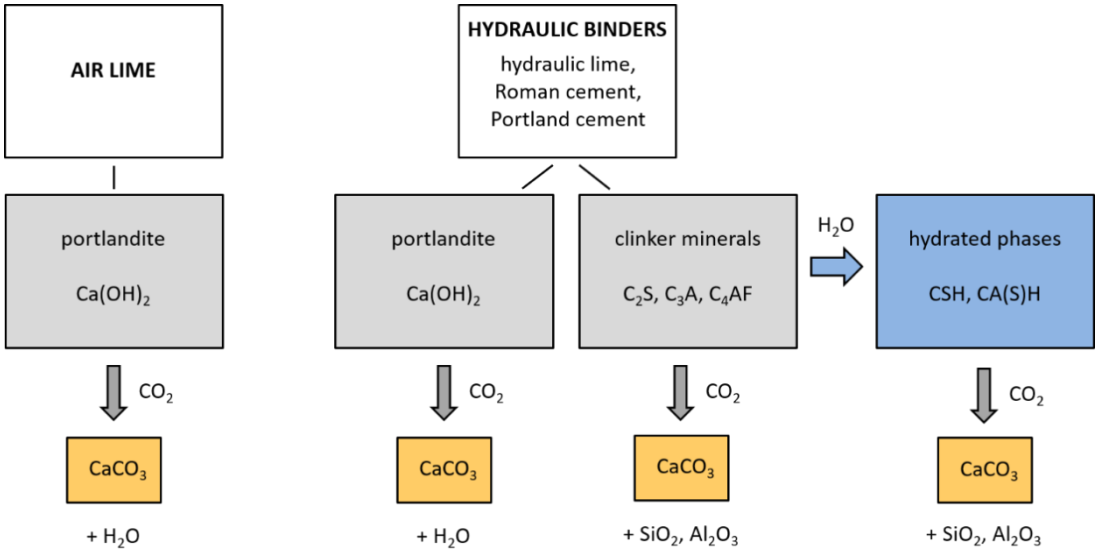

Figure 3. Schematic display of carbonation and hydration mechanism of carbonatic binders. After **[11]**.

The degradation of mortars can be caused by physical factors (changes of moisture and temperature), chemical factors (formation of salts) and biological factors (mechanical cracks due to plant roots or fungi mycelia or dissolution of the binder by acids produced by organisms). Exterior mortars are threatened by aggressive compounds contained in the atmosphere or surrounding environment. Apart from naturally occurring CO_2, which dissolves in rain water, atmospheric pollutants such as SO_2, SO_3 and NO_x can form acid solutions that wash binder particles out of the mortar or react with the binder to inorganic salts.

Mosaic mortars can also be corroded by salts migrating from wet masonry or from capillary moisture. The most common salts are sulphates, chlorides and nitrates. Crystallization pressures of these salts can cause mechanical damage to mortars. Lime binder is prone to the sulphate attack with results in the formation of calcium sulphate (gypsum) $CaSO_4 \cdot 2H_2O$. This salt can form a dark crust on the mortar´s surface. Moreover, the crystallisation of its large crystals can induce stress leading to the development of cracks.

Sulphates migrating in capillary water also pose a threat to Portland cement binders. They typically react with cement to gypsum $CaSO_4 \cdot 2H_2O$ or ettringite $3CaO \cdot Al_2O_3 \cdot 3CaSO_4 \cdot 32H_2O$. Their formation is accompanied by the increase of volume and consequent cracking.

The formation of thaumasite $CaSiO_3 \cdot CaSO_4 \cdot CaCO_3 \cdot 15H_2O$ can come about when cement binder is attacked both by sulphates and aggressive carbon dioxide. The reaction consuming the silicates of the binder can lead to harmful decohesion and

softening. Thaumasite often develops at the junction of cement plaster and sulphate-containing brick masonry [14].

The presence of nitrates in mortars is associated with bacteria activity [14]. Nitrates occur in ground parts of plaster mortars on sites rich in organic contamination (stables, cemeteries etc.). They are easily soluble in water. Organisms such as bacteria and fungi can also produce water-insoluble biogenic calcium oxalates which were identified in historic lime mortars [53], [54] and other works of arts [55].

4 DEVELOPMENT OF MOSAIC FIXING TECHNIQUE

Mosaic technique developed during the Antiquity. World´s most famous examples of this art have been associated with ancient Greeks and Romans [56] and with early Christian, Byzantine and Italian medieval art [44]. Mosaic technique experienced its revival in the half of the 19th century after several hundred years of decline. Their much longer durability compared to wall paintings, perceived as "eternity" at the moment of the artwork´s origin [57], made mosaics a popular decoration of facades, building interiors or sepulchres. (After decades or centuries the condition of many mosaics reveals, the faith in the "immortality" of these artworks was often exaggerated.)

Another important factor contributing to the spread of mosaic art at that time was the invention of the so-called *indirect method* of tesserae setting (see Section 4.5). This made it possible to create a complete lay-out in the studio.

Although mosaic predecessors made of ceramic cones fixed in mud or bituminous binder were designed in Mesopotamia as early as 3000 B.C. [44], ancient Greece is regarded to be the cradle of classic mosaic art form, *opus tessellatum* (mosaic made of cut cubes of stone or glass). The earliest Greek mosaics were made of pebbles and applied on floors. Pebbles were replaced with tessellated stone *tesserae* during the Hellenistic period (4th – 2nd cent. B. C.). At this time artificially produced materials, such as beads, faience and glass were also introduced into classic mosaic art. However, their use was rather sporadic. Pavimental form prevailed until the Christian era [56].

Glass tesserae became the most common material used in wall and vault mosaics from the mid-first century onward [56]. The spread of Christianity in the 4th century A.D. significantly helped the transition from floor to wall mosaic decoration of early Christian and later Byzantine churches. Mosaic became an illustrative medium of an almost exclusively religious nature [44]. "Eternal" monumental technique transmitting "eternal" sacred ideas plus its essential connection to architecture and public space – this might be the reason why mosaic form later became so preferred in totalitarian regimes´ art (see e.g. [58], [59] for deeper discussion). The strictly religious character was partially broken as late as 19th century when mosaics began to be applied also to representative profane structures.

The research into glass tesserae has been more intensive than in case of mosaic fixing materials. Numerous papers on ancient [60]–[64], Byzantine and medieval [65]–[70] mosaic glass have been performed. Several studies have been dedicated to the classification and characterization of Czech mosaics´ glass tesserae [71], [72], [35], [48]. As the materials nature of mosaic glass differs significantly from the mortars, mosaic tesserae stand outside the scope of this study.

Ceramic tiles, the third common material for modern mosaic tesserae, became widespread in European design tradition as late as early 20th century during the Art-Nouveau period [73].

Fixing mortars are applied universally, regardless the material of the tesserae. The following sections describe the development of mosaic fixing techniques that have been used since the Antiquity up to the 20th century and onward. The overview concerns European mosaic art.

4.1 Antiquity

4.1.1 Floor mosaics

In the Antiquity, mosaics were displayed mostly on floors (Fig. 4). Even though aesthetic factors significantly came to play, mosaics served as functional architectural elements above all. Their fixing technique had to be adopted to their daily use as walking surfaces. Most of the mosaics were made *in situ* [56], the tesserae were set *alla prima*, i.e. pressed directly into the mortar. Due to the mosaics´ practical use, several layers of ground mortars were applied. The process of the floors´ preparation was described by Vitruvius in the 1st cent. B.C. The mortars were laid on oak-wood boards which had to be separated from the upper parts by a layer of straw or fern not to be affected by lime. Vitruvius then starts with a layer of the so called *statumen*, a bedding of fist-sized aggregates. This is followed by the *rudus*, which is a mortar made of 3 parts of aggregates and 1 part lime in case of a newly-built floor (or 2 parts of lime and 5 parts of rubble if an old floor is renovated). This mixture is beaten solid to the thickness no thinner than ¾ feet (20 cm). The uppermost layer, the *nucleus*, consists of a finer mixture made of 3 parts crushed bricks and 1 part lime. After being beaten down, it should be at least 6 inches (11 cm) thick. Above this, mosaic tesserae or tiles are to be laid using level and rule. The floor is subsequently ground and polished. Finally, a covering grout of lime, marble dust and sand is applied [26].

Special instructions are provided for the laying of foundations for outdoor pavements. The preparation must be extremely careful so that the wooden parts do not shrivel or deform. The wooden layer must be made of two sets of boards – the upper laid perpendicularly to the lower. Boards must be nailed at the extremities, to prevent them from warping. The *statumen* should consist of 5 parts aggregates and 2 parts lime. The aggregates should contain ⅔ stones and ⅓ crushed bricks. The *nucleus* should be at least 1 foot (30 cm) thick. It is followed by a marble dust, sand and lime cover, into which tiles are squeezed. This mortar cover is recommended to be impregnated by boiled olive oil in order to protect it from frost [26].

The wooden support concerned rather pavimental works situated on elevated floors, the *statumen* of the ground floor mosaics was commonly laid directly on rammed ground [74], [75].

Pliny the Elder [76] repeats the general procedure of laying the foundations for outdoor terrace-roof pavements after Vitruvius [26] but his description is briefer.

The technique recorded by Vitruvius developed in Greece in the 4th cent. BC [77]. The 5th BC pebble mosaics from the ancient town Olinthos are reported to have been fixed in a single-layered, extremely well compacted bedding mortar with lime and pozzolana binder and coarser aggregates of various rock types [5]. Stratigraphy corresponding to the Vitruvian mortar sequence was discovered in Hellenistic mosaic floors dating back to 4th cent. B.C. [78]. Vitruvius´ ideal rules were not followed strictly by all mosaicists but the general stages he distinguishes can be found in most mosaic floors of the Graeco-Roman world [56]. Multilayer mortar system has been documented in Roman excavations dating back to 1st cent. BC – 6th cent AD from present-day Greece [78], Italy [74], [75], [79], Spain [80], Turkey [81], Israel [82] or Hungary [83].

Figure 4. Mosaic floor from a late antiquity Roman villa in Desenzano by Lago di Garda, northern Italy.

In practice, the multilayer mortar system (Fig. 5) was often much thinner compared to Vitruvius´s instructions, reaching about half of the recommended total thickness [78], [80]. The mosaicists usually laid the mosaic tesserae into a thin (0.5-1 cm) bedding layer – the *supranucleus* – which was applied over the *nucleus* mortar and consisted of lime [74], [83] or lime with fine siliceous or carbonate aggregates with a high binder/

aggregate ratio [80], [84], [85]. The bedding mortar sometimes contained crushed bricks [78].

Crushed bricks and pozzolana represented an important compound of the *nucleus* mortars, which frequently provided a hydraulic character [74], [78], [81]. According to Pachta et. al. [77], the addition of brick dust and crushed bricks enhances the adhesion between the layers as well as their resistance to humidity. Ancient masons were able to achieve an extremely stable interface between the layers due to a careful compaction of mortars. That is why the compressive strength of mosaic mortars is higher and their porosity generally rather lower compared to ancient structural mortars [78].

Deviations from Vitruvius´s guidelines have also been reported. Late antiquity floor mosaics from a Roman villa near Barcelona, Spain, were built on the older pavement with a clearly distinguishable rudus and nucleus stratigraphy. The older pavement served as a base for a 5 cm thick preparatory layer made of lime, sand and crushed ceramics, followed by a very thin fine lime-based bedding mortar [84]. Miriello et al. describe the absence of the *nucleus* layer with *rudus* being followed directly by a fine-grained bedding mortar rich in lime [75]. Although the general idea of a multi-layered system, recorded by Vitruvius in the 1st cent BC, spanned many centuries from classic Greece period to the late Antiquity, its certain development and modification in time was observed [79]. Lime and *cocciopesto* (i.e. lime and crushed bricks) mortars became traditional mosaic fixing materials which were used in mosaic art until as late as early 20th century.

4.1.2 Emblemata

Since the second half of the 3rd century BC prefabrication of small-scale mosaic motifs was implemented into mosaic floor decoration. Transferable small-scale panels – the so called *emblemata* – were assembled in mosaic workshops [56], [86]. The tesserae were bedded in a mortar consisting of calcitic binder and sand and fixed into a transferable terracotta or stone tray. The mortars were often painted by various pigments (yellow ochre, hematite, green earth, cinnabar, carbon black or Egyptian blue) in order the mosaics to resemble a painting [86].

4.2 Early Christian and Byzantine mosaics

The early Christian and subsequent Byzantine period is associated with the transfer of mosaics from floors to walls. The multilayer fixing system continued to have been applied with certain modifications related to the transition to walls (Fig. 5).

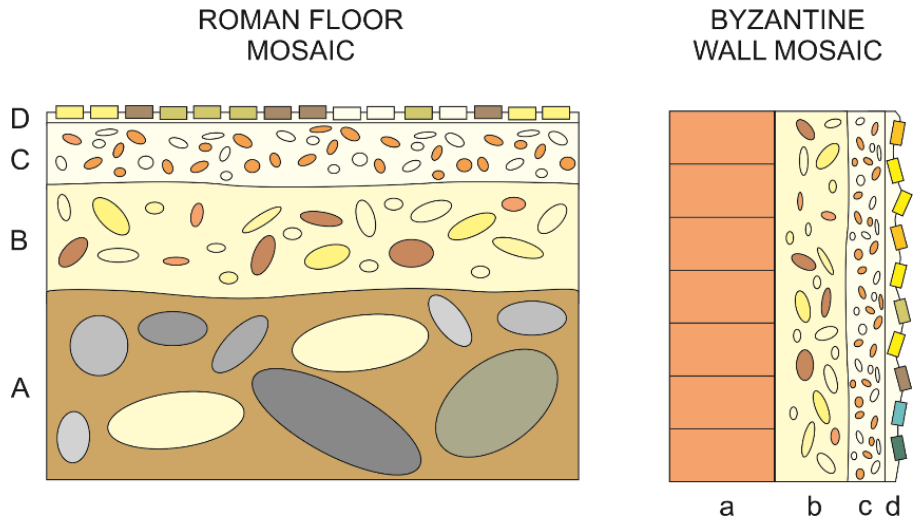

Figure 5. Comparison of multilayer mortar systems in Roman mosaic floors and Byzantine wall mosaics. Roman floor – A – statumen, B – rudus, C – nucleus, D – supranucleus. Byzantine wall mosaic – a – masonry, b – ground mortar, c – finer plaster equivalent to *arriccio* layer in fresco painting, d – fine bedding mortar equivalent to *intonaco* in fresco painting.

According to Haswell [44], the wall was coated with a waterproofing agent such as bitumen, tar or resin prior to the application of mosaic fixing mortars. The fixing multilayer consisted of three lime-based coatings. A bottom-most (adjacent to the wall), fairly coarse foundation coat was made up of crushed bricks and sand aggregates. The foundation coat was usually thicker than subsequent mortars. It was followed by a second coat of finer texture. The surface of the underlying mortars was roughened with a pick to provide better adhesion for the next layer. The final coat usually contained lime putty. This uppermost mortar was applied in sections of suitable size for a day´s work. The final layer was sometimes coloured to avoid compromising the visual effect of the tesserae [44] or painted in order to outline preparatory drawings [42], [87]. The total thickness of the coats usually did not exceed a maximum of 8 cm. To enhance the efficiency of fixing mortars, a reinforcement made up of clamps or flat-headed nails was sometimes driven into the lowest mortar layer [44].

Byzantine artists invented a special method of laying the upper-most mortar layer so as to produce an undulating surface. The surface irregularities enabled mosaicists to achieve glittering visual effect of glass (especially gold) tesserae [44] (Fig. 6).

The above-described technological and materials features were reported from the mosaics of the Durres amphitheatre, Albania, dated to 7th – early 8th century [88]. Moropoulou et al. [42] identified straw fibres in bedding mortars of Hagia Sophia mosaics. Bonnerot et al. [89] reported the use of gypsum in mortar fragments of 5-7th century wall mosaics in Cyprus. However, the application of gypsum was caused by the availability of local gypsum deposits and seems to be rather exceptional.

Figure 6. Masterpieces of Byzantine mosaic art: wall and vault mosaics at Mausoleum of Galla Placidia, Ravenna, Italy. The glittering effect of the mosaics occurs due to a special technique of glass tesserae setting. Photo by S. Zucker, licence CC BY-NC-SA 2.0, downloaded from https://www.flickr.com/photos/profzucker/8619566122/in/photostream/

4.3 Medieval mosaics

Medieval mosaics followed older Byzantine tradition not only from the point of style but also from the point of materials and technique. Lime-based mortars continued to be a basic bedding material in medieval mosaics. Literature on the technique and materials of European medieval mosaics is not rich (perhaps because medieval mosaics are not as abundant as Byzantine works). However, as far as we can deduce from only few available sources, mosaic laying technology slightly modified. In the literature, a certain simplification of the technology (reducing the number of plaster coatings to a double layer system - [90], [91] and the use of organic additives [43], [48], [90], [92] are described.

An instruction how to prepare a mosaic mortar can be found in the early medieval treatise *Compositiones ad tigenda musiva* dated to late 7th/ early 8th centuries: *"Take one part of lime, four parts of sand and 1/3 part of brick powder, obligatorily one congius* (3,3 l) *water and two sextars* (approx.. 1 l) *pig fat. Mix altogether and let stand for one week…"* ([45], p. 74).

In the late 11th century, first mosaics were introduced in the famous St. Mark´s basilica in Venice. The structure of mosaic mortars follows the Byzantine routine, i. e. three layers of wall coatings of decreasing grain size towards the top. The intermediate coating clearly contained fibrous material, supposedly straw. Interestingly, a thin film of egg white was painted over the surface of the uppermost mortar bed. This might have

improved the adhesion between the mortar and tesserae and the overall workability [43].

A double- layer mosaic mortar system is reported from some 12th century mosaics in the Norman cathedral in Salerno [91]. The lower layer was composed of a lime mortar with dolomite and feldspar aggregates while the bedding mortar has practically no inert fraction. A double-layer consisting of a preparatory plaster and a mortar bed was also found in mosaic fragments from the former Székesfehérvár basilica, Hungary, built in the 11th cent. [90]. The preparatory plaster is equivalent to *arricchio* in fresco painting, while the fine-grained mortar bed´s structure corresponds to *intonaco*. The intonaco´s surface was painted and remnants of *sinopia* (support sketches) were identified in the underlying preparatory plaster. The basic mortar was made of lime binder and limestone aggregates. Moreover, the material contained a large amount of organic vegetal elements [90].

Madonna of Malbork, an 8 meter high statue decorating the outer façade of a castle church in Malbork, Poland, represents a unique example of sculpture piece covered by mosaic tesserae. Mosaic replaced the original painted polychromy around 1380 to provide a longer durability of the artwork. The statue´s body is made of artificial stone based on gypsum and sand. Micritic calcium carbonate binder, siliceous aggregates and crushed bricks were identified in the pinkish mortar used for the fixation of the mosaic layer. The Madonna´s mosaic decoration, as well as a gothic mosaic from the façade of the near-by Kwydzin cathedral are considered to have a relation to the Last Judgment mosaic from the Prague Castle [93].

4.3.1 Last Judgment Mosaic at the Prague Castle

The Last Judgment mosaic decorating the southern façade of St. Vitus Cathedral at the Prague castle (Fig. 7) originated in 1370s. According to the results of its detailed investigation and careful conservation [48], [92], two layers of preparatory plasters were applied prior to laying the tesserae. At first, the surface of the cathedral´s stone wall was roughed and an iron wire mesh was stretched between double hooked nails placed in regular 37.5 cm intervals along the whole area of the future mosaic. The first mortar layer (several centimetres thick) was applied over the mesh afterwards. Subsequently, a bedding mortar consisting of lime, sand and brick powder was laid in sections corresponding to daily work progress. Mosaic tesserae were installed into this mortar bed immediately. Analytical study of the original mortar bed brought evidence on the presence of organic compounds – egg proteins and linseed oil coming from later 19th century conservation treatment [48].

Figure 7. The Last Judgment Mosaic at the Prague Castle, Prague.

4.4 Early modern mosaics

In the 16th century the centre of mosaic production shifted from Venice to Rome. Mosaic decoration of St. Peter´s basilica, Vatican, brought significant modification in the preparation of fixing mortars – the application of *"oil"* or *"Roman stucco"*, a composite mastic rich in linseed oil. The application of linseed oil or stand oil in mosaic mortars has been recently documented both by materials and archival research..

The so called "oil stucco" was reportedly designed by Italian painter Girolamo Muziano (c. 1532 – 1592) exclusively for the completion of St. Peter´s mosaics [94], [95]. Indeed, Fiori et al. [96] identified linseed oil in St Peter´s mosaic mortars. The analysed mortar layers technologically correspond to archival historic recipes cited by the authors [96].

Anonymous records on the composition of the mastic have appeared since the 16th century. The oldest one gives details on the mastic´s preparation: *"They don´t use stuccos but glue made as follows: they take a recently made caustic lime and, after purification by sieving, they wet it immediately […], then they mix it with an equal part of the following material. They take a kind of grass called "malmischio", barley with bark and linseeds in equal parts and boil them together in water until the two thirds of it are eliminated. Mixing this material with the above mentioned lime makes a very good glue for the work…"* ([96]; p. 249)

After several months of setting, the glue was ground to dust and mixed with linseed oil prior to the application [96].

Belmonte and Salermo [94] point out, the composition of mosaic mortars used in the basilica changed repeatedly during the mosaic installation. Interestingly, in some parts of the cathedral´s vault more traditional, Venetian-style mosaic mortars-with vegetable fibres were used instead of oil stucco [94].The authors also mention three similar early 17th century oil stucco recipes listed in various contracts for St. Peter´s mosaic decoration. The principal components were slaked lime mixed with marble dust and raw linseed oil. The mixture had to be carefully blended in order to get rid of water and let dry prior to application on the wall. Drying should last 3-4 days according to one recipe, 8-10 days according to the other and its purpose is to improve the adhesion of the mortar to the wall. The third recipe allows for an initial step in this process. The wall had to be coated with a layer of stand oil prior to the application of oil stucco. No stand oil was added in the stucco itself [94].

A later, 1760s record describes oil stucco as a mixture of equal parts lime, travertine powder and linseed oil [96].

Despite continuing completion of mosaic decoration of some churches, such as St. Peter basilica, and the inventions it has brought, the slow decline of the monumental mosaic craft began during the 15th century, coinciding with new developments in painting and sculpture [44]. Nevertheless, since the 17th century mosaic technique was used to create mosaic “paintings” and reproduce famous painted artworks into more stable mosaic image [97].

A special technique called *micromosaic* or *mosaico minuto* was developed in the newly established Vatican mosaic studio around 1730. *Mosaico minuto* masters also used a stucco consisting of linseed oil, travertine dust and slaked lime to fix minute glass tesserae as a decoration of art and craft objects and jewellery [98].

In 1880s, during the revival of traditional mosaic art, a modified version of Muziano´s recipe for lime and linseed oil based mosaic mastic was recommended by Gerspach [95]. Gerspach´s recommendations seem to have been followed by Austrian mosaicists from Albert Neuhauser/ Tiroler Glasmalerei- und Mosaikanstalt workshop [37].

The main difference from the abovementioned recipes lies in including the stand oil directly in the mortar. Gerspach even gives the ratios of particular compounds – 60 parts of travertine dust, 25 parts of white slaked lime of the same travertine, 10 parts of raw linseed oil and 6 parts of standoil [95]. Unfortunately, a note on whether it regards weight or volume parts is missing.

The author states the ratios can slightly vary and so can the material (travertine can be replaced with a raw material of similar composition) [95]. The relatively high amount of linseed oil compound as well as the combination of raw and stand oil make the main specifics of this recipe.

Gerspach [95] adds further details on the use of this oil mastic: *"…To demonstrate the advantages of Muziano´s invention, it is necessary to mention that lime cement is plastic only for several hours while this oil mastic keeps its plasticity for three to four days in summer and twice as long in winter. This makes the work significantly easier and faster. The oil mastic is much more adhesive than cement, it adheres well to any type of stone, metal wood or glass grounds provided they are rough and coated with oil. The mastic is light as it can be applied in one layer only. Since Muziano´s time it has been used mostly in interiors and portable mosaics."* ([95]; p. 238)

4.5 Indirect method of setting and the 19th century revival of mosaic art

The revival of traditional mosaic art arose from the need of more appropriate restoration of dilapidated medieval mosaics, namely the mosaics of St Mark basilica in Venice. Venetian lawyer Antonio Salviati (1816-1890), sensed a chance and in 1859 he and his business partner, glassmaker Lorenzo Radi (1803-1874), opened a mosaic workshop which supplied St. Mark´s restorers with a newly developed mosaic glass material. What is more, thanks to the owner´s social contacts and business talent, Salviati dott. Antonio Company received numerous contracts for new mosaic decoration from both inland and abroad [99]. The company brought up many mosaic masters who soon founded mosaic studios in other European cities [100].

The increasing demand for mosaics´ renovation and increasing new production needed an effective solution to accelerate the whole mosaic-laying process. The invention of the so-called *indirect method of setting* (Fig.8), a mid-19th century breakthrough in making mosaics, paved the way to a semi-industrialized mosaic production. Thanks to indirect setting, mosaics started to be manufactured in the studio and transported to sites in sections. Smaller-scale mosaics could be fixed in portable metal frames. This considerably reduced the production costs and opened the door to a widespread marketing area.

The method has been widely used to this day. Mosaic tesserae are first adjusted on a temporary support – a canvas or a paper. The support usually serves as a 1:1 scale cartoon with a reversed mosaic motif. The tesserae are laid reversely, i.e. face side down. Starch paste or gum Arabic with honey can be used to fix the tesserae [39]. Once the mosaic laying has been completed, it is transferred to its final site. The mosaic (at this point visible from the reverse. i.e. with reversely laid tesserae on the top), is squeezed into a permanent bed made of fresh mortar so that the temporary support remains on top. When the bedding mortar sets, the temporary support is washed away with water. What remains is the original, unreversed mosaic motif. Unfortunately, greater efficiency results in the loss of quality and expression in design [44]. Exposed surfaces of indirectly set mosaics remain uniformly flat. Thus, the play of light scattering on undulating tesserae notably reduced.

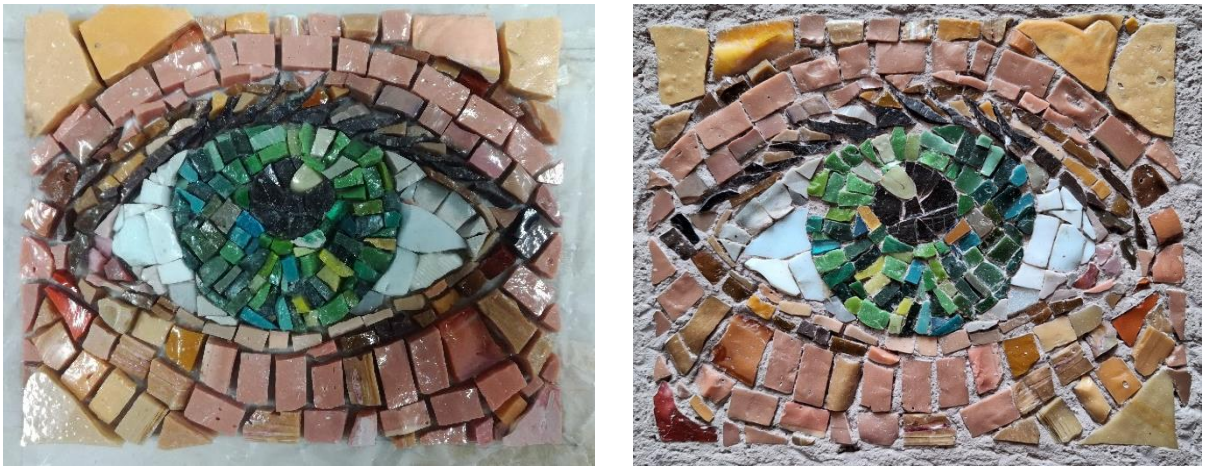

a) b)

Figure 8. Indirect method of setting. Mosaic glued reverse on top on a temporary paper support (a), final mosaic image fixed to a cement mortar (b). The images are inverted.

Italian mosaicist Giandomenico Facchina (1826-1903) usually gets credit for the invention of indirect method while performing mosaic restoration works in France [97]. On the other hand, Salviati´s son and colleagues claim, Salviati Company came up with this improvement [100]. According to some authors the method might have been known even before Salviati [101]. Dunbabin [56] discusses the possibility of indirect method being used in mosaic floor production as early as by ancient Romans but finds it rather improbable.

Beside the innovation of mosaic technique, 19th century brought revolution in the application of new building materials in civil engineering. Due to the lack of published data it is quite difficult to estimate when exactly and to what extend traditional mosaic mortar materials started to be replaced by cement-based binders. In Central Europe, cement-based concrete structures spread extensively during 1880s [102]. The penetration of progressive new binders to mosaic art seems to have taken a longer time. To our knowledge, the first documented use of Portland cement in mosaic mortars comes from 1900s [36], [39].

From sporadic materials studies of late 19th century and early 20th century mosaic fixing mortars we can conclude, a relatively wide range of materials – both traditional and new – were applied. Interestingly, most of the published papers describe mosaics from the present-day Czech Republic. Lime mortars with carbonate aggregates were identified in mosaic mortars of Austrian provenance [37], [103] – (see Section 6.3.1). Some of them contained a high amount of degraded linseed oil [37], [104]. Their composition corresponds to the recipe published by Gerspach [95] in 1880s [37].

Hungarian mosaicist Miksa Róth (1865-1944) also applied traditional lime-based mortars with angular carbonate aggregates (crushed marble or limestone) in his early 20th century Art Nouveau mosaics located at various places in Budapest [39]. In order to achieve the painterly effect of the whole composition, Róth added hematite pigment, not crushed bricks nor brick powder. Apart from this, Róth experimented with the

addition of tiny coloured glass splinters to his mosaic mortar beds, which gave the mortars a brighter and more glittering look [105].

Perná et. al. [106] identified a *cocciopesto* lime mortar containing ceramic shards on an early 20th century mosaic in Pfeiffer-Kral family sepulchre in Jablonec nad Nisou. According to the authors, the addition of crushed ceramics increased the mortar´s durability by adding hydraulic properties. However, hydraulic properties of the mortar have not been confirmed by later analysis [37].

Rohanová et al [35] analysed the samples of two art nouveau glass mosaic mortar beds by Viktor Foerster (1867-1915), the pioneer of Czech mosaic tradition. With the help of XRF, x-ray powder diffraction and SEM they found out, the mortars were of gypsum and gypsum-lime type which makes them easily attackable by rising capillary water. They also identified an interlayer at the interface between the glass and the fixation mortars caused by inter-diffusion of sodium and calcium cations.

The use of early Portland cement binder was proved in Viktor Foerster´s mosaics. He seems to have applied cement to fix his works from the very beginning of his mosaic career. In some cases he combined cement with crushed bricks and lime or gypsum. The aggregates in his mortars consisted mostly of silicates [36]. As Kürtösi [39] indicates, Roth´s mosaics from the Monument of the Fiume Road Cemetery, Budapest, were embedded in a mixture of early Portland cement and lime.

4.6 The 20th century – prefabrication and cement domination

In the 20th century Portland cement became the most frequent fixing material. Cement´s way to domination started in the 1900s. In the first two decades of the 20th century Portland cement competed with traditional fixing and bedding materials (see section 3.2.4). In the Czech Lands, the door to a wider application of novel cement binder seems to have been opened due to an increasing demand for mosaic decoration as well as an increasing awareness of new materials options among mosaic suppliers. The opening of the first local Czech studio run by mosaicist Viktor Foerster in 1903 or 1904 seems to have played a pioneering role not just in mosaic art history but also from the materials point of view [36]. Interestingly, Foerster seems to have started with traditional lime + linseed oil fixing mortars – such a material was identified at his Our Lady of the Rosary mosaic in České Budějovice [107], [108], whose assembly commenced in 1903 making it one of the first, if not the very first Foerter´s completed mosaic works in the Czech Lands [109]. Other exterior mosaics, including ornaments and signs at Our Lady of Sorrows chapel in Prague completed in 1903, were fixed by cementitious mortars [36], Section 6.3.2).

There is an archival evidence on the use of Portland cement by Foerster´s wife Marie [110] who continued her husband´s commissions after his untimely death. In 1929, she assembled a 40 m^2 large mosaic vault in the crypt of Slavín, Vyšehrad Cemetery, Prague. We can read in the preserved invoices issued by Schlafer a Nový building company (Fig. 9), their workers applied 2 cm thick bedding mortar made of cement,

finely crushed bricks, “white dust” and “black dust” [110]. We have not been able to figure out undoubtedly, what the chemical nature of white or black dust was. However, based on the recipes for artificial stone in early 20th century literature [111], we assume “white dust” represents marble dust and “black dust” might be slag, as the author of the book recommends using best of all “black glossy Příbram dust”. In the vicinity of Příbram, a town located 60 km SW from Prague, large pyrometallurgical slag dumps (1.8 Mt) were deposited in 18th – 20th century during industrial silver-lead mining and processing. Local slag was used as a building material [112].

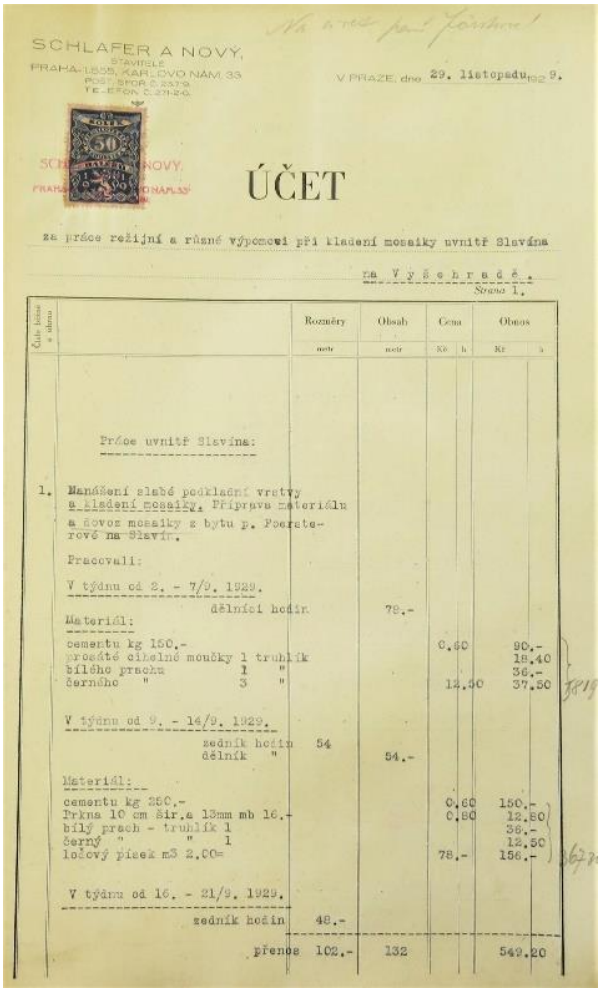

SCHLAFER A NOVY,
STAVITELÉ
PRAHA-ÚSTŘ.-KARLOVO NÁM. 33
POŠT. SPOR. Č. 2379.
TELEFON Č. 271-20.

V PRAZE, dne 29. listopadu 1929.

ÚČET

za práce režijní a různé výpomoci při kladení mosaiky uvnitř Slavína

na Vyšehradě.

Strana 1.

Číslo řádku a účtu		Rozměry	Obsah	Cena	Obnos
		metr	metr	Kč h	Kč h
	Práce uvnitř Slavína:				
1.	Manášení slabé podkladní vrstvy a kladení mosaiky. Příprava materiálu a dovoz mosaiky z bytu p. Foersterové na Slavín.				
	Pracovali:				
	V týdnu od 2. - 7/9. 1929.				
	dělnící hodin		78.-		
	Materiál:				
	cementu kg 150.-			0.60	90.-
	prosáté cihelné moučky 1 truhlík				18.40
	bílého prachu 1 "				36.-
	černého " 3 "			12.50	37.50
	V týdnu od 9. - 14/9. 1929.				
	zedník hodin 54				
	dělník "		54.-		
	Materiál:				
	cementu kg 250.-			0.60	150.-
	Prkna 10 cm Šir.a 13mm mb 16.-			0.80	12.80
	bílý prach - truhlík 1				36.-
	černý " 1				12.50
	ložový písek m3 2.00=			78.-	156.-
	V týdnu od 16. - 21/9. 1929.				
	zedník hodin	48.-			
	přenos	102.-	132		549.20

Figure 9. Invoice issued by Schlafer a Nový building company including a list of materials provided for the installation of a vault mosaic by Marie V. Foersterová in the crypt of Slavín, Vyšehrad Cemetery.

The use of early Portland cement has also been reported from the mosaic decoration in the Dittrich crypt in Krásná Lípa, Northern Bohemia [107]. Samples from this site were also analysed within this study (see Section 6.3.3) and the presence of Portland cement was confirmed. To our knowledge no other materials research has been published on mosaic mortars from the 1st half of the 20th century. However, Portland cement is supposed to take over the leading role among mosaic mortar binders in other countries too.

Due to the reasons briefly mentioned in an introduction to Section 4, many new monumental mosaic works appeared in socialistic countries in the latter half of the 20th

century. In Czechoslovakia, almost no private art and craft studios existed. Most of the mosaic installations of the time were made by state-run mosaic workshops. The largest mosaic studio existed within the so-called Central Art and Craft Studio (Ústředí uměleckých řemesel - ÚÚŘ) [113]. The company developed standardized techniques of mosaic installations over time (they differed according to the type and size of the planned mosaic). These techniques were summarized in the textbook [49] written by long-term employees of the ÚÚŘ mosaic workshop.

Indirect method of setting seems to have been applied less frequently than in previous periods. Mosaics were mostly fixed to concrete slabs *alla prima* (e.g. directly on the final support) with a cement-based mortar. This work could have taken place either *in situ*, i.e. on the site where the mosaic would be situated, or in a studio [49].

The slabs usually consisted of steel grating on which Rabitz wire mesh was laid (Fig. 10). This system was either welded to an L-profile steel frame or left unframed. If unframed, slabs were casted in removable steel moulds. The space was filled with a fine-grained concrete [38], [49].

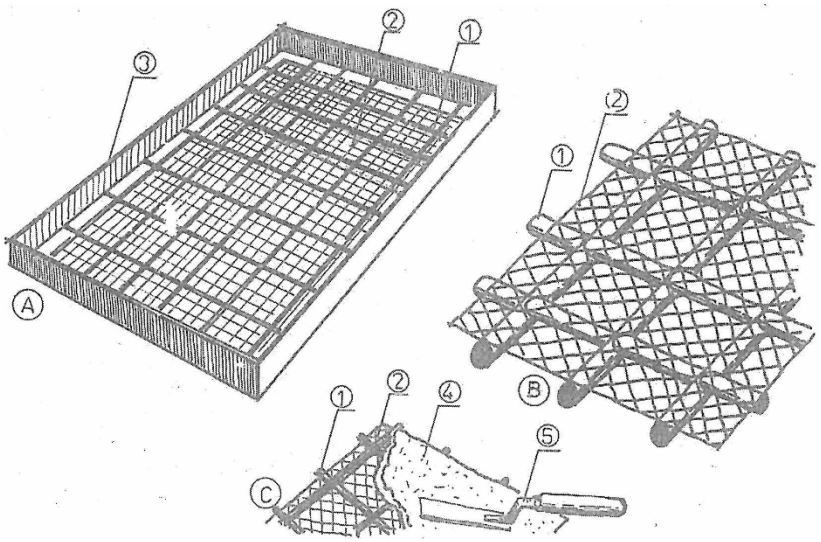

Figure 10. Schematic drawing of mosaic slab system. A: 1 – steel grating welded to the structure, 2 – Rabitz wire mesh, 3 – steel angle frame; B – frameless slab: 1 – steel grating, 2 – Rabitz wire mess; C: 1 – steel grating, 2 – Rabitz wire mesh, 3 – mortar, 4 – spatula. **[49]**

Prior to the assembly several cartoons (i. e. sketches) of the mosaic motif had been prepared including sketches in 1:1 scale. The motif was subsequently divided into sections corresponding to the size of the slabs. These sections were transferred on the slab surface and an underdrawing was drawn with an ink or latex paint [49]. Finally, mosaic tesserae (glass or stone cubes) or irregular stones were fixed with a cement mortar (Fig. 11a) [38].

Tesař and Klouda [49] state: *"The binding mortar for mosaic assembly consist approximately of two parts of cement 250-300* (strength class – older classification) *and one part of sieved river sand. A small amount of Acronex (ratio 1:10 – one part of Acronex and 10 parts of water) is mixed with the mortar to provide better binding characteristics and smooth hardening. Acronex is a water-based latex suspension. […]*

It is added to renders and mortars in order to avoid irregular hardening or powdering of the materials." ([49], p. 91)

Akronex "latex" suspension (i.e. water dispersion of synthetic polymers) was a commercial product based on water-dispersed poly vinyl acetate (PVAc). Besides PVAc, Akronex water dispersions contained dibutyl phthalate as a softener [38] [114].

After the completion mosaic blocks made in the studio were transported to the site and anchored to bricked walls of the façade (Fig. 11b). The space in between the slabs had to be filled with *tesserae in situ*.

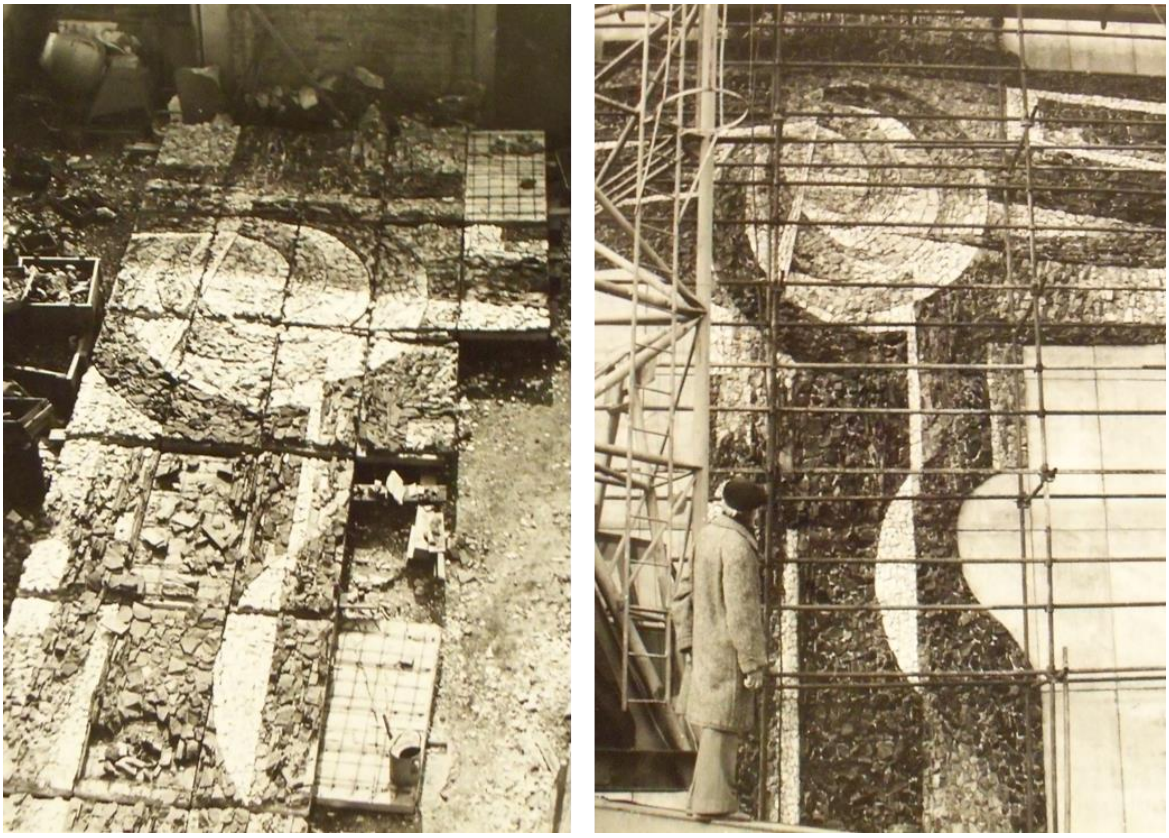

a) b)

Figure 11. Assembly of the mosaic "Architects´s Reason and Sense" by Martin Sladký. *Alla prima* tesserae laying on frameless slabs in a mosaic studio (a); installation of the slabs on the façade of the Faculty of Civil Engineering. CTU supervised by the author (b). Courtesy of Martin Sladký, Jr. Previously published in **[38]**.

As the final step of mosaic completion, Tesař and Klouda [49] recommend impregnating a mosaic´s surface with a solution of a "methyl silicone varnish" in order to protect the work from weather oscillations and reduce its water permeability.

This is in agreement with the memories of an ex-employee of ÚÚŘ who participated in the installation of Sladký´s ČVUT mosaic. He remembers impregnating the mosaic with a product called Lukofob which "smelled like mineral oil" [115]. The product is still available on the market and used for the waterproofing of stones and concrete. Its classic version consists of a silicone resin and organics solvents (mineral oil derivates, xylen) [38].

Koch and Galstyan [116] describe the most common way of mosaics´ assembly in former Soviet Union. It differs from the Czechoslovak procedure. It is in fact based on indirect method of setting. The original-sized mosaic motif was divided into square sections which were drawn on a paper. Such cartoon was populated with the tesserae and placed in a mould subsequently filled with concrete. The hardened mosaic slabs were then transported to the site and either installed on a wall or built in as load-bearing slabs [116].

Indirect method of setting was also frequently applied in the production of pressed glass mosaics in Czechoslovakia, a technique associated with *Železnobrodské sklo* state company [71], [98]. The tesserae were first glued to a temporary sulphate paper support, transferred to a site and fixed into a cement bed [98]. As the final step, the mosaic was grouted [71].

4.6.1 Alternative methods of mosaic fixation

Since 1950s mosaicists searched for innovative ways to fix their artworks. Some mosaics were set into an epoxy resin bed – namely a famous mosaic fountain by *Dana Hlobilová* awarded a medal at EXPO 1958 [104], mosaic image of a Barricader by *Arnošt Paderlík* or circular mosaic slabs from a former rock lift in Děčín [117]. However, the adhesion of tesserae to the resin bed does not show a long-term durability due to the deterioration of the resin. Restoration treatment of such works usually involves total transfer of mosaic cubes to substitutional supports [118], [104].

Czechoslovak company *Železnobrodské sklo* came up with many innovative elements in mosaic production, including the invention of prefabricated rectilinearly pressed glass mosaic cubes in the 1950s, which were originally laid into a cement mortar bed [71]. Since the latter half of the 1960s they were fixed on glass, mirror plates and later to polished aluminum sheets (Kučerová, 2023). In the latter half of the 20th century, mosaicist *Eliška Rožátová* (1940) invented a new method of fixation – tesserae adhered to the support thanks to a polyvinyl butyral foil which had been placed in between glass or aluminum sheet and mosaic cubes. After assembly, the mosaic was heated up to 200 °C which led to the fixation of cubes due to the foil´s melting. Subsequently, the mosaic was grouted [98]. An acrylate-modified cement mastic or the Bakol tile glue based on acrylic dispersion were used for grouting (Kučerová, 2023).

Despite the experiments with organic resins and special foils in the latter half of the 20th century, the domination of cement continues to this day. More traditional binders such as hydraulic lime are applied in restoration works. A common way of restoration is to transfer loose mosaics onto portable honeycomb slabs [119], [120].

5 BRIEF HISTORY OF MOSAIC ART IN THE CZECH LANDS

5.1 The rising of mosaic art in the Czech Lands (1880s – 1918)

In the Czech Lands mosaics have widely been used in architecture since as late as late 19th century. The only medieval mosaic situated at St. Vitus Cathedral in Prague (Fig. 7) dates back to 1370s. It represents a unique solitaire [104] followed by several centuries lasting "mosaic dark period" [121]. The mosaic depicting the Last Judgement was commissioned by Emperor Charles IV after the return from his second journey to Rome made on the occasion of crowning his wife Elisabeth of Pomerania roman empress. The imperial couple was portrayed praying in the lower "earthy" sphere of the mosaic.

Almost since its installation the mosaic tesserae faced severe corrosion due to less resistant composition of the glass which was produced locally. Local Bohemian glass-makers used potassium glass instead of more durable sodium material [113].

It was just the Last Judgement mosaic´s poor state and an urgent call for its restoration in late 1870s that resulted in an increasing interest in mosaic technique and its application in the decoration of Czech contemporary architecture [100]. At that time there was no local mosaic studio and so the conservation treatment of the dilapidated mosaic had to be discussed with foreign experts from Italy and Austria. One of them was *Luigi Solerti* (1846-1902), an art director of an Austrian mosaic workshop from Tyrol named after its owner *Albert Neuhauser* (1832-1901). This consultancy as well as the company´s presentation at the Art Exhibition in Prague in 1879 [100] probably opened Neuhauser the door to mosaic commissions in Bohemia and Moravia (present-day Czech Republic). The company supplied both large-scale façade mosaics as well as smaller works such as mosaic decorations of sepulchres. At the turn of the 19th and 20th century the company occupied a significant position in the Bohemian mosaic market due to its collaboration with outstanding Czech architects *Antonín Barvitius* (1823 – 1901) and most importantly *Osvald Polívka* (1859 – 1931) who made mosaics an integral part of his structures. The mosaic motifs were designed by famous Czech artists (Mikoláš Aleš, Jan Preisler, Karel Špillar etc.) but the actual mosaic work was carried out by Austrian mosaicists. The most famous installations can be found for example on the Municipal House (Fig.12) and UOváků commercial centre in Prague material [113].

Neuhauser´s history started in Wilten near Innsbruck in 1877 when Albert Neuhauser (1832 – 1901) founded the first mosaic studio in Austria – *Die Mosaikwerkstätte Albert Neuhausers* (Albert Neuhauser´s Mosaic Workshop) [122]. One of the leading mosaicists working for the company at that time was *Josef Pfefferle the elder* (1862 - 1939) who had been employed there since the workshop´s foundation. In 1900 the mosaic workshop merged with a stain-glass producing company Tiroler Glasmalerei to form a new, still existing workshop called *Tiroler Glasmalerei- und Mosaikanstalt* [123].

In the same year Josef Pfefferle established his own mosaic workshop in Zirl close to Innsbruck. Pfefferle´s studio operated mostly in Tirol [122].

Figure 12. Mosaic “Apotheosis of Prague” on the façade of Prague´s Municipal House.

Neuhauser´s twenty-year lasting monopoly on mosaic supplies to the Czech Lands was broken at the turn of the 19th and 20th centuries. Apart from new local studios, Neuhauser had to face increasing competition from other foreign companies – namely Berlin-based *Puhl & Wagner*, Neuhauser´s ex-employee Luigi Solerti´s *Königlich Bayerischen Mosaik-Hofkunstanstalt* from Munich and Austrian workshop *Wiener Werkstätte* represented by designer Leopold Forstner above all [99], [124].

In the first years of the 20th century mosaicist *Viktor Foerster* (1867 – 1915) established the first local Czech mosaic studio. The circumstances and a precise date of the workshop´s foundation still have not been satisfactorily cleared up. What is for sure, he participated in the design of Our Lady of the Rosary mosaic together with his friend Pantaleon Major as early as 1902 [125], [126]. Foerster designed and assembled about 35 mosaic works (Štorkánová, Hemelík, 2017) – mostly spiritual themes commissioned by church institutions (e.g. Our Lady of the Rosary in České Budějovice (Fig. 13), mosaics for the Emauzy monastery in Nové Město, Prague, mosaic on the façade of Mary of the Snows Church in the same location, Czech patron saints on the façade of St. Bartholomew church in Pardubice, Virgin Mary on the façade of the basilica in Svatý Hostýn etc.). Apart from larger religious commissions, Foerster is the author of numerous sepulchral mosaics [125]. His mosaics decorate also profane buildings such as the façade of the present-day Evropa hotel in Prague or mosaic portals of hotel Paris, Prague, or Česká spořitelna bank in Nový Bydžov. Recently, several publications have been dedicated to the activities of this “first Czech mosaicist” [125]–[127]. All Foerster´s works are listed in Kracík Štorkánová and Hemelík´s monography [128]. The

mortars of some Foerster´s mosaics were studied within this project ([36], Section 6.3.2).

Figure 13. Main part of the mosaic on the façade of Our Lady of the Rosary Church in České Budějovice. Designed by Viktor Foerster and Pantaleon Major.

After his untimely death, Foerster´s studio was taken over by his wife *Marie Viktorie Foersterová* (1867 – 1952) who received mosaic commissions for example for St. Vitus Cathedral, orthodox church in Olšany Cemetery, Fénix palace in Prague (Fig. 14) or for a unique vault mosaic decorating the crypt of Slavín at Vyšehrad Cemetery [128].

Besides Foersters, several minor mosaic workshops existed in Moravia. The most important of them was Brno-based company *Škarda* which produced mosaics mostly of flat stained glass [129].

The first Czech Art Nouveau ceramic mosaics are associated with artist *Jano Koehler* (1873-1941). They were designed in a close collaboration with the RAKO tile manufacturing company which developed a unique technique of ceramic cut mosaic [130].

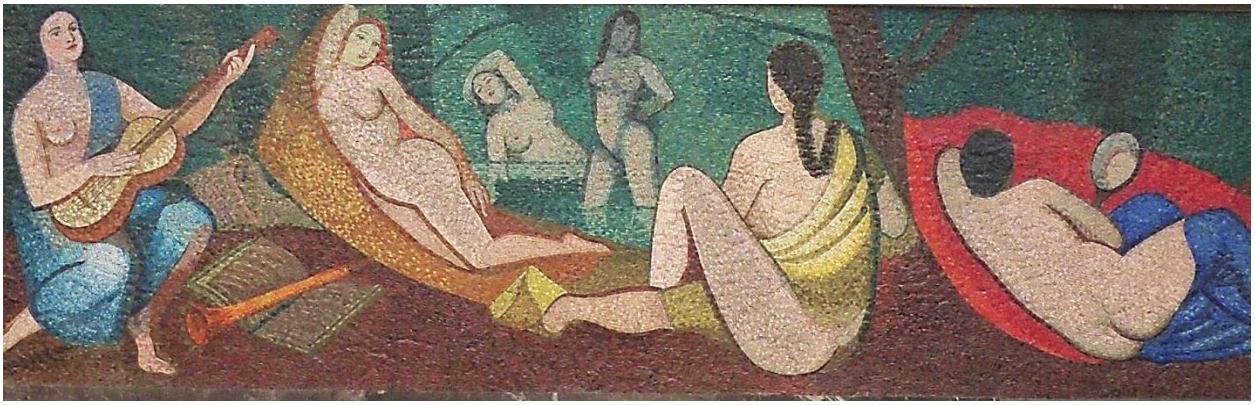

Figure 14. Bathing women. A detail of a mosaic belt installed in the passage way of Fénix Palace, Wenceslas Square, Prague. The mosaic lais by M. Foersterová, the motif designed by painter Rudolf Kremlička.

5.2 Mosaics in inter-war Czechoslovakia (1918-1938)

In inter-war Czechoslovakia, mosaic received reputation as a specific art medium. It had become an essential part of the First Republic (time period 1918-1938) decorative style (Vicherková and Kracík Štorkánová, 2017). Thanks to *Jan Tumpach´s mosaic workshop* Czechoslovakia ranked among three countries in the world producing local mosaic glass (*smalti*). Their production commenced in 1931 [131]. Besides the workshop´s founder *Jan Tumpach* (1883-1937), glass specialist *Michail Ajvaz* (1904-1994) must be given credits for the invention of Czech smalti. Despite initial issues, Ajvaz soon developed around 3500 shades of mosaic glass [131]. Tumpach´s studio gained prestigious mosaic commissions at St. Vitus Cathedral at the Prague Castle, in the Old Town Hall in Prague or in the National Liberation Memorial on the Vítkov hill [131].

Figure 15. Shepherd by Josef Novák. The first modern stone mosaic in Czechoslovakia awarded by gold medal at World exhibition in Paris in 1937. Private property of Novák´s son.

Besides Tumpach and Marie Foersterová (introduced in the previous section), other personalities contributed to the development of mosaic art in the pre-war period – namely painter *Max Švabinský* (1873-1962), teacher and designer *Oldřich Žák* (1900-1983) or mosaicists *Stanislav Ulman* (1898-1982) and *Josef Novák* (1902-1987), the author of the first stone mosaic in Czechoslovakia [132] – Fig. 15.

5.3 Mosaics under socialism (1948 – 1989)

The latter half of the 20th century can be called the heyday of Czechoslovak mosaic art even though it is just this period that caused the negative connotation of mosaic art as the tool of communist propaganda. As Vicherková and Kracík Štorkánová remark, monumental art performed in high-quality and long-term materials was a preferred manifestation of socialist culture which was meant to last eternally [113]. Mosaics frequently appeared both on the facades and in interiors of newly constructed buildings. Smaller inter-war and early post-war studios were nationalized and in 1954 united into a central mosaic workshop incorporated into *Ústředí uměleckých řemesel* (ÚUŘ - Central Art and Craft Studio) which received by far the most of mosaic commissions of that time. Notably in the 1950s, some mosaics reflected the change of the political regime both thematically (adoration of folk, workers or straightforward communist symbols) and technically (socialist realism style). However, despite strict state control over art and active censorship, mosaic art differentiated in many styles and forms. The 1960s brought new trends both to topic (less straightforward ideology, more abstract subjects), form (abstraction) and materials (more frequent use of unprocessed stone and ceramics due to lower costs, newly developed prefabricated pressed and sintered glass). Mosaics were assembled in numerous public buildings all over the country – railway stations, schools, factories etc. The most prestigious set of mosaics was installed in Prague metro.

In 1970 – 1993 (company´s collapse), ÚUŘ mosaic workshop assembled over 300 works all over Czechoslovakia and also abroad [113]. To mention only few personalities of this era´s mosaic art, let´s name *Vladimír Sychra* (1903-1963), *Josef Kaplický* (1899-1962), *Martin Sladký* (1920-2015), *Radomír Kolář* (1924-1993) and *Sauro Ballardini* (1925-2010). Sychra participated at the post-war mosaic reinterpretation of the National Liberation Memorial on the Vítkov hill [113] and created a mosaic at Ležáky memorial site. Kaplický´s mosaics represented Czech glass art at the EXPO 1958 exhibition in Brussels, winning a gold medal [99]. Kolář is the author of large-scale stone mosaic in former Officers´House in Milovice, glass mosaic slabs at Vlasta housing estate in Vršovice (Fig. 16), Prague and a stone mosaic depicting Charles IV and his achievements at Karlovo náměstí metro station, Prague. The most attention has recently been paid to works of Martin Sladký, the author of three mosaics of Prague metro (two abstract mosaics at Dejvická station and one figurative at Staroměstská station, now covered by a plasterboard wall) [132] and Sauro Ballardini [133] whose masterpiece “Mankind Conquering the New Space Horizons” was saved from destruction three years ago [134]. Ballardini stood outside the ÚUŘ workshop, he

created his mosaics in his studio at the Academy of Fine Arts [134]. A 14-metres long “Battle of Sokolovo” mosaic situated at Florenc metro station, which Ballardini made with his colleague Oldřich Oplt, was also assembled at the Academy.

Figure 16. ZOO (Radomír Kolář, 1980). A detail of an exterior mosaic decoration of Vlasta housing project, Prague – Vršovice.

An innovative role of Železnobrodské sklo state company in the development of Czech mosaic glass and fixing techniques was briefly discussed in section 4.6. The company´s fruitful mosaic workshop performed hundreds of mosaic works and employed numerous artists including *Eliška Rožátová* (1940), who played a crucial part in the company´s innovative achievements [99]. Rožátová soon became an independent artist [99] but continued to make prefabricated glass mosaics fixed to metal support by melted polyvinyl butyral foils.

5.4 After 1989

After 1989 (the fall of socialism) mosaics lost their position of a privileged art medium. The system of state mosaic commissions collapsed. The ÚUŘ mosaic workshop ceased to exist as a result of privatisation in 1993. Yet, several new mosaic realisations appeared in the public space. Political change brought the revival of religious and sepulchral mosaics which had been shadowed by profane mainstream in the previous era. Religious themes are reflected in the mosaics by *Antonín Klouda*, *Petr Štěpán* or *Jiří Šťasta* [99]. Profane glass mosaics are represented by municipal coats of arms (made by *Jiří Louda* and *Jiří Libinský* in Havířov or by *Eva and Svatopluk Kasalí* in Panenská Rozsíčka). *Free Mosaic* art group (Tereza Podová and Jan Pancíř) assembled a series of ceramic mosaics in Vršovice district, Prague in the last decade [135]. In 2022 a set of public mosaic benches was installed at several public places in

the village of Únětice (Fig. 17) within an international mosaic symposium organized by *Magdalena Kracík Štorkánová* [136]. This artist also founded the mosaic association Art & Craft Mozaika, aimed at the promotion and rescue of mosaics [137], and organized exhibitions of contemporary mosaic art [121], [138].

Last decade brought an increasing interest of restorers and art historians in modern mosaics. Mosaics produced in Tyrolean workshops have been mapped within an Austrian-Czech Mosaic Connection project [139]. Special attention of both domestic and foreign enthusiasts and experts has been drawn to “socialist” art [140]–[145].

In the Czech Republic, a detailed on-line map and database of exterior glass mosaics [146] and a comprehensive book dedicated to Czech glass mosaic [147] represent the most remarkable results of several recent research projects [148], [149].

Figure 17. Mosaic benches located in different public places in the village of Únětice. They were made during an international mosaic symposium in 2022.

6 CHARACTERISATION OF AUTHENTIC MOSAIC MORTARS

6.1 Samples

Authentic mosaic mortar samples were provided by restorers. Their collection was usually associated with an intended or already performed restoration of a particular mosaic. Mortars from 26 historic mosaic works dating back to late 19th and early 20th century were investigated within this study. These mosaics represent minute mosaic decoration of sepulchres as well as large-scale mosaics situated on the facades of public architectural objects (both profane and sacral). A brief history of the artworks as well as their description and photodocumentation can be found in a separated "catalogue" attached to this work (Appendix 1). Investigated samples and a summary of analytical tools used for their characterization are listed in Tab. 3.

The studied mosaics cover one-hundred-year period from 1880s to 1980s. They can be divided into four groups according to their provenance and time of their origin. The first group includes mosaics produced or ascribed to Tirolean mosaic workshops, namely the studios of Albert Neuhauser and his former employee Josef Pfefferle who later founded his own mosaic workshop. Neuhauser´s company known since 1900 as Tiroler Glasmalerei- und Mosaikanstalt (see Section) had been supplying mosaics to the Czech Lands for approximately 40 years, our samples come from 1880s and the turn of the 19th/ 20th century. Pfefferle operated mostly in his homeland Tirol but the samples of his mosaic fixing mortars were included in this study as an interesting comparative material.

Other samples come from five mosaics designed by the first Czech mosaicist Viktor Foerster (early 20th century). One studied mosaic (Slavín) was made by his wife Marie Foersterová over a decade after his death.

The third group of samples comes from mosaics dating back to early 20th century whose provenance remained under question at the start of this PhD. project but recently one of the mosaics (Dittrich sepulchre in Krásná Lípa) has been undoubtedly ascribed to German Puhl&Wagner company [150] and one (Pfeiffer-Kral) to Solerti´s Munich-based Königlich Bayerische Mosaik- Hofkunstanstalt [124], [151]. Mortar beds from the 1950s-1980s mosaics fall into the last group of samples. Besides four works designed by renowned mosaic authors of that era, a unique mosaic statue by sculptor Eva Kmentová (1928-1980) was analysed. A material from her husband Olbram Zoubek´s (1926-1917) statue was taken as a reference sample. Zoubek is known for the use of asbestos cement in his works [152].

Table 3. List of investigated mosaic samples, their brief visual description and methods applied in their study. ÚUŘ – Ústředí uměleckých řemesel (Central Art and Craft Studio); SEM-EDS – scanning electron microscopy, PM – polarising microscopy, LM – reflected light microscopy, TG – thermal analysis, XRD – powder x-ray diffraction, FTIR – infrared spectroscopy, GC-MS – gas chromatography, HCl – dissolution in HCl, TOC – total organic carbon assesment. Dashed lines separate provenance or period groups. * - the method was employed.

sample label	mosaic	location	date	author/ workshop	description	SEM-EDS	PM	LM	TG	XRD	FTIR	GC-MS	HCl	TOC
PB1702 Sladkovský	Greek cross surrounded by laurel twigs	Karel Sladkovský´s sepulchre; Olšany Cemetery, Prague	1884	Albert Neuhauser	fine-grained beige mortar bed, sweety smell	*		*	*	*	*	*	*	*
PB1704 Bittnerová	Mosaic torzo, illegible motif	Marie Bittnerová´s sepulchre; Olšany Cemetery, Prague	1899	Tiroler Glassmalerei- und Mosaikanstalt	corroded mortar bed, powdery texture, beige colour, dark corrosion crust on the surface	*		*	*	*	*	*		
PB1706 Beneš	Plant wreath	Beneš family sepulchre; Olšany Cemetery, Prague	1890s	Albert Neuhauser	fine-grained beige mortar bed, sweety smell	*		*	*	*	*	*	*	*
PB1707 Peluněk	Resurrected Christ	Peluněk family sepulchre; Malvazinky Cemetery, Prague	late 19th cent.	Tiroler Glassmalerei- und Mosaikanstalt	fine-grained beige mortar bed, sweety smell	*		*	*	*	*	*	*	*
PB2003 Mašek	Christ with a lamb	František Mašek´s sepulchre; Olšany Cemetery, Prague	1890s	Albert Neuhauser	beige fine-grained mortar, corroded	*		*	*	*	*	*		
PB2106 Pfannerer	Mosaic torzo, illegible motif, tesserae imprints in the mortar	canon Pfannerer´s sepulchre, upper gable; Olšany Cemetery, Prague	late 19th cent.?	Albert Neuhauser (?)	pinkish mortar with a black corrosion layer	*		*	*	*	*			

Table 3. List of investigated mosaic samples, their brief visual description and methods applied in their study. ÚUŘ – Ústředí uměleckých řemesel (Central Art and Craft Studio); SEM-EDS – scanning electron microscopy, PM – polarising microscopy, LM – reflected light microscopy, TG – thermal analysis, XRD – powder x-ray diffraction, FTIR – infrared spectroscopy, GC-MS – gas chromatography, HCl – dissolution in HCl, TOC – total organic carbon assesment. Dashed lines separate provenance or period groups. * - the method was employed.

sample label	mosaic	location	date	author/ workshop	description	SEM-EDS	PM	LM	TG	XRD	FTIR	GC-MS	HCl	TOC
PB2204 Krip	Getzner coat of arms	townhall facade; Hall, Austria	1897	Albert Neuhauser	double layer – beige fine-grained mortar bed with a thin coarser underneath plaster	*		*						
PB2205 Getzner	Krip coat of arms	townhall facade; Hall, Austria	1897	Albert Neuhauser	white-grey fine-grained mortar bed	*		*	*	*	*			
PB1709 Reith	Madonna with a Child	roofed outdoor staircase, cemetery; Reith bei Seefeld, Austria	before 1906	Josef Pfefferle	white fine-grained mortar bed, at the bottom corroded from the enclosing iron frame	*		*	*	*	*		*	
PB2206 Oberhofen	St. Michael the Archangel	church facade; Oberhofen, Austria	1903/1904	Josef Pfefferle	white-grey mortar bed	*		*	*	*	*			
PB2207 Hopfgarten	Madonna with a Child	chruch facade; Hopfgarten, Austria	1905	Tiroler Glassmalerei- und Mosaikanstalt	whitish-grey mortar bed	*		*	*	*	*			
PB1705 Lauschmann	Wall decor and medallion with Christ	Lauschmann family sepulchre, Vyšehrad Cemetery, Prague	1908	Viktor Foerster	pinkish mortar bed with visible brick shards	*		*	*	*				*

Table 3. List of investigated mosaic samples, their brief visual description and methods applied in their study. ÚUŘ – Ústředí uměleckých řemesel (Central Art and Craft Studio); SEM-EDS – scanning electron microscopy, PM – polarising microscopy, LM – reflected light microscopy, TG – thermal analysis, XRD – powder x-ray diffraction, FTIR – infrared spectroscopy, GC-MS – gas chromatography, HCl – dissolution in HCl, TOC – total organic carbon assesment. Dashed lines separate provenance or period groups. * - the method was employed.

sample label	mosaic	location	date	author/ workshop	description	SEM-EDS	PM	LM	TG	XRD	FTIR	GC-MS	HCl	TOC
PB1802 Dolín-portal	Ornamental belt	mosaic border of the portal; St. Simon and Juda church, Dolín (near Slaný)	1908	Viktor Foerster	pinkish mortar bed with visible brick shards and lumps, from the portal	*		*	*	*				
PB1802-2 Dolín-Crist	Christ the Good Shepherd	gable above the portal, St. Simon and St. Jude Church, Dolín (near Slaný)	1908	Viktor Foerster	bedding mortar from the mosaic,seems identical to the bed of portal mosaic border	*	*	*		*	*			
PB1902 Pelhřimov	Mascron	mosaic panel originally exposed at Pelhřimov Cemetery, now stored in The Highlands Museum, Pelhřimov	1906	Viktor Foerster	grey cement taken from the corner of the mosaic panel, possible contamination by rust from the enclosing metal frame	*		*	*	*				
PB1903 Evropa hotel	Sign and plant ornament on a blue background	Evropa hotel, gable; Wenceslas Square, Prague	1905	Viktor Foerster	mortar bed, greyish	*	*	*	*	*				
PB1904 Barrandov	Sign and Christian symbols	Virgin Marry of the Sorrows Chapel, gable; Prague - Hlubočepy (under Barrand Rock)	1903	Viktor Foerster	grey mortar bed near A letter from the inscription on the lower mosaic belt	*	*	*	*	*				
PB2007 Slavín	Ornamental decor (reminiscence of Starry Sky)	Vault of the Slavín crypt; Vyšehrad Cemetery, Prague	1929	Marie Foersterová	greyish fine-grained mortar bed from the back side of the crypt	*		*						

Table 3. List of investigated mosaic samples, their brief visual description and methods applied in their study. ÚUŘ – Ústředí uměleckých řemesel (Central Art and Craft Studio); SEM-EDS – scanning electron microscopy, PM – polarising microscopy, LM – reflected light microscopy, TG – thermal analysis, XRD – powder x-ray diffraction, FTIR – infrared spectroscopy, GC-MS – gas chromatography, HCl – dissolution in HCl, TOC – total organic carbon assesment. Dashed lines separate provenance or period groups. * - the method was employed.

sample label	mosaic	location	date	author/ workshop	description	SEM-EDS	PM	LM	TG	XRD	FTIR	GC-MS	HCl	TOC
PB1708 Pfeiffer-Kral	Plant ornament	Pfeiffer-Kral Family Sepulcher; Jablonec nad Nisou	1902	Königlich Bayerischen Mosaik-Hofkunstanstalt	white-pinkish mortar bed with visible brick shards	*		*	*	*	*		*	
PB1803 Dittrich	Golden decor and medallions on the crypt´s vault	Dittrich Family Sepulcher; Krásná Lípa	1920	Pull&Wagner	a) fine-grained mortar bed, b) coarser underlying plaster ("arriccio")	*	*	*	*	*	*			
PB2005 Liberec	Holy Family	mosaic panel; stored in Liberec Museum, Liberec	1910?	?	dark grey fine-grained mortar bed, small amount			*		*				
PB2108 Schicht	Golden decor	Schicht Family Sepulcher; Ústí nad Labem	around 1912	?	dark grey mortar bed, fine-grained	*	*	*		*				
PB1901 Ballardini	Mankind Conquering New Space Horizons	large panel in the former Central Telecommunication Building; Prague; now transferred (saved from demollition)	1980	Sauro Ballardini/ AVU	two layers – a) grey cementitious mortar bed; b) coarser grey concrete of the panel support	*		*	*	*				
PB2006 Sladký	Architect´s Reason and Sense	Faculty of Civil Engineering, CTU facade; Prague	1977	Martin Sladký/ ÚUŘ	greyish mortar; samples from the central and upper part of the mosaic	*		*	*	*	*	*		

Table 3. List of investigated mosaic samples, their brief visual description and methods applied in their study. ÚUŘ – Ústředí uměleckých řemesel (Central Art and Craft Studio); SEM-EDS – scanning electron microscopy, PM – polarising microscopy, LM – reflected light microscopy, TG – thermal analysis, XRD – powder x-ray diffraction, FTIR – infrared spectroscopy, GC-MS – gas chromatography, HCl – dissolution in HCl, TOC – total organic carbon assesment. Dashed lines separate provenance or period groups. * - the method was employed.

sample label	mosaic	location	date	author/ workshop	description	SEM-EDS	PM	LM	TG	XRD	FTIR	GC-MS	HCl	TOC
PB2009 Pardubice	Map of Czechoslovakia	Pardubice Train Station hall, eastern wall; Pardubice	1957	Richard Lander, Česká mosaika/ ÚUŘ	dark corroded mortar bed released from the mosaic	*	*	*		*				
PB2103 Milovice	Fighting Friendship with Soviet Troops	entrance hall, former Soviet Officers´ House (now museum), Milovice	1980-1982	Radomír Kolář	grey mortar bed from the central lower part of the mosaic	*		*	*	*				
PB2201 Kmentová	Listening Woman	mosaic statue	1957	Eva Kmentová	1 – grey fine concrete statue´s body with asbestos fibres; 2 – corroded body; 3- grey mortar bed (two layers)	*		*	*	*				
PB2202 Zoubek	Figure	concrete statue	1990s	Olbram Zoubek	fine grey concrete containing asbestos, used as reference material to PB2201	*		*	*					

6.2 Methods

A multianalytical approach, generally recommended for the analysis of historic mortars [153], [154], was applied to characterise authentic mosaic mortar samples. However, not all the samples were studied by a complete set of methods employed. The key methods were scanning electron microscopy, thermal analysis and x-ray powder diffraction.

6.2.1 SEM-EDS

Scanning electron microscopy – energy dispersive X-ray spectroscopy (SEM-EDS) was employed to study the mortar´s microstructure and chemical composition. SEM-EDS characterisation was performed using a MIRA II LMU SEM microscope (Tescan corp., Brno) equipped with an energy dispersive x-ray detector (Bruker corp., Berlin). Mortar samples were embedded in an acrylic resin and polished. Polished sections were carbon-coated prior to analysis to ensure specimen surface conductivity. Elemental analysis was performed at 15 kV accelerating voltage and 15 mm working distance. Applying the methodology of Frankeová [11], the binders´ chemical composition presented in this work was calculated as an average of at least 5 measurements in various representative parts (showing minimum deterioration or carbonation) of cross-sections studied. EDS spectra were mostly collected from areas of 150 x 150 µm.

6.2.2 Light microscopy (LM)

Mortars´ microstructure was observed in an Olympus BX53M reflected light microscope both in the bright field and dark field mode. The same polished sections as for SEM-EDS (without carbon coating) were used. The device is a property of the Institute of Physics, CAS.

6.2.3 Polarised light microscopy (PLM)

Polarised light microscopy is a very useful tool to get a closer insight into a mortar´s microstructure. It makes it possible to determine mineralogical phases present both in the aggregates and the binder, the nature of the binder and the degree of its carbonation. As the light transmits through a sample, mortar specimens have to be embedded in an acrylic resin, fixed onto a microscopic glass and subsequently ground and polished to a maximum of 30 µm thick thin sections. The thin sections of selected samples (Tab. 3) were prepared in Geological Laboratories of the Faculty of Science, Masaryk University in Brno. Microscopic observation was performed in collaboration with dr. Farkas Pintér at the University of Applied Arts in Vienna, Austria. A Nikon stereomicroscope was employed for overall observations, while detailed analyses were done in a polarised light microscope (Olympus BX-40) in plane- and cross-polarised light.

6.2.4 Thermal analysis coupled with EGA mass spectroscopy

Thermogravimetry/ differential thermogravimetry coupled with evolved gas analysis – mass spectroscopy (TG/DTG-EGA) makes it possible to identify the composition of mortars and to determine the nature of their binders. The mass-spectroscopic analysis provides information on gases evolved at various temperatures from a heated sample. This can help find out whether there is some organics present.

Two TG/DTG devices were used within this study The TG/DSC-EGA results for Neuhauser´s and Foerster´s authentic mortars were obtained by Setaram Setsys Evolution-16 MS system in scan mode. Powdered samples were placed into an alumina crucible without a lid with argon or synthetic air flowrate being 60 ml/min and heating rate 10 °C/min. The measurement was performed from ambient temperature (21 °C) to 1000 °C, the mass spectrometer was operated in “Multiple Ion Detection” mode. The measurement was carried out at the Institute of Inorgannic Chemistry, CAS.

The rest of historic samples was analysed at the Institute of Theoretical and Applied Mechanics, CAS (dr. Dita Frankeová). The analysis was performed on a Discovery SDT 650 instrument from TA Instruments in the temperature range of 25-1000 °C. For analysis, 30-40 mg of the sample was weighed into a ceramic crucible, combustion took place in an N_2 atmosphere at a heating rate of 10 °C/ min. Analysis of gases released during heating was performed using a TA Instruments mass spectrometer.

6.2.5 X-ray powder diffraction (XRD)

X-ray powder diffraction analysis (XRD) enabled to determine mineralogical composition of the mortars studied. An X’Pert MPD device equipped with Cu tube and PIXcel1D detector was used to obtain the results. The metadata were evaluated by Rietveld refinement performed by Profex software version 4.1.0 [155]. The device does not enable to determine the percentage of an amorphous phase.

6.2.6 ATR-FTIR

Attenuated total reflectance Fourier-transformed infrared spectroscopy (ATR-FTIR) was employed to identify an organic substance in selected samples (Tab. 3). Apart from the bulk analysis, the organic compound was extracted by isopropanol in order to minimize overlapping with the intensive bands of the inorganic phases. Mortars´ extracts were prepared by two-step extraction. At first, 5 g of powder mortar was mixed with 20 ml of IPA and equilibrated for 5 days. In the subsequent step, the sample was extracted again with 15 ml of IPA. Eventually, both extracts were mixed and the resulting solution was analysed by ATR. The final extract was dried on a watch glass to evaporate the IPA solvent prior to spectra collection.

The spectra measurements were performed using an external module iZ10 of Nicolet iN10 spectrometer (Thermo Scientific) equipped with a DTGS detector, KBr beam splitter and ATR accessory with diamond crystal. The spectra were collected in the spectral range 4000–525 cm^{-1} with a resolution of 4 cm^{-1}. The collected signal was subsequently processed by Fourier transformation to an absorbance infrared spectrum. FTIR measurements took place in collaboration with Mgr. Petra Mácová at the Institute of Theoretical and Applied Mechanics, CAS in Telč.

6.2.7 Gas chromatography

Selected samples were analysed by the GC-MS (gas chromatography – mass spectrometry) in order to identify and quantify possible organic content. Prior to GC analysis powdered samples had been extracted using a mixture of organic solvents (dichlormethan: methanol, 4:1) and ASE 150 device (Accelerated Solvent Extractor, Dionex). The evaporated extract was dissolved in 5 ml of dichlormethan and 2 ml methanol, subsequently derivated in 2 ml 14% solution BF_3 in methanol at 90°C for one hour. The resulting solution was washed in distilled water and analysed by Trace 1310 GC device coupled with ISQ single quadrupole mass spectrometer (Thermo Scientific). The chromatogram was recorded in SIM (selected ion monitoring) mode. The measurements were carried out by dr. Martina Havelcová at the Institute of Structure and Rock Mechanics, CAS.

6.2.8 TOC

Total organic carbon (TOC) was assessed by RC 612 device (Leco) according to DIN 19539 (method B) [156]. This method does not enable to identify particular organic compounds. It was included as a complementary method to other techniques used for the identification of organics. The measurement was performed at the Institute of Chemical Technology, Prague.

6.2.9 Binder/ aggregate ratio assessment - HCl dissolution test

In order to separate soluble carbonates from insoluble aggregates, HCl was applied to dissolve the mortars. Each mortar sample was crushed and dried at 75°C for 24 h. A total of 10 g of mortar were dissolved in 100 ml of HCl (diluted 1:3) and subsequently filtered. The undissolved filtration residue representing the non-carbonate aggregates was dried at 75°C for 24 h and weighted before further analysis. However, the method turned out to be inappropriate for the assessment of binder/aggregate ratios as the aggregates in most samples were identified as carbonates during subsequent analyses. The undissolved residues were used for the XRD assessment of the non-carbonate aggregates´ mineralogical composition. The method was then no longer applied to other samples.

6.3 Results and discussion

6.3.1 Tirolean workshops – Neuhauser/Tiroler Glasmalerei and J. Pfefferle

Eleven samples of mortars fixing the mosaics from Tirol-based mosaic workshops were analysed within this study. A part of the results was previously published in a paper [37], yet some of the published conclusions had to be revisited due to new findings.

All the investigated mosaics were made in a studio by an indirect method of mosaic setting (see Section 4.5), most of the mosaics installed on Czech sepulchres were delivered as ready-made pieces embedded in transferable metal frames (with the exception of Mašek and Peluněk mosaics which were fixed with an on-site mixed mortar directly into a stone niche). Pfefferle´s Madonna from Reith was also fixed in a circular metal frame prior to its installation on a wall. The rest of mosaics from Austrian locations were installed directly on walls, inserted iron-wire reinforcement was found at some spots in both Hall and Oberhofen mosaics.

As for the samples from Czech cemeteries´ mosaics, some remarkable features could be observed even by unaided senses. Mortar beds of Beneš, Peluněk and Sladkovský mosaics are fine-grained, beige and have an intensive sweetish smell indicating the presence of an organic compound. Bittnerová mosaic mortar was similar but much more deteriorated. After more than 100 years the surface of mortars became powdery due to humidity and rain precipitations which resulted in the loss of tesserae in some parts of the mosaics. Dark corrosion layer was visible on the surface of Bittnerová, Pfannerer and Mašek mosaics where most of the tesserae had already fallen off due to strong deterioration of mortar beds.

6.3.1.1 Microstructure and chemical composition (LM, SEM-EDS)

Tab. 4 summarizes an average chemical composition of the mortars and their identified compounds. The mortars´ microstructure, as seen in a light microscope and SEM-EDS, is depicted in Fig. 18 and Fig. 19. In general, the mortars are rather fine-grained with aggregate particles up to 2 mm. All mortars contained Ca-bearing carbonate aggregates which could be interpreted as a very pure crystalline calcite based on their chemical composition (Tab. 4) and the shape and characteristic cleavage planes preserved in some grains (see e.g. Fig. 18a, b or 19e). This indicates the use of marble dust. Fig. 18 represents mosaics from two Prague cemeteries which show similar features in the microscopes. As can be seen from SEM-BSE images and EDS analysis results (Tab. 4), all mortars consist of calcium carbonate aggregates and calcareous binder showing no striking signs of hydraulicity. According to their cementation indices (CI) calculated according to Equation 2 (Section 3.1.1), the binders can be characterised as air lime. Sladkovský, Peluněk and Beneš mosaic mortars look very

Table 4. Chemical composition of "Tirolean" mosaic mortar samples as obtained by SEM-EDS. The results are an average of at least 5 measurements.

sample	mortar compounds	wt%															Cl
		CaO	SiO_2	Al_2O_3	MgO	Na_2O	K_2O	SO_3	Fe_2O_3	TiO_2	MnO	P_2O_5	Cl	Pb	Cu	F	
Sladkovský PB1702	binder	78.1	0.9	0.7	18.0	-	-	2.3	-	-	-	-	-	-	-	-	0.03
	$CaCO_3$ aggr.	99.5	-	-	0.5	-	-	-	-	-	-	-	-	-	-	-	-
Beneš PB170	binder	94.5	1.9	1.1	2.0	-	-	0.4	0.1	-	-	-	-	-	-	-	0.07
	$CaCO_3$ aggr.	99.4	-	-	0.6	-	-	-	-	-	-	-	-	-	-	-	-
Peluněk PB1707	binder	74.6	2.7	9.8	12.9	-	-	-	-	-	-	-	-	-	-	-	0.20
	lime lump	84.1	4.6	4.0	7.4	-	-	-	-	-	-	-	-	-	-	-	0.15
	Ca-aggregate	97.5	-	1.8	0.7	-	-	-	-	-	-	-	-	-	-	-	-
Bittnerová PB1704	binder	87.5	3.8	0.9	4.3	0.3	0.1	3.4	-	-	-	-	-	-	-	-	0.12
	S-rich crust	67.0	2.6	0.6	2.2	-	-	27.6	-	-	-	-	-	-	-	-	-
	Ca-aggregate	96.5	0.4	0.2	2.3	-	-	1.1	-	-	-	-	-	-	-	-	0.01
Mašek PB2003	binder	87.1	7.8	2.0	1.3	0.5	0.4	0.6	0.7	-	-	0.6	0.4	-	-	-	0.28
	Ca-aggregate	98.5	-	-	1.5	-	-	-	-	-	-	-	-	-	-	-	-
Pfannerer PB2106	binder	81.2	7.5	2.4	4.9	0.9	0.4	1.6	0.7	0.3	-	0.3	0.6	-	-	-	0.27
	brick aggr.	6.4	53.3	25.0	4.8	1.9	2.6	0.4	8.7	0.6	-	-	0.0	-	-	-	-
	crust	49.9	3.0	1.4	1.5	0.1	0.5	43.3	0.2	-	-	-	-	-	-	-	-
	$CaCO_3$ aggr.	98.6	-	-	1.4	-	-	-	-	-	-	-	-	-	-	-	0.00
Getzner PB2204 - layer A	binder	61.0	20.2	6.8	5.0	-	0.3	5.8	1.0	1.0	-	-	-	-	-	-	0.95
	lime lump	84.7	3.6	1.3	2.5	-	0.2	7.7	-	-	-	-	-	-	-	-	0.13
	brick aggr.	0.7	56.9	38.9	0.7	0.3	1.5	-	1.4	1.3	-	-	-	-	-	-	-
	Pb "glass"*	2.6	74.8	14.5	0.2	1.3	4.0	-	0.9	2.0	0.8	-	-	3.7	-	-	-
Getzner PB2204 - layer B	binder	61.3	22.6	8.2	4.0	-	0.5	2.8	0.8	0.6	-	-	-	-	-	-	1.09
	lime lump	87.3	3.4	0.7	5.0	-	-	3.6	-	-	-	-	-	-	-	-	0.11
	brick aggr.	1.5	62.0	31.8	0.2	0.3	1.4	-	1.5	1.2	-	-	-	-	-	-	-
Krip PB2205	binder	66.7	16.0	7.6	5.4	0.8	0.4	2.0	1.0	-	-	-	-	-	-	-	0.73
	brick aggr.	1.2	69.8	23.4	1.2	0.9	1.8	-	1.3	1.8	-	-	0.3	-	-	-	-
	Pb glass*	0.2	56.8	0.6	-	5.2	1.9	-	0.2	0.1	-	-	-	34.7	0.3	0.1	-
Madonna Reith (PB1709)	binder	89.9	4.3	1.5	3.6	-	-	0.9	0.4	-	-	-	-	-	-	-	0.15
	lime ump	91.8	4.3	2.5	2.0	-	-	-	-	-	-	-	-	-	-	-	0.16
	$CaCO_3$ aggr.	98.6	0.4	0.2	0.9	-	-	-	-	-	-	-	-	-	-	-	0.01
Oberhofen PB2206	binder	78.5	7.4	2.3	9.5	0.6	0.1	0.7	0.8	-	-	0.3	0.2	-	-	-	0.26
	lime lump	71.8	12.2	2.0	12.1	0.7	0.1	0.8	0.8	-	-	0.4	0.1	-	-	-	0.41
	$CaCO_3$ aggr.	98.6	0.2	-	1.3	-	-	-	-	-	-	-	-	-	-	-	0.01
Hopfgarten PB2207	binder	90.8	5.0	1.8	1.9	0.4	-	0.6	-	-	-	-	-	-	-	-	0.17
	lime lump	96.0	2.3	0.6	1.5	-	-	-	-	-	-	-	-	-	-	-	0.07

* only 1 measuement; aggr. = aggregates

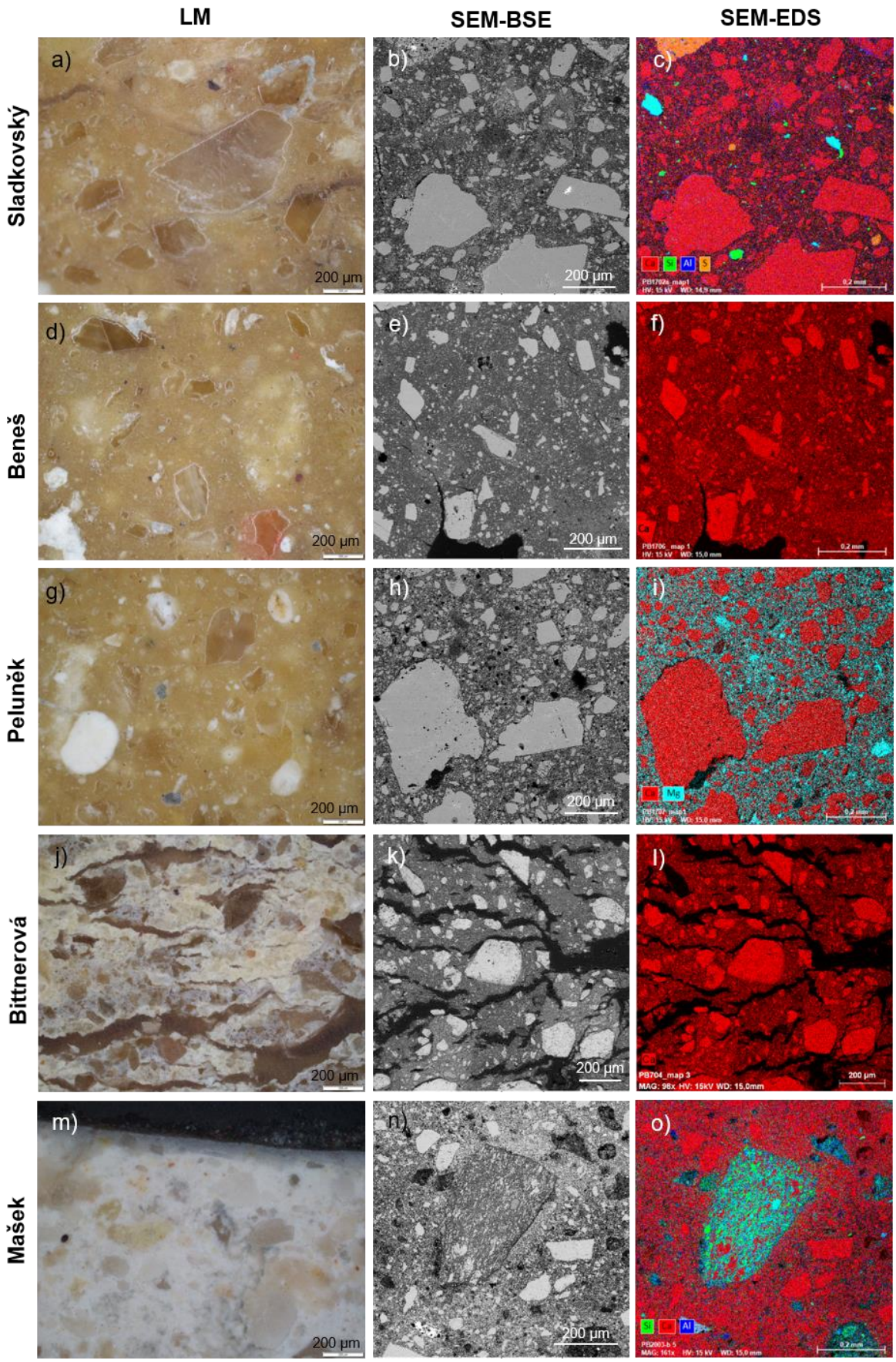

Figure 18. Microstructure of lime and marble aggregate-based bedding mortars of ready-made sepulchral mosaics from Prague cemeteries. LM-light microscopy images; SEM-BSE – back scattered electron images; SEM-EDS – maps of Ca (red), Si (green) and Al (blue) distribution.

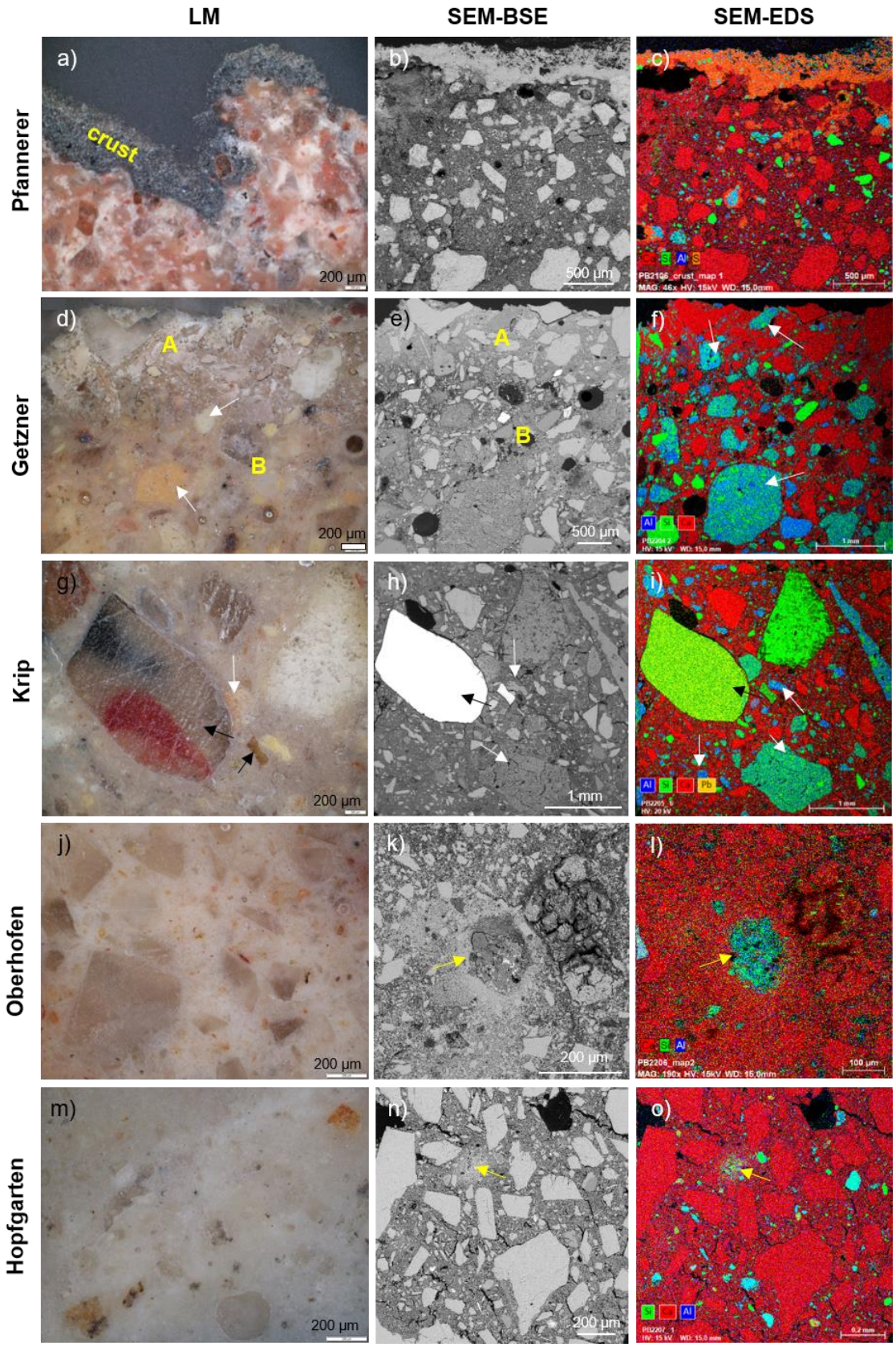

Figure 19. Microstructure of *cocciopesto* and lime-cement bedding mortars of mosaics made by Neuhauser and Pfefferle mosaic studios. LM-light microscopy images; SEM-BSE – back scattered electron images; SEM-EDS – maps of Ca (red), Si (green) and Al (blue) distribution. Black arrows mark glass splinters, white arrows mark ceramic particles and yellow arrows mark residual clinker grains.

similar both under the light microscope and SEM (Fig. 18a-i). Bittnerová mortar is affected by a high degree of corrosion associated with the formation of sulphate crust, extremely inconsistent texture and the development of vast horizontal microcracks (Fig. 18j-l).

Mašek occupies a special place in this sample set (lighter colour; CI almost reaches the hydraulicity limit of 0.3; no sweetish smell) but the main characteristic remains – lime-based binder mixed with fine marble dust aggregates (although some metamorphic rock fragments can be occasionally found too – see Fig. 18n, o).

Chemical composition of the aggregates, as assessed by SEM-EDS (Tab. 4), differs from the composition of the binder which has a higher Mg content and is richer in silica and alumina. This means most aggregates represent a very clean calcium carbonate added as a filler. According to the Mg content exceeding 5 wt% MgO, Sladkovský and Peluněk mortar binders can be classified as dolomitic lime [10]. Apart from $CaCO_3$ grains other aggregates such as SiO_2 (quartz) or K, Na-Ca rich aluminosilicates (probably feldspars) and Ca-S phases (corresponding most likely to gypsum) were identified in some samples to a lesser extent. Their occurrence will be discussed in section 6.3.1.3.

The mortars shown in Fig. 19 represent a more diverse set in terms of materials composition. Their common feature is the presence of fine (up to 0.5 mm) calcium carbonate aggregates (marble dust). The Pfannerer mortar (Fig. 19a-c) can be characterised as a *cocciopesto* – a mixture of lime and finely crushed bricks. Its CI balances at the border between air and hydraulic lime. The mortar has been affected by sulphate attack resulting in the development of a dark, up to 400 µm thick crust consisting of calcium sulphate. Locally, sulphate corrosion penetrates deeper to the mortar affecting predominantly the brick aggregates (Fig. 19c).

Mosaics from the town hall of Hall (Getzner and Krip) were also fixed by mortars based on lime, calcium carbonate aggregates and brick-like aluminosilicate particles (Fig. 19d-i). In contrast to the Pfannerer mortar, some of these Si-Al rich particles reach significantly larger size (up to 2 mm) compared to the carbonate aggregates. The Getzner mortar consists of two layers (Fig. 19d-f), the upper (layer A) is finer and thinner (thickness around 600 µm). It probably represents the uppermost bedding mortar which is missing in the Krip sample. Chemically, both mortar layers (A and B) are very similar. Microscopic observation showed a finer and more compact structure of the upper layer A. Ceramic aluminosilicate grains are less frequent compared to layer B. Apart from ceramics, random glassy particles were identified in both Getzner and especially Krip samples. Both types of aggregates will be discussed in a special section (6.3.1.4).

In Hopfgarten, Oberhofen (Fig. 19j-o) and Reith mortars neither intentionally added brick aggregates nor pieces of glass can be found. Judging solely on their chemical composition, namely the CI values of their binders (Tab. 4), the binders do not seem to be much hydraulic. However, clinker residues appeared under the SEM (Fig. 20). The SEM-EDS analysis of lime lumps identified in the sample of the Oberhofen mortar

uncovered their hydraulic character (Tab. 4). The unhydrated clinker residues were rather rare in this sample. Their shape (Fig. 20) corresponds rather to natural hydraulic lime clinkers formed in random “hot spots” of calcination kilns due to inhomogeneous temperature distribution rather than to clinkers occurring in Portland cement (nests of fine round belite-like crystals enclosed by a dense carbonation rim). Due to their decalcification it was not possible to determine their original chemical composition in order to confirm or exclude the presence of C_3S (alite, a characteristic phase of Portland cement). But the presence of aluminous and ferrous interstitial phases in between these (assumingly) belite grains lets us assume the clinker represents residual early Portland cement grains [50].

On the contrary, in the Hopfgarten and Reith mortars the composition of lime lumps as well as the general binder composition corresponds to air lime. However, early Portland cement clinker residues were detected in both samples (Fig. 20). Hence, the binder of these mortars seems to be a mixture of lime and Portland cement (added in a significantly smaller amount in proportion to lime, that is why its addition did not affect the generally “air lime” character of the binder in terms of the EDS results).

Magnesium was present in the binders of all these samples. The mortars showed dolomitic composition (i.e. > 5 wt% MgO [10]) with the exception of Reith and Hopfgarten, where the Mg amount was slightly lower. However, no phenomena associated with dolomitic mortars were observed in the microscope.

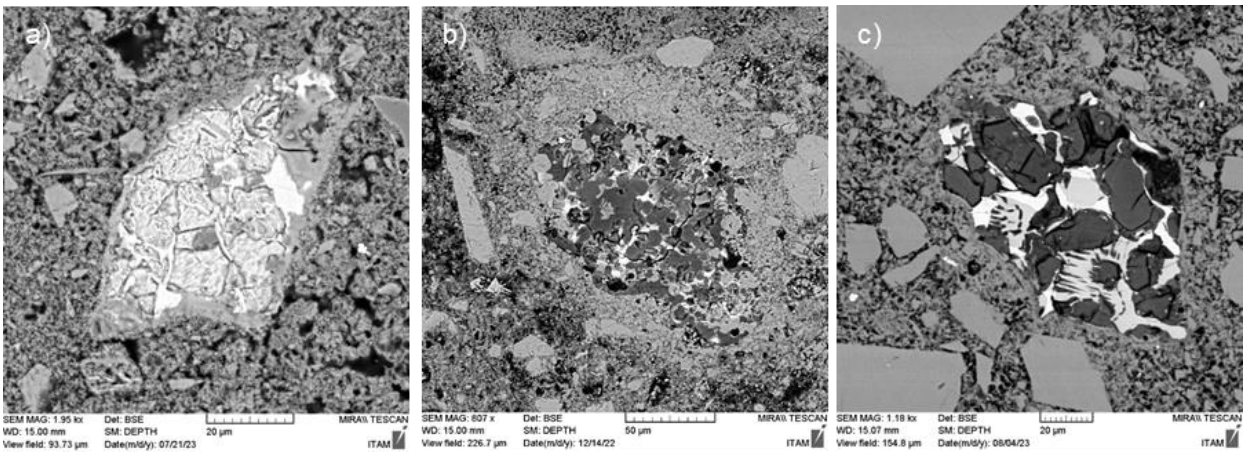

Figure 20. Early Portland cement clinkers found in Hopfgarten (a), Oberhofen (b) and Reith samples. Hopfgarten clinker (a) is less decalcified than the other samples. In Reith sample (c), decalcified belite shows finger-like extensions, a sign of this early PC´s slow cooling.

Dissolution in HCl and binder/ aggregate ratio assessment

As all mortars contained HCl soluble carbonate aggregates (see 6.3.1.1), the assessment of binder/ aggregate ratio was estimated based on visual analysis of SEM images after Shvetsov [157]. However, the method provides only approximate results. They are summarized in Tab. 5.

Table 5. Binder/ aggregate ratio estimated after Shvetsov **[157]**, expressed in area percentages of aggregates.

aggre-gates	Slad-kovský	Beneš	Pelu-něk	Bittne-rová	Ma-šek	Pfan-nerer	Getz-ner A	Getz-ner B	Krip	Reith	Ober-hofen	Hopf-garten
% area	30	25	30	30	25	30	50	50	50	30	35	40

Yet, the binder/ aggregate ratio assessment by the samples´ dissolution in HCl was tested on Beneš, Peluněk and Sladkovský mosaic mortars. Despite the experiment´s failure (in terms of binder/ aggregate ratio assessment), the dissolution of these samples in HCl uncovered the presence of an organic compound which was later identified as deteriorated linseed oil (see Section 6.3.1.5). Large brownish greasy stains remained on filtration papers after the samples´ filtration (Fig. 21). The dissolution residues were subsequently analysed by XRD.

Figure 21. Filtration residues after the HCl dessolution and subsequent filtration of the Sladkovský (left), Beneš (centre) and Peluněk (right) bedding mortars.

6.3.1.2 Mineralogical composition (XRD)

Tab. 6 displays crystalline phases identified in bulk mortars. Mineralogical composition of HCl dissolution residues (Beneš, Sladkovský, Peluněk) is shown in Tab. 7. The phase composition of bulk samples and residues does not fully match due to low concentrations of less abundant phases such as feldspars, muscovite and hematite in the bulk. The main crystalline constituent of all the mortars is calcite $CaCO_3$, accounting for over 90 wt% of some samples (Sladkovský, Mašek, Pfannerer, Oberhofen, Hopfgarten). Quartz (SiO_2) was also identified in all samples. The development of thermodynamically metastable $CaCO_3$ polymorphs, aragonite and vaterite, corresponds to the carbonation of C–S–H, C-A-H or to the recrystallization of the pore solution [51], [158]. Aragonite seems to occur less frequently in carbonated hydraulic and cementitious mortars compared to vaterite but its formation might be enhanced by the presence of Mg ions [159]. Therefore the aragonite identified in the dolomite-containing Reith mosaic mortar (characterised as a mixture of lime and early PC in 6.3.1.1) might be associated with the carbonation of its hydraulic cementitious binder.

Table 6. Mineralogical composition of mosaic mortars coming from analysed mosaics of Tirolean provenance.

wt%	calcite	Mg-calcite	aragonite	vaterite	portlandite	dolomite	quartz	cristobalite	kaolinite	mullite	albite	hydrotalcite	merwinite	akermanite	gypsum	epsomite	alunogen	whewellite
PB1702	91.4	-	-	-	1.5	2.6	4.5	-	-	-	-	-	-	-	-	-	-	-
PB1706	87.4	-	-	-	7.0	1.2	4.4	-	-	-	-	-	-	-	-	-	-	-
PB1707	85.2	-	-	-	1.5	1.8	11.5	-	-	-	-	-	-	-	-	-	-	-
PB1709	80.3	-	16.2	-	-	1.4	2.0	-	-	-	-	-	-	-	-	-	-	-
PB1704	65.0	16.0	-	3.0	-	-	2.0	-	-	-	-	-	-	-	3.0	6.0	6.0	3.0
PB1704 crust	64.0	4.0	-	4.0	-	-	4.0	-	-	-	-	-	-	-	16.0		3.0	-
PB2003	98.0	-	-	-	-	-	2.0	-	-	-	-	-	-	-	-	-	-	-
PB2003 crust	56.0	-	-	-	-	-	1.0	-	-	-	-	-	-	-	43.0	-	-	-
PB2106 a	91.0	-	-	-	-	-	7.0	-	-	-	-	-	-	-	2.0	-	-	-
PB2106 b (crust)	53.0	-	-	-	-	-	8.0	-	-	-	-	-	-	-	39.0	-	-	-
PB2204 layer A	76.0	-	-	-	-	-	16.0	1.0	-	-	-	2.0	3.0	2.0	-	-	-	-
PB2204 layer B	67.0	-	-	-	-	-	20.0	4.0	-	-	-	2.0	4.0	3.0		-	-	-
PB2205	66.0	-	-	-	-	1.0	9.0	6.0	6.0	8.0	2.0	2.0	-	-	-	-	-	-
PB2206	99.0	-	-	-	-	-	1.0	-	-	-	-	-	-	-	-	-	-	-
PB2207	97.0	-	-	-	-	-	3.0	-	-	-	-	-	-	-	-	-	-	-

Table 7. Phases identified in HCl undissolved residues. The presence of a phase is denoted with an asterisk.

sample	HCl undissolved residue (qualitative)				
	quartz	albite low	muscovite	calcite	portlandite
Sladkovský	*	*	*	-	-
Beneš	*	-	-	*	*
Peluněk	*	*	*	*	*
Reith	*	-	-	-	-

The detection of vaterite in the Bittnerová sample can be linked to the presence of linseed oil in the mortar. Vaterite was previously identified in “oil stucco” plaster used for the fixation of mosaics in St. Peter´s basilica in Rome [96].

The presence of portlandite ($Ca(OH)_2$) in Sladkovský, Beneš and Peluněk samples caught our attention. In more than 120 years old mortars complete carbonation of portlandite to calcite ($CaCO_3$) would be expected. Yet, some non-carbonated portlandite remains have been reported even in much older mortars, typically in inner parts of an extremely thick masonry or in an environment of high humidity [8], [9], [160]. However, in this case portlandite´s occurrence has something to do with the presence of linseed oil which will be discussed in section 6.3.1.6 in detail. The unusual presence of calcite and portlandite in Beneš and Peluněk mortars´ acid dissolution residues (Tab. 7) can be also explained by the greasy organic content. The oil probably “enveloped” a part of calcite and portlandite particles and isolated them from the acid.

The surface of some mortars (Bittnerová, Mašek, Pfannerer) was affected by biodegradation and an intensive sulphate attack which is manifested by the formation of blackened crust with gypsum ($CaSO_4 \cdot 2H_2O$) as a basic compound and (in case of Bittnerová) with epsomite ($MgSO_4 \cdot 7H_2O$) and alunogen ($Al_2(SO_4)_3 \cdot 17H_2O$) as minor phases. Whewelite, a calcium oxalate ($CaC_2O_4 \cdot H_2O$), frequently forms on the surface of deteriorated lime mortars, carbonatic rocks or mural paintings due to the concomitant action of specific environmental conditions and microorganisms such as bacteria, algae, fungi, yeasts or lichens [161]–[163].

Kaolinite ($Al_2Si_2O_5(OH)_4$), mullite ($Al_6Si_2O_{13}$), cristobalite (SiO_2), merwinite (Ca_3MgSiO_4) and akermanite ($Ca_2MgSi_2O_7$) are associated with the aluminosilicate ceramic and glass aggregates found in the Getzner and Krip bedding mortars. So is hydrotalcite ($Mg_6Al_2CO_3(OH)_{16}$), a product of pozzolanic reaction between these grains and lime binder (see section 6.3.1.4 for a detailed discussion).

6.3.1.3 Thermal analysis (TG/DTG-EGA)

Fig. 22 shows the TG/DTG curves of the four organics-containing mosaic mortars from Prague (Peluněk, Sladkovský, Beneš and Bittnerová). They exhibit small mass changes (weight loss less than 10%) in the 0 – 350 °C temperature range. In case of cement-based binders, these changes could be attributed to the dehydration of C-S-H phases. However, no evidence of clinker residues was found by SEM-EDS and the binders of the mortars were therefore characterised as air-lime. The weight loss was

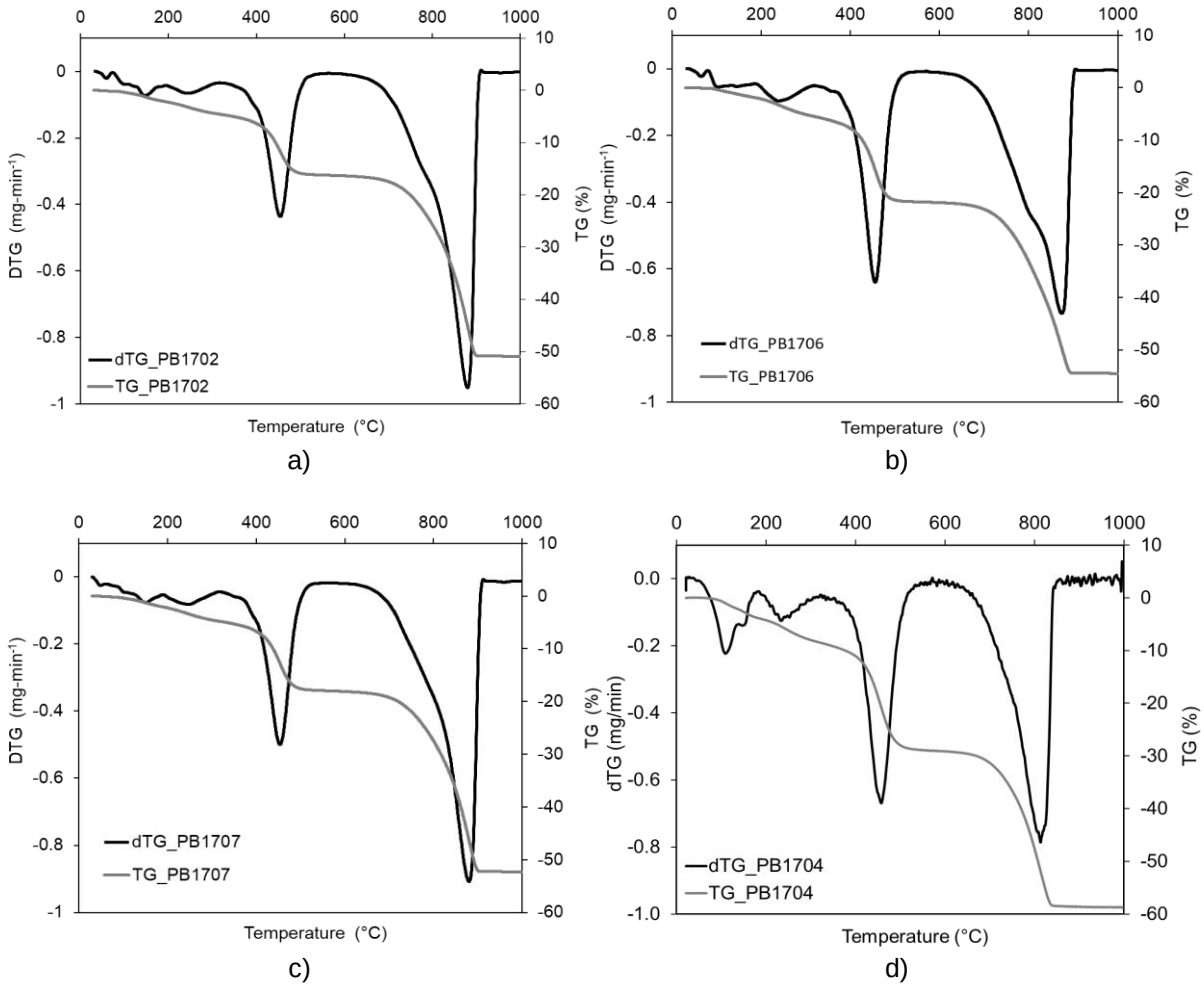

Figure 22. TG/DTG curves of a) Sladkovský, b) Beneš, c) Peluněk, d) Bittnerová bedding mortars.

partially caused by the dehydration of gypsum whose decomposition peak (150 °C) was identified in all the DTG curves. In some samples, the presence of gypsum was confirmed by SEM-EDS, FTIR spectra of bulk mortars and by XRD. But the main part of the mass loss in this interval is due to the decomposition of the organic matter present - identified by FTIR as oil (see section 6.3.1.5). The fatty acids contained in oil decompose at 150 – 250 °C [164]. Fiori et al. [96] detected mass changes due to the presence of linseed oil-based organic admixture in 16th century mosaic binders between 200 – 550 °C.

A significant peak at 455 °C indicates the presence of portlandite. This phase was confirmed in three of the samples (not in the Bittnerová mortar) by XRD (Tab. 6). It has been experimentally proved substantial portion of thermally induced oil disintegration

resulting in CO_2 and water release takes place in this region as well [165], overlapping portlandite decomposition peak. Thus, the intensity of “portlandite” peak is “amplified” by the contribution of oil decomposition. This explains why portlandite and calcite content calculated from the ratios of their DTG peaks´ intensities gives misleading results.

X-ray diffraction did not provide any evidence of portlandite in the Bittnerová mortar. However, the “portlandite” peak, i.e. the peak at 455 °C is extremely distinct in the DTG curve (Fig. 22d). We assume, the peak can be fully attributed to the decomposition of the organic matter. As can be seen from the TG curve of the Bittnerová mortar, the total mass change in the temperature range of 0 - 600 °C was 29.5%. Of this, 1.2 % is due to sulphur decomposition (mass loss between 125 - 155 °C). Thermal decomposition of the oil therefore accounts for 27.9 % of the mass change in the temperature range studied. At the same time, it was found that at higher temperatures there is no significant mass change due to oil decomposition anymore (see Section 7 or [165]). Thus, the figure of 27.9% represents the total contribution of oil to the mass loss of the sample. This is also evident from the results of the EGA-MS analysis (Fig.23), which show that even in the case of the Bittner mortar, there is a significant release of the main mass fractions attributed to oil decomposition (m/z 55 and 95) at 450 °C (i.e. at the same temperature as the potential release of CO_2 from portlandite if it were present in the sample) [165].

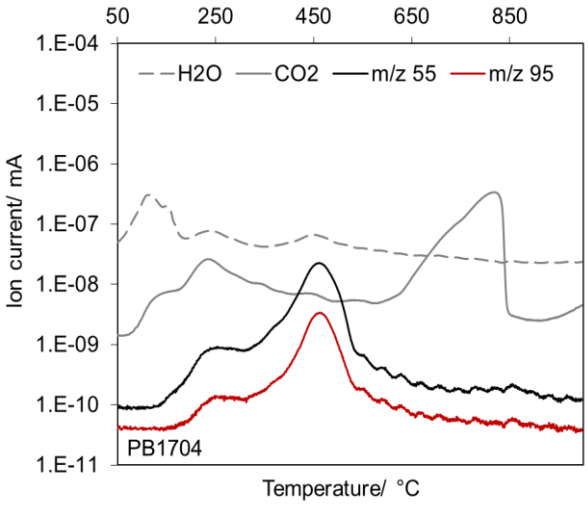

Figure 23. EGA-MS curves of the Bittnerová mortar.

If the contribution of the oil to the total mass change is known, its content in the sample can be calculated from Eq. 11 (Section 7.3.3.3). The amount of organics (oil) contained in the Bittnerová sample was thus estimated to be 37.1%.

Calcium carbonate decomposes at around 880 °C. In two mosaic mortars (Sladkovský, Beneš) the doublet at 780 °C/ 800 °C and 880 °C might correspond to the presence of dolomite [166]. This phase was identified by XRD in all samples.

The TG/DTG curves of the Mašek and Pfannerer samples are shown in Fig. 24. The curves representing “fresh” mortars (i.e. parts without visible degradation or corrosion) indicate a lime nature of both bedding mortars with $CaCO_3$ being the main constituent (Fig. 24 a, c). Based on TG/DTG, the binder of the Mašek mortar bed can be characterised as air lime which is in agreement with the EDS results.

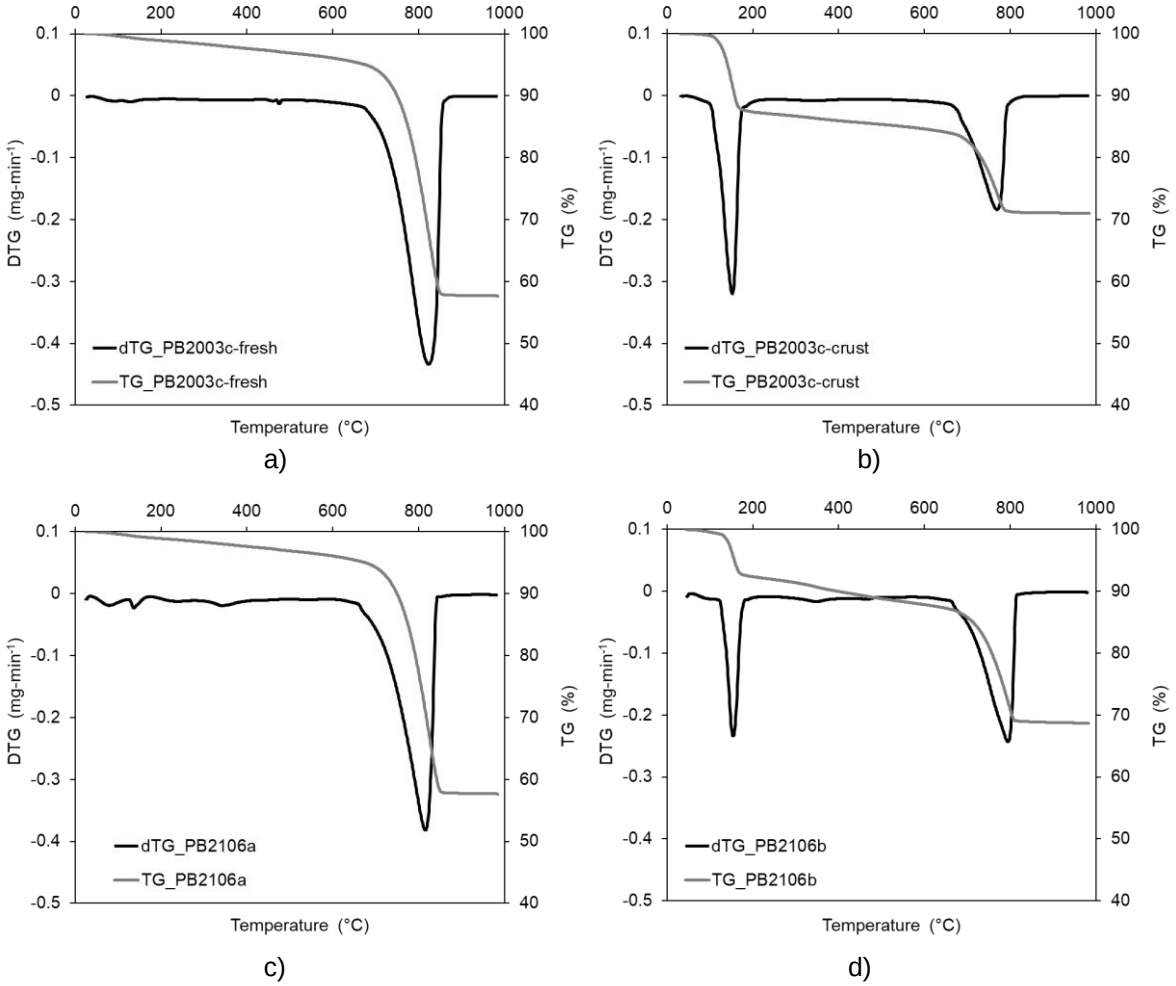

Figure 24. TG/DTG curves of a) uncorroded Mašek mortar, b) corroded surface crust of the Mašek mortar, c) uncorroded Pfannerer mortar, d) corroded surface crust of the Pfannerer mortar.

The mortar bed of the Pfannerer mosaic was described by SEM-EDS as a *cocciopesto* consisting of lime with brick aggregates. According to the cementation index, the hydraulicity of the binder still corresponds to air lime, but the TG/DTG curve indicates a slight pozzolanic reaction between the lime and the bricks.

Most of the Mašek and Peluněk mosaics´ tesserae had fallen off due to an extreme deterioration of their mortar beds. Dark corrosion crusts developed on the surface of the naked mortars. Fig.24b,d displays the TG/DTG curves of these crusts with gypsum (peak at 150 °C) and calcium carbonate (peak at 780 °C) being the most abundant compounds.

EGA-MS analysis did not prove the presence of organics but uncovered other deterioration products besides sulphates in the corrosion crust of the Pfannerer mortar. The fraction m/z 30 represents NO^+, the most intensive fraction evolved during the decomposition of hydrated nitrates [167] (Fig. 25).

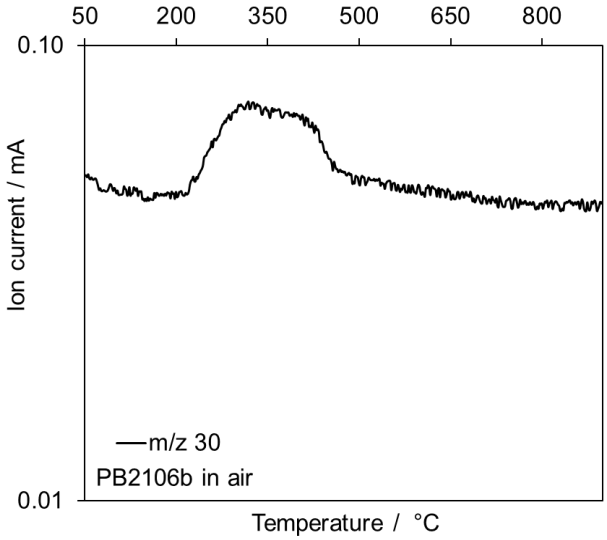

Figure 25. EGA-MS curve illustrating the decomposition of nitrates (represented by m/z 30) in the Pfannerer mosaic mortar bed.

Fig. 26 shows the TG/DTG curves of five bedding mortars of mosaics installed in Austria. Fig. 26a,b displays the thermal decomposition of the Getzner and Krip mortars. As shown by SEM-EDS (Section 6.3.1.1) and XRD (Section 6.3.1.3), these mortars contained reactive pozzolanic aggregates. Similarly to the Pfannerer sample (Fig. 24c), an evidence of the pozzolanic reaction between these grains and the binder is distinct in both graphs. In Fig. 26a (Getzner) pozzolanic reaction is represented by a broader peak between 100-200 °C. The Krip mortars´ TG/DTG curves look identical to the Pfannerer sample – an unassuming peak at 85 °C associated with the release of hygroscopic water [168] and another at 340 °C representing the dehydration of hydrogarnet [169].

Based on the TG/DTG analysis alone, the binders of the three remaining mortars could be classified as air lime. There was no significant evidence of C-S-H phases thermal decomposition. However, the presence of residual Portland cement clinkers was clearly demonstrated by SEM-EDS. This is another indication that lime-cement binders were used and that cement was a much smaller part of the mix.

A broad peak between 600-780 °C in Fig. 26d (Reith) could be attributed to the presence of another $CaCO_3$ polymorph other than calcite. Based on the TG curve, its content was calculated to be 9.4 wt%. This is in a relatively good agreement with the results of the XRD analysis where aragonite was detected in the amount of 16 wt%. (The XRD values are generally slightly overestimated as the amount of amorphous

fraction cannot be determined.) Aragonite is supposed to be a product of the C-S-H phases´ carbonation [11].

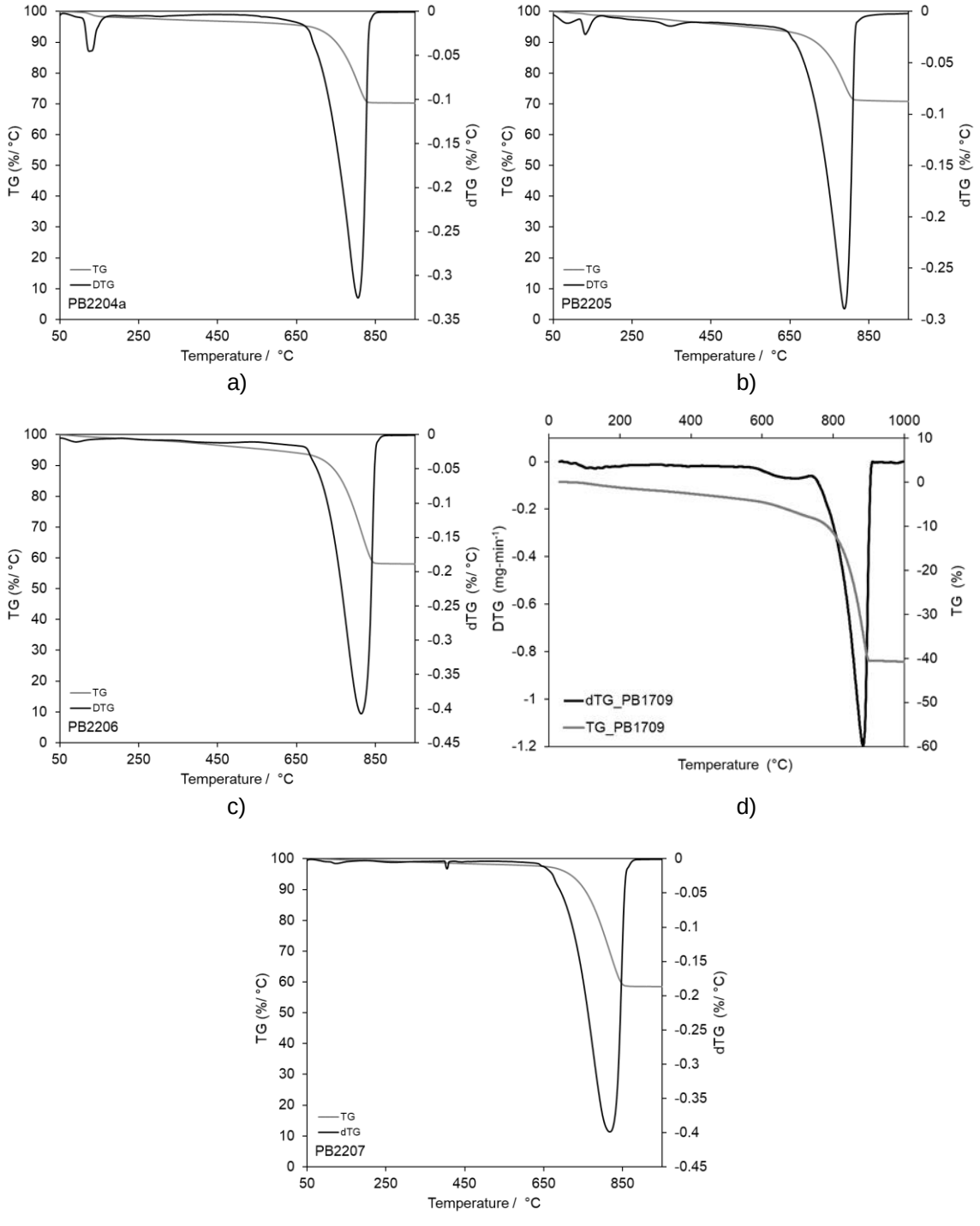

Figure 26. TG/DTG curves of a) Getzner, b) Krip, c) oberhofen, d) Reith and e) Hopfgarten samples.

6.3.1.4 Aggregates of Getzner and Krip bedding mortars

Besides $CaCO_3$ aggregates which were used in all the bedding mortars, frequent ceramic (Fig. 27) and less abundant glassy grains were identified in Getzner and Krip samples. Both mortars coming from the mosaic decoration of Hall town hall´s façade show very similar features. According to the CIs (Tab. 4), their binders are highly hydraulic. However, in the Getzner sample, lime lumps of air lime nature have been preserved (no binder-related lumps were observed in the Krip mortar). Hence we assume, the original lime binder itself was rather not hydraulic and the high overall hydraulicity of the mortar was induced by the pozzolanic reaction between lime binder and reactive ceramic shards. Weak reaction rims detected by light microscopy developed around some ceramic particles (Fig. 27e). The presence of hydrotalcite $Mg_6Al_2CO_3(OH)_{16}{\cdot}4H_2O$ in both samples also indicates pozzolanic reaction [170]. This phase can be formed during the hydration in an Mg-rich environment. In the presence of water, Al^{3+} ions (in this case available from the ceramics) combine with Mg^{2+} ions from MgO (contained in Mg-rich or dolomitic binders) which leads to the formation of hydrotalcite crystals [171]. Hydrotalcite as a product of pozzolanic reaction has been reported from ancient structures [172], especially from ancient harbours whose concrete had been slaked by sea water serving as the source of Mg^{2+} ions [173], [174].

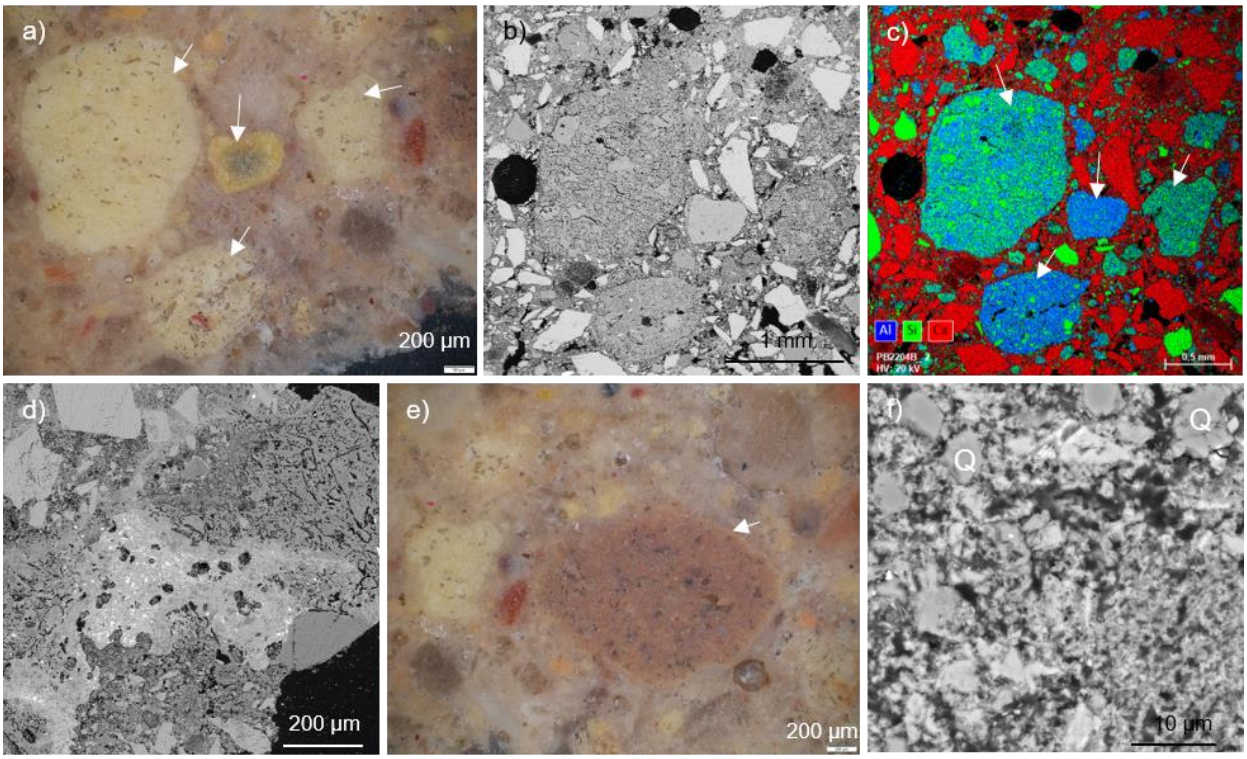

Figure 27. Ceramic (chamotte) shards from the Krip and Getzner mortars. The ceramics shards are marked with white arrows – a) chamotte grains in a light microscope, b) the same grains in a SEM-BSE image and c) in an EDS map of element distribution; d) ceramic grains with a different degree of calcination (SEM-BSE image), e) weak light red reaction rim around a ceramic particle, d) lime binder with residual quartz grains (marked Q) indicating former fine ceramic grains consumed during the pozzolanic reaction with the binder (SEM-BSE image).

Frequent microscopic SiO_2 (quartz?) grains dispersed in the binder (Fig 27f) might be the relics of smaller reactive ceramic fragments consumed almost completely by the pozzolanic reaction [17].

The ceramic brick-like shards are rich in alumina but have a very low calcium and alkali content (Fig. 28) and an absence of feldspars and micas. The amount of Fe is also quite low (around 1%). This as well as light colours in light microscopy images (Fig.27a), untypical for common bricks, let us assume fire clay was used as a raw

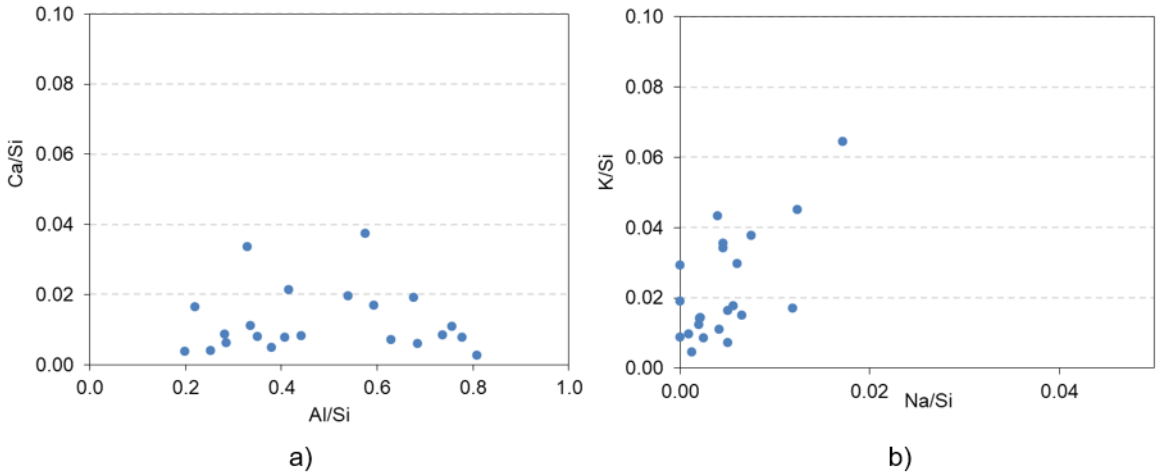

Figure 28. Chemical composition of analysed ceramic aggregates obtained by SEM-EDS – a) Ca and Al content and b) alkali content.

material for their firing. Fireclays are used as mined or after calcination, during which their main constituent, kaolinite ($Al_2Si_2O_5(OH)_4$), breaks down to mullite ($Al_6Si_2O_{13}$) and siliceous glass [175].

Shards showing varying degree of calcination occur in both mortars (Fig. 29). Some particles are extremely compact (Fig. 29a) showing a high degree of vitrification, some exhibit a partial collapse of the original clayey microstructure due to partial sintering (Fig 29b) and in some aggregates the relics of the original foliated microstructure corresponding to clay minerals (kaolinite) have been preserved (Fig.29c). In general, two groups of aggregates can be distinguished – (1) “low-fired” aggregates – generally more porous, probably associated with kaolinite identified by XRD in the Krip sample and (2) “high fired” aggregates – showing a higher degree of sintering, dense structure, richer in Al and containing cristobalite and (in case of the Krip sample) mullite detected by both XRD and SEM (Tab. 4, Fig. 29d-f).

These two aggregate groups are distinguishable also in terms of their alumina content (Fig. 28a). The alumina content in Ca-poor ceramics tends to increase at higher firing temperatures [176]. This is because higher temperatures promote the sintering process, leading to densification and reduced porosity in the ceramic material. As the porosity decreases, alumina particles can pack more closely together, resulting in a higher alumina content. However, the microstructure can significantly vary within a single grain indicating inhomogeneous thermal load.

The detection of kaolinite in the Krip sample indicates some of the clayey aggregates or their parts must have not been exposed to temperatures exceeding 630 °C (the decomposition of kaolinite [177]). However, the clayey texture with the relics of foliation can be observable in clays fired up to 800 °C [178]. According to Böke et al. [20], this temperature interval (700 – 800°C) is optimal for the development of pozzolanic properties in ceramics.

The formation of mullite and sintering, typical for the denser, Al-rich aggregates, takes place at temperatures above 1000 °C [177], [179]. Vitreous phase content increases with the rising of temperature [178]. Mineralogical association of these aggregates (mullite, cristobalite, quartz) as well as their chemical composition corresponds to chamotte [179]–[181]. Due to its refractory properties, chamotte ceramics was frequently used during glass-making process [182].

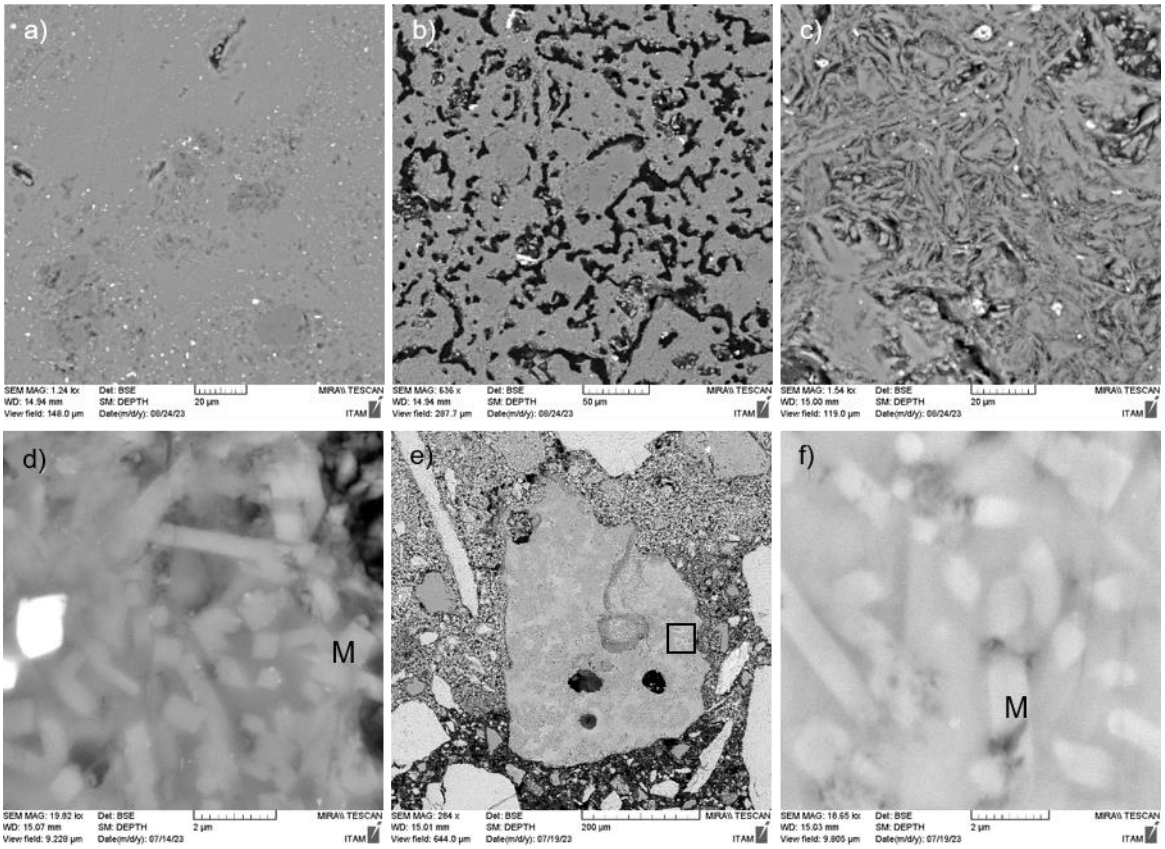

Figure 29. Different textures of ceramic aggregates. a) dense glassy aggregate, b) vitrified aggregate, c) aggregate with residual clayey foliation, d) mullite srystals (M) identified in the Getzner sample, e) dense agreegate in the Pfannerer sample, black square denotes an area magnified for a detailed image, f) a detail of the particle with mullite crystals. SEM-BSE images.

Apart from fired clayey and chamotte compounds, glassy aggregates were observed in both Krip and Getzner mortars (Fig 30). Their chemical composition is displayed in Tab. 8. The glassy aggregates are very inhomogeneous in terms of their composition. Some of these aggregates contain lead and common glass opacifiers (F, Sb, Cu), some resemble frits or slags. The slag-like frit grains are more frequent in the Getzner mortar, while glass shards in the Krip sample.

The occurrence of high-temperature minerals akermanite ($Ca_2MgSi_2O_7$) and merwinite (Ca_3MgSiO_4) detected by XRD in the Getzner mosaic mortar might be associated with these frit aggregates. Merwinite and akermanite commonly occur in blast furnace slags

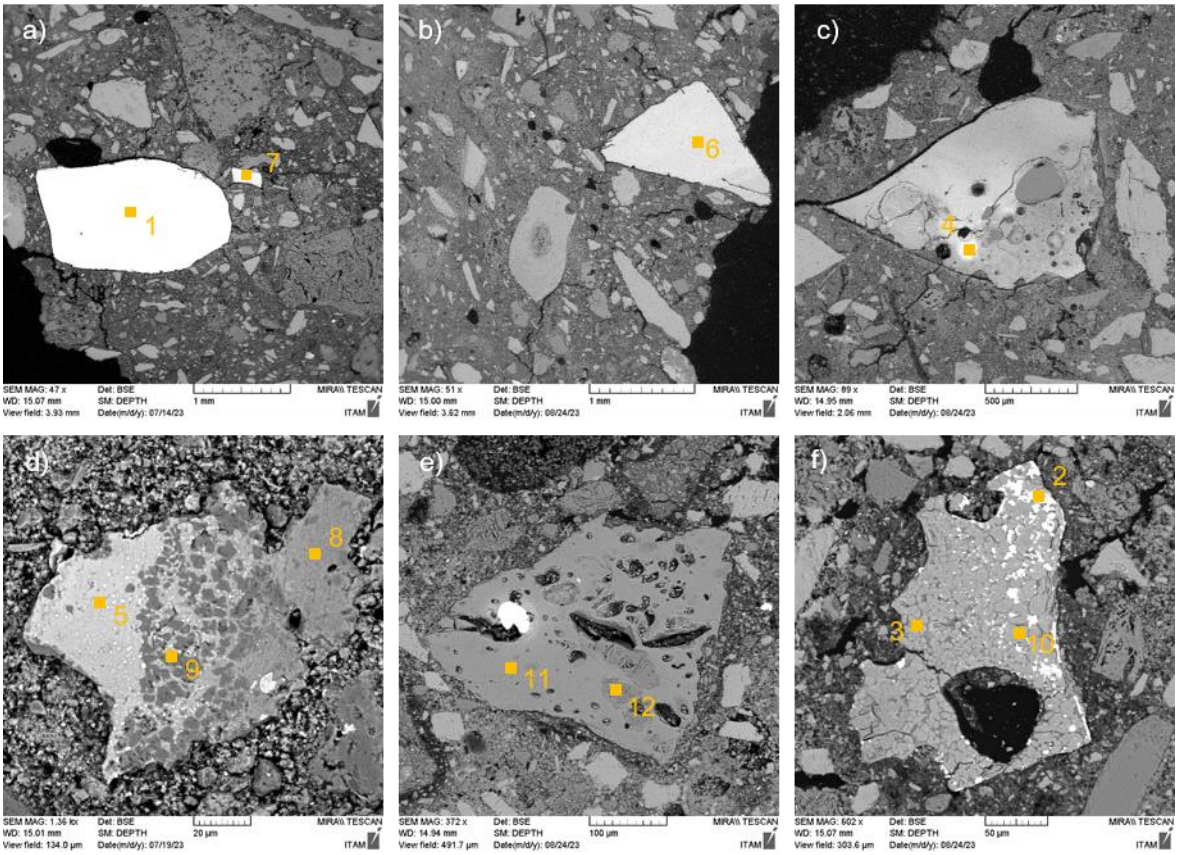

Figure 30. Glassy aggregates from the Krip (a-c) and frits from the Getzner mortar (d-f). Yellow dots indicate the points from which the EDS spectra shown in Tab. 8 were collected.

[183], [184]. On the other hand, no magnesium necessary for the formation of these phases was detected in the slag-like frits by EDS. Moreover, akermanite has also been reported to have crystallized in bricks fired above 1040 °C [185] and synthetic merwinite has been suggested as a suitable material for bioactive ceramics [186]. This means these phases might also come from ceramic aggregates discussed in previous paragraphs. In order to unambiguously identify the source of these minerals more focused methods such as x-ray microdiffraction could be employed.

Due to their inhomogeneity (varying chemical composition, varying texture and degree of sintering) we assume, the frit and glass aggregates as well as the chamotte shards probably represent waste materials from Neuhauser workshop´s own glass production. Neuhauser Company produced its own mosaic tesserae. A glassworks was a part of the company from the beginning. Apart from glass supply it carried out numerous chemical experiments [187]. Some of the experimental samples have been preserved in Tiroler Glasmalerei´s materials archive (Fig. 31)

Neuhauser´s mosaic cubes can be characterised as sodium-potassium-calcium glass with a higher content oxide [72]. This roughly corresponds to the chemical composition of glass aggregates in the studied mortars.

The reason why these aggregates were incorporated into Getzner and Krip mortars remains under question. We might only speculate whether Neuhauser mosaicists added these particles intentionally due to their pozzolanic activity enhancing mechanical strength of the binder or whether they simply wanted to recycle waste products. Esthetic aspects should also be considered. The addition of glass splinters to bedding mortars in order to achieve a brighter effect was documented in the mosaics of Hungarian mosaicist Miksa Róth [105]. However, varying chemical composition of both Hall mosaic mortars does not indicate a well-developed mosaic glass but resembles rather waste or experimental frits.

Table 8. SEM-EDS analysis of glassy shards from the Getzner and Krip samples. The spots of spectra collection are illustrated in Fig. 30.

	CaO	SiO2	Al_2O_3	MgO	K_2O	Na_2O	FeO	TiO_2	MnO	Cr_2O_3	F	Cu	Sn	Sb	Pb
spec 1	0.2	56.8	0.6		5.2	1.9	0.2	0.1			0.1	0.3			34.7
spec 2	28.1	10.2	3.1		1.2	2.2	1.3	11.1		0.2				15.3	27.2
spec 3	4.2	55.0	14.0	0.4		7.3	2.8	2.8							13.6
spec 4	3.2	64.1	7.6	1.5	2.9	7.5	1.4	1.4							10.3
spec 5	1.8	72.2	11.2	0.3	5.7	0.9	0.8		0.8						6.3
spec 6	8.9	67.6	1.5	0.6	10.5	3.9			1.3						5.7
spec 7	1.4	63.1	3.5	0.1	8.0	3.9	2.0	0.4	12.0						5.5
spec 8	5.5	54.3	31.1	0.1	2.3	2.5	1.1	2.0							1.2
spec 9	0.6	97.8	1.1			0.4									
spec 10		56.2	21.5	0.2	0.2	21.0	0.8								
spec 11	0.3	55.5	37.8	0.4	0.3	2.4	2.1	1.2							
spec 12		99.1				0.0	0.1	0.0					0.8		

Figure 31. Experimental mosaic glasses from the Tiroler Glasmalerei archive with a label containing the recipe for their preparation.

6.3.1.5 Organic compound identification (FTIR, GC)

As outlined in the previous sections, the bedding mortars of four sepulchral mosaics from Prague cemeteries (Sladkovský, Beneš, Peluněk, Bittnerová) contained large amounts of organic matter, which showed a peculiar odour, left greasy stains when the samples were dissolved in acid and affected TG/DTG curves of the samples. According to TOC analysis which also indicated the presence of some organics, the total organic carbon content ranged between 9 – 16 wt% in the Peluněk, Beneš and Sladkovský samples. To identify this compound infrared spectroscopy (FTIR) and gas chromatography (GC) were employed.

FTIR

FTIR analysis of powdered bulk mortars revealed that the bands of the inorganic matrix of the samples (mainly carbonates) have a significantly higher intensity compared to the organic bands and in the spectrum they completely overlap even the most characteristic bands of the organic component (Fig. 32). This problem has been encountered previously by other authors [188];. The organic component had to be

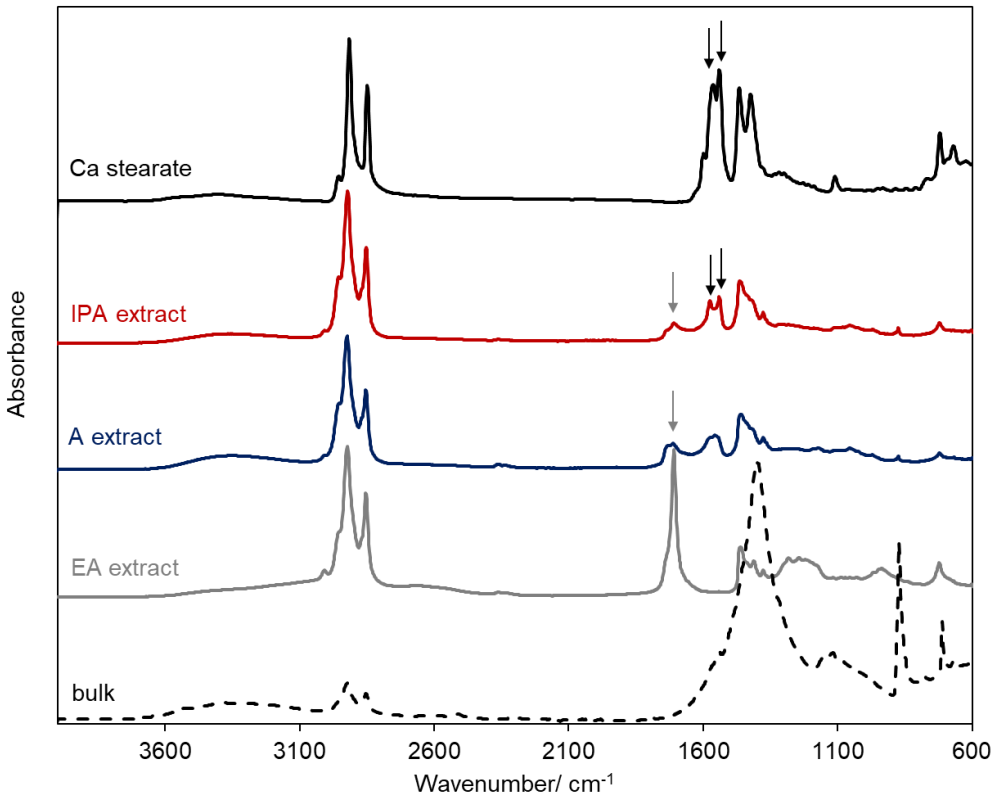

Figure 32. Comparison of the FTIR spectra of the bulk Peluněk mortar (dashed line; the most prominent bands belong to calcite overlapping organics) and mortar extracts in different solvents. A reference spectrum of Ca-stearate is also shown (black line). A – acetone, EA – ethyl acetate, IPA – isopropanol. Grey arrows indicate a C=O stretching vibration band representing tryglicerides from oil; black arrows point to bands of carboxylate soaps (products of lime and oil reaction).

extracted from the sample using a suitable solvent. Three extraction reagents - ethyl acetate, acetone and isopropanol (IPA) - were tested on the Peluněk mortar sample. The results of the test are shown in Fig. 32. It was found that the measured spectra corresponded to degraded vegetable oil. Vegetable oils are composed of triglycerides, i.e. esters of glycerol and several different fatty acids. The most suitable solvent was found to be isopropanol, as it was able to extract both the residues of the original triglycerides (characteristic band at 1740 cm^{-1}) and the newly formed products of the reaction of the oil with the alkaline binder of the mortar (carboxylate bands at 1570 and 1540 cm^{-1}) from the sample. Isopropanol was therefore used to extract the organic compound also from the remaining samples.

The FTIR spectra of authentic mortars´ IPA extracts are shown in Fig. 33. The figure provides their comparison with an IPA-extracted MO-20 reference sample containing 20 wt% linseed oil in proportion to dry compounds (see Section 7). A very close similarity between the reference sample and the Bittnerová mortar was observed. The remaining authentic mortars´ spectra were less similar but the bands undoubtedly pointing at the presence of oil compounds could still be identified. Tab. 9 gives an overview of the peaks identified in the FTIR spectra.

Similarly to oil paints, the processes resulting from an interaction of oil and a lime mortar can be grouped into polymerization, hydrolysis and oxidation of oil and soap

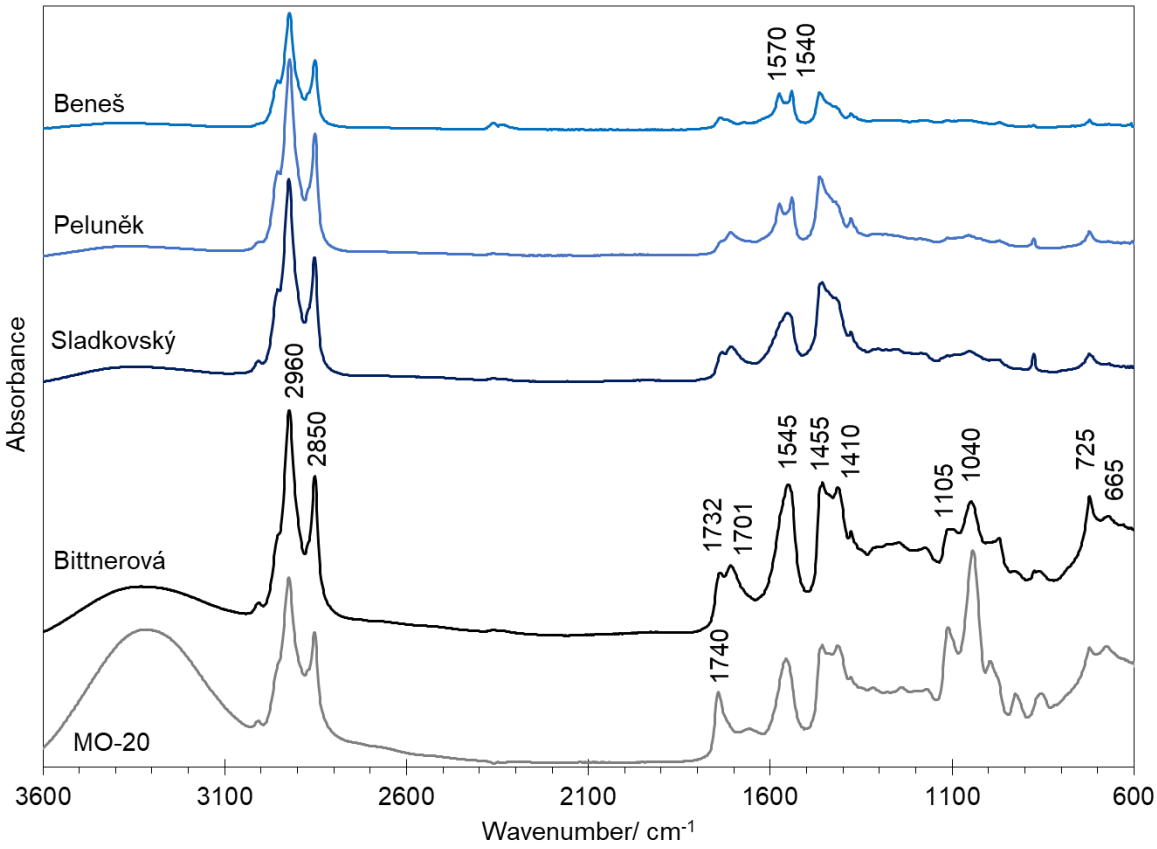

Figure 33. FTIR spectra of isopropanol (IPA) extracts of authentic mosaic mortars containing organics. MO-20 represents an IPA extract from a reference mortar with thhe addition of 20 wt% linseed oil.

formation (reaction between oil and Ca from lime). During the oil´s drying smaller molecules crosslink (polymerize) [189]. Photooxidative degradation of linseed oil eventually leads to the formation of aldehydes which can be further oxidised to carboxylic acids [164]. In addition, the amount of free fatty acids increases due to the hydrolysis of the original triglycerides. A portion of them may react with calcium to form insoluble metal soaps (carboxylates) [189]. In the FTIR spectra, the formation of a soap is marked by the disappearance of the very broad O-H stretching band around 3300 cm^{-1} and the replacement of the bands attributed to the C=O stretching around 1740 cm^{-1} with the bands of COO^- asymmetric and symmetric stretch around 1550 and 1400 cm^{-1} [190].

Table 9. Characteristic FTIR vibration bands identified in linseed oil-containing bedding mortars. The bands in bald are associated with linseed oil autoxidation and carboxylate formation.

position (cm^{-1})	intesity	vibration assignment
3310	b	v(OH) hydroperoxides and hydroxyl
3010	w	v(CH) unconjugated cis double bonds in FA chain
2960	s	v_a(CH) CH_2 in FA chain
2850	s	v_s(CH) CH_2 in FA chain
1740	s	v(C=O) in saturated esters
1732	ms	v(C=O) in esters
1701	w	v(C=O) in unsaturated esters or aldehydes
1570	ms	v_a(C-O) in carboxylates (COO^-)
1545	s	v_a(C-O) in carboxylates (COO^-)
1540	ms	v_s(C-O) in carboxylates (COO^-)
1455	w	δ(CH_2, CH_3) in tryglicerides (FA chain)
1410	w	v(C-O) in carboxylates
1105	w	v(C-O) in triglycerides ester linkage
1040	ms	deformation COOR
725	ms	$(CH2)_n$ rocking of the FA chain in tryglycerides (n>4)
665	w	Ca-O bond in carboxylates

v – stretching, a – antisymmetric, s – symmetric, δ – bending; b - broad, w - weak, ms - medium strong, s – strong; in bald – bands representing carboxylates

All these phenomena were observed in the authentic mortars´ spectra. The most striking features indicating saponification (metal soap formation) include the disappearance of the O-H stretching band at 3305 cm^{-1} and the appearance of one (Bittnerová, Sladkovský) or two (Beneš, Peluněk) stretching vibration bands around 1550 cm^{-1} representing the carboxylates. The reason why the vibration sometimes

splits into two bands and sometimes remains as a single band is not clear. Poulenat et al [189] observed a carboxylate vibration doublet in crude glycerol soaps, whereas pure Ca-palmitates and laurates gave only a single vibration band around 1530 cm^{-1}. In addition to saponification, the drop of the ester carbonyl stretching signal at 1740 cm^{-1}, its shift to lower wavenumbers and the formation of a second carbonyl stretching band at around 1700 cm^{-1} are illustrated in the spectra. These changes indicate the degradation of the original triglycerides and their breakdown into free fatty acids and other products such as aldehydes, whose carbonyl band appears at lower wavenumbers.

Due to the similarity of various vegetable oils´ spectra [191] it is very problematic to unambiguously identify a particular oil type in the mortars by FTIR. However, the use of linseed oil - either crude or polymerised by heating (stand oil) - seems by far the most likely option. Linseed oil was readily available in central Europe. Moreover, in the past it was quite often added to mortars as a water proofing agent [37], [188], [192], [193]. Its addition to mosaic mortars has been documented in historic recipes [94], [95] as well as in authentic mosaic works [96], [108].

Gas chromatography

Gas chromatography was employed in order to confirm the type of the organic compound. Palmitic, linoleic, oleic and stearic acid methyl esters were identified in the extracts of the Peluněk, Beneš and Sladkovský mortar samples (Fig. 34). The triglycerides of these fatty acids are the main constituents of linseed oil.

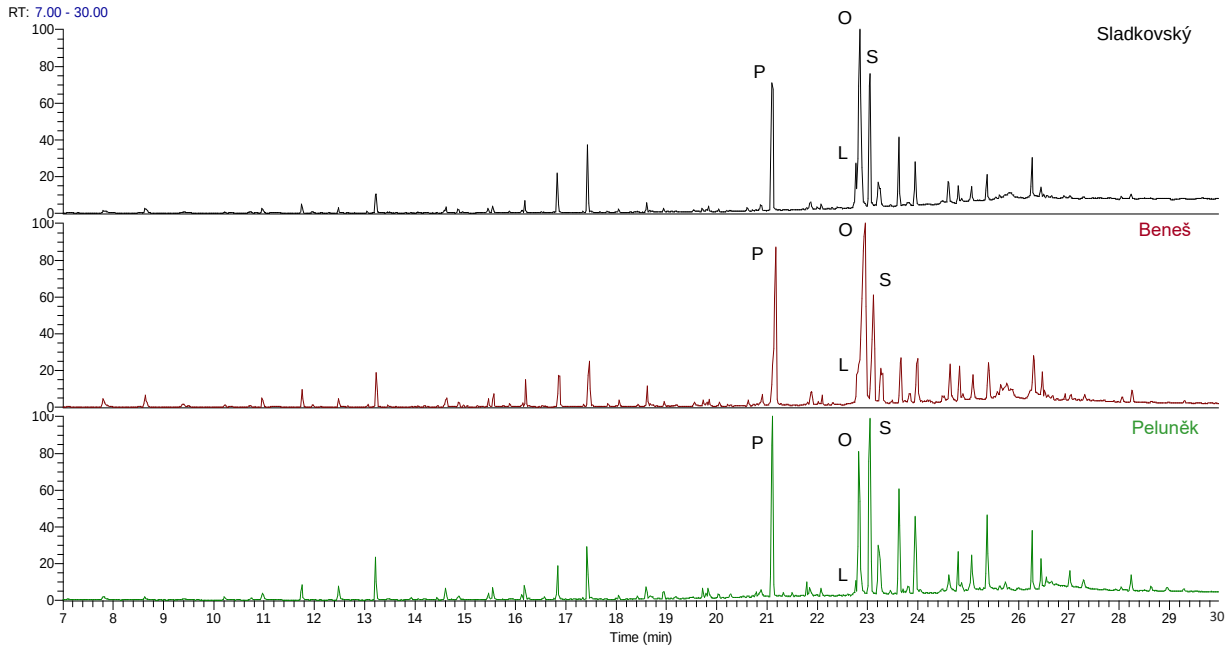

Figure 34. Full chromatographic records of the Peluněk, Beneš and Sladkovský mortar extracts´ derivatives. Detected compounds were P – palmitic acid methyl ester, L – linoleic acid methyl ester, O – oleic acid methyl ester, S – stearic acid methyl ester.

The presence of oil was confirmed in the Bittnerová sample too (Fig. 35). A calibration curve was constructed using model samples of known linseed oil concentration (Section 7). This made it possible to quantify the oil content in the mortar to be 38.5 wt%.This value seems to be enormously high. However, it is in a surprisingly good agreement with an estimation of linseed oil content using TG/DTG and EGA-MS (section 6.3.1.4) which was 37.1 wt%.

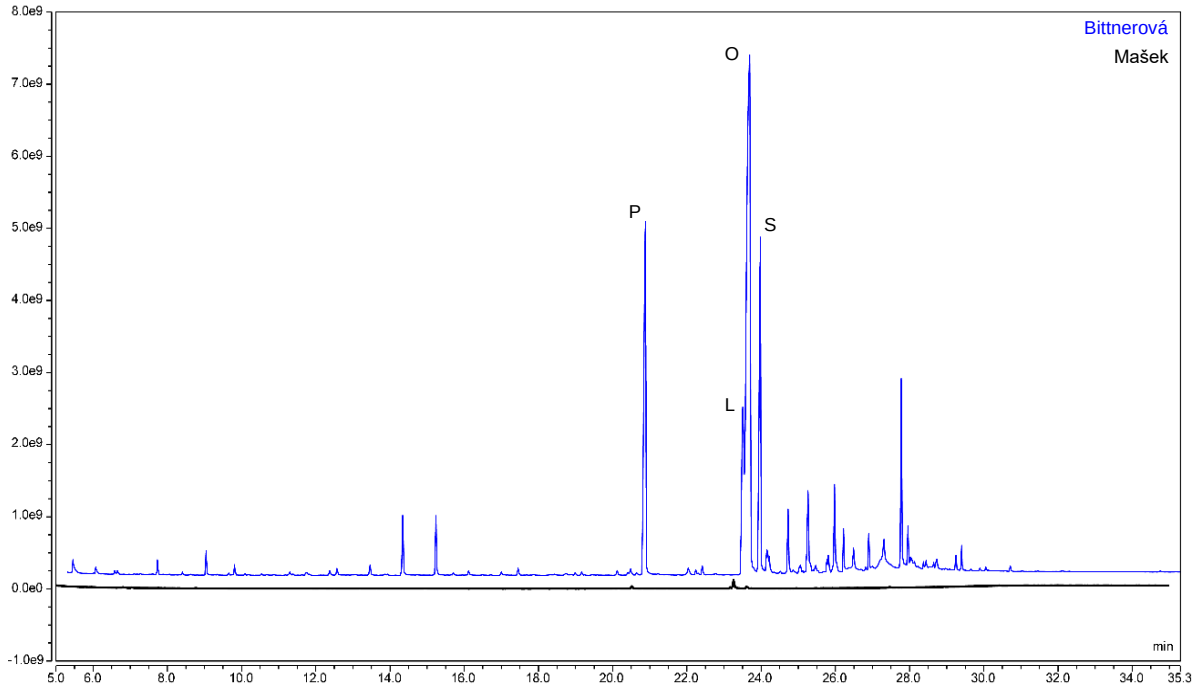

Figure 35. Full chromatographic records of the Bittnerová and Mašek mortar extracts´ derivatives. Compounds detected in the Bittnerová sample were P – palmitic acid methyl ester, L – linoleic acid methyl ester, O – oleic acid methyl ester, S – stearic acid methyl ester. The Mašek mortar was used as a reference representing samples with neglibile concentration of fatty acid derivatives.

As discussed in detail in section 4.4, linseed oil was a traditional compound of mosaic mortars. Water proofing effect of oil was known since Vitruvius´s times [26]. However, in the case of mosaic mortars linseed oil was added primarily not as a water repellent but as a plasticizer enabling longer workability. The presence of linseed oil reduces the contact of calcium hydroxide with CO_2 due to the high surface tension between the CO_2 transporting pore water and the hydrophobic matrix. This leads to the inhibition of calcium carbonate growth [188]. Thus, linseed oil slows down the carbonation process [165], [188], [192]–[194] and the mortar remains plastic for a longer time. This also explains the detection of non-carbonated portlandite in the Peluněk, Beneš and Sladkovský bedding mortars (Tab. 6).

Despite certain differences between the Sladkovský, Peluněk, Beneš and Bittnerová mosaic mortars (different contents of linseed oil and additives, different MgO/CaO ratios), they show a high degree of similarity. Their method of preparation (lime + marble dust aggregates + linseed oil) seems to have been inspired by the recipe

published by Gerspach [95] (see section 4.4). This author recommends this type of mortar for fixing small mosaics in easily transportable metal frames. The examined mosaics from Prague cemeteries generally fall into this category. Gerspach's book was easily available to Neuhauser mosaic masters - a copy is still kept in the company's library.

Due to its hydrophobicity, linseed oil improves frost resistance of mortars. On the other hand, it has a negative effect on the mechanical strength [194], [195]. In order to balance the advantages and disadvantages of its use, Čechová et al. [192] suggest that the optimum concentration of linseed oil in mortar is 1% by mass. However, the amount of oil recommended by Gerspach [95] is about an order of magnitude higher. The amounts of oil found in authentic samples are roughly in line with Gerspach's recipe. This could explain the severe deterioration of the mosaics, which resulted in the 'powdering' of the bedding mortar and subsequent loosening of the tesserae. An enormously high concentration of oil was found in the Bittnerová mortar bed (almost 40 wt%). This mortar showed the highest degree of deterioration of all oil-containing mosaics.

6.3.1.6 Summary I – Tirolean workshops´ mosaics

Late 19th/ early 20th century mosaics coming from two Austrian mosaic workshops (Neuhauser/ Tiroler Glasmalerei and Josef Pfefferle) showed quite a wide diversity of composition and technological features.

Four small portable mosaics from Prague cemeteries (Sladkovský, Peluněk, Bittnerová and Beneš) were probably transported as ready-made works fixed mostly in metal frames by mortars corresponding to the traditional 16th century recipes later adopted by Gerspach [95]. The mortars´ main compounds are lime + marble dust aggregates + linseed oil. The mortar from the Mašek mosaic is also based on lime and marble aggregates but the oil was missing. The Pfannerer mortar was characterised as a traditional *cocciopesto* with bricks and calcium carbonate aggregates. An introduction of innovative techniques and materials can be traced in Neuhauser´s as well as Pfefferle´s works – the use of early PC (Reith, Oberhofen, Hopfgarten) and, assumingly, the processing of the worshop´s glass production waste materials (chamotte ceramics, waste glass splinters and frits in the Krip and Getzner mosaic mortars).

Some mosaics (Bittnerová, Pfannerer, Mašek) have been affected by a severe deterioration due to moisture, atmospheric pollution and a special location (cemetery). The degradation was manifested by the formation of dark surface crusts rich in sulphates and nitrates, the disintegration of the binder and the loss of mosaic tesserae.

6.3.2 Foerster´s workshop

Czech mosaicist Viktor Foerster opened the first local mosaic studio in the Czech lands at the beginning of the 20th century, and by the time of his untimely death in 1915 he had completed more than 30 outdoor mosaic works [128]. The bedding mortars of five of his mosaics from an early stage of his mosaic career have been studied in this project. Their list can be found in Tab. 3. They include both sacral works (the façade of the Chapel of Our Lady of Sorrows in Barrandov, mosaics on the façade of the Church of St. Simon and St. Jude in Dolín, the Lauschmann family sepulchre or mosaic panels originally designed for a cemetery gate in Pelhřimov) and profane works (an ornamental mosaic in the gable of the Art Nouveau Hotel Evropa in Prague). The mosaic decoration of the Dolín church includes an attractive mosaic of Christ the Good Shepherd and a mosaic belt framing the portal of the church. Samples were excavated from both sites (Dolín Christ and Dolín Portal), but they turned out to be almost identical. Therefore, only a single representative sample labelled "Dolín" is sometimes presented in the results. Preliminary results of the research into Foerster´s mosaic mortars were published in a conference paper [36] which became the basis for this section. After Foerster's death, the family's mosaic tradition was continued by his wife Marie Viktorie. She designed a unique mosaic vault in the crypt of the Slavín monument in the Vyšehrad cemetery in Prague. Despite a gap of more than twenty years between the installation of the Slavín mosaic and Viktor Foerster's works, the results of the Slavín fixing mortar´s investigation were also included in this section. Marie Viktorie became an active mosaicist only after meeting her husband and learning this artistic technique from him [128]. Therefore, we assumed a certain materials similarity between her and her husband's works.

6.3.2.1 Microstructure and chemical composition (SEM-EDS)

As in the case of the Tyrolean mosaics, SEM-EDS proved to be the most useful tool for characterising Foerster´s mosaic fixing materials. Tab. 10 shows the average chemical composition of the analysed samples. Due to their hydraulic nature and degradation, the binders of most of the mortars investigated showed a significant degree of inhomogeneity. Therefore, EDS spectra were collected from areas representing an "average" binder and several measurements (at least 6) were made within each cross section.

All mortars consist of silicate aggregates (mostly SiO_2) and a hydraulic binder with Portland cement clinker residues. Their aggregates are made up of sand consisting mostly of quartz, feldspars and micas. Their size usually does not exceed 500 µm. Three samples (Dolín – Christ, Dolín – portal and Lauschmann) contained a large amount of brick fragments (Fig. 36). Moreover, frequent lime lumps were preserved in the Dolín sample. In the Foersterová's bedding mortar (Slavín), frequent grains of slag were identified (Fig. 36j-l), confirming our hypothesis about the nature of the "black dust" listed among the items in an archival invoice for the assembly of the Slavín mosaic (Section 4.6).

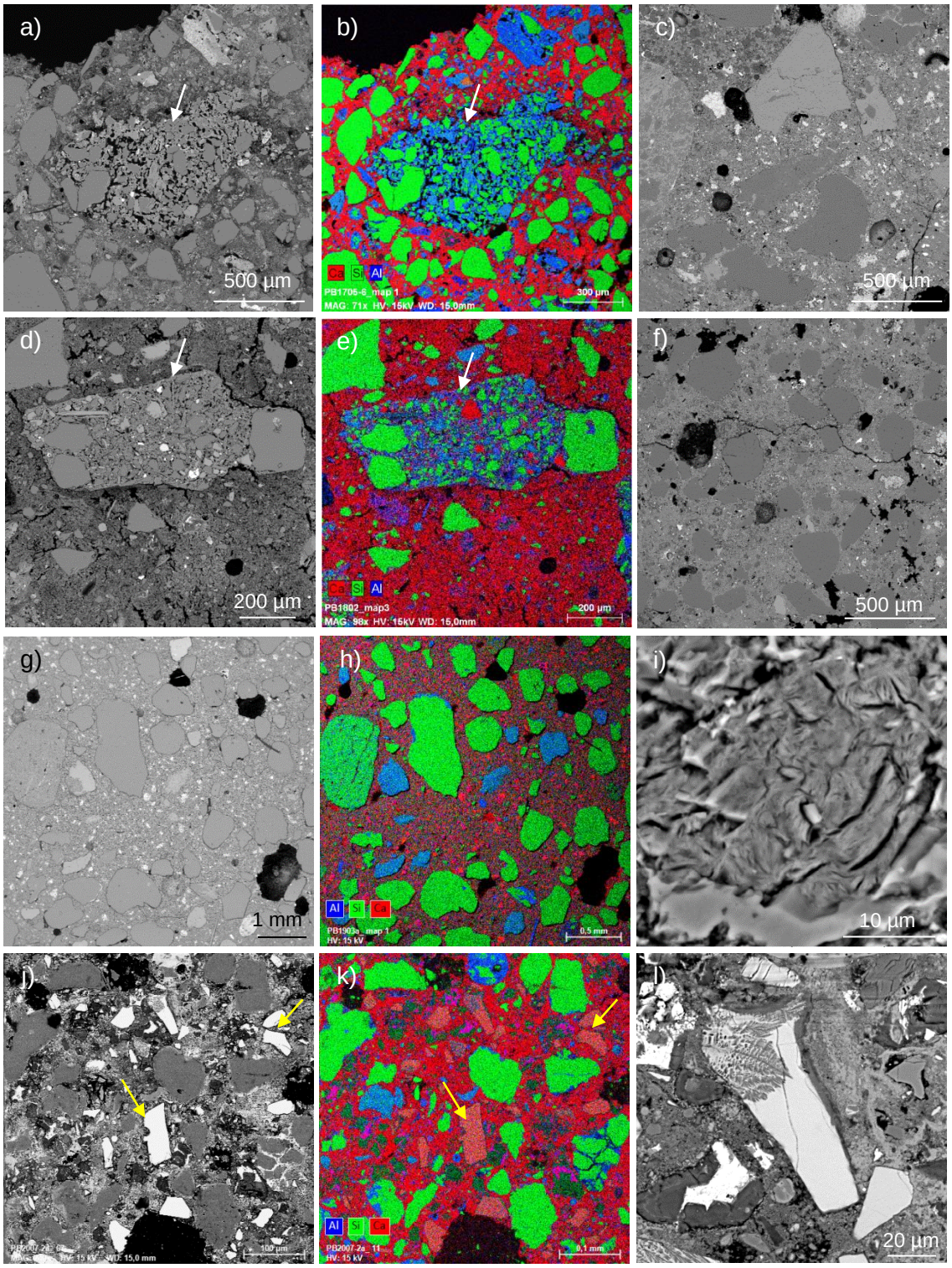

Figure 36. SEM images of Foerster´s mosaic mortar beds - a) Lauschmann – a brick particle in the centre, SEM-BSE image; b) Lauschmann – a brick particle in the centre, EDS map of the distribution of Al,Si and Ca; c) Pelhřimov – SEM-BSE image; d) Dolín – a brick particle in the centre, SEM-BSE image; e) Dolín – a brick particle in the centre, EDS map of the distribution of Al,Si and Ca; f) Barrandov – SEM-BSE image; g) Evropa hotel – BSE image; h) Evropa hotel – EDS map of the distribution of Ca. Si and Al; i) a detail of a clayey part of the Evropa hotel mortar binder; M. Foersterová´s Slavín bedding mortar with slag particles (marked with yellow arrows) – j) SEM-BSE image, k) EDS map of Ca, Si and Al distribution; l) a detail of a slag grain in the Slavín sample – SEM-BSE image.

Table 10. Chemical composition of the Foersters´ mosaic bedding mortars calculated from EDS spectra.

wt%	Lausch-mann	Dolín portal	Dolín mosaic	Pelhřimov	Barrandov	Evropa	Slavín
CaO	63.6	77.3	78.3	67.5	56.4	29.3	59.5
SiO_2	18.5	11.1	12.7	19.7	32.1	49.3	21.2
Al_2O_3	5.8	4.4	4.3	2.3	5.0	6.5	5.1
MgO	5.6	2.0	1.3	7.2	1.9	3.4	2.2
Na_2O	1.6	0.6	0.8	0.5	2.5	2.8	3.0
K_2O	0.8	1.7	0.7	0.3	1.0	0.4	3.1
SO_3	2.1	1.3	0.7	0.9	0.6	2.5	3.7
Cl	0.5		0.6	0.2	-	-	0.2
FeO	1.9	5.8	1.1	2.2	2.3	3.9	1.9
TiO_2	-	1.1	-	-	-	-	0.7
MnO	-	-	-	-	-	-	-
ZnO	-	-	-	-	-	4.9	-
C.I.	0.83	0.50	0.51	0.76	1.65	4.34	1.06

6.3.2.2 Mineralogical composition (XRD)

XRD Rietveld quantification results of Foerster´s bedding mortars are illustrated in Tab. 11. Rietveld analysis does not involve amorphous hydrates, therefore it should be taken just as indicative. Calcite (from the binder) and quartz (from aggregates) are the most abundant crystalline phases in all samples. Higher calcite content presumably indicates higher rate of carbonation.

Table 11. X-ray powder diffraction results. Asterisks indicate the presence of the compound.

(wt %)	Lauschmann	Dolín	Pelhřimov	Barrandov	Evropa hotel
calcite	18	54	*	46	41
quartz	66	33	*	35	46
feldspars	-	-	-	12	
albite	-	3	*	-	
microcline	-	3	-	-	7
micas	-	-	-	5	2
muscovite	-	2	-	-	
kaolinite	-	**	-	2	4
gypsum	16	**	-	-	
whewellite	-	*	-	-	

Contrary to SEM-EDS, no clinker phases were identified by x-ray powder diffraction. This might be explained by their low amount and also by their deterioration (see next section). In the Lauschmann sample 16 wt% of gypsum was detected. In the sample from Dolín (Christ the Good Shepherd) traces of whewellite, a hydrated calcium oxalate, were found. This mineral indicates a biological activity of microorganisms [161]–[163]. The identification of quartz, feldspars and other aluminosilicates confirms the SEM-EDS results and proves that sand aggregates were used in all mortars.

6.3.2.3 Thermal analysis

TG/DSC-EGA-MS signal of investigated mortars (Fig. 37, 38) can be divided to several regions. In the first region up to ca. 200 °C, water bound physically and chemically to C-S-H hydrates and gypsum is evolved. Physically bound water adsorbed on the surface of clayey components of bricks is also released at temperatures around 100 °C (scrivener). The gypsum peak (at 150°C) is strong in the Lauschmann sample indicating a large amount of gypsum in the mortar. Using TG data, gypsum amount was calculated to be 15 wt%. This is in a very good agreement with the XRD results (16 wt%). Gypsum was also detected in the Dolín bedding mortars both by XRD and thermal analysis. While the XRD method was not able to quantify this phase, the amount of gypsum calculated from TG mass loss was approximately 3 wt%.

Most of the samples showed no signal corresponding to portlandite decomposition around 450°C. The absence of the portlandite peak indicates that the mortars were heavily carbonated. However, one exception can be found (Evropa Hotel). According to the DTG data, this sample contains about 3 wt% of non-carbonated portlandite (presumably a product of C-S-H hydration). The DTG curve of this sample shows a rather significant peak at 120 °C. Its origin remains uncertain. The peak could be attributed to the release of water from some hydrated aluminosilicates such as kaolinite detected by XRD or some earthy compounds. A certain amount of ettringite could also be present [169], although this phase was not detected by XRD. But some ettringite-like grains were observed in SEM (Fig. 40c).

The Pelhřimov sample was collected from the corner of a steel frame into which the mosaic had been fixed. Only a limited amount of the mortar could be taken. The sample was apparently contaminated by the dust from the frame. In Fig. 38c the DTG peak around 250 °C corresponds to the thermal decomposition of iron hydroxides [196].

The EGA-MS curves indicate the presence of organic matter. As discussed in the previous sections, the use of linseed oil was quite common in traditional bedding mortars of portable mosaics produced by the Neuhauser Company. However, the presence of oil was not confirmed by either EGA-MS (weak or zero m/s 95 signals) or FTIR. On the basis of EGA-MS (see Section 7 for the methodology), the presence of organic matter in the Lauschmann, Dolín, Evropa and Pelhřimov samples can be excluded. On the contrary, an organic substance seems to be present in the Barrandov

sample (a distinct "hump" of the m/z 55 signal at 450 °C), but more detailed examination of the sample would be required to confirm the presence of oil.

Due to a very limited amount of sample, neither thermal analysis nor XRD diffraction could be performed on the Slavín sample.

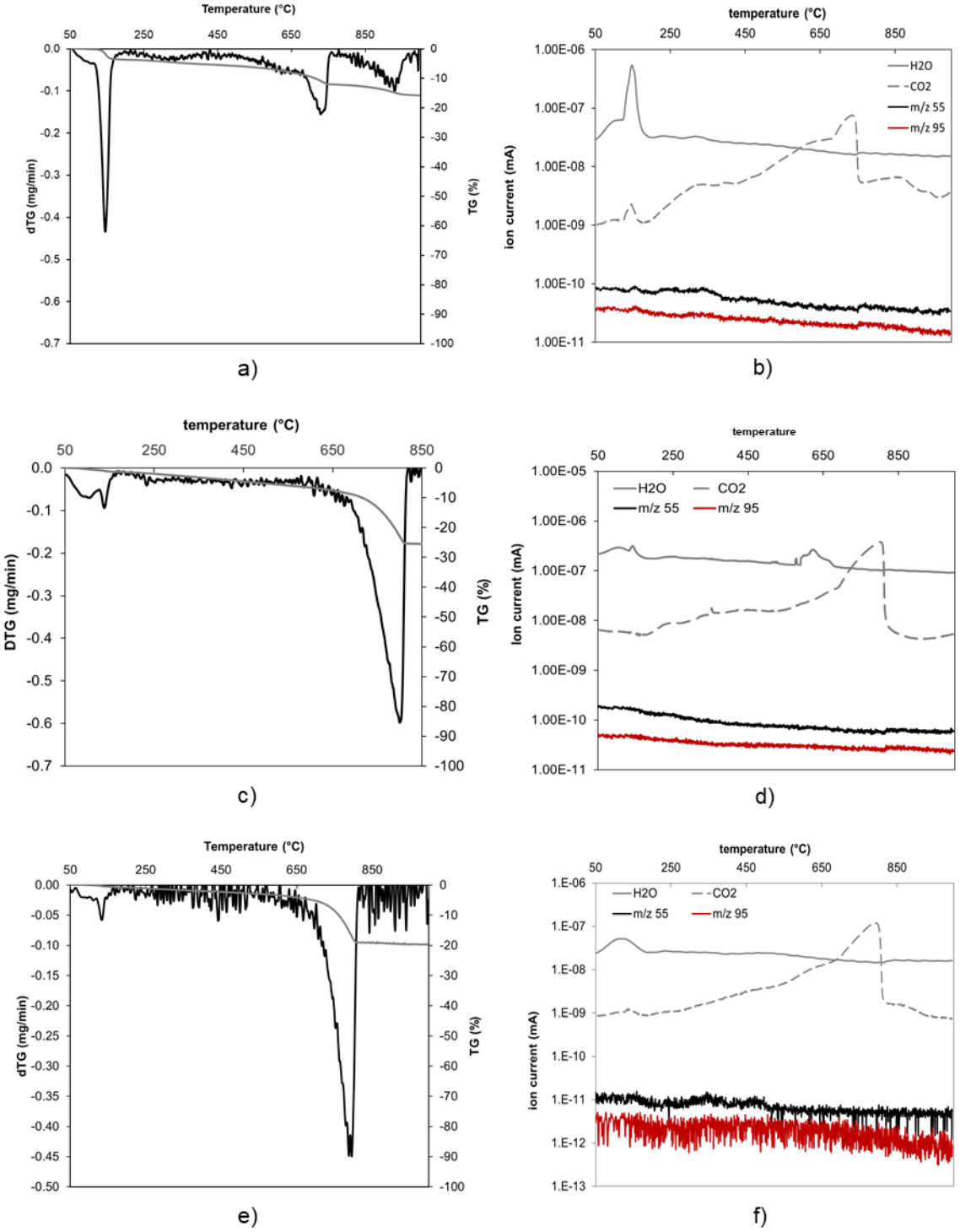

Figure 37. TG-DTG (left) and EGA-MS (right) curves of Foerster´s mosaic mortar beds (TG – grey line, DTG – black line). EGA graphs show evolved H_2O (solid line) and CO_2 (dashed line). Samples – a, b) Lauschmann, c,d) – Dolín-portal, e,f) Dolín-Christ.

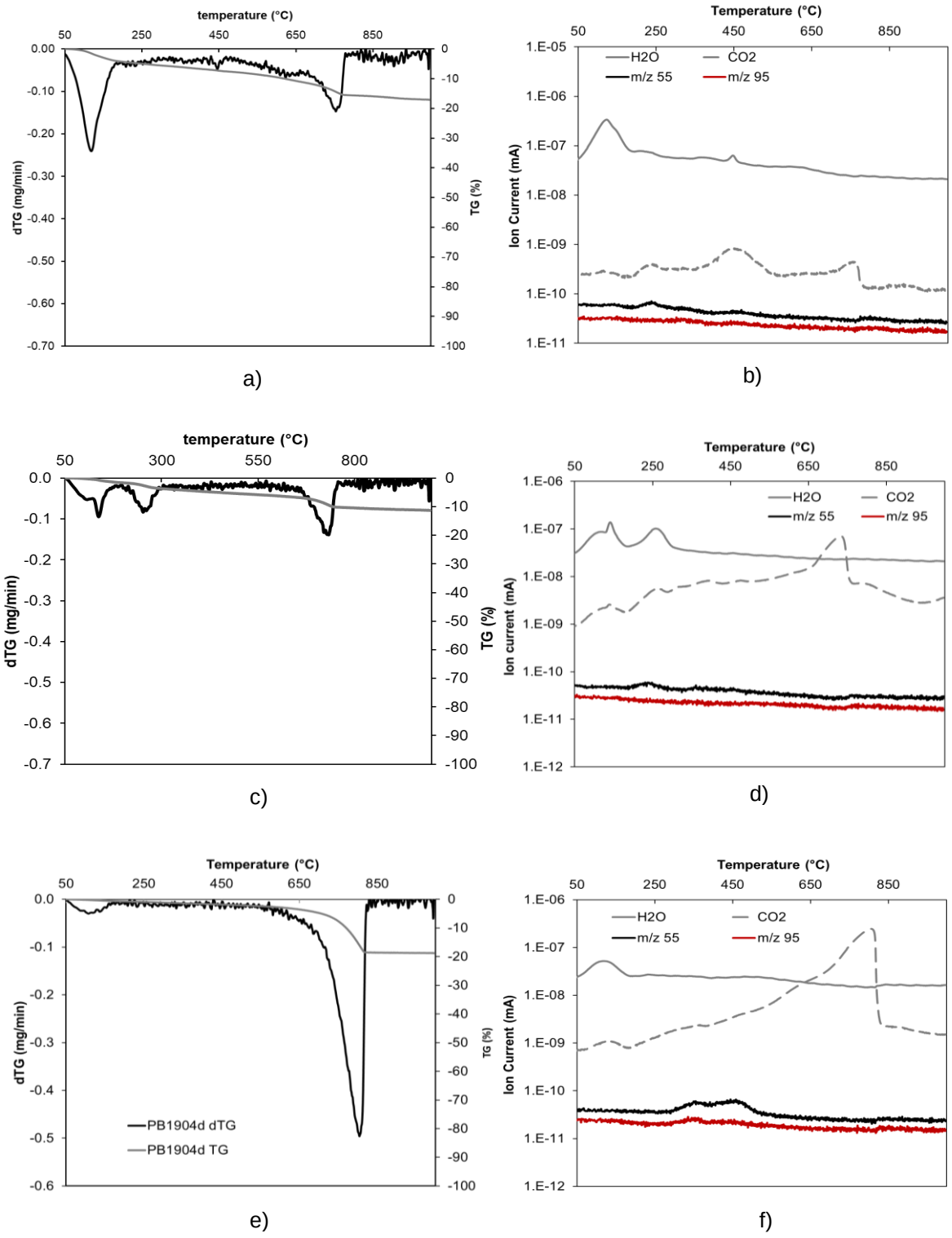

Figure 38. TG-DTG (left) and EGA-MS (right) curves of Foerster´s mosaic mortar beds (TG – grey line, DTG – black line). EGA graphs show evolved H_2O (solid line) and CO_2 (dashed line). Samples – a, b) Evropa hotel, c,d) – Pelhřimov, e,f) Barrandov.

6.3.2.4 Comparison of analysed bedding mortars

Two samples (Dolín and Lauschmann) looked quite similar both macroscopically and in the microscope. Apart from mostly SiO_2 aggregates and frequent clinker residues, particles of crushed bricks were identified in them (Fig. 36). While the original shape of many clinker residues has been preserved (Fig. 39-41), their chemical composition has changed dramatically due to the redistribution of Ca in the mortar system during hydration and subsequent carbonation. The original clinker calcium silicates have been decalcified. However, the shape of their crystals suggests that the clinkers were mostly of belitic composition although some sharp-edged grains, presumably originally alite, were also observed (Fig. 39a). Round belite crystals often occur in relatively coarse nests with distinct carbonated hydration rims (Fig. 39b). Optimally fired clinker residues consisting of amorphous silica cores surrounded by Ca-enriched rims (Fig. 39c) were also observed in both samples. These particles resemble those occurring in 19th century Roman cements (type 2-A in Gadermayr´s classification) [30]. However, the relatively large size (>10 µm) of the belite crystals or their hydrated and altered structures as well as the sporadic presence of alite relics may be indicative for Portland cement rather than hydraulic lime [197]. The microstructure with coarser clinker residues and the dominance of belite over alite lets us assume these early cements were fired at lower temperatures than modern Portland cements. The inhomogeneous distribution of firing temperature in the kiln can be documented by the abundance of overfired vitreous particles (Fig. 39d).

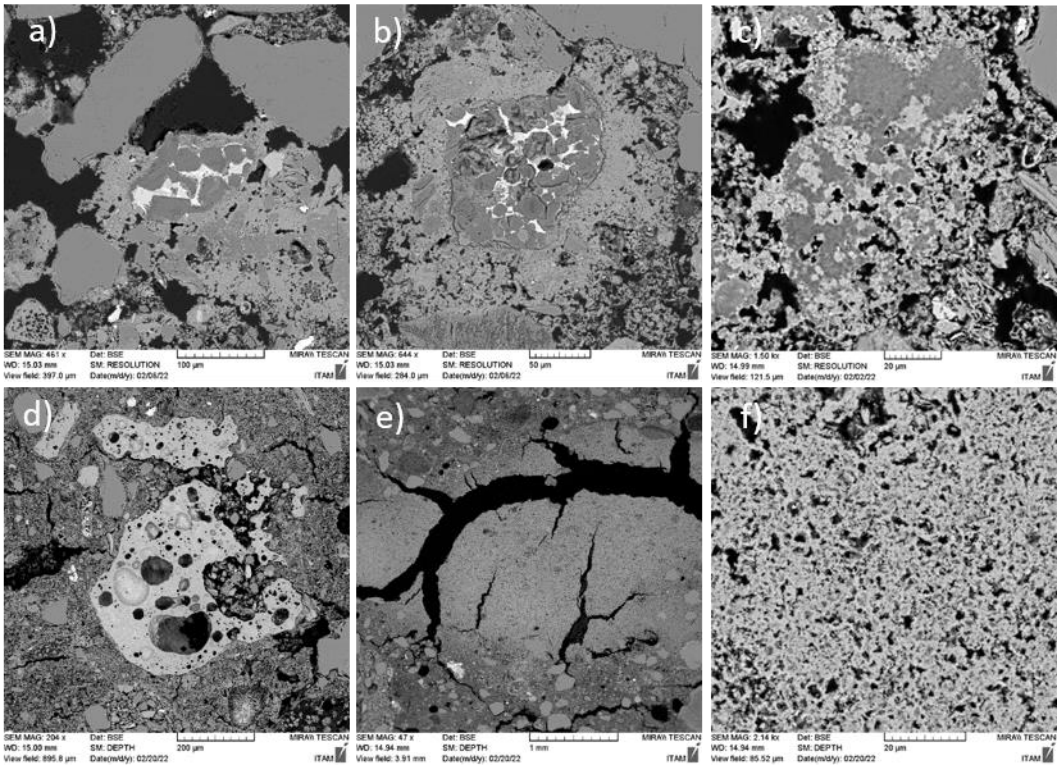

Figure 39. SEM-BSE images of (a-c) PB1705 (Lauschmann) and (d-f) PB1802 (Dolín).

However, despite these similarities the Lauschmann and Dolín mortars cannot be characterised as the same material. In the Lauschmann sample significant amount of gypsum was identified by both xrd and thermal analysis (16 wt% by xrd, TG mass loss calculations showed approximately 15 wt%). This amount of gypsum is considered to be too high to be attributed solely to the deterioration of the mortar. No gypsum crystals were found in the cross sections examined, and SEM-EDS showed a rather uniform distribution of sulphur in the binder. However, considering the TG and XRD results, gypsum seems to have been deliberately added. Similar to linseed oil in traditional mosaic mortars, the added gypsum could play the role of a setting retarder, extending the time within which some changes in tesserae arrangement could be made. Thus, the mortar used to fix the mosaic in the Lauschmann sepulchre was prepared by mixing Portland cement, gypsum, sand and crushed bricks.

As can be deduced from Tab. 10, the average chemical composition of the Dolín sample shows a higher CaO/SiO_2 ratio than the other samples. This is in agreement with the TG results (Fig. 37), where the Dolín sample shows the maximum mass loss associated with $CaCO_3$ decomposition. In addition, larger areas or sharp-edged grains filled with recrystallized $CaCO_3$ were observed (Fig. 39e, f). These represent fully carbonated fragments (lumps) of lime that had been hand-mixed with hydraulic Portland cement. Irregular porosity and cracks in the binder indicate that lime was the main constituent of the lime-cement mixture.

Our results do not support the conclusions of Rohanová et al [35], who focused on glass tesserae and also examined the mortar bed of the Dolín mosaic. Based on XRD results alone, they identified 34 wt% of gypsum and characterised the binder as a gypsum-lime mixture [35]. Their different interpretation of the mortar´s nature may be partly explained by the inhomogeneity of the binder and the lack of microscopic methods in the study.

Residual Portland cement clinkers from both Dolín and Lauschmann samples vary in size. The variation in clinker dimensions is a typical feature of early Portland cements [29]. The brick aggregates showed no evidence of pozzolanic reaction with the binder. We suggest that bricks were added for aesthetic reasons. Hydraulicity (and the consequent improved mechanical strength and durability) was provided by the addition of Portland cement.

An inhomogeneous distribution of clinker phases in terms of size and microstructure was also observed in the cross section of the Barrandov sample. The binder was fully carbonated and most of the clinker residues were decalcified. The micrographs from both the SEM and the polarising microscope allowed to distinguish different degrees of firing - from underfired particles rich in wollastonite and gehlenite (Fig. 40a,b), through “optimally” fired clinkers with “finger-like” belite extensions (Fig. 40c,d), to overfired glassy particles. The wide range of sizes and phases indicates an inhomogeneous temperature distribution in a shaft kiln. The “finger-like” belite is indicative of rapid cooling [198]. Both features are characteristic of early 20^{th} century Portland cements [29].

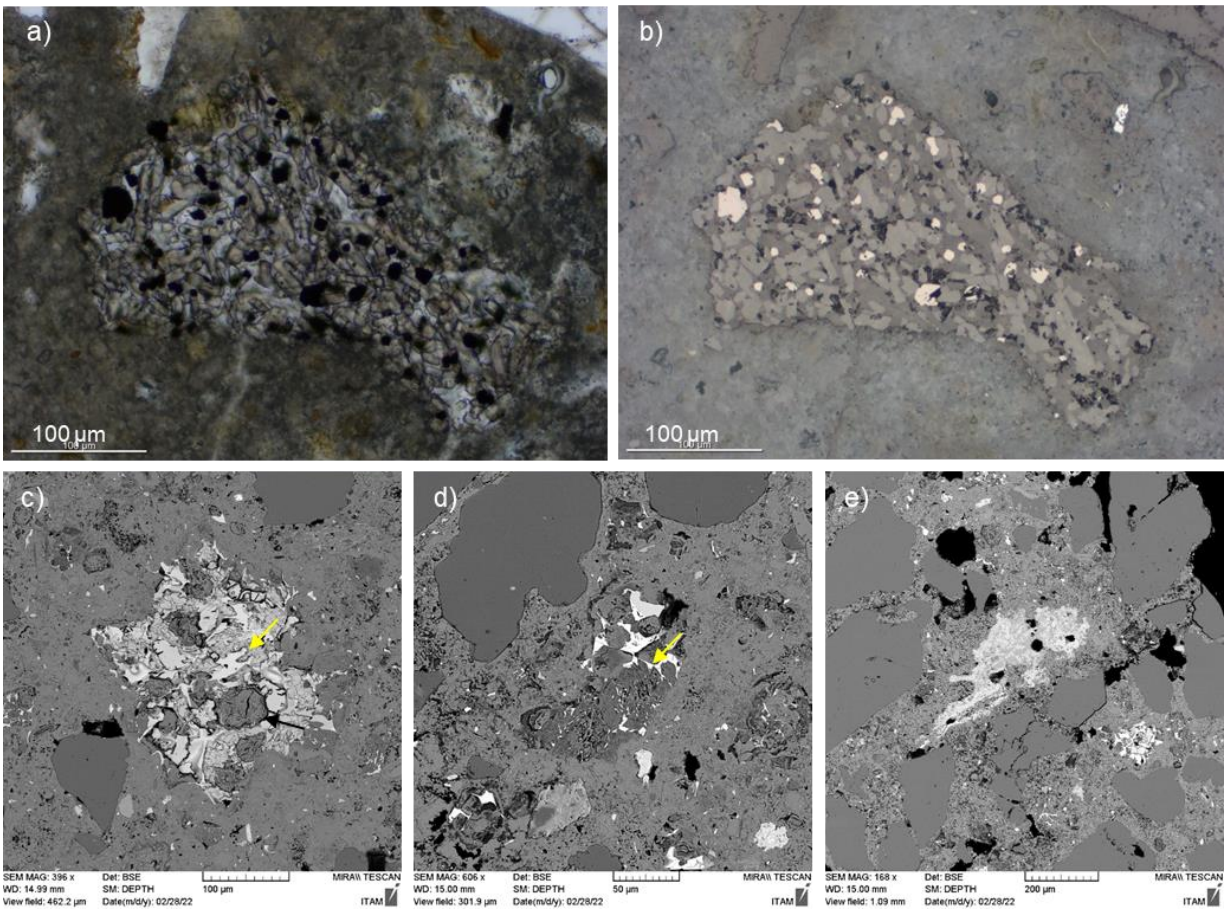

Figure 40. Clinker phases identified in the Barrandov early Portland cement binder - a) underfired cement grain, polarising microscope (PM), plane-parallel polars; b) underfired cement grain, PM, reflected light; c) belite-rich clinker phase with finger-like belite extensions (marked with yellow arrow) and ettringite (dark round particle in the centr of the clinker), SEM-BSE image; d) decalcified clinker phase with finger-like belite extensions (yellow arrow), SEM-BSE image; e) overfired glassy cement lump, SEM-BSE image. Photos a) and b) by Farkas Pintér.

In contrast to the clinker residues of other Foerster's samples, the unhydrated clinker residues of the Evropa hotel mosaic bedding mortar were almost non-carbonated (Fig. 41). They represent clear evidence for the use of Portland cement. The clinker grains are more homogeneous and two distinct interstitial phases (CA and CAF) can be clearly distinguished between the alite and belite grains (Fig. 41b). Although the chemical composition of the interstitial phases is not fully equivalent to today's C_4AF and C_3A, the formation of distinct interstitial phases is an indication of faster cooling [198]. The Portland cement used to fix the Evropa hotel mosaic was probably produced in a more advanced cement plant than the cements in other Foerter´s mosaics investigated.

Despite a lower degree of clinker carbonation (indicated by TG - Fig. 38a, b), the calcium content in an average binder matrix is extremely low (only 29.3 wt% Ca compared to 49.9% Si). In addition, the texture of the binder is extremely cracked. This suggests that Portland cement was probably mixed with a silica-rich compound to produce the Evropa hotel mosaic mortar. However, the nature of this compound remains in question. Some kaolinite was identified in the sample by XRD (Table 11). However, its content (7 wt %) is too low to dramatically affect the overall composition of

the binder. However, some clay-like structures were found in the binder by SEM-EDS (Fig. 36i). In the DTG curve, an intense peak appeared at 118 °C, but this should rather be attributed to the decomposition of ettringite [169] attacking the clinker residues, as indicated by SEM (Fig. 40c). The use of some earthy pigment would probably be

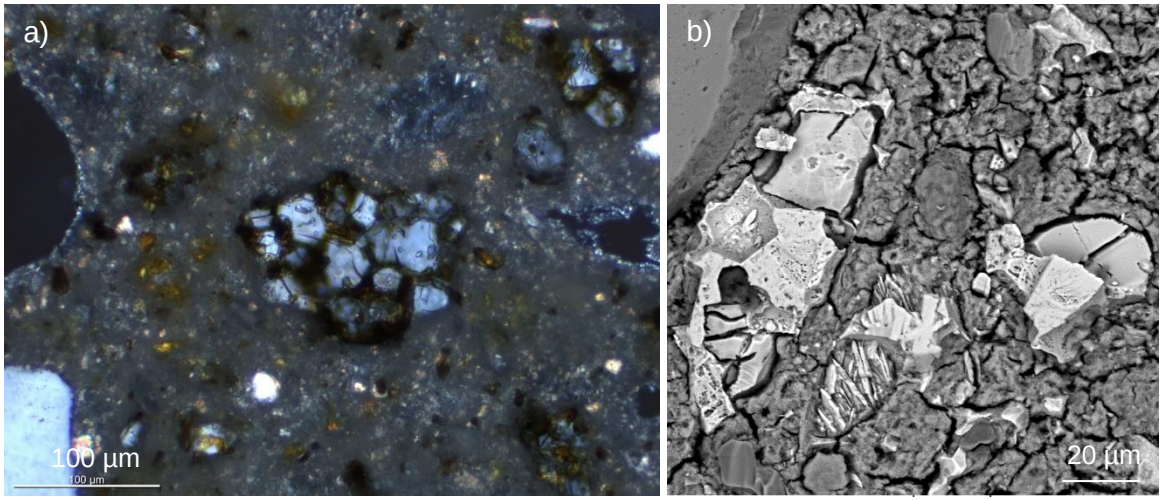

Figure 41. Portland cement clinkers in the Evropa hotel mosaic mortar – a) polariding microscope image, crossed polars; b) SEM-BSE image with two distinct interstitial phases.

reflected in the XRD and also EDS spectra, but they did not provide any evidence.

Viktor Foerster seems to have used Portland cement from the very beginning of his mosaic career. (The Chapel of Our Lady of Sorrows in Barrandov is considered to be his first completed mosaic commission [128]). However, the mosaic on the façade of the Church of Our Lady of the Rosary in České Budějovice, one of his very early works, sometimes referred to as the very first Czech mosaic commission he began [109], is said to have been fixed with a traditional lime mortar containing 25% fatty acids [107], [108]. In this study we were only able to examine about one seventh of Foerster's works. More research would be needed to make the following statement less speculative. It seems, however, that Foerster soon abandoned the traditional binders and, like his Austro-Hungarian colleagues Josef Pfefferle (Section 6.3.1) and Miksa Roth [39], was quite open to the use of Portland cement, a material that was still quite new in mosaic art at the time.

Foerster's widow Marie Viktorie commissioned Portland cement as the main component of the bedding mortar for the Slavín mosaic (section 4.6). In addition to Portland cement, the surviving invoice lists “black dust” (identified in this work as blast furnace slag - see Fig. 36), “white dust” and crushed bricks as components of the mortar. However, neither crushed bricks nor particles that could be attributed to "white dust" were identified.

6.3.2.5 Summary II – Foerster´s mosaic bedding mortars

Viktor Foerster used cement to fix his works at an early stage in his mosaic career. All the mortars extracted from his mosaics contained siliceous sand and hydraulic binders

with abundant clinker residues. In addition to the cementitious binder (early Portland cement), the Dolín and Lauschmann samples contained crushed brick fragments and other admixtures. In the Lauschmann sample cement and brick were combined with gypsum, in the Dolín sample the binder is a mixture of lime, cement and crushed brick. The binder used to fix the Evropa Hotel mosaic was probably not pure Portland cement, but a mixture of cement and an unspecified siliceous (clayey?) compound. Grains of blast furnace slag have been identified in the cement-based mortar of the Slavín mosaic designed by Foerter's wife Marie.

6.3.3 Other early 20th century mosaics

Apart from Foerster´s studio and Neuhauser/Tiroler Glasmalerei other mosaics workshops performed their work in the Czech Lands. Their activities have recently been studied in depth by other authors [124], [151] which has led us to reconsider some of our assumptions. For example, it has been proven that the mosaic from the Pfeiffer-Kral family's cemetery in Jablonec was made by Luigi Solerti's company Königlich Bayerishe Mosaik-Hofkunstanstalt [124], [151]. Říhová and Křenková [150] were also able to attribute the mosaic from the crypt of the Dittrich family sepulchre in Krásná Lípa to the Berlin company Pull & Wagner. The provenance of the other two mosaics included in the study (a mosaic panel depicting the Holy Family and a gold décor from the Schicht family sepulchre in Ústí) remains unknown. Due to the small amount of sample available, the Schicht and Holy Family mortars were analysed using only two or three basic methods (light microscopy, XRD and, in the case of the Schicht mortar, SEM-EDS and polarising microscopy).

6.3.3.1 Microstructure and chemical composition

All the mortars studied contain residual unhydrated Portland clinker. However, the Portland cement content of the binder varies among the samples. While the Dittrich and Pfeiffer-Kral mortars appear to have been prepared from a mixture of Portland cement and lime (with the Pfeiffer-Kral mortar containing a higher proportion of lime), no binder other than early PC was identified in the Schicht and Holy Family mortars. For these mortars, however, only a small amount of sample was available and therefore only a cursory examination was carried out. The samples also differed in aggregate composition. While some mortars (Schicht core mortar and Pfeiffer-Kral) were characterised as containing traditional mosaic aggregate in the form of angular marble dust, other mortars contain siliceous sand as an aggregate. The chemical composition of the mortars is shown in Tab. 12.

The mosaic decorating the sepulchre of Pfeiffer-Kral family (Fig. 42) appears to have been fixed in the most traditional way of all the mosaics from this group. It contains marble aggregates and crushed bricks. However, the Portland cement content, indicated by the presence of unhydrated clinker residues (Fig. 42c,f), does not allow the mortar to be characterised as a traditional *cocciopesto*. Brick particles are

inhomogeneous in size ranging from 10 – 500 µm. Apart from crushed bricks abundant quartz and carbonate grains ($CaCO_3$) can be identified by SEM-EDS.

Table 12. Chemical composition of early 20th century mortars determined by SEM-EDS.

	Pfeiffer-Kral (PB1708a)			Dittrich (PB1803)		Schicht (PB2009)
wt%	binder	Ca-aggregate	brick	bedding mortar	core mortar	bedding mortar
CaO	77.2	99.5	2.3	65.8	52.6	61.7
SiO_2	13.3	-	61.7	20.3	28.8	23.2
Al_2O_3	2.9	0.1	24.9	6.4	10.1	6.4
MgO	3.0	0.4	1.7	1.6	1.7	3.3
Na_2O	1.3	-	0.7	1.0	1.2	0.3
K_2O	1.3	-	2.0	1.5	1.5	0.1
SO_2	1.6	-	-	1.1	1.3	2.6
Cl	0.5	-	-	0.2	0.3	0.0
P_2O_5	-	-	-	0.6	0.3	0.1
Fe_2O_3	1.0	-	6.2	1.7	2.0	2.0
TiO_2	-	-	0.6	-	0.5	0.4
C.I.	0.50	-	-	0.95	1.70	1.11

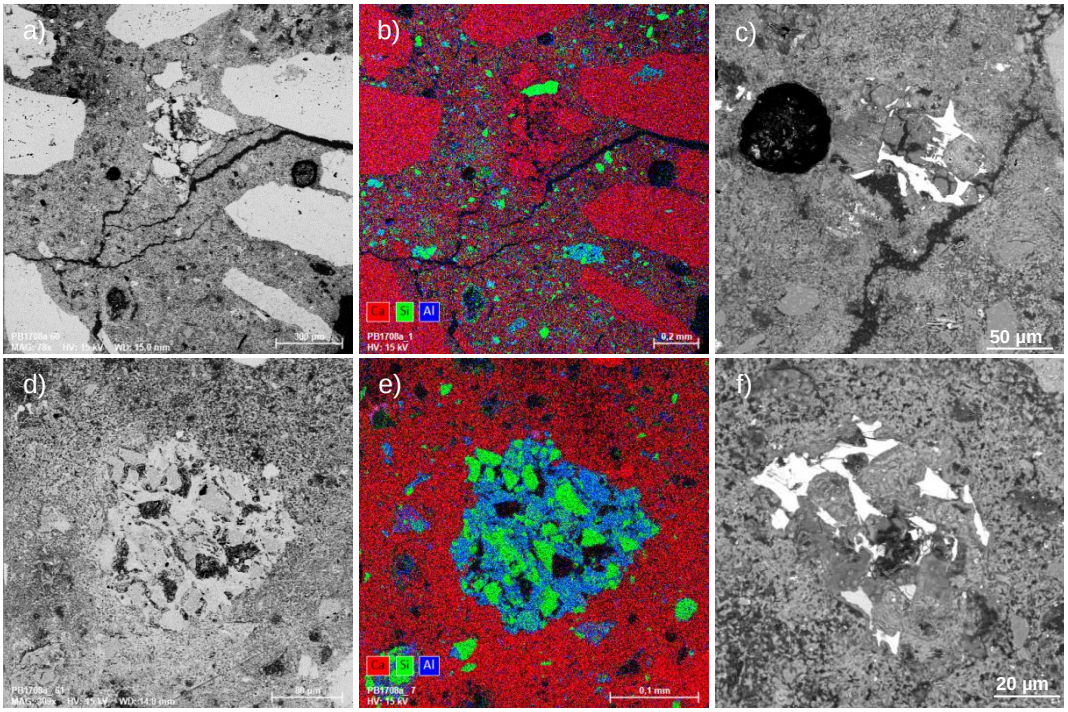

Figure 42. SEM-EDS micrographs of the Pfeiffer-Kral bedding mortar – a) SEM-BSE image and b) EDS map distribution of Ca, Si and Al in the mortar with carbonate (red) and fine brick aggregates (green-blue), c) SEM-EDS image and d) EDS map distribution of Ca, Si and Al in the matrix, a detail of a brick particle in the centre.; e,f,) unhydrated clinker residues, SEM-BSE images.

In the past, the Pfeiffer-Kral mortar was studied by Perná et al. [106] The authors found that the binder of the mortar was hydraulic. They attributed the hydraulicity to the pozzolanic reaction between the bricks and the binder. However, our results do not fully confirm their hypothesis. The bricks, if fired optimally, can react with the alkaline binder. This results in the formation of C-S-H and C-A-H phases, which provide greater mechanical strength and durability [19]. The hydrated C-S-H and C-A-H gel forms dense reaction rims [9], [8], [20], [21]. No reaction rims were observed around the brick particles in the Pfeiffer-Kral mortar. The cracked texture of the sample indicates a significant amount of air lime. On the other hand, the C.I. of the binder (Table 12) corresponds to a weakly hydraulic lime. Furthermore, the abundant fine SiO_2 and feldspar grains observed in the binder could represent the inert relics of otherwise fully reacted fine bricks [17], indicating a pozzolanic reaction. However, given the presence of Portland cement clinkers in the system (Fig. 42c,f), the hydraulicity of the binder should not be attributed solely to the pozzolanic reaction.

As can be seen in Fig. 43a, the mosaic on the ceiling and walls of the crypt of the Dittrich family sepulchre is attached to the wall by two layers of mortar. Both are carbonated and heavily altered by moisture. Both contain quartz aggregates and numerous relics of unhydrated decalcified clinkers. The lower core mortar is approximately 3 cm thick. The aggregates are coarser grained than in the bedding mortar, with some grains up to 2 mm in size. The bedding mortar of the mosaic is approximately 1.5 cm thick. The main compound of the aggregate is SiO_2. These

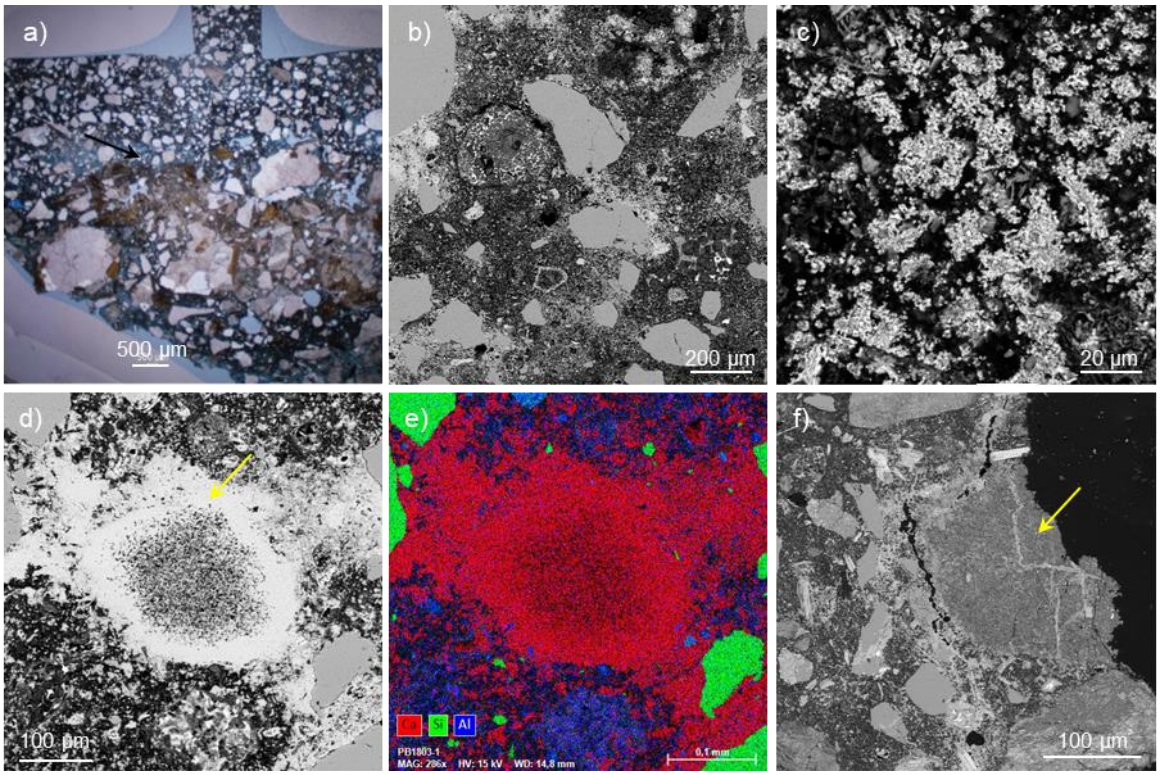

Figure 43. Micrographs of the Dittrich mosaic – a) overall view of the two mortar layers, b) detail of the binder with clinker residues and SiO2 aggregates, c) decalcified matrix of the bedding mortar with “popcorn-like” secondary CaCO3, d, e) lime lump in the bedding mortar, f) binder of the core mortar with lime lumps (arrow). a) – polarising microscopy, photo by F. Pintér, b-d, f) SEM-BSE; e) EDS map of Ca,Al and Si distribution.

observations are consistent with archival sources. Postal correspondence between the firm Puhl&Wagner and an architect's office designing the Dittrich family sepulchre provides interesting evidence of the application of two layers of mortar and also reveals the source of some of the sand aggregates [150]: *"… the two sand samples are also sufficient, namely the one from Tollenstein, partly mixed with coarser particles, for the lower ground* (core mortar) *and the one from the upper ground* (mortar bed) *for the upper mortar required for the actual setting of the mosaics."* ([150], p.224)

Tollenstein, present-day Tolštejn, is a village located about 8 km south east from Krásná Lípa. The existence of a small sand factory in a local area called Rozhled is documented as recently as mid 1940s [199].The correspondence also shows that the Berlin mosaicists did not directly install the mosaic in the sepulchre, but in letters to the architect's office they instructed the workers working on site how and of what to prepare the mortar mixtures. The architect's office even sent test samples of the mixed mortars to Puhl&Wagner by post for approval [150].

Both mortars are highly inhomogeneous. Due to carbonation and the effect of moisture, the calcium in the sample has been redistributed. Some parts are enriched with calcium (e.g. carbonated edges around the lime lumps - Fig. 43), while in other parts it has been leached out. In some places, a so-called "popcorn structure" can be observed, i.e. newly formed $CaCO_3$ crystals in a silicate matrix composed of amorphous SiO_2 , or Al_2O_3 (Fig.43c). In general, the binder of the underlying core mortar is more homogeneous compared to the mortar bed and contains coarser clinkers. The contact between the two layers represents a weak zone along which extensive detachment of the mosaic, including the mortar bed, from the crypt wall occurs. The weak zone probably developed due to different porosities of both mortars.

Lumps of lime were found in both layers. This, together with cracks in the binder, indicates that the binder was prepared by mixing Portland cement and lime. The lime lumps in the bedding mortar appear to be more frequent and less hydraulic than those in the core mortar. This is consistent with the C.I. values (Tab. 12). The core mortar appears to be generally more hydraulic, consisting of a mixture of early PC and hydraulic lime. Its lower part (Fig. 43) is heavily leached (dark colour in Fig. 43a).

The mosaic mortar from the Schicht family sepulchre (Fig. 44) also consists of two layers, which differ in their aggregates. The upper bedding mortar contains quartzitic grains, whereas the lower core mortar has carbonate aggregates (Fig. 44a,b). The mortar is generally less carbonated. The transition between the two layers is smooth and gradual. This indicates that the two layers were probably applied wet in wet. At the boundary between the two layers there is a large round lump of Roman cement. Its origin remains unclear due to the lack of comparable sections. The remaining clinkers are very coarse and not very hydrated. The low degree of hydration may indicate a low water/binder ratio. The interstitial phases of the clinkers are rather fine-grained, indicative of a faster cooling rate and suggesting the use of a clinker cooler. [198].

Although the Holy Family mortar was examined only by light microscopy, the method was sufficient enough to confirm the Portland cement binder (Fig. 45).

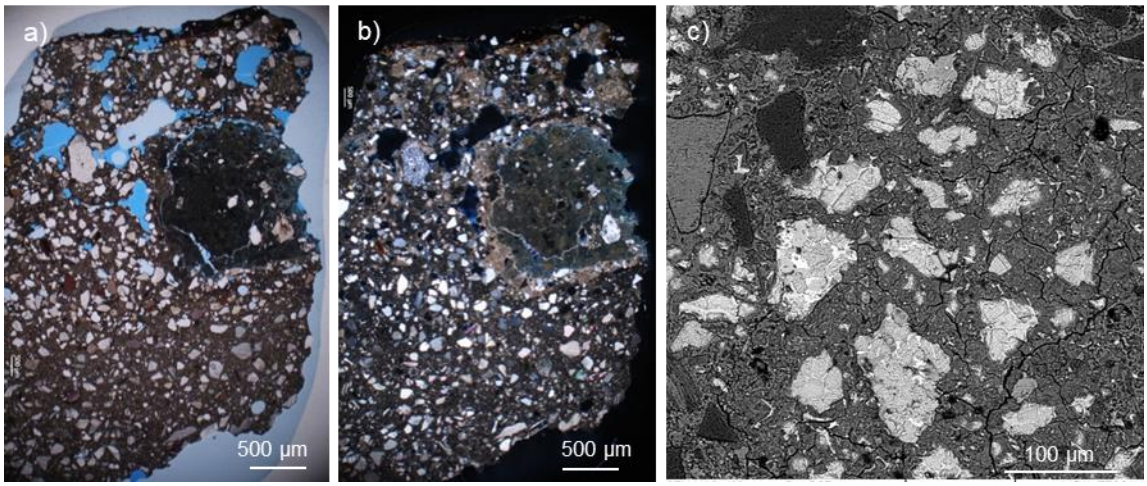

Figure 45. Schicht mosaic mortars – two layers of plaster a) polarising microscope, plane polars, b) polarising microscope, crossed polars, c) SEM-BSE image. In a,b) a round distinct Roman cement lump, c) a detail of the bedding mortar with coarse clinker (light).

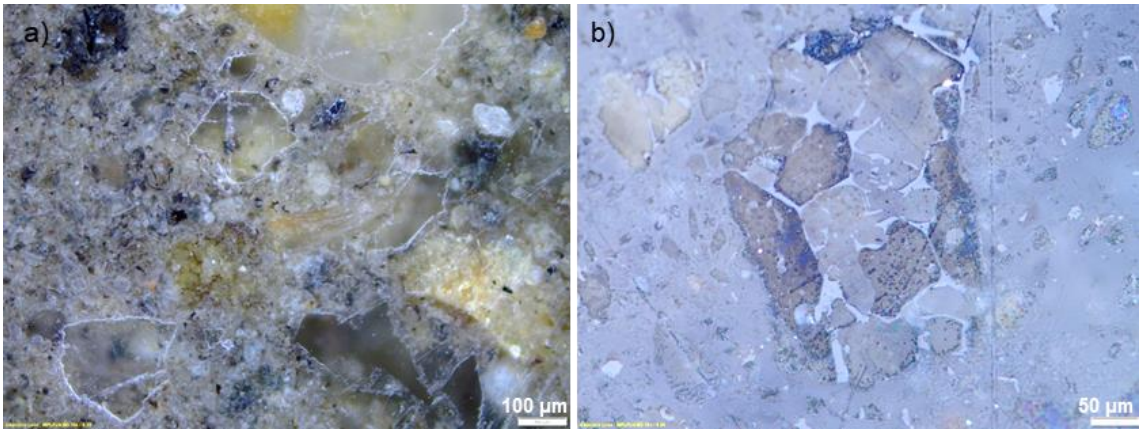

Figure 44. Holy Family bedding mortar in a light microscope, reflected light – a) mortar, bright field mode, b) a detail of a residual clinker with distinguishable alite (brown) and belite (grey) crystals, dark field mode.

6.3.3.2 Mineralogical composition

Tab. 13 summarises the results of the XRD analysis. Due to the limited amount of the samples and to the impossibility of estimating the percentage of an amorphous phase, the XRD results must be taken rather as indicative. Yet they are in a good agreement with microscopic observations and measurement.

The presence of clinker phases was only confirmed in the Schicht and Holy Family samples. As observed by microscopic methods (Fig. 44 and 45), both samples contained extremely coarse-grained (up to 200 µm) and relatively unhydrated and unaltered clinkers. Such particles can be easily detected by XRD. Vaterite detected in the Schicht sample can be attributed to the carbonation of C-S-H [51]. However, the detection of portlandite in the same sample suggests that the mortar´s carbonation has not been completed.

Table 13. X-ray powder diffraction results of the mosaics from the early 20th century.

wt%	**PB1708a** Pfeiffer-Kral	**PB1803-1a** Dittrich (bed)	**PB1803-1b** Dittrich (core)	**PB2005** Holy Family	**PB2108** Schicht
calcite	91.4	41.0	17.0	15.0	62.0
vaterite	-	-	-	15.0	-
dolomite	1.0	-	-	-	-
quartz	7.8	46.0	28.0	19.0	12.0
microcline	-	7.0	19.0	6.0	-
albite	-	-	19.0	-	-
kaolinite	-	4.0	-	-	-
biotite	-	2.0	17.0	-	-
muscovite	-	-	-	-	1.0
portlandite	-	-	-	-	8.0
C_3S	-	-	-	26.0	6.0
C_2S	-	-	-	19.0	8.0
C_3A	-	-	-	-	3.0

The dominance of calcite in the Pfeiffer-Kral mortar (91 wt%) is associated with a relatively high carbonation rate, the presence of lime in the binder and with carbonate aggregates. On the other hand, mineralogical composition of the remaining samples indicates the presence of sand (SiO_2 rich aggregates). Dolomite identified in the Pfeiffer-Kral sample indicates a dolomitic admixture in the binder. Other phases represent less abundant aggregate grains.

6.3.3.3 Thermal analysis

Fig. 46 presents the TG/DTG curves of the Pfeiffer-Kral and Dittrich bedding mortars. In this temperature interval water is released from the C-S-H phases [169]. The TG/DTG curves of the Pfeiffer-Kral mosaic look almost like the curves of an air lime. Mass changes in the temperature range up to 200 °C account for only 0.7 % of the total mass change. This supports microscopic observations indicating that the Pfeiffer-Kral binder is made up of lime and Portland cement with lime being the dominant compound (Section 6.3.3.1). Calcite´s dominance was also confirmed by XRD (Section 6.3.3.2). In the case of the Dittrich mortar bed, the total mass loss is generally lower (-13 wt%) compared to the Pfeiffer-Kral. The mass loss in the discussed temperature range

accounts for 0.5 %. This mortar was also described as a mixture of lime and Portland cement by SM-EDS.

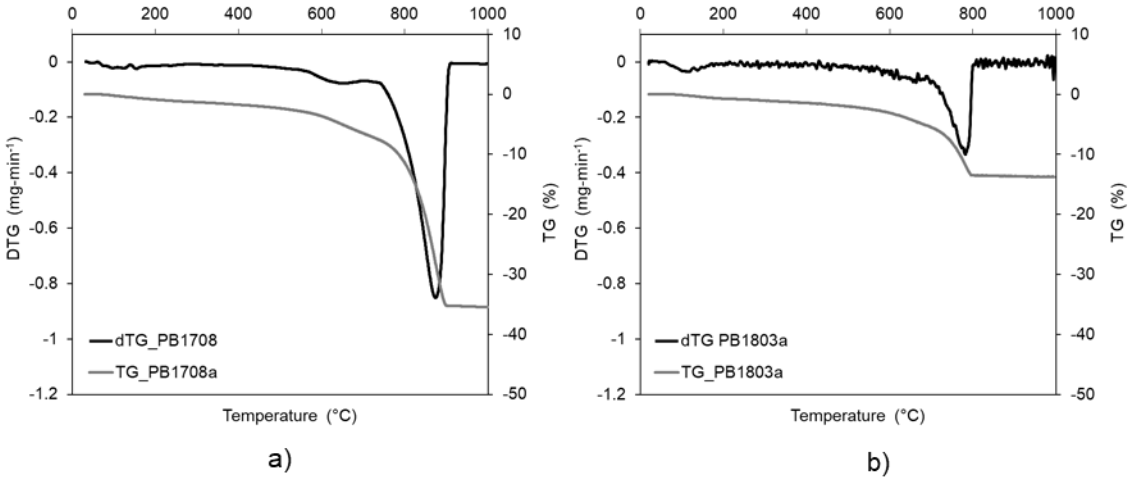

Figure 46. TG/DTG results – a) Pfeiffer-Kral bedding mortar, b) Dittrich mosaic mortar bed.

6.3.3.4 Summary III – Other early 20th century mosaics

Mosaics from the beginning of the 20th century were already commonly fixed with mortars based on Portland cement. The samples studied differed mainly in the composition of the aggregates. Crushed brick and marble dust were identified in the Pfeifer-Kral sample. The mortar binder is a mixture of lime and Portland cement, similar to the Dittrich mosaic from Krásná Lípa. The latter, however, contained sand as an aggregate. Schicht mortar is an intermediate type of mosaic mortar. Its binder is Portland cement, similar to the Holy Family mosaic. Different types of aggregates – siliceous sand as well as carbonate grains - have been found in its two layers.

6.3.4 Mosaics of the socialistic period

Six artworks of the socialistic period were included in this study. This period, i.e. the latter half of the 20th century was the time of centralisation. Most official mosaic works were produced after the design of renowned artists by professional mosaicists in a state-run studio Ústředí uměleckých řemesel (ÚUŘ – Central Art and Craft Studio). The mosaicists followed standardised procedures discussed in section 4.6. Portland cement is supposed to be an ultimately prevailing fixing material. Cement and sand are recommended for the mosaics´ fixation in a 1980s textbook written based on a decades-lasting experience of the ÚUŘ employees [49]. That is why quite a uniform composition of the mosaic mortars was expected.

Three of the art works studied were assembled by ÚUŘ - Sladký's mosaic on the façade of the Faculty of Civil Engineering, Kolář's stone mosaic in the former Officers' House in Milovice and an interior mosaic in the Pardubice railway station (signed by the

Česká mosaika studio, a direct predecessor of ÚUŘ). Ballardini's mosaic from the demolished Central Telecommunication Building was made by the artist himself in his studio at the Academy of Fine Arts in Prague. The tesserae were embedded in a bed of grey cement mortar and fixed to a concrete slab. Both the bedding mortar and the slab were analysed as part of this study. The last two works are sculptures made by Eva Kmentová and her husband Olbram Zoubek, outstanding sculptors of the time, in their private studio. Kmentová's mosaic sculpture consists of four layers - (1) the original cement body of the sculpture, (2) a corroded body with some remnants of metal reinforcement, (3) mosaic fixing mortars - 3a) a core mortar and 3b) mosaic bedding mortar into which stone tesserae were placed. Zoubek's work has no mosaic decoration on the top, but the material of the body has been studied as a reference to the statue of his wife.

6.3.4.1 Microstructure and chemical composition

The EDS results of the analysed samples are shown in Tab. 14. The chemical composition of all mortars roughly corresponds to an expected use of a Portland cement binder (in various degrees of carbonation) and quartzitic or aluminosilicate aggregates. Despite an almost fourty-year difference, Kmentová core mortar (from the 1950s) and Zoubek mortar (1990s) have a very similar chemical composition with a slightly increased CaO content (around 70 wt%).Figure 47 shows the microstructure of the Pardubice mosaic mortar bed as seen in the polarising microscope and in the SEM. The mortar shows dark colours in crossed polars (Fig. 47b), indicating a generally low degree of carbonation. Frequent quartz and feldspar aggregates (Fig. 47a,b) and abundant unhydrated clinker residues can be observed (Fig. 47e,f). Glass fragments were identified in the surface layer of the bedding mortar (Fig. 47a,b,g). Contrary to the splinters deliberately added to some of the mosaic mortars from the Neuhauser studio (section 6:3.1), these glass grains seem to represent the remains of a cracked and later partially released mosaic tessera, as they were observed only on the very surface of the bedding mortar. The main constituents of the glass are Si and Na, other elements detected were F, Zn, P, K, Al, Ca, Cl, Cr and Cu. The mortar also contains occasional foraminifera microfossils (Fig. 47c,d), which represent the original siltstone raw material and survived the firing process. Their shells are filled with a secondary siliceous incrustation.

Table 14. SEM-EDS chemical composition of the mortars from mosaics of the 2nd half of the 20th century.

wt%	**Ballardini** mortar bed	**Ballardini** panel	**Sladký**	**Pardubice**	**Milovice**	**Kmentová** body	**Kmentová** corroded body	**Kmentová** core mortar	**Kmentová** mortar bed	**Zoubek**
CaO	64.9	52.8	40.4	44.8	55.4	54.3	65.6	70.9	53.2	69.3
SiO_2	23.7	29.4	29.9	29.0	28.1	30.8	27.5	18.0	27.9	21.9
Al_2O_3	5.9	6.1	9.6	12.1	8.1	4.0	3.8	4.5	8.2	4.1
MgO	2.4	2.0	2.1	3.6	1.6	4.3	1.9	2.0	3.2	2.4
Na_2O	0.2	0.8	2.9	1.0	0.5	0.4		0.2	0.4	0.7
K_2O	1.4	3.9	0.8	1.7	0.5	0.9	0.3	0.3	0.8	0.1
SO_3	-	-	-	2.5	2.1	2.3	0.9	0.8	3.7	1.5
Cl	-	1.6	0.4	0.6	-	-	-	-	-	-
P_2O_5	-	-	-	0.3	-	-	-	0.0	-	-
FeO	1.7	3.7	2.4	3.7	3.4	2.6	-	3.2	1.7	-
TiO_2	0.6	-	0.8	0.6	0.6	0.2	-	0.3	0.5	0.2
MnO	0.1	-	1.1	0.3	-	0.6	-	-	0.6	-
ZnO	-	-	10.5	-	-	-	-	-	-	-
C.I.	1.1	1.7	2.2	1.9	1.6	1.5	1.2	0.8	1.5	0.9

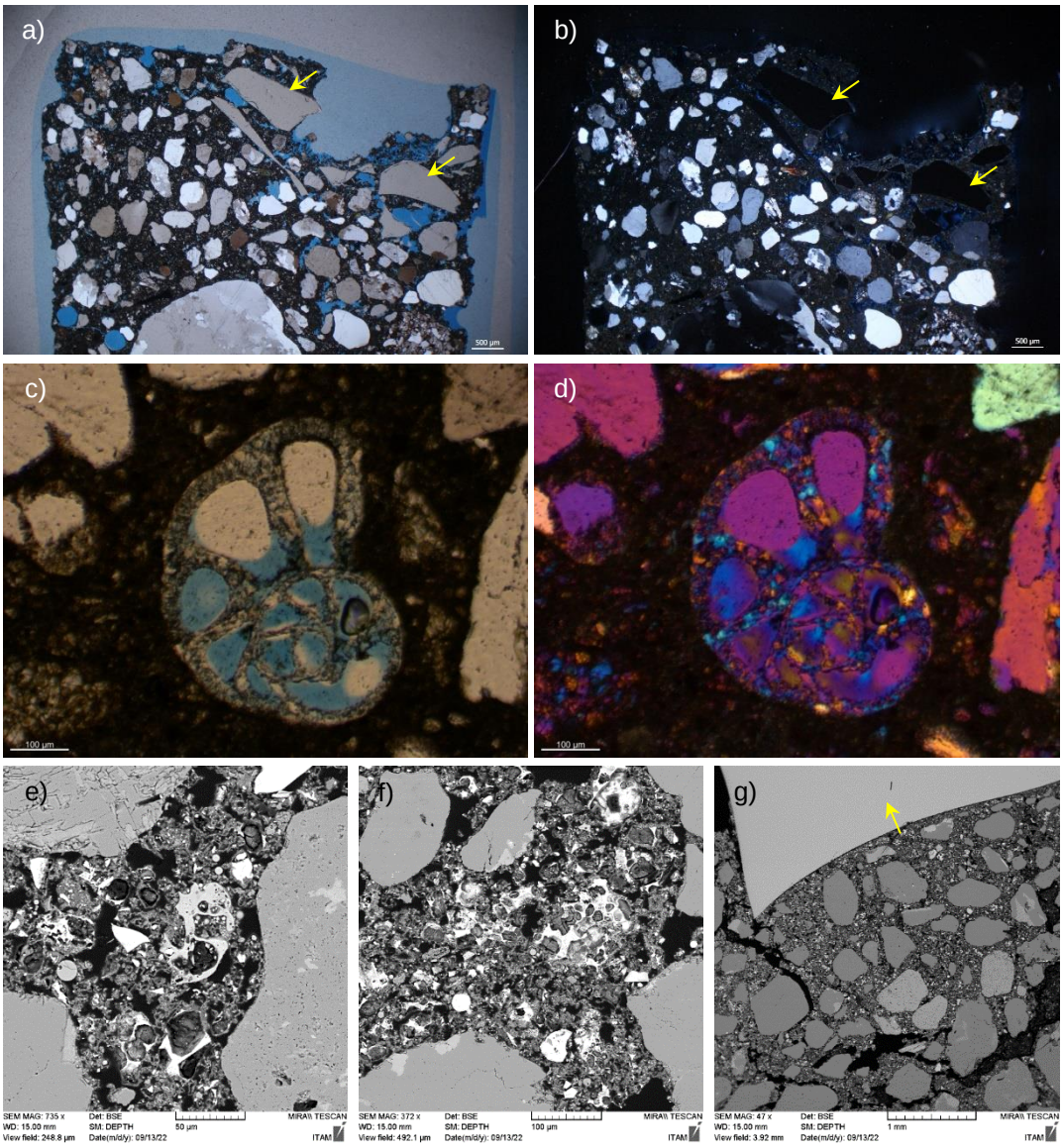

Figure 47. Pardubice bedding mortar in the polarising microscop (a-d) and in the SEM (e-f). Figure a) polarising stereomicroscope, plane parallel polars, b) crossed polars, c) a microfosil in plane parallel polars and d) in crossed polars; e,f) SEM-BSE image of clinker residues, g) tessera fragment in SEM-BSE image. Photos a-d by Farkas Pintér.

Figure 48 displays the microstructure of the Ballardini, Sladký and Milovice mosaic mortars. Compared to the other two samples, the Ballardini mortar shows a lower degree of carbonation. Undecalcified clinker residues (Fig. 48f) with clearly identifiable undecomposed alite and belite crystals occur both in the bedding mortar and in the underlying concrete slab. The concrete slab material (Figs 48 d-f) is coarser - with frequent aggregates over 1 and sometimes 2 mm (as observed macroscopically). On the other hand, the bedding mortar (Fig. 48 a-c) consists of fine sand made up of rock fragments rich in quartz and feldspar. Contrary to the slab, which appears to be made of a standard Portland cement, the Ballaradini bedding mortar contains frequent blast furnace slag particles. Unlike the slab, which appears to be made of standard Portland cement, the Ballaradini bedding mortar often contains blast-furnace slag particles.

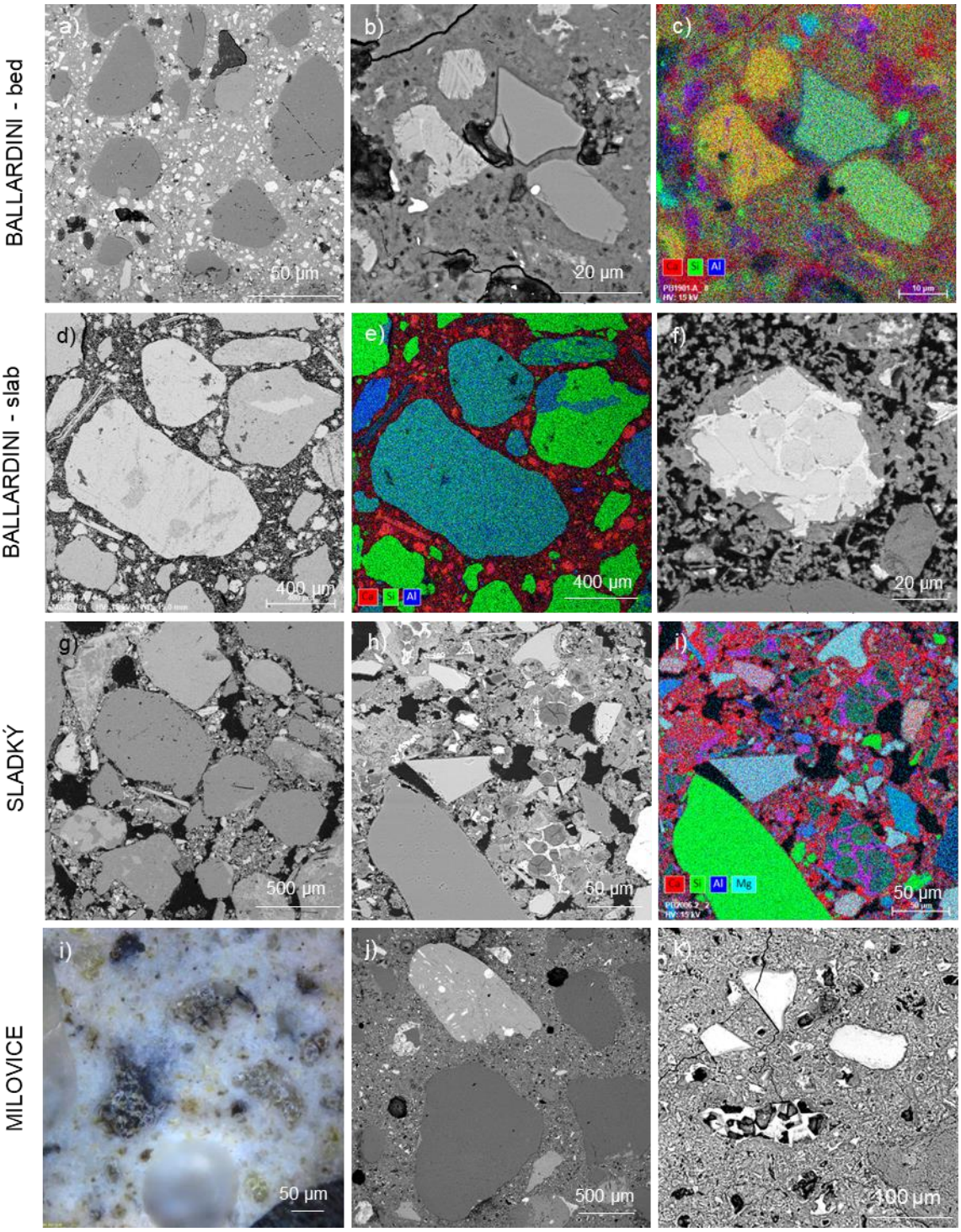

Figure 48. Micrographs of the Ballardini (a-f), Sladký (g-i) and Milovice (i-k) mosaic mortars – a) dark quartz aggregates and slag and clinker rich binder, SEM-BSE image; b) detail of residual clinkers (centre left) and blast-furnace slag grains (centre right), SEM-BSE; c) EDS map of Ca, Si and Al distribution in the same area (clinkers – yellow, slags – light green); d) SEM-BSE image and e) EDS map of aluminosilicate aggregates and clinker (bright red spots) rich binder, f) a detail of an unhydrated clinker residue, SEM-BSE; g) aluminosilicate aggregates and binder, SEM-BSE; h) SEM-BSE image and g) EDS map of the binder with frequent clinker residues and sharp-edged slag grains; i) LM image, reflected light of a binder with clinker residues (dark grains), i) SEM-BSE image of quartz and aluminsilicate aggregates and a binder with clinker residues; k) a detail of slag grains (light) and a decalcified clinker, SEM-BSE.

Slag aggregates were also identified in the Sladký and Milovice samples. While in the case of the Sladký bedding mortar slag grains were very abundant, in the Milovice mortar they occurred rather sporadically. Sand, consisting of round grains of quartz and feldspar, constitutes the inert fraction in both mortars. The average size of the sand aggregates is 500 µm. In contrast to the Ballardini sample, a higher rate of carbonation (the presence of decalcified clinker residues) is observed.

The Sladký sample used for the EDS analysis was taken from the very top of the mosaic. An increased concentration of zinc was detected in the EDS spectrum. The zinc was most likely leached from the zinc sheets of the roof [38].

According to SEM-EDS four different mortar materials could be distinguished in Eva Kmentová´s sculpture (Fig. 49). The most characteristic feature of her and her husband´s works is the use of asbestos cement. This material was found in the body of both Kmentová´s and Zoubek´s sculptures. While in Zoubek´s sculpture chrysotile asbestos ($Mg_3(Si_2O_5)(OH)_4$) was present, two types of asbestos were identified in the Kmentová-body sample – (1) fibrous crystals with a chemical composition corresponding to amphibol (probably amosite – $Fe^{2+}_2Fe^{2+}_5(Si_8O_{22})(OH)_2$ in the original uncorroded body and (2) chrysotile asbestos which appears darker in the SEM-BSE due to the lack of iron. Less harmful and generally more encountered chrisotile was found in a broken piece of corroded mortar from the inner part of the body as the traces of a corroded metal reinforcement have been preserved in the sample. An inert compound was missing in both the Kmentová and Zoubek mortars from the bodies of the sculptures. They both contained frequent grains of blast-furnace slag and unhydrated residues of Portland cement clinker.

In the case of Kmentová´s work, a core mortar adheres to the body of the sculpture. It separates the sculpture´s body from a very fine-grained grey mosaic mortar bed. The core mortar is the only material within Kmentová´s sculpture with inert aggregates (prevailingly quartz and feldspars). Its binder is hydraulic and contains numerous clinker residues. Due to a slightly increased CaO content we might speculate whether the binder is not a mixture of Portland cement and lime. However, no binder-related particles that could prove this assumption were found. On the contact with the upperlying mortar bed a denser and Ca-enriched zone was formed. The smooth transition between these two layers could indicate the upper layer was laid on the wet core mortar. The upper bedding mortar contains residual Portland cement clinker and blast-furnace slag.

The addition of blast furnace slag adversely affects the mechanical strength of cement. On the other hand, it acts as a hardening retarder and also reduces cement shrinkage during drying [6]. Both of these properties may have played a role in the choice of this material for the use in mosaic, as well as its more favourable price compared to pure Portland cement. In the In their mosaic textbook [49], Tesař and Klouda recommend working with cement labeled 250-300 when fixing mosaics. These numbers are based on the now obsolete classification of cements into classes based on strength. Class 300 is not mentioned in the classification (the authors of the textbook probably had class 325 in mind). Two types of blended cements correspond to these categories -

slag-portland cement (class 250-300) or blast-furnace cement (class 250) [200]. Slag-portland and blast-furnace cements are distinguished by their slag content (blast-furnace cement contains more slag). The identification of slag grains in all the ÚUŘ-made “socialistic” mosaic mortar beds studied indicates the standardised process of mosaic bedding mortars preparation recorded by Tesař and Klouda was indeed commonly applied in practice.

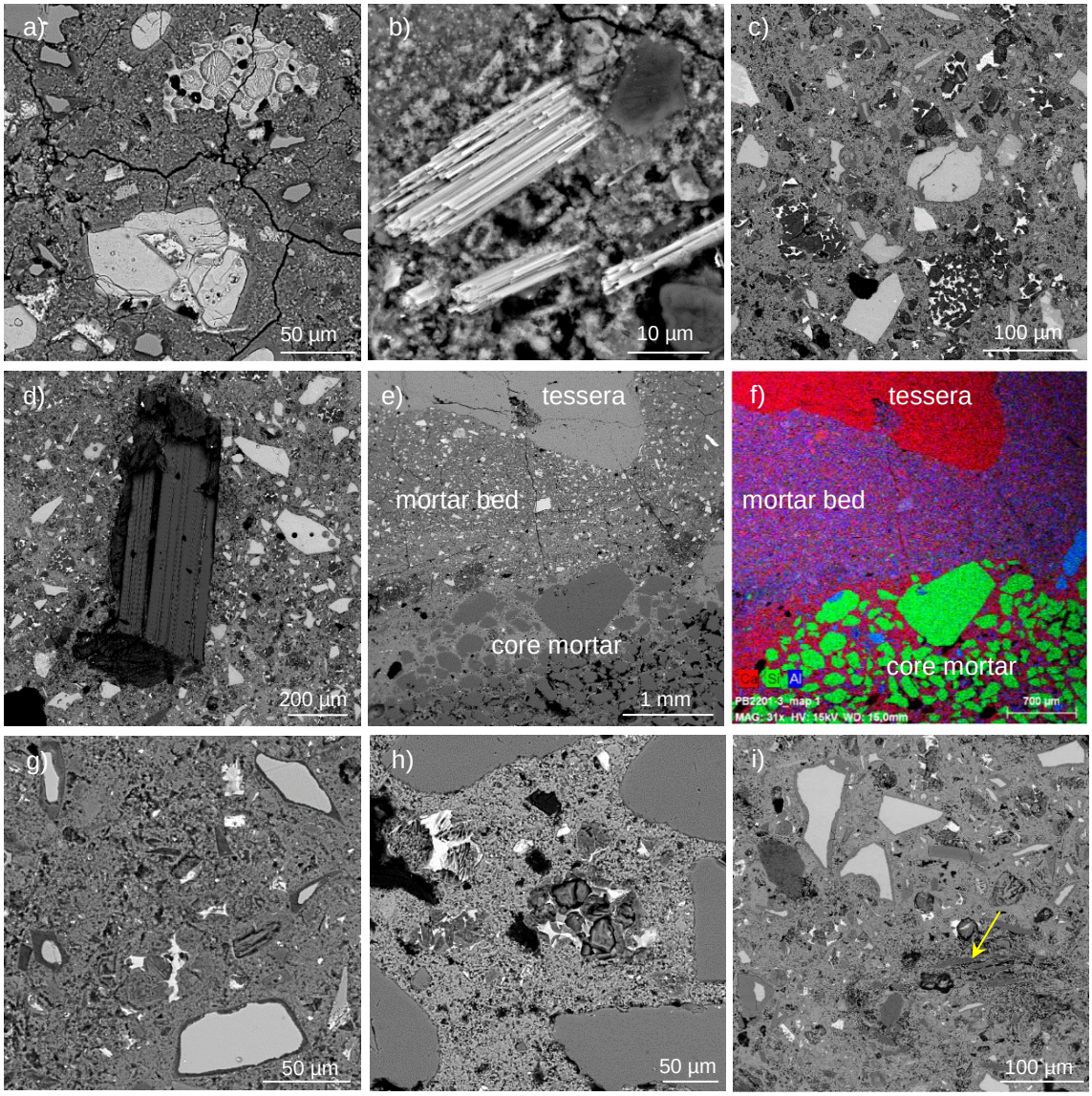

Figure 49. Micrographs of Kmentová and Zoubek mortars. Asbestos cement mortar of the sculpture´s body, BSE images – a) unhydrated and non-carbonated clinker residues; b) a detail of amphibole asbestos; Kmentová corroded body mortar, SEM-BSE – c) binder with light slag grains and decalcified clinkers (dark grains embedded in white interstitial phases), d) chrysotile asbestos; Kmentová mosaic mortars – e) SEM-BSE, f) EDS map of Ca, Si and Al distribution which enables to distinguish individual layers; g) a SEM-BSE detail of the Kmentová bedding mortar with light slag grains and no inert aggregates, h) a SEM-BSE detail of the Kmentová´s core mortar without slag grains and with quatzitic aggregates (grey) and residual clinkers; i) a SEM-EDS image of Zoubek mortar – light slags, residual clinkers and chrysotile asbestos (arrow).

Zoubek and Kmentová combined blast-furnace slag with asbestos cement. The basic raw materials of the common asbestos cement were made up of a mixture of asbestos and PC400 cement. [201], i.e. Portland cement (without slag). It is therefore believed that both artists did not use common commercial mixtures, but developed a material tailored to their needs.

6.3.4.2 Mineralogical composition

The mineralogical phases identified in the samples by XRD (Table 13) confirm the microscopic observations and measurements. In most samples (with the exception of Zoubek and some Kmentová mortars) a high amount of quartz and to a lesser extent feldspars and micas were identified as the main constituents of the aggregates. Unhydrated clinker phases, indicative of Portland cement, occur in all samples with the exception of Kmentová corroded body mortar and Kmentová core mortar (but SEM-EDS revealed the presence of decalcified clinker residues even in these). In addition, other $CaCO_3$ polymorphs (besides calcite), i.e. vaterite and/or aragonite, were detected in all samples except Kmentová core mortar, where only quartz and calcite were found. Vaterite and aragonite are formed during the carbonation of hydraulic binders [51], [158]. Therefore, in most cases the binders can be characterised as carbonated Portland cement. XRD analysis did not shed any light on the nature of the Kmentová core mortar. As indicated in the previous section, this mortar contains 71 wt% CaO (Tab. 11), which appears to be quite high for pure Portland cement. Both EDS and XRD results suggest that the binder may be a mixture of Portland cement and lime. However, more evidence would be needed to decide.

SEM-EDS analysis revealed different types of asbestos in the Kmentová and Zoubek samples. These results were confirmed by XRD. Both amphibole and chrysotile were found in the Kmentová mosaic, while only the less harmful chrysotile occurred in the Zoubek sample.

The carbonation rate differed between the samples. In some of them (Ballardini bedding mortar, Zoubek, Kmentová body, Kmentová bedding mortar) portlandite was detected, indicating incomplete carbonation of the binder.

Table 15. Mineralogical composition of mortars from “socialistic” mosaics.

wt%	Pardubi-ce	Ballardi-ni bedding	Sladký	Milovi-ce	Kmen-tová body	Kmen-tová corrod. body	Kmento-vá bedding	Kmento-vá core	Zou-bek
calcite	6	6	45	18	25	51	68	28	42
aragonite	-	-	-	5	-	21	5	-	9
vaterite	3	31	3	13	9	12	7	-	10
quartz	62	25	19	31	2	1	-	72	9
feldspars	12	21	12	19	-	-	-	-	-
biotite	-	3	-	-	-	-	-	-	-
muscovite	-	-	1	4	-	-	-	-	-
clinker	-	12	-	-	-	-	-	-	-
alite	13	-	4	9	11	-	-	-	3
belite	1	-	3	2	6	-	4	-	9
C_3A	2	-	3	-	0	-	-	-	3
C_4AF	-	-	5	-	7	-	-	-	2
gypsum	-	-	4	-	-	-	2	-	-
merwinite	-	-	-	-	4	-	-	-	4
ettringite	-	-	-	-	8	-	8	-	1
monophase	-	-	-	-	7	-	-	-	2
portlandite	-	2	-	-	9	-	3	-	1
amphibole	-	-	-	-	13	-	-	-	-
chrysotile	-	-	-	-	-	15	-	-	5

6.3.4.3 Thermal analysis

Figure 45 illustrates TG/DTG results of the mortar beds from the studied mosaics. The measured TG/DTG curves are in agreement with the SEM-EDS and XRD results. Ballardini bedding mortar, Sladký bedding mortar and Kmentová bedding mortar (Fig. 50a-c) show curves corresponding to Portland cement. There are two peaks in the temperature range 0-250 °C indicating dehydration of C-S-H phases (at 110 °C) and dehydration of gypsum (at 150 °C). The presence of gypsum was also demonstrated by XRD in two of the corroded samples (Sladký and Kmentová bedding mortar). Thermal

decomposition of portlandite occurs in the region around 450 °C. This reaction was observed in two samples (Ballardini bedding mortar and Kmentová bedding mortar), which is again in agreement with the XRD results that showed the presence of portlandite in these samples. The thermal decomposition of carbonates occurs in the temperature range of approximately 500-850 °C. Metastable $CaCO_3$ polymorphs (vaterite, aragonite) decompose at lower temperatures than calcite. In the DTG curves of the Ballardini, Sladký and Kmentová bedding mortar samples (Fig. 50a-c) their decomposition corresponds to a broad "hump" of the main carbonate peak representing calcite decomposition (around 800 °C).

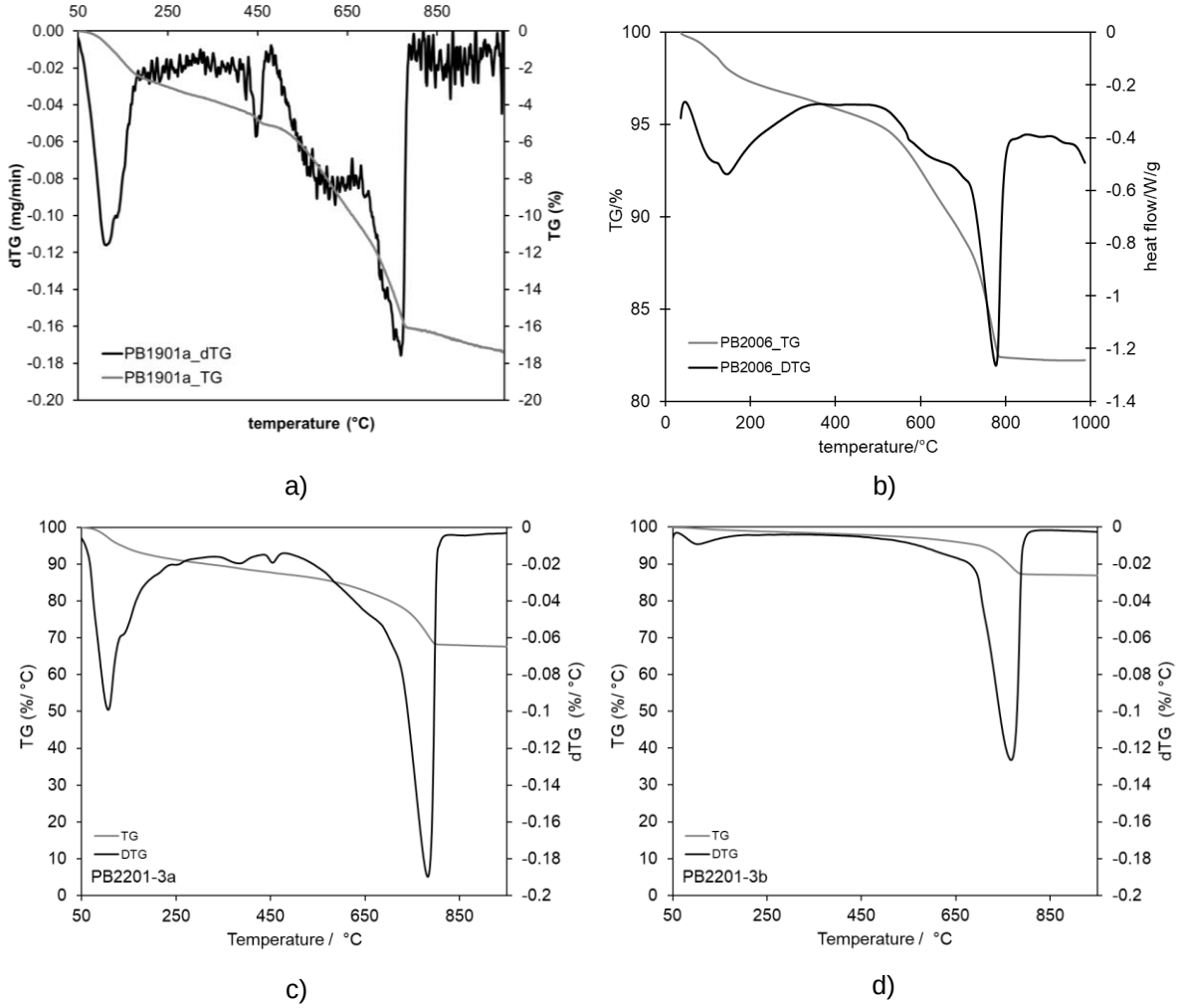

Figure 50. TG/DTG analysis of mosaic mortars from the “socialistic” mosaics – a) Ballardini bedding mortar, b) Sladký bedding mortar, c) Kmentová bedding mortar, d) Kmentová core mortar.

Similar to the SEM-EDS and XRD, the Kmentová core mortar sample (Fig. 50d) is distinguished from the other analysed mortars by a less pronounced peak representing C-S-H gel decomposition. Therefore, the results of the thermal analysis of this sample support the hypothesis that the core mortar is not purely composed of Portland cement, but probably also of lime addition.

6.3.4.4 Organic compound assessment (GC)

As stated in Section 4.6, in the 2nd half of the 20th century the mosaicists applied some synthetic organic admixtures and coatings [38], [49]. The presence of organics was tested on Sladký´s mosaic “Architect´s Reason and Sense” situated on the façade of the Faculty of Civil Engineering. The results presented here were previously published in a paper [38].

The results of the gas chromatographic analysis are shown in Fig. 51. Esters of palmitic, stearic and erucic acids were identified in significant amounts in the mortar extract. Esters of linoleic and oleic acids and other oxygenated compounds were identified in lower concentrations. The organic content was quantified to 8 wt% of the mortar.

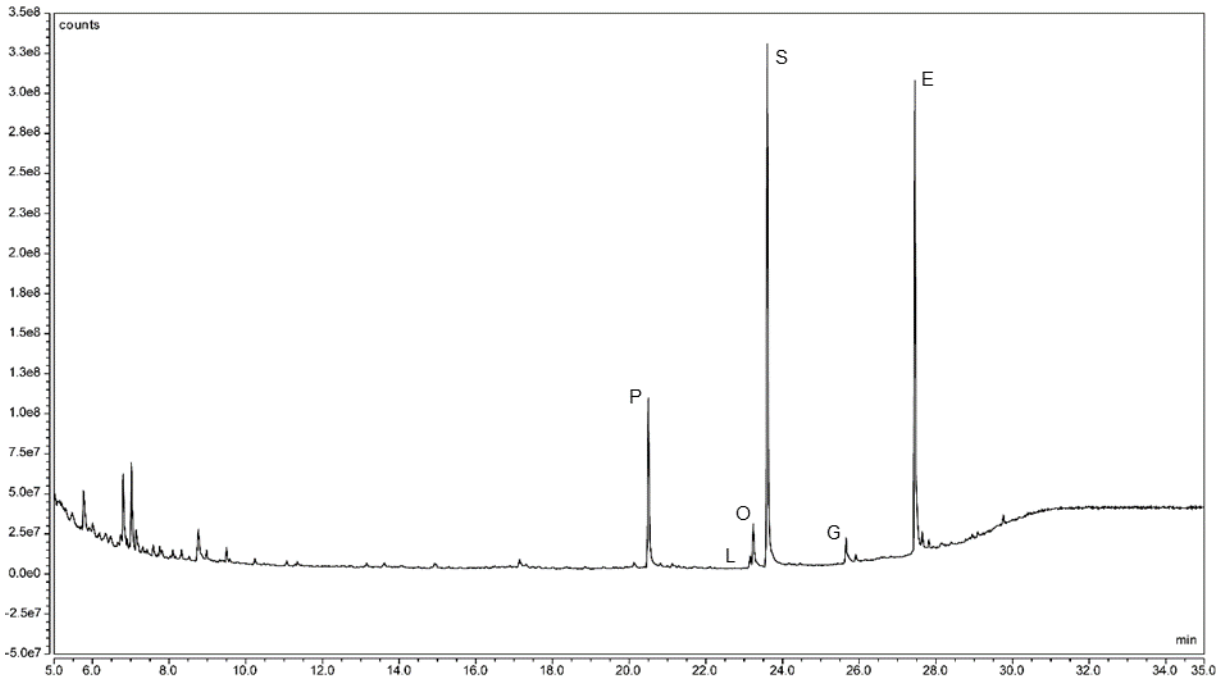

Figure 51. GC-MS spectrum of the Sladký bedding mortar. P – palmitic acid, L – linoleic acid, O – oleic acid, S – stearid acid, G – gondoic acid, E – erucic acid.

The acids identified belong to the group of fatty acids that form the main compounds of oils when they react with glycerol. However, the composition of the identified fatty acids and other compounds does not correspond to traditionally applied linseed oil.

Furthermore, the mosaic literature available at the time only mentioned the addition of PVAc dispersions and the use of hydrophobic silicone finishes [49]. PVAc degrades to polyvinyl alcohol in an alkaline environment. Microorganisms, if present, may convert the polyvinyl alcohol to acetic acid, which may be corrosive [202]. No degradation products indicating the presence of PVAc or siloxanes in the original mortar were detected by the methods used. The use of more specific chromatographic techniques (pyrolysis gas chromatography) is planned for future experiments.

Contrary to common vegetable oils, which consist mainly of triglicerides of unsaturated fatty acids (C18:3 linolenic acid ester is the most abundant compound in linseed oil, C18:1 oleic acid ester in rapeseed oil), the oily substance found in the mortar contained compounds derived mainly from saturated acids (mainly C18:0 stearic acid and to a lesser extent C16:0 palmitic acid). This could indicate that the mixture of fatty acids identified in this mortar may have come from an oil of animal origin.

On the other hand, the high content of erucic acid (C22:1) casts doubt on the purely vegetable origin of the compounds identified. Erucic acid occurs in large quantities in seeds of the Brassicaceae family, such as rapeseed and mustard seed. Although natural forms of rapeseed contain high levels of erucic acid (usually more than 40% of the total fatty acids), the concentration of erucic acid in present-day commercially bred rapeseed varieties typically reaches levels below 0.5% of the total fatty acids. The need to significantly reduce erucic acid levels in food-grade oilseed rape is driven by the potential adverse effects of the acid on human health. High erucic acid cultivars are still grown for industrial, non-food purposes [203]. In Czechoslovakia, the cultivation of low erucic acid oilseed rape varieties was introduced in the mid-1970s.

Low concentrations of erucic acid are naturally present in other food sources, such as fish [203], but the amount of erucic acid found cannot be considered low. Therefore, we assume that an artificial mixture of fatty acid salts was added to the mortar of Sladký's CTU mosaic. This assumption is supported by the fact that waterproofing agents based on fatty acid salts were available at the time. However, contemporary witnesses do not mention any such treatment [115].

In the mid-1960s, a new method of mortar waterproofing was patented, based on the addition of fatty acid salts of metals (namely Ca) dispersed in water. The authors came up with a cheap saponification of "bone fatty acids" (probably slaughterhouse waste) with powdered CaO in the presence of a surfactant [204]. Later a commercial product called "Betofix" was produced in Czechoslovakia. This was a water emulsion of fatty acid salts. It was added to the mixing water in a ratio of 1:15 - 1:25 [205]. This or similar products could have been used in the mortar investigated.

6.3.4.5 Summary IV – Mosaics of the socialistic period

The results of the analysis of the mosaic mortars of the second half of the 20th century confirm that at this time Portland cement was already fully established as the main mortar binder for fixing mosaics, and polymictic river sand was used as a filler, in which, in addition to the predominant quartz grains, rock fragments containing feldspars and micas were also identified. The technology of the studied mosaic mortars generally corresponds to the standardized procedure established in the UUŘ workshop [49]. In most of the studied mosaic beds, numerous grains of blast furnace slag were identified in addition to Portland clinkers. The sample of mosaic sculpture by Eva Kmentová containing asbestos cement represents an authorial exception in the analysed set of

"socialist" mosaics. An organic waterproof coating was identified on the surface of Sladký´s mosaic, probably consisting of a synthetic mixture based on fatty acid salts.

7 MODEL MORTARS FOR THE ESTIMATION OF LINSEED OIL CONTENT →PAPER [165]

Linseed oil turned to be an important part of some of the authentic mosaic mortar samples. The addition of linseed oil to portable mosaics´ fixing mortars seems to have been a common practice at the Tirolean workshop founded by A. Neuhauser. Linseed oil was added in surprisingly high quantities [37] compared to the recommended dosage for optimal water repelling effect [192], [195]. Moreover, its identification and especially quantification in lime-based mortars is not always straightforward – the signal of oil or its derivates is often affected by overlapping stronger calcium hydroxide or calcium carbonate bands [37], [188]. That is why this compound deserves a special attention.

The experiment aims at the investigation of the possibility to estimate linseed oil admixture content in lime-based mortars by thermal analysis. The method is compared with other common analytical techniques conventionally applied to the identification of organics such as FTIR spectroscopy and TOC (total organic carbon).

7.1 Materials

A set of model samples with varying linseed oil content was prepared after the model of authentic mosaic mortar beds from Neuhauser´s workshop [37], i.e. air lime mortars with a carbonatic filler.

Table 16. Composition of model mortars. $W_{oil\text{-}total}$ represents the mass fraction of oil with respect to all mortar´s components including mixing water; $w_{oil\text{-}mortar}$ – mass fraction of oil over lime calcite and oil (water excluded).

	$Ca(OH)_2$ (g)	$CaCO_3$ (g)	H_2O (g)	oil (g)	$w_{oil\text{-}total}$ (%)	$w_{oil\text{-}mortar}$ (%)
M-0	100	100	90	0	0.0	0.0
M-1	100	100	90	2	0.7	1.0
M-2	100	100	88	4	1.4	2.0
M-5	100	100	86	10	3.4	4.8
M-10	100	100	84	20	6.6	9.1
M-15	100	100	84	30	9.6	13.0
M-20	100	100	82	40	12.4	16.7

Model samples were prepared of slaked lime CL 90 S and finely ground $CaCO_3$ in 1:1 mass ratio. Food grade quality linseed oil was added to dry components in the proportion 0 – 20 wt% (Tab. 16). The amount of mixing water was not constant – water

was added until a proper plastic consistency for mosaic laying was reached. The amount of added water was measured (Tab. 16)

Model mortars were placed to silicon moulds and cured in laboratory environment. The samples were kept moist by water spraying in order to enable their carbonation. After 28 days, samples were crushed and stored in plastic sealed containers until the moment of analysis, which was carried out in two weeks after the 28 days, i. e. 42 days after the samples´ preparation.

7.2 Methods

Model mortars, as well as the linseed oil alone and reference historic sample PB1707 (Peluněk), were analysed by TG/DTG analyser Setaram Setsys Evolution-16-MS coupled with Evolved Gas Analysis by mass spectrometer (EGA-MS). The crushed mortar sample was placed in alumina crucible without a lid, in argon atmosphere (flowrate 60 ml/min), the heating rate was 10 °C/min. The measurement was performed from ambient temperature (21 °C) to 1000 °C, the mass spectrometer was operated in "Multiple Ion Detection" mode.

Powder X-ray diffraction (XRD) was employed to study phase composition of the samples; diffractograms were recorded by Malvern PANalytical Aeris diffractometer equipped with CoKα source operating at 7.5 mA and 40 kV. The incident beam path consisted of iron beta-filter, Soller slits 0.04 rad and divergence slit 1/2°. The diffracted beam path was equipped with 9 mm anti-scatter slit and Soller slits 0.04 rad. The used detector was PIXcel1D-Medipix3 detector with active length 5.542°. Data were evaluated by Rietveld refinement performed by Profex software (ver. 4.0.3) [155].

The FTIR spectra of mortars and their isopropanol (IPA) extracts were acquired by Nicolet iN10 spectrometer with connected external module iZ10 with diamond ATR crystal. The spectra were collected in the range 4000–525 cm^{-1} at 2 cm^{-1} spectral resolution. Mortars´ extracts were prepared by two-step extraction in the same way like authentic samples. In the first step, 5 g of powder mortar was mixed with 20 ml of IPA and equilibrated for 5 days. In the second step, the same sample was extracted again with 15 ml of IPA. Both extracts were mixed and the resulting solution was analysed by ATR. The final extract had been dried on a watch glass to evaporate the IPA solvent prior to spectra collection. The total organic carbon (TOC) was determined by Leco RC 612 combustion analyser according to standard DIN 19539(A) [156].

The SEM (Scanning Electron Microscopy) microphotographs were acquired by Tescan Mira LMU II device in BSE (back-scattered electron) regime at 15 kV accelerating voltage and 15 mm working distance.

7.3 Results and discussion

7.3.1 Reference pure linseed oil

To obtain reference data for the identification and quantification of linseed oil in mortars, pure linseed oil was analysed. Linseed oil is in fact a mixture of various unsaturated fatty acids´ triglycerides – esters derived from glycerol. Table 17 shows main fatty acids (FA) constituting linseed oil.

Table 17. Fatty acids constituting linseed oil **[164]**.

Fatty Acid	Number of carbons: number of double bonds	Weight %
Linolenic	18:3	48-60
Oleic	18:1	14-24
Linoleic	18:2	14-19
Palmitic	16:0	6-7
Stearic	18:0	3-6

7.3.1.1 Thermal analysis (TG/DTA and EGA-MS)

TG/DTA and EGA-MS of pure linseed oil were performed in argon and air atmosphere (Fig. 52). The temperature range of the oil´s thermal decomposition was much broader in air (220-600 °C) than in argon. As expected, the oxidative decomposition was more exothermic than the decomposition in argon atmosphere. Linseed oil´s decomposition in argon atmosphere yielded more intensive and narrower EGA-MS signal; the mass loss ended at 500 °C. Hence the argon atmosphere was found to be more suitable for thermal analysis of oil-containing mortars.

Besides water (*m/z* 18; *m/z* stands for mass-to-charge ratio) and CO_2 (*m/z* 44), the EGA-MS showed a large number of other released ions. The most intensive signal was provided by ion with *m/z* 55. This signal corresponds to $[C_4H_7]^+$ ion, which is frequently found in mass spectra of monounsaturated fatty acids [206]. This ion was generated in both inert and oxidative conditions. Unfortunately, an ion of *m/z* 55 is intensively generated also during the thermal decomposition of proteins which were also broadly used as mortars admixtures – casein and animal glue [207]. Hence the *m/z* 55 ion was not found enough “oil-specific” to be used for the oil content estimation. A little less intensively abundant ion *m/z* 95 $[C_7H_{11}]^+$ ion was chosen instead (Fig. 52). A ion of *m/z* 95 also occurs in protein pyrolysis mass spectra [207] but much less frequently than that of *m/z* 55.

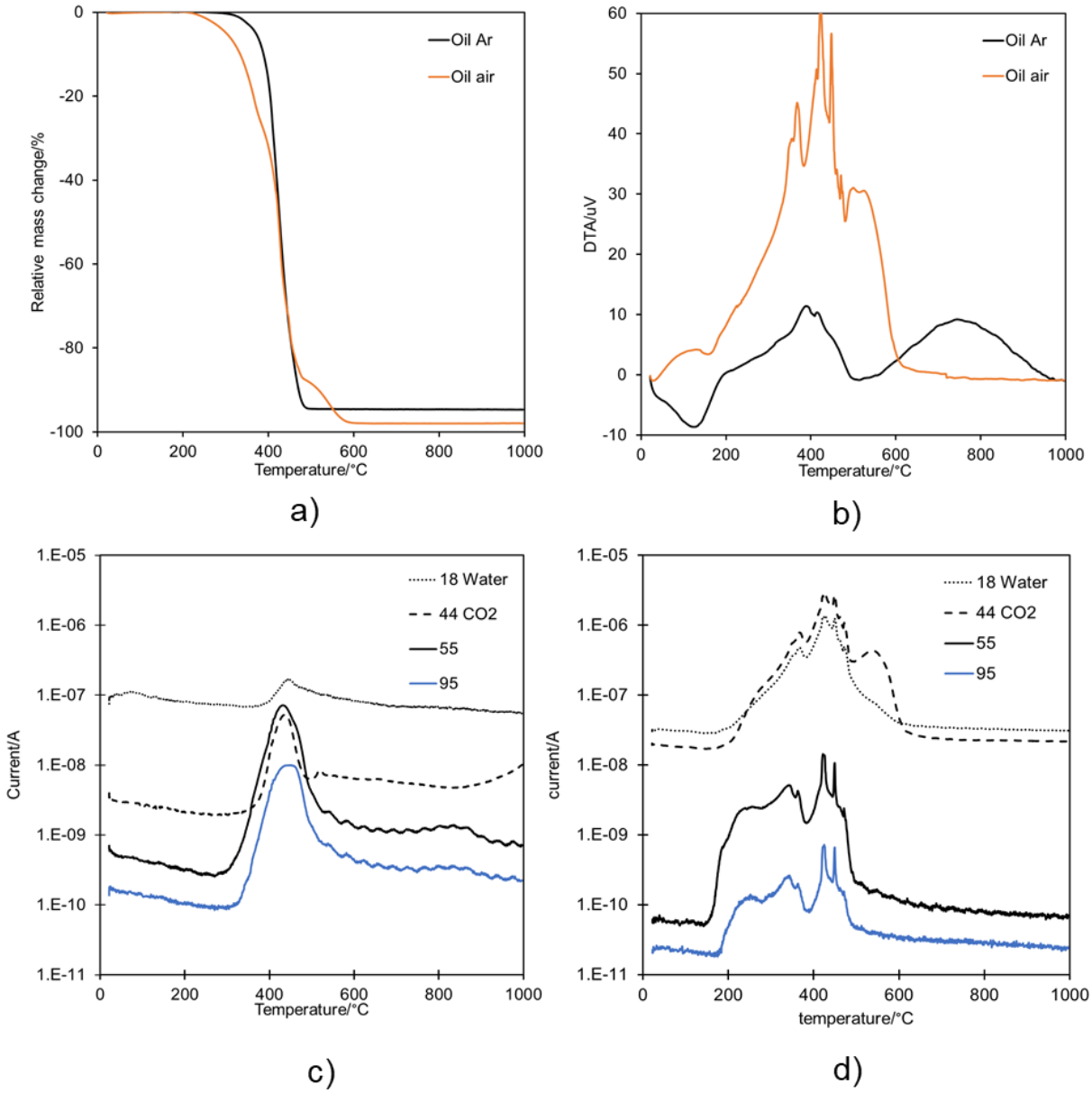

Figure 52. Pure linseed oil – results of thermal analysis. a) Thermogravimetry in argon and air, b) DTA in argon and air, c) EGA-MS of oil in argon, d) EGA-MS of oil in air.

7.3.1.2 FTIR spectroscopy

FTIR spectrum of pure linseed oil is depicted in Fig. 53a. The most significant band occur at 3010 cm^{-1} – stretching vibration of unconjugated cis double bonds in FA bound in triglycerides; 2920 and 2850 cm^{-1} – asymmetric and symmetric stretching of CH_2 units (in FA); 1740 cm^{-1} – stretching in C=O bond in ester group; 1460 cm^{-1} – bending of CH; 1160 cm^{-1} – stretching of C-O in triglycerides; 717 cm^{-1} – rocking of CH_2 [208].

7.3.2 Model mortars

7.3.2.1 FTIR spectroscopy

Fig. 53a clearly shows the spectra of model mortars´ powders do not provide representative information on the mortar´s composition as the signal of organic compounds coming from the linseed oil is substantially suppressed by the inorganic matrix, i. e. by the bands assigned to the stretching vibrations of carbonate anion in calcite at 1410, 874 and 712 cm^{-1}. This phenomenon was observed in the previous research into authentic mosaic mortar samples ([37], Section 6.3.1.6) as well as in other works investigating lime-based mortars with a high dosage of lined oil [188].

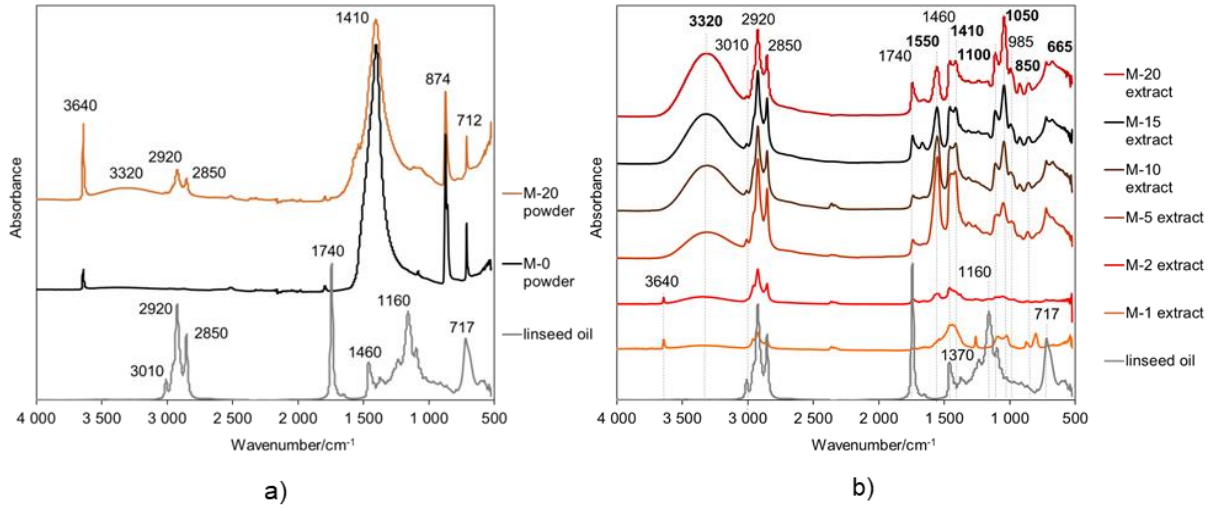

Figure 53. ATR-FTIR spectra of linseed oil and model mortars – a) powdered bulk samples, b) isopropanol extracts

Even though the presence of linseed oil cannot be fully detected from the powdered mortars´ spectrum, some evidence of organics can be read out of it. Besides an OH-stretching vibration in portlandite at 3640 cm^{-1} and the vibrational bands representing calcite, a broad band appears between 3500-3100 cm^{-1} peaked at 3320 cm^{-1}. It corresponds to stretching vibration of O-H in hydroxyls and hydroperoxides; the increase of this band is caused by oxidative polymerisation (autoxidation) of the oil, i.e. of its “drying” from liquid to solid state [208]. The peaks apparent at 2920 cm^{-1} and 2850 cm-1 generally represent stretching vibrations of -CH_2- group in aliphatic hydrocarbon chain (here assigned to FA bound in triglycerides). The peaks at 1740 cm^{-1} (C=O in esters) and 1160 (C-O in esters) have somewhat diminished; it might indicate that ester groups in the oil were transformed to Ca^{2+} carboxylates (“soaps”). Unfortunately, the absorption bands of carboxylates are found between 1200 and 1600 cm^{-1} [209], [208], [210] where also an intensive stretching vibration of carbonate (1410 cm^{-1}) is found.

To overcome the issue of carbonate interference with the expected carboxylate vibration bands, mortars´ organic compound was extracted by isopropanol (IPA). The

“removal” of carbonate from the samples disclosed number of absorption bands (Tab. 18, Fig. 53b).

Table 18. FTIR vibrational (absorption) bands identified in linseed oil and IPA extract of M-20 model mortar. The bands in bald are assiciated with linseed oil autoxidation and carboxylate formation. Abbreviaations: v – stretching, a – antisymmetric, s – symmetric, δ – bending; b - broad, w - weak, ms – medium strong, s – strong.

position (cm-1)	linseed oil	mortar extracts (M-20)	vibration assignment
3320		b	v(OH) hydroperoxides and hydroxyl
3010	ms	sh	v(CH) unconjugated cis double bonds in FA chain
2920	s	s	v_a(CH) CH2 in FA chain
2850	s	s	v_s(CH) CH2 in FA chain
1740	s	ms	v(C=O) in esters
1550		s	v_a(C-O) in carboxylates
1460	ms	ms	δ(CH2, CH3) in tryglicerides (FA chain)
1410		ms	v(C-O) in carboxylates
1370	w		ω(CH2) deformation CH in methyl groups
1160	s		v(C-O) in triglycerides ester linkage
1100	w	w	v(C-O) in triglycerides ester linkage
1050	sh	s	deformation COOR
985		sh	ω(CH) trans-trans conjugated
850		ms	glycerol
717	s		$(CH2)_n$ rocking of the FA chain in tryglycerides (n>4)
665		w	Ca-O bond in carboxylates

The bands identified in the FTIR spectra of mortars´ extracts indicate the transformation (deterioration) of linseed oil in the alkaline environment of the lime matrix. The first deterioration process is *polymerization* followed by *autoxidation*, i. e. the “drying” of oil which is a natural process associated with the aging [164], [189], generally independent of the lime matrix. Its mechanism is very complex and not fully understood [211] but simply said its most remarkable result is the formation of cross-linked structure through the unsaturated hydrocarbon chains of fatty acids constituting the original oil´s triglycerides. This reflects as a broad band with a peak at 3320 cm^{-1} in the FTIR spectra. Its intensity seems to be proportional to linseed oil content in the mortar.

The second deterioration process observable in the FTIR spectra is the reaction of oil and calcium contained in lime – *saponification*, i.e. the formation of Ca-carboxylates with glycerol as a by-product. According to the literature, this is accompanied by the disappearance of the carbonyl ester group stretching vibration at 1745 cm^{-1} [210] and the rising of new absorption peaks at 1550 cm^{-1}, 1410 cm^{-1} and 665 cm^{-1} corresponding to carboxylate ion symmetric and antisymmetric stretching vibrations and metal-oxygen bond vibration [210], [212]. All these carboxylate-related absorption bands were

identified in the investigated model mortars documenting the oil transformation. These processes are clearly apparent as early as in a few-week-old samples. However, the presence of the 1740 cm^{-1} band (C=O in esters), as well as those at 1050 and 1100 cm^{-1} (stretching in –CO–O–C– in triglycerides) in our spectra indicates that the conversion of triglycerides to carboxylates was not completed [213].

Some of the bands might be seemingly used for the oil content quantification as their intensities seem to be proportional to the amount of linseed oil added to the mortars (e.g. the bands at 3320 or 1050 cm^{-1}) (Fig. 53b). However, one must bear in mind that the deterioration of oil and its interaction with the lime matrix is a very complex and dynamic process with an up-to-now not precisely described kinetics. For example, the hydroxyl and hydroperoxides content represented by the seemingly applicable band at 3320 cm^{-1} decreases during the proceeding cross-linking of the fatty acid chains [214]. This means the stability of the autoxidation and saponification products is not guaranteed. That is why the FTIR spectra are not suitable for the quantification of linseed oil in the mortars.

7.3.2.2 XRD

Selected representative diffractograms of model mortars were plotted in Fig. 54. Unsurprisingly, calcite (PDF# 04-008-0788) and portlandite (PDF# 04-010-3117) were identified as principal components of all model mortars. However, the ratio of these two phases significantly differed in the samples after 28 days of curing. In mortars with low oil content lime carbonation (transformation of lime to calcium carbonate) was more intensive (Fig. 55). Lime carbonation takes place in the water pore solution [215] but linseed oil acts as a water-repealing agent in mortars and thus slows down the carbonation process (and strength increase) [194]. As ATR-FTIR spectroscopy indicated, the addition of linseed oil induces Ca-carboxylates formation, although not consuming the whole amount of oil – a part of it remains in the mortar in a polymerized form.

In general, carboxylates can crystallize, but the formation of carboxylate crystals is difficult [216] due to the hydrocarbon chains length and ongoing polymerization. However, a small diffraction, which could be assigned to a Ca-carboxylate, was detected in MO-20 mortar (Fig. 54) at 6.5 ° 2θ (d = 15.479 Å); the most intensive diffraction lines of carboxylates are found at low diffraction angles [217]. Fig. 55 shows the results of Rietveld refinement indicating some general trends in the samples showing an increasing amount of non-carbonated portlandite with the increasing oil content in model samples.

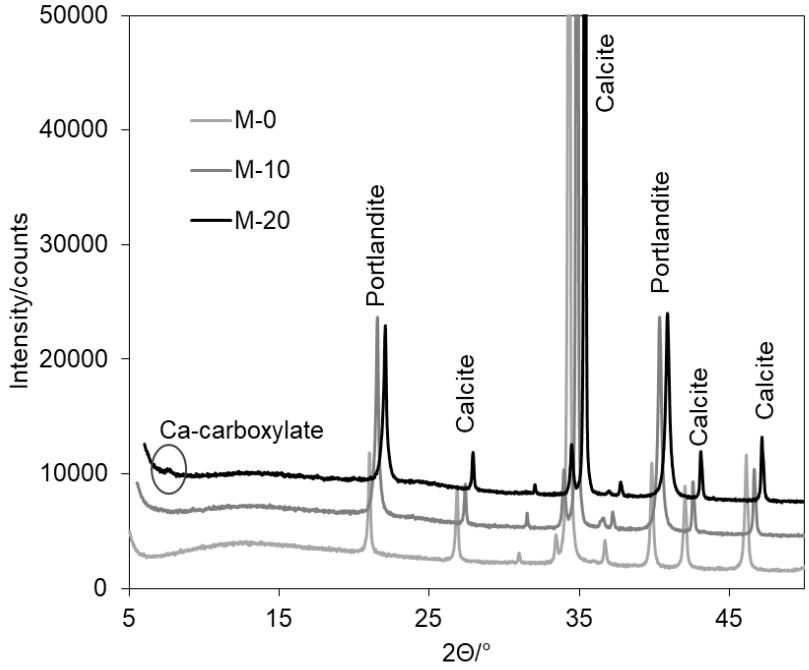

Figure 55. X-ray diffractograms of studied model mortars.The diffractograms are shifted for a better clarity.

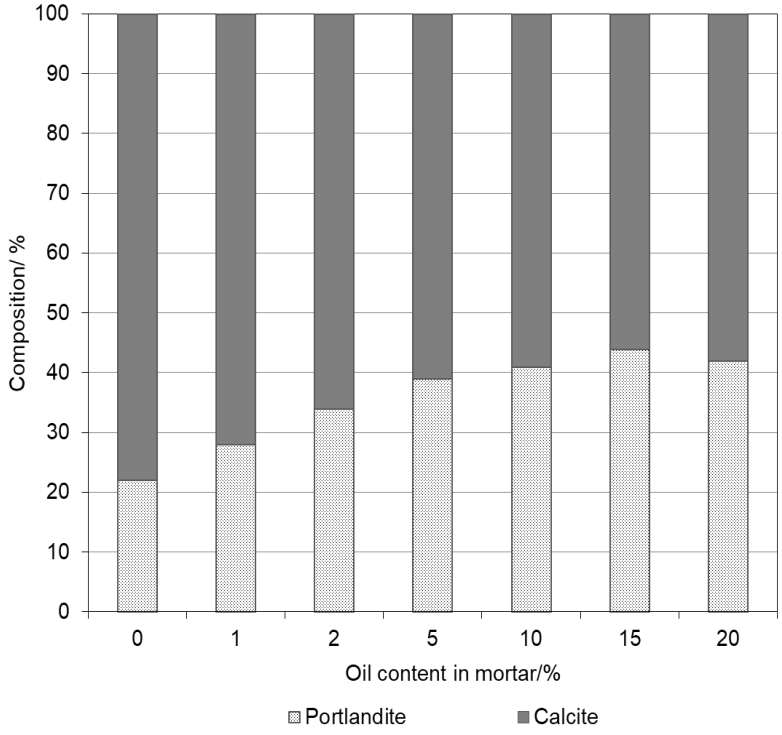

Figure 54. Portlandite/ calcite ratio in model mortars after 28 days of curing as obtained by Rietveld refinement (% by mass).

7.3.2.3 SEM-EDS

The SEM images of selected samples´ microstructure are displayed in Fig. 56. The microstructure of the reference M-0 sample differs from the two samples with the largest linseed oil dosage (M-10 and M-20). At the lowest magnification (150x) one can observe an increased number of large round pores (50-200 µm in diameter) in linseed oil-containing samples. According to Nunes et al. [188], an occurrence of such macropores is a characteristic feature of oil-containing mortars which has been documented also by other authors experimenting with carboxylate admixtures [218],

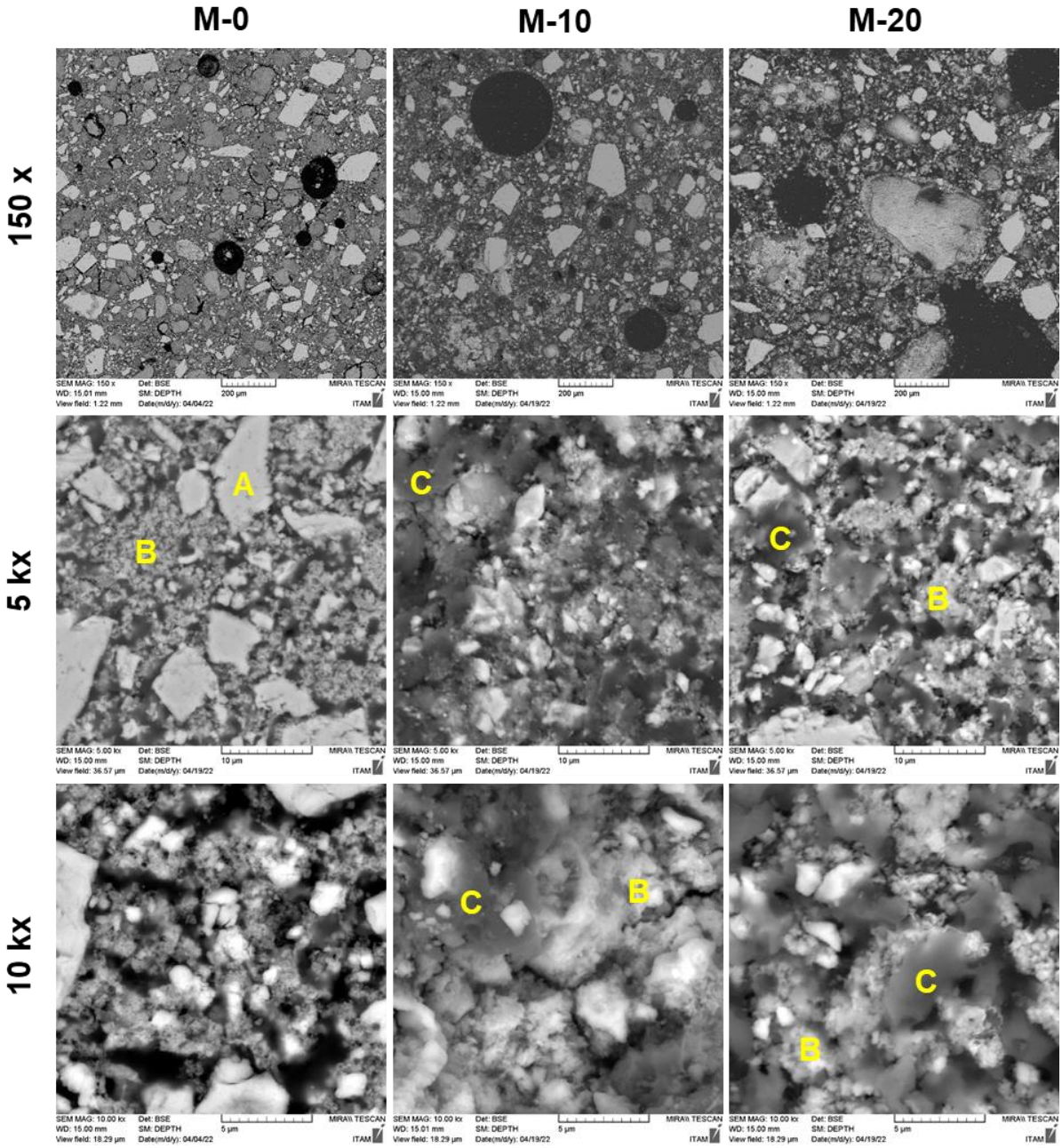

Figure 56. Microstructure of selected model mortars with different oil content as recorded by SEM (BSE regime) at different magnifications (150x, 5000x (5kx) and 10000x (10kx)). M-0 – reference mortar with 0% linseed oil, M-10 – mortar with the addition of 10% of linseed oil, M-20 – mortar with the addition of 20% of linseed oil; A – carbonatic filler, B – lime binder, C – lime-oil reaction products (carboxylate soaps).

[219]. Nunes et al. [188] assign the formation of such pores to the saponification reaction between oil and the alkaline components of the binder. The fatty acid anions resulting from the reaction of oil with the binder consist of hydrophobic non-polar hydrocarbon chains linked with hydrophilic poplar carboxyl groups (–COO^-). Their bipolar nature enables the carboxylates to be absorbed and concentrate at the air-binder interface thus promoting the formation of pores [188] and stabilizing them [219].

At higher magnifications (5 kx and 10 kx), darker flaky structures can be observed in the oil-containing mortars M-10 and M-20 (Fig. 56). They represent the products of lime-oil reaction. Similar structures have been identified as calcium oleate and calcium stearate deposits in Izagguire´s et al. model samples prepared in order to investigate the water-repelling effect of commercial Na- and Ca-carboxylates on lime mortars [219].

7.3.2.4 Thermal analysis

In the thermogravimetric curves of the model mortars (Fig. 57) there is no specific sign of linseed oil admixture´s thermal decomposition. Their shape, reflecting the thermally-induced decompositional processes, is similar to thermogravimetric curves of authentic linseed-oil containing mortars (a previously analysed [37] mosaic mortar sample from the Peluněk family sepulchre was chosen as a reference in Fig. 57). On the other hand, the lime-linseed oil mortars (both model and authentic) show an unusually high total

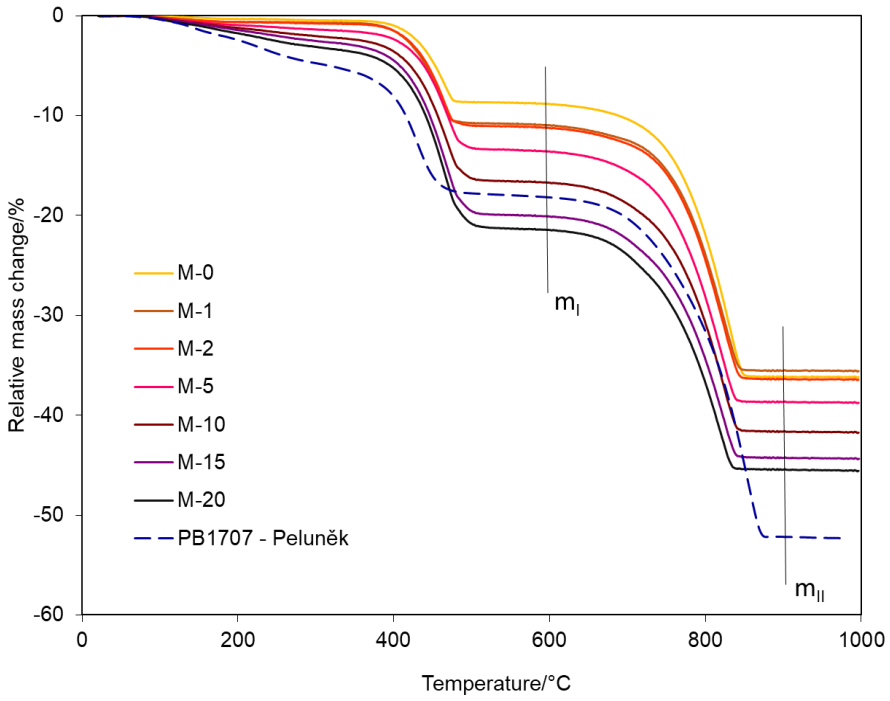

Figure 57. Thermogravimetric curves of model mortars M-0 – M-20 and PB1707 sample of authentic mosaic mortar bed from Peluněk family sepulchre.

relative mass change compared to “pure” air lime mortars. This contradiction lets us assume, thermally induced decomposition of linseed oil reaction products identified by FTIR spectroscopy (Ca-carboxylates and polymerized oil) must overlap with the well-known decomposition processes of $Ca(OH)_2$ and $CaCO_3$ (decomposition of $Ca(OH)_2$ to CaO and released H_2O at about 450 °C; thermal $CaCO_3$ decomposition to CaO and released CO_2 at about 750-800 °C).

In order to distinguish the contribution of “oil” and “inorganics” to the relative mass change, i.e. to determine the mortar composition, EGA-MS was employed. The results of two “extreme” samples M-0 and M-20 are depicted in Fig. 58. The reference mortar M-0 (Fig. 58a) provided well separated signals of free (physical) water (to 200 °C), $Ca(OH)_2$ decomposition (peak at 450 °C) and CO_2 evolution from $CaCO_3$.(500-900 °C).

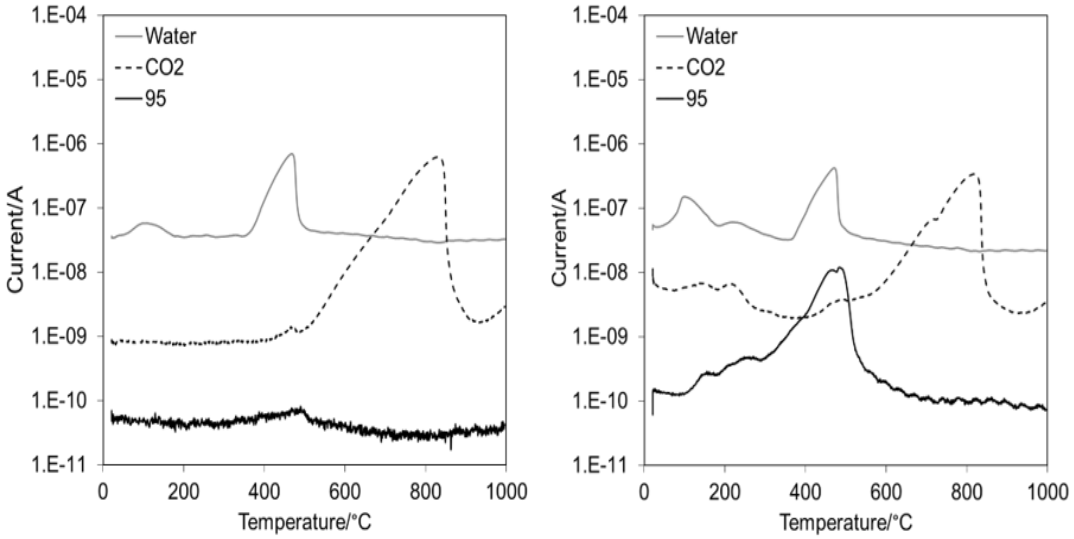

Figure 58. The results of model mortars´ EGA-MS analysis – a) M-0 and b) M-20.

The “oil-related” signal *m/z* 95 showed just a small hump at 500 °C (of unspecific origin). The gas evolution process of M-20 sample with the highest oil content looks much more complicated (Fig. 58b). One can observe somewhat more intensive water release bellow and also above 200 °C and an expected high peak at 450 °C. At the same temperature, a peak belonging to *m/z* 95 can also be found. This signal began to grow at 100 °C. The CO_2 evolved at low temperature (up to 300 °C) and then again more intensively from 400 to 900 °C. It means “oil products” (polymerized oil, partially in a form of Ca-carboxylates, glycerol) must have been thermally decomposing in a wide temperature range between 100 and 600 °C.

Operating under several assumptions, themogravimetric analysis results were used to estimate the composition of mortars: the total mass of sample m_s (let assume it to be 1 g) is a sum of mass of $CaCO_3$ (m_{CC}), a mass of $Ca(OH)_2$ (m_{CH}) and a mass of “oil products”, i.e. Ca-carboxylates and polymerized oil (m_{OP}) (Eq.6). The amount of physically bound water, even though apparent at EGA-MS of M-0, was neglected due to a very low relative mass change up to 100 °C (Fig. 57).

$$\mathrm{ms} = m_{CC} + m_{CH} + m_{OP} \quad (6)$$

The mass of $CaCO_3$ (m_{CC}) was determined conventionally from the relative mass loss m_{II}. The EGA-MS of M-0 and M-20 samples (Fig. 58) indicates certain overlap between the "oil" and $CaCO_3$ decomposition. On the other hand, the TG curve featured well-distinct plateau around 600 °C – thus the m_{CC} was determined simply from m_{II} - difference of relative mass changes (in %, Fig. 57) between the final plateau and the plateau around 600 °C by (Eq. 7). Individual values of m_{II} were obtained by tangential method:

$$m_{CC} = 0.01 m_{II} \frac{M_{CaCO3}}{M_{CO2}} \qquad (7)$$

The relative mass change m_I (%) involves two contributions: water evolved from the $Ca(OH)_2$ and the volatile portion of "oil products" (Eq. 8); where x means non-volatile (or thermally stable) fraction of "oil products".

$$m_I = 100 \cdot \left(\frac{M_{H2O}}{M_{Ca(OH)2}} + (1 - x) m_{OP} \right) \qquad (8)$$

The third equation necessary to calculate the three unknowns (m_{CH}, m_{OP} and x), is the analysis of the residual mass (m_r), after the thermogravimetry experiment. The m_r is composed of non-volatile fraction of "oil products" (x) and CaO coming from $CaCO_3$ and $Ca(OH)_2$ thermal decomposition (Eq. 9)

$$m_r = 100 \cdot \left(m_{CC} \frac{M_{CaO}}{M_{CaCO3}} + m_{CH} \frac{M_{CaO}}{M_{Ca(OH)2}} + x \cdot m_{OP} \right) \qquad (9)$$

The solution of Eq. 5-8 system provides an estimation of model mortars´ composition. As can be seen in Fig. 60, as low as 1% linseed oil dosage was enough to cause certain carbonation decrease, which is in agreement with previously published papers [194]. Moreover, the amount of "oil products" was clearly increasing with the linseed oil content. The initial mortar contained $CaCO_3$ and $Ca(OH)_2$ mixed in the 1:1 ratio by mass (Tab. 16); the calculated composition of hardened mortars indicates that a higher oil content means more intensive $Ca(OH)_2$ depletion in favour of "oil products" – specifically to Ca-carboxylates. However, this does not mean calcite is not formed in the oil-containing mortars at all – its content is higher than would correspond to the amount added to mixture at the time of mortars´ preparation.

The composition of mortars determined from thermogravimetry (Fig. 59) reflects the real situation better than quantitative XRD (Fig. 55) since XRD cannot cope with mostly amorphous organic components of the mortars.

Parameter x representing the residual non-volatile portion of "oil products" (the third unknown from Eq. 6-9) ranged between 0% - 0.64% (Tab. 19). It could be interpreted as CaO having its origin in Ca-carboxylates. There is a certain increasing trend of x with the oil dosage, which could indicate that a higher oil admixture means a higher degree of its saponification. However, the confirmation of this speculative assumption requires further research.

Table 19. Composition of model mortar samples and Peluněk historic mosaic mortar as determined by thermal analysis and TOC.

sample	m_{CC} (%)	m_{CH} (%)	m_{op} (%)	TOC (%)	x (%)
M-0	62.0	38.0	0.0	0.23	0.0
M-1	55.9	43.9	0.2	0.54	0.0
M-2	57.1	41.8	1.1	0.80	0.2
M-5	57.0	38.8	4.2	1.56	0.2
M-10	56.6	35.3	8.1	2.99	0.2
M-15	54.9	33.1	12.1	6.01	0.2
M-20	54.3	31.8	13.9	7.50	0.6
Peluněk	78.3	5.3	16.5	9.30	0.0

m_{CC} – $CaCO_3$ content, m_{CH} – calcium hydroxide content, m_{op} – "oil products" content, x – non-volatile residual fraction of "oil products"

The methodology of linseed oil characterisation and quantification, developed on a set of model mortars, was tested on a mosaic mortar bed from Peluněk family sepulchre. The authentic mortar´s "oil products" content was estimated by thermal analysis and EGA-MS presented as well as by TOC analysis.

7.3.2.5 Thermal analysis

Peluněk mortar´s thermogravimetric curve (Fig. 57) was evaluated with the help of Eq. 6-9 in the same way as model mortars. Its composition was thus calculated as 78.3% (by mass) of $CaCO_3$, 16.5% of "oil products" (m_{OP}) and 5.3% of $Ca(OH)_2$. The presence of portlandite (somewhat surprising in 120 years old mortar) was confirmed previously by XRD as well [37]. The calculated m_{OP} value of 16.5% indicates – with respect to the model mortar results and assuming carbonation is increasing the total mortar mass – that the initial oil dosage in Peluněk mortar was about 22%.

7.3.2.6 EGA-MS

The second approach to the authentic mortar´s analysis was based on the EGA-MS. The intensity of signal *m/z* 95, corresponding to $[C_7H_{11}]^+$ ion, was used as a parameter for comparison of the oil content in model samples and the authentic Peluněk mortar. As discussed in section 7.3.1.1, the $[C_7H_{11}]^+$ ion signal was chosen due to its intensive evolution during the thermal decomposition of linseed oil and at the same time negligible occurance in thermally decomposed proteins´ mass spectra. In the mass spectra of both model mortars and Peluněk mortar this ion provided an intensive signal.

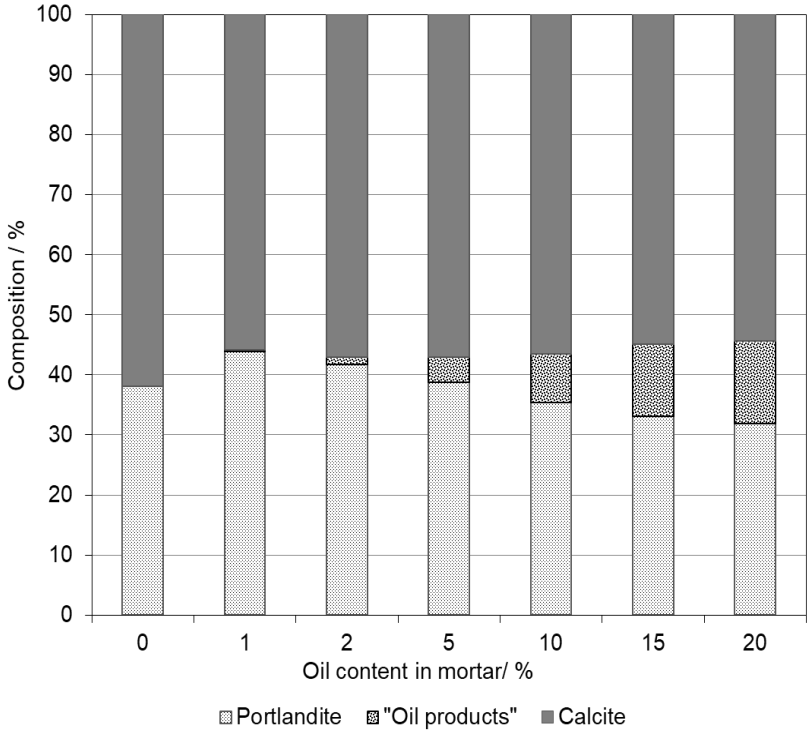

Figure 59. The composition of model mortars as determined by thermogravimetry (% by mass).

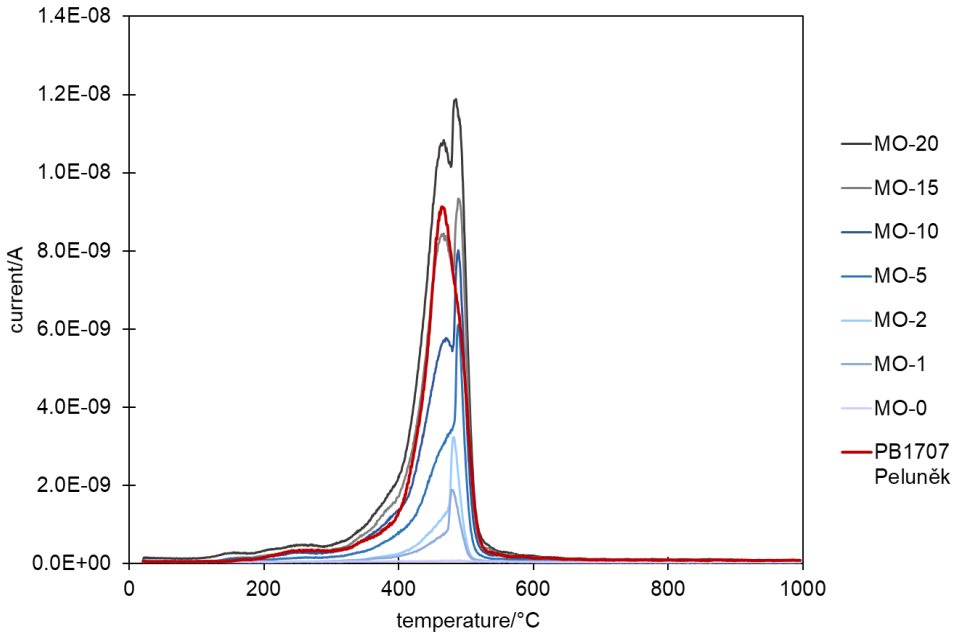

Figure 60. The EGA-MS signal of *m/z* 95 ion detected in model mortars (bluish lines; the intensity increased with the oil content from M-0 to M-20) and historic mortar Peluněk (red line).

In model mortars, the electric signal detected for *m/z* 95 (Fig. 60) was growing with the increasing amount of added linseed oil. The quantification of EGA-MS signal was performed based on several premises: Since the heating is constant (10 °C/min), the x-

axis may be expressed in the form of time. Then the area of the peak between 300 and 600 °C can be integrated and expressed in the form of an electric charge passed through the relevant detector channel. The dependence of the charge upon the oil content in the mortar was found to be linear (Fig. 61). Such linear dependence was used as a “calibration curve” for the authentic mortar analysis. The EGA-MS *m/z* 95 ion curve of historic mortar is very close to the M-15 model mortar (Fig. 60). Moreover, its peak area (passed charge) $5x10^{-6}$ C correspond to about 17% of linseed oil admixed to the fresh model mortar. This is in a very good agreement with the linseed oil dosage (16%) recommended by Gerspach who recorded an authentic 19th century recipe for mosaic mastic [95].

7.3.2.7 TOC

The third possible approach is based on the TOC determination. The TOC of model mortars (Fig. 61) is proportional to the linseed oil content. The TOC of authentic Peluněk mortar was 9.20% which correspons to the oil dosage about 25%.

The quantitative results of model experiments (value of m_{OP} from thermogravimetry; TOC and electric charge corresponding to *m/z* 95 ion), as well as those obtained for Peluněk mortar, are summarized in Fig. 61 and Tab. 19. Empty markers in Fig. 61 represent results of model mortars´ analyses while full markers correspond to the estimated oil dosage in the authentic Peluněk mortar. Model mortars served as

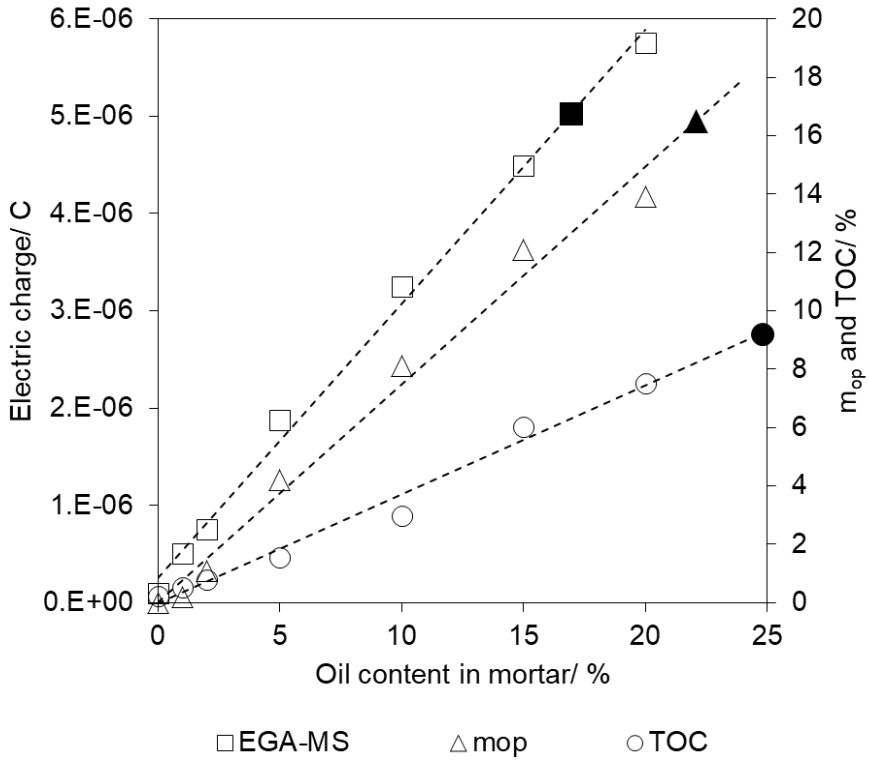

Figure 61. Quantitative results of model mortars thermal analysis and TOC (empty symbols) and estimated positions of historic mortar (full symbols).

"calibration curves" for these estimations. When the searched mass fraction of oil in mortar (with respect to dry components) is signed w_{oil}, the following Eq. 10 – 12 enable to estimate w_{oil} [% by mass] on basis of results of respective experiment (data shown in Fig. 61):

$$w_{oil}[\%] = 3.546 \cdot 10^6 \, Q\,[C] - 0.897 \qquad R^2 = 0.996 \qquad (10)$$

$$w_{oil}[\%] = 1.339 \, m_{op}\,[\%] - 0.006 \qquad R^2 = 0.985 \qquad (11)$$

$$w_{oil}[\%] = 2.695 \, TOC\,[\%] - 0.02 \qquad R^2 = 0.982 \qquad (12)$$

7.3.3 Evaluation of methods

Each of the three methods proposed for the quantification of linseed oil in historic mosaic mortars has its pros and cons. Total organic carbon (TOC) method is fast and easily accessible but it can not distinguish the nature of organic admixtures (e.g. to identify particular type of organics such as lipids, proteins, waxes etc.). Since the method is not specific to particular kinds of organic admixtures, it gives just the "bulk" content of all organic compounds present. If there were some other minor organic substances besides linseed oil undetected by our investigation methods in the Peluněk sample, this might explain why TOC gave the highest "oil" content – 25 wt%.

The determination of m_{op} based on thermogravimetry can be directly applied only to mortars based on air lime and $CaCO_3$ aggregates. These materials do not contain chemically bound water in the form of hydraulic lime hydration products. Peluněk mortar basically meets this condition as it was characterised as an air lime mortar with carbonatic filler [37]. Thermogravimetry results indicated the mortar contained 16.5% "oil products" (Tab. 19) which corresponds to about 22% of original oil admixture.

EGA-MS approach does not depend on mortar composition as neither non-calcareous aggregates nor hydraulic binder affect the *m/z* 95 signal intensity. The method based on the detection and analysis of $[C_7H_{11}]^+$ ion (its *m/z* 95 signal) provided the lowest "oil products" estimation (17%). This result is the closest to Gerpsach´s linseed oil dosage recommendation [95].

The three values calculated based on the three abovementioned methods (i.e. 25%, 22% and 17% of oil admixture) should be discussed closer to evaluate which of them is the most realistic. As mentioned above, the TOC assessment can be affected by the presence of other organics – no matter whether intentionally added or results of biodegradation processes [161]. An unidentified organic compound admixture (other than oil or its alteration products) would also affect thermogravimetric results. However, we should note neither a previous analysis of Peluněk mortar sample [37] nor Gerspach´s mosaic mortar recipe [95] indicate the presence of other organics but oil. Yet, possible overestimations due to interfering components (such as moisture, bound water, aggregates or other organics) can not be exluded. From this point of view, the

determination of “oil” content based on EGA-MS seems to be the least susceptible to interfering effects of all the three investigated methods.

7.4 Summary – Model samples

A set of model mortars imitating the composition of lime-based historic mosaic mortar beds was prepared in order to study the identification and quantification options of linseed oil content in authentic (not only mosaic) mortar samples by thermal analysis (thermogravimetry), evolved gas analysis (EGA) and total organic carbon (TOC) assessment. It was experimentally proved, linseed oil and its alteration or reaction products thermally decompose in the same temperature range as $Ca(OH)_2$ during thermogravimetric analysis. The overlapping $Ca(OH)_2$ peak “hides” the “oil products” peak which may lead to $Ca(OH)_2$ content overestimation. On the other hand, it was shown the addition of linseed oil slows down the carbonation process and so a certain amount of unconsumed portlandite (proportional to linseed oil content) still remained in lime-linseed oil model mortars as well as in the authentic Peluněk mosaic mortar bed sample. Even though the proposed methods proved to be suitable for the identification of organics admixed to the mortars, their combination with other methods, namely FTIR of the samples´ extracts, is recommended to get a better insight into the nature of “oil products” present in the samples.

A methodology of linseed oil content estimation in the historic mortars was proposed based of the three methods (TG coupled with EGA-MS and TOC) with model mortars measurements serving as “calibration curves”. The approach based on EGA-MS (identification and analysis of *m/z* 95 signal corresponding to “oil-specific” $[C_7H_{11}]^+$ ion) provided the closest results to a popular mosaic recipe available at the time of the reference authentic mortar´s origin. Moreover, this approach seems to be the least sensitive to possible interfering effects of other mortar´s components.

8 CONCLUSIONS

The thesis followed the development of mosaic fixing technique within a period of approximately one hundred years from the late 19th century to the late 20th century The characterisation of authentic mosaic mortar samples proved, diverse materials were used for mosaics´ fixation. An expected shift from traditional lime-based materials to an almost exclusive use of Portland cement fixing mortars was documented. Although the analysed set of 27 mosaic works is too small to make general conclusions, some trends and preferences in the use of materials can be traced in the works of different workshops.

- Samples from Prague-located portable sepulchral mosaics ascribed to Tirol-based Neuhauser workshop, the first mosaic studio operating in the Czech Lands, follow the traditional technology invented as early as the 16th century (and later recorded by Gerspach [95] whose book is a part of the company´s archive) – bedding mortars based on lime binder + marble aggregates + high amount of linseed oil (up to almost 40%) as a plasticizer. Canon Pfannerer´s mosaic from the upper gable of his sepulchre exhibits the signs of traditional *cocciopesto* technique.

- In order to fix larger-scale mosaics installed directly on the facades, Neuhauser/ Tiroler Glasmalerei applied hydraulic mortars made of lime, marble dust, random waste glass splinters and reactive ceramic aggregates (bricks, chamotte) or Portland cement based materials with carbonate aggregates.

- Josef Pfefferle´s mosaic mortars were characterised as mixtures of lime and early Portland cement. Similarly to his former employer, the Neuhauser studio, Pfefferle kept the addition of traditional carbonate aggregates to his mosaic bedding mortars.

- "The first Czech mosaicist" Viktor Foerster seems to have started to use new, progressive materials from the very beginning of his mosaic career. Mortar beds of Foerster´s mosaics studied within this project consist of siliceous sand, early Portland cement or mixtures of Portland cement and lime and crushed bricks or gypsum. His wife Marie who continued running Foerster´s studio after his death used blended Portland cement with blast furnace slag grains to fix the vault mosaic of the Slavín crypt.

- The analysed bedding mortars from mosaics produced by other early 20th century mosaic workshops also inndicate the on-going transition from traditional calcium carbonate aggregates and *cocciopesto* technique to the application of sand and Portland cement based mortars.

- Portland cement was the main compound in the binders of the studied "socialistic" mosaics of the latter half of the 20th century. In general, the technique of their preparation corresponds to the guidelines described in a

1980s textbook on mosaic making [49]. The materials nature of the cement recommended for the mosaics´ fixation was not explicitly specified in the textbook. However, this work brought evidence of a common use of blended cements containing granulated blast furnace slag.

- Linseed oil turned out to be an important compound of some late 19th/ early 20th century. Therefore a methodology of linseed oil content estimation in the historic mortars was proposed based of the three methods (TG coupled with EGA-MS and TOC). The approach based on EGA-MS (identification and analysis of *m/z* 95 signal corresponding to "oil-specific" $[C_7H_{11}]^+$ ion), developed on a set of model mortars and tested on authentic mosaic mortars´ samples, provided the most satisfactory results.

9 FUTURE PERSPECTIVES

In recent years, modern mosaics have been attracting more and more attention, not only from professionals but also from the general public. However, information on their materials composition is still very scarce. It is in the interest of the protection and preservation of the mosaic works that the group of works under study should be expanded. This will provide us with more objective information on the use and development of the mosaic technique. The thesis outlines several directions for possible further research: (1) better integration of the results of materials, restoration and art historical research, (2) evaluation of the materials and artistic qualities of mosaics from the Czech Lands in an international context, (3) development and improvement of the methods for determining organic components in mortars and (4) raising awareness of the tradition and quality of Czech mosaic works.

REFERENCES

[1] C. J. W. P. Groot, G. J. Ashall, and J. J. Hughes, *Characterisation of old mortars with respect to their repair: state-of-the-art report of RILEM Technical committee 167-COM*. in RILEM report, no. 28. Bagneux: RILEM publications, 2007.

[2] J. Jirásek, M. Sivek, and P. Láznička, *Ložiska nerostů*. Ostrava: Anagram, 2017. [Online]. Available: http://geologie.vsb.cz/loziska/suroviny/anorganicka_pojiva.html

[3] W. H. Gourdin and W. D. Kingery, 'The Beginnings of Pyrotechnology: Neolithic and Egyptian Lime Plaster', *Journal of Field Archaeology*, vol. 2, no. 1–2, pp. 133–150, 1975, [Online]. Available: https://www.jstor.org/stable/529624

[4] J. D. Frierman, 'Lime Burning as the Precursor of Fired Ceramics', *Israel Exploration Journal*, vol. 21, no. 4, pp. 212–216, 1971.

[5] I. Papayianni and M. Stefanidou, 'Durability aspects of ancient mortars of the archeological site of Olynthos', *Journal of Cultural Heritage*, vol. 8, no. 2, pp. 193–196, Apr. 2007, doi: 10.1016/j.culher.2007.03.001.

[6] S. Somayaji, *Civil engineering materials*, 2nd ed. Upper Saddle River, N.J: Prentice Hall, 2001.

[7] A. Arizzi and G. Cultrone, 'The influence of aggregate texture, morphology and grading on the carbonation of non-hydraulic (aerial) lime-based mortars', *QJEGH*, vol. 46, no. 4, pp. 507–520, Nov. 2013, doi: 10.1144/qjegh2012-017.

[8] A. Moropoulou, A. Bakolas, and S. Anagnostopoulou, 'Composite materials in ancient structures', *Cement and Concrete Composites*, vol. 27, no. 2, pp. 295–300, Feb. 2005, doi: 10.1016/j.cemconcomp.2004.02.018.

[9] A. Moropoulou, A. Bakolas, and K. Bisbikou, 'Investigation of the technology of historic mortars', *Journal of Cultural Heritage*, vol. 1, no. 1, pp. 45–58, Jan. 2000, doi: 10.1016/S1296-2074(99)00118-1.

[10] 'ČSN EN 459-1 ed. 3 (722201) Stavební vápno - Část 1: Definice, specifikace a kritéria shody'. Úřad pro technickou normalizaci, metrologii a státní zkušebnictví, 2015.

[11] D. Frankeová, 'Změny vlastností hydraulických vápenných pojiv vlivem zrychleného stárnutí', dissertation thesis, Czech Technical University in Prague, Prague, 2021.

[12] G. Mertens, P. Madau, D. Durinck, B. Blanpain, and J. Elsen, 'Quantitative mineralogical analysis of hydraulic limes by X-ray diffraction', *Cement and Concrete Research*, vol. 37, no. 11, pp. 1524–1530, Nov. 2007, doi: 10.1016/j.cemconres.2007.08.002.

[13] K. Callebaut, J. Elsen, K. V. Balen, and W. Viaene, 'Nineteenth century hydraulic restoration mortars in the Saint Michael's Church (Leuven, Belgium) Natural hydraulic lime or cement?', *Cement and Concrete Research*, 2001.

[14] P. Rovnaníková, *Omítky*, 1st ed. Praha: Společnost pro technologie ochrany památek, 2002.

[15] E. C. Eckel, *Cements, limes, and plasters, their materials, manufacture and properties*, 2nd ed. New York: Wiley, 1922.

[16] H. Böke, Ö. Çizer, B. İpekoğlu, E. Uğurlu, K. Şerifaki, and G. Toprak, 'Characteristics of lime produced from limestone containing diatoms', *Construction and Building Materials*, vol. 22, no. 5, pp. 866–874, May 2008, doi: 10.1016/j.conbuildmat.2006.12.010.

[17] J. Weber, A. Baragona, F. Pintér, and C. Gosselin, 'Hydraulicity in Ancient Mortars: Its Origin and Alteration Phenomena under the Microscope', presented at the 15th Euroseminar on Microscopy Applied to Building Materials, Delft, the Netherlands, Jun. 2015, pp. 147–156.

[18] M. J. McCarthy and T. D. Dyer, 'Pozzolanas ans Pozzolanic Materials', in *Lea's chemistry of cement and concrete*, P. C. Hewlett and M. Liska, Eds., Fifth edition.Oxford [England] ; Cambridge, MA: Butterworth-Heinemann, 2019, pp. 363–468.

[19] I. Papayianni and M. Stefanidou, 'Strength–porosity relationships in lime–pozzolan mortars', *Construction and Building Materials*, vol. 20, no. 9, pp. 700–705, Nov. 2006, doi: 10.1016/j.conbuildmat.2005.02.012.

[20] H. Böke, S. Akkurt, B. İpekoğlu, and E. Uğurlu, 'Characteristics of brick used as aggregate in historic brick-lime mortars and plasters', *Cement and Concrete Research*, vol. 36, no. 6, pp. 1115–1122, Jun. 2006, doi: 10.1016/j.cemconres.2006.03.011.

[21] V. Nežerka, J. Němeček, Z. Slížková, and P. Tesárek, 'Investigation of crushed brick-matrix interface in lime-based ancient mortar by microscopy and nanoindentation', *Cement and Concrete Composites*, vol. 55, pp. 122–128, Jan. 2015, doi: 10.1016/j.cemconcomp.2014.07.023.

[22] F. Turco, P. Davit, F. Chelazzi, A. Borghi, L. Bombardieri, and L. Operti, 'Characterization of Late Prehistoric Plasters and Mortars from Erimi - Laonin tou Porakou (Limassol, Cyprus): Plasters and mortars from Erimi - Laonin tou Porakou (Limassol, Cyprus)', *Archaeometry*, vol. 58, no. 2, pp. 284–296, Apr. 2016, doi: 10.1111/arcm.12168.

[23] G. Artioli, M. Secco, and A. Addis, 'The Vitruvian legacy: Mortars and binders before and after the Roman world', in *The Contribution of Mineralogy to Cultural Heritage*, Mineralogical Society of Great Britain and Ireland, 2019, pp. 151–202. doi: 10.1180/EMU-notes.20.4.

[24] A. Bakolas, G. Biscontin, A. Moropoulou, and E. Zendri, 'Characterization of structural byzantine mortars by thermogravimetric analysis', *Thermochimica Acta*, vol. 321, no. 1–2, pp. 151–160, Nov. 1998, doi: 10.1016/S0040-6031(98)00454-7.

[25] M. Theodoridou, I. Ioannou, and M. Philokyprou, 'New evidence of early use of artificial pozzolanic material in mortars', *Journal of Archaeological Science*, vol. 40, no. 8, pp. 3263–3269, Aug. 2013, doi: 10.1016/j.jas.2013.03.027.

[26] M. Vitruvius Pollio, *Deset knih o architektuře*, 5. Prague: Arista : Baset, 2021.

[27] R. Tišlová, *Hydration of natural cements*, V Tribunu EU vyd. 1. Brno: Tribun EU, 2009.

[28] K. Bayer, ‘Mikrostruktura a vlastnosti malt z románského cementu’, in *Románský cement - historie, vlastnosti a možnosti použití*, Prague: Společnost pro technologie ochrany památek, 9 2011, pp. 16–20.

[29] F. Pintér, C. Gosselin, T. Köberle, I. Vidovszky, and J. Weber, ‘From marlstone to rotary kilns – the early development of Portland cements in Central Europe’, in *Proceedings of the 5th Historic Mortars Conference*, Pamplona, Spain, Jun. 2019.

[30] N. Gadermayr, F. Pintér, and J. Weber, ‘Identification of 19th century Roman cements by the phase composition of clinker residues in historic mortars’, in *Proceedings of the 12th International Congress on the Deterioration and Conservation of Stone*, New York, Oct. 2022.

[31] H. F. W. Taylor, *Cement chemistry*, 2nd ed. London: T. Telford, 1997.

[32] E. A. R. Trout, ‘The History of Calcareous Cements’, in *Lea’s chemistry of cement and concrete*, P. C. Hewlett and M. Liska, Eds., Fifth edition.Oxford [England] ; Cambridge, MA: Butterworth-Heinemann, 2019, pp. 1–30.

[33] ‘ČSN EN 197-1 ED.2 (722101) Cement - Část 1: Složení, specifikace a kritéria shody cementů pro obecné použití’. Úřad pro technickou normalizaci, metrologii a státní zkušebnictví, 2013.

[34] J. Láník and M. Cikrt, *Dvě tisíciletí vápenictví a cementárenství v českých zemích*. Praha: Svaz výrobcít cementu a vápna Čech, Moravy a Slezska, 2001.

[35] D. Rohanová, S. Švarcová, and T. Hájek, ‘Signs of degradation of czech art nouveau mosaic glasses’, in *Znalost a praxe ve výtvarném umění: sbornik 4. mezioborové konference ALMA ; znalost a praxe ve výtvarném umění - cesta od poznání materiálů k technologickému uplatnění ; 21. - 23.11.2012, Strahovský klášter v Praze = Knowledge and experience in the fine art - from understanding materials to technological applications*, D. Hradil, J. Hradilová Eds., in Acta artis academica, no. 2012. Praha: Akademie Výtvarných Umění v Praze, 2012, pp. 227–243.

[36] P. Bauerová, M. Kracík Štorkánová, D. Frankeová, Z. Slížková, and M. Keppert, ‘Czech mosaic pioneer Viktor Foerster and the mortars of his mosaics’, in *Proceedings of the 6th Historic Mortars Conference*, V. Bokan Bosiljkov, A. Padovnik, T. Turk, and P. Štukovnik, Eds., Ljubljana: University of Ljubljana, 2022, pp. 40–49.

[37] Bauerová, M. Kracík Štorkánová, P. Mácová, M. Pavlíková, L. Scheinherrová, and M. Keppert, ‘Searching for common technological features of 19th–20th-century mosaic mortars ascribed to the Neuhauser company’, *Archaeometry*, vol. 63, no. 6, pp. 1216–1235, 2021, doi: 10.1111/arcm.12678.

[38] Bauerová *et al.*, ‘What fixes architect’s reason and sense? Materials study of CTU façade mosaic mortar’, *AIP Conference Proceedings*, no. 1, p. 020024, Feb. 2021, doi: 10.1063/5.0041947.

[39] B. M. Kürtösi, ‘Examination of Hungarian Art Nouveau Mosaics: the Róth Workshop’, in *What comes to mind when you hear mosaic? Conserving mosaics from ancient to modern*, R. Nardi and M. Pugès i Dorca, Eds., Firenze: International Committee for the Conservation of Mosaics.Edifir edizioni Firenze, 2020, pp. 663–667.

[40] P.-N. Maravelaki *et al.*, ‘RILEM TC 277-LHS report: additives and admixtures for modern lime-based mortars’, *Mater Struct*, vol. 56, no. 5, p. 106, Jun. 2023, doi: 10.1617/s11527-023-02175-z.

[41] L. B. Sickels, ‘Organic Additives in Mortars’, *Edinburgh architecture research*, vol. 8, pp. 7–20, 1981.

[42] A. Moropoulou, A. Bakolas, M. Karoglou, E. T. Delegou, K. C. Labropoulos, and N. S. Katsiotis, ‘Diagnostics and protection of Hagia Sophia mosaics’, *Journal of Cultural Heritage*, vol. 14, no. 3, pp. e133–e139, Jun. 2013, doi: 10.1016/j.culher.2013.01.006.

[43] G. C. Allen, D. D. Edwards, E. Cilibeto, and S. La Delfa, ‘Investigation of lime mortar/tesserae adhesion in medieval mosaics from the Basilica di San Marco, Venice’, in *Historical Mortars Conference: Characterization, Diagnosis, Conservation, Repair and Compatibility*, Lisbon, Portugal: LNEC, 2008.

[44] J. M. Haswell, *The Thames and Hudson manual of mosaic*. in The Thames and Hudson manual. London: Thames & Hudson, 1973.

[45] J. Höferová, ‘Technologický vývoj mozaikářského řemesla’, Univerzita Karlova v Praze, Katolická teologická fakulta, Praha, 2012. [Online]. Available: https://dspace.cuni.cz/handle/20.500.11956/42620

[46] A. Izaguirre, J. Lanas, and J. I. Álvarez, ‘Characterization of aerial lime-based mortars modified by the addition of two different water-retaining agents’, *Cement and Concrete Composites*, vol. 33, no. 2, pp. 309–318, Feb. 2011, doi: 10.1016/j.cemconcomp.2010.09.008.

[47] Y. Fang, J. Wang, X. Qian, L. Wang, Y. Dong, and P. Qiao, ‘Low-cost, ubiquitous biomolecule as a strength enhancer for cement mortars’, *Construction and Building Materials*, vol. 311, p. 125305, Dec. 2021, doi: 10.1016/j.conbuildmat.2021.125305.

[48] D. C. Stulik, ‘Scientific Research in the Conservation of the last Judgment Mosaic’, in *Conservation of the Last Judgment Mosaic, St. Vitus Cathedral, Prague*, Los Angeles: Getty Conservation Institute, 2005, pp. 135–156. [Online]. Available: http://hdl.handle.net/10020/gci_pubs/last_judgment_mosaic

[49] F. Tesař and A. Klouda, *Mozaikářství. Učební text pro 1. až 3. ročník učebního oboru mozaikář*. Prague: Institut Ministerstva kultury ČSR, 1988.

[50] J. P. Ingham, *Geomaterials under the microscope: a colour guide building stone, roofing slate, aggregate, concrete, mortar, plaster, bricks, ceramics, and bituminous mixtures*. London: Manson, 2011.

[51] D. Frankeová and V. Koudelková, ‘Influence of ageing conditions on the mineralogical micro-character of natural hydraulic lime mortars’, *Construction and Building Materials*, vol. 264, p. 120205, Dec. 2020, doi: 10.1016/j.conbuildmat.2020.120205.

[52] J. Elsen, K. Van Balen, and G. Mertens, ‘Hydraulicity in Historic Lime Mortars: A Review’, in *Historic Mortars*, J. Válek, J. J. Hughes, and C. J. W. P. Groot, Eds., in RILEM Bookseries, vol. 7. Dordrecht: Springer Netherlands, 2012, pp. 125–139. doi: 10.1007/978-94-007-4635-0_10.

[53] M. Jia *et al.*, ‘Characterization of archaeological lime mortars in a Ming dynasty tomb: A multi-analytical approach’, *Archaeometry*, vol. n/a, no. n/a, pp. 1–18, 2023, doi: 10.1111/arcm.12855.

[54] T. Karche and M. R. Singh, ‘Biologically induced calcium oxalate mineralization on 15th century lime mortar, Murud Sea fort, India’, *Journal of Archaeological Science: Reports*, vol. 39, p. 103178, Oct. 2021, doi: 10.1016/j.jasrep.2021.103178.

[55] L. Rampazzi, ‘Calcium oxalate films on works of art: A review’, *Journal of Cultural Heritage*, vol. 40, pp. 195–214, Nov. 2019, doi: 10.1016/j.culher.2019.03.002.

[56] K. M. D. Dunbabin, *Mosaics of the Greek and Roman world*. Cambridge ; New York: Cambridge University Press, 1999.

[57] K. B. Mádl, ‘Mosaika’, *Národní listy*, Prague, p. 13, Feb. 05, 1906.

[58] V. Vicherková, ‘Novodobá česká mozaika jako specifický druh umění v architektuře druhé poloviny 20. stol.’, diploma thesis, Charles University in Prague, Faculty of Arts, Prague, 2014. [Online]. Available: http://hdl.handle.net/20.500.11956/70919

[59] A. Břehová, ‘Vývoj a užití mozaiky v 50. letech 20. století v českém prostředí’, Palacky University in Olomouc, Faculty of Arts, Olomouc, 2009. [Online]. Available: https://theses.cz/id/oqfgyd/

[60] D. Bersani, L. Saviane, A. Morigi, L. Mantovani, M. Aceto, and L. Fornasini, ‘Multi-technique characterization of glass mosaic tesserae from Villa di Teodorico in Galeata (Italy)’, *Journal of Raman Spectroscopy*, vol. 52, no. 12, pp. 2234–2245, 2021, doi: 10.1002/jrs.6180.

[61] E. Basso, C. Invernizzi, M. Malagodi, M. F. La Russa, D. Bersani, and P. P. Lottici, ‘Characterization of colorants and opacifiers in roman glass mosaic *tesserae* through spectroscopic and spectrometric techniques: Characterization of colorants and opacifiers in roman glass mosaic *tesserae*’, *J. Raman Spectrosc.*, vol. 45, no. 3, pp. 238–245, Mar. 2014, doi: 10.1002/jrs.4449.

[62] P. Ricciardi, P. Colomban, A. Tournié, M. Macchiarola, and N. Ayed, ‘A non-invasive study of Roman Age mosaic glass tesserae by means of Raman spectroscopy’, *Journal of Archaeological Science*, vol. 36, no. 11, pp. 2551–2559, Nov. 2009, doi: 10.1016/j.jas.2009.07.008.

[63] S. Galli, M. Mastelloni, R. Ponterio, G. Sabatino, and M. Triscari, ‘Raman and scanning electron microscopy and energy-dispersive x-ray techniques for the characterization of colouring and opaquening agents in Roman mosaic glass tesserae’, *J. Raman Spectrosc.*, vol. 35, no. 89, pp. 622–627, Aug. 2004, doi: 10.1002/jrs.1181.

[64] P. Colomban *et al.*, ‘Raman identification of materials used for jewellery and mosaics in Ifriqiya’, *J. Raman Spectrosc.*, vol. 34, no. 3, pp. 205–213, Mar. 2003, doi: 10.1002/jrs.977.

[65] S. Fiorentino, T. Chinni, and M. Vandini, ‘Ravenna, its mosaics and the contribution of archaeometry. A systematic reassessment on literature data related to glass tesserae and new considerations’, *Journal of Cultural Heritage*, vol. 46, pp. 335–349, Nov. 2020, doi: 10.1016/j.culher.2020.06.003.

[66] A. Moropoulou, N. Zacharias, E. T. Delegou, B. Maróti, and Zs. Kasztovszky, ‘Analytical and technological examination of glass tesserae from Hagia Sophia’, *Microchemical Journal*, vol. 125, pp. 170–184, Mar. 2016, doi: 10.1016/j.microc.2015.11.020.

[67] V. S. F. Muralha, S. Canaveira, J. Mirão, S. Coentro, T. Morna, and C. S. Salerno, ‘Baroque glass mosaics from the Capela de São João Baptista (Chapel of Saint John the Baptist, Lisbon): unveiling the glassmaking records: Baroque glass mosaics from the Capela de São João Baptista’, *J. Raman Spectrosc.*, vol. 46, no. 5, pp. 483–492, May 2015, doi: 10.1002/jrs.4669.

[68] N. Schibille, P. Degryse, M. Corremans, and C. G. Specht, ‘Chemical characterisation of glass mosaic tesserae from sixth-century Sagalassos (south-west Turkey): chronology and production techniques’, *Journal of Archaeological Science*, vol. 39, no. 5, pp. 1480–1492, May 2012, doi: 10.1016/j.jas.2012.01.020.

[69] M. Verità, ‘Technology of Italian Glass Mosaics’, in *Conservation of the Last Judgment mosaic, St. Vitus Cathedral, Prague*, F. Piqué and D. Stulik, Eds., Los Angeles: Getty Conservation Institute, 2004.

[70] P. Costagliola, G. Baldi, C. Cipriani, E. Pecchioni, and A. Buccianti, ‘Mineralogical and chemical characterisation of the Medicean glass mosaic tesserae and mortars of the Grotta del Buontalenti, Giardino di Boboli, Florence, Italy’, *Journal of Cultural Heritage*, vol. 1, no. 3, pp. 287–299, Nov. 2000, doi: 10.1016/S1296-2074(00)01085-2.

[71] I. Kučerová, Z. Křenková, V. Říhová, Z. Zlámalová Cílová, and M. Knězů Knížová, ‘Typology of glass tesserae used for mosaic production in the Czech Republic´s territory’, in *Česká skleněná mozaika: historie, technologie, katalog exteriérových děl = Czech glass mozaic: history, technology, catalogue of exterior works*, Z. Křenková, I. Kučerová, and V. Říhová, Eds., Vydání: první.Praha: Vysoká škola chemicko-technologická v Praze, 2022, pp. 269–288.

[72] Z. Zlámalová Cílová, S. Randáková, and M. Knězů Knížová, ‘Mosaic glass technology’, in *Česká skleněná mozaika: historie, technologie, katalog exteriérových děl = Czech glass mozaic: history, technology, catalogue of exterior works*, Z. Křenková, I. Kučerová, and V. Říhová, Eds., Vydání: první.Praha: Vysoká škola chemicko-technologická v Praze, 2022, pp. 235–268.

[73] M. Kracík Štorkánová, ‘Keramická mozaika’, *Obklady, dlažba & sanita*, vol. 6, no. 5, pp. 22–25, 2013.

[74] F. Izzo *et al.*, ‘The art of building in the Roman period (89 B.C. – 79 A.D.): Mortars, plasters and mosaic floors from ancient Stabiae (Naples, Italy)’, *Construction and Building Materials*, vol. 117, pp. 129–143, Aug. 2016, doi: 10.1016/j.conbuildmat.2016.04.101.

[75] D. Miriello *et al.*, ‘Compositional study of mortars and pigments from the “Mosaico della Sala dei Draghi e dei Delfini” in the archaeological site of Kaulonía (Southern Calabria, Magna Graecia, Italy)’, *Archaeol Anthropol Sci*, vol. 9, no. 3, pp. 317–336, Apr. 2017, doi: 10.1007/s12520-015-0285-9.

[76] J. Bostock and H. T. Riley, ‘Pliny the Elder, The Natural History, BOOK XXXVI. THE NATURAL HISTORY OF STONES.’ http://www.perseus.tufts.edu/hopper/text?doc=Perseus%3Atext%3A1999.02.0137%3Abook%3D36 (accessed Jan. 23, 2023).

[77] V. Pachta, P. Marinou, and M. Stefanidou, ‘Development and testing of repair mortars for floor mosaic substrates’, *Journal of Building Engineering*, vol. 20, pp. 501–509, Nov. 2018, doi: 10.1016/j.jobe.2018.08.019.

[78] V. Pachta and M. Stefanidou, ‘Technology of multilayer mortars applied in ancient floor mosaic substrates’, *Journal of Archaeological Science: Reports*, vol. 20, pp. 683–691, Aug. 2018, doi: 10.1016/j.jasrep.2018.06.018.

[79] M. Secco, S. Dilaria, A. Addis, J. Bonetto, G. Artioli, and M. Salvadori, ‘The Evolution of the Vitruvian Recipes over 500 Years of Floor-Making Techniques: The Case Studies of the *Domus delle Bestie Ferite* and the *Domus di Tito Macro* (Aquileia, Italy): Evolution of Vitruvian recipes over 500 years of floor-making’, *Archaeometry*, vol. 60, no. 2, pp. 185–206, Apr. 2018, doi: 10.1111/arcm.12305.

[80] F. Puertas, M. T. Blanco-Varela, A. Palomo, J. J. Ortega-Calvo, X. Ariño, and C. Saiz-Jimenez, ‘Decay of Roman and repair mortars in mosaics from Italica, Spain’, *Science of The Total Environment*, vol. 153, no. 1–2, pp. 123–131, Aug. 1994, doi: 10.1016/0048-9697(94)90109-0.

[81] Z. Karayazili, B. Ipekoglu, and H. Böke, ‘Characteristics of Mortars of Mosaics From A Roman Villa in Antandros Ancient City, Turkey’, presented at the 6th International Congress on “Science and Technology for the Safeguard of Cultural Heritage in the Mediterranean Basin”, Athens, Greece, October 22-25, 2013, 2013. [Online]. Available: https://www.researchgate.net/publication/322100243_Characteristics_of_Mortars_of_Mosaics_From_A_Roman_Villa_in_Antandros_Ancient_City_Turkey

[82] R. Piovesan, L. Maritan, and J. Neguer, ‘Characterising the unique polychrome sinopia under the Lod Mosaic, Israel: pigments and painting technique’, *Journal of Archaeological Science*, vol. 46, pp. 68–74, Jun. 2014, doi: 10.1016/j.jas.2014.02.032.

[83] B. M. Kürtösi, ‘Copy at the Site, Original in the Museum: Sociopolitical Context, Circumstances of the Preparation and Display of the Mosaics, and Impacts, Villa Romana Baláca, Hungary’, in *The conservation and presentation of mosaics: at what cost? proceedings of the 12th ICCM conference, Sardinia, October 27-31, 2014*, Sardinia, October 27-31, 2014: The Getty Conservation institute, 2017, p. 372. [Online]. Available: https://d2aohiyo3d3idm.cloudfront.net/publications/virtuallibrary/9781606065334.pdf

[84] S. Llobet i Font, M. Pugès i Dorca, and A. Bertral i Arias, ‘Discovering and Safeguarding the Mosaics at the Pont del Treball Roman Villa in Barcelona’, in *The conservation and presentation of mosaics: at what cost? proceedings of the 12th ICCM conference, Sardinia, October 27-31, 2014*, Sardinia, October 27-31, 2014: The Getty Conservation institute, 2017, pp. 136–144. [Online]. Available: https://d2aohiyo3d3idm.cloudfront.net/publications/virtuallibrary/9781606065334.pdf

[85] J. Neguer, ‘The Lod Mosaic: Discovery and History of the Intervention’, in *The conservation and presentation of mosaics: at what cost? proceedings of the 12th ICCM conference, Sardinia, October 27-31, 2014*, Sardinia, October 27-31, 2014: The Getty Conservation institute, 2017, pp. 210–216. [Online]. Available: https://d2aohiyo3d3idm.cloudfront.net/publications/virtuallibrary/9781606065334.pdf

[86] C. Boschetti, A. Corradi, and P. Baraldi, ‘Raman characterization of painted mortar in Republican Roman mosaics’, *Journal of Raman Spectroscopy*, vol. 39, no. 8, pp. 1085–1090, 2008, doi: 10.1002/jrs.1970.

[87] P. Baraldi, S. Bracci, E. Cristoferi, S. Fiorentino, M. Vandini, and E. Venturi, ‘Pigment characterization of drawings and painted layers under 5th–7th centuries wall mosaics from Ravenna (Italy)’, *Journal of Cultural Heritage*, vol. 21, pp. 802–808, Sep. 2016, doi: 10.1016/j.culher.2016.03.001.

[88] E. Neri, B. Gratuze, and N. Schibille, ‘Dating the mosaics of the Durres amphitheatre through interdisciplinary analysis’, *Journal of Cultural Heritage*, vol. 28, pp. 27–36, Nov. 2017, doi: 10.1016/j.culher.2017.05.003.

[89] O. Bonnerot, A. Ceglia, and D. Michaelides, ‘Technology and materials of Early Christian Cypriot wall mosaics’, *Journal of Archaeological Science: Reports*, vol. 7, pp. 649–661, Jun. 2016, doi: 10.1016/j.jasrep.2015.10.019.

[90] B. M. Kürtösi, ‘Archaeometric Investigation of Medieval Wall Mosaic Fragments of Székesfehérvár, Hungary.’, in *ATTI Classe di Scienze Fisiche, Matematiche e Naturali 173-1, 2014-2015, Study Days on Venetian Glass Approximately 1700’s*, Venice: Istituto Veneto di Scenze Lettere ed Arti, 2015, pp. 137–145. [Online]. Available: http://www.istitutoveneto.org/pdf/GV_1700_Kurtosi

[91] B. Marchese and V. Garzillo, ‘An Investigation of the Mosaics in the Cathedral of Salerno. Part I. Characterization of Binding Materials’, *Studies in Conservation*, vol. 28, pp. 127–132, 1983, doi: https://doi.org/10.2307/1506115.

[92] A. Martan and M. Martan, ‘Restaurování mozaiky “Poslední soud” umístěné nad jižním vstupem do Svatovítské katedrály na Pražském hradě’, *Zprávy památkové péče*, vol. 62, no. 6, pp. 178–189, 2002.

[93] M. Kozarzewski, ‘Rekonstrukce středověké sochy Panny Marie s děťátkem z hradního kostela v Malborku a konzervace mozaiky v katedrále v Kwidzynu’, *Zprávy památkové péče120-*, vol. 77, no. 3, pp. 275–285, 2017.

[94] C. Belmonte and C. S. Salerno, ‘Mosaic glass made in Rome between the sixteenth and seventeenth centuries: Rome glassmakers for the Fabrica di San Pietro’, *Journal of Cultural Heritage*, vol. 9, pp. e93–e96, Dec. 2008, doi: 10.1016/j.culher.2008.06.003.

[95] E. Gerspach, *La Mosaique*. Paris: A. Quentin, 1880. [Online]. Available: https://archive.org/details/lamosaique00gers_0/page/271/mode/1up

[96] C. Fiori, M. Vandini, S. Prati, and G. Chiavari, ‘Vaterite in the mortars of a mosaic in the Saint Peter basilica, Vatican (Rome)’, *Journal of Cultural Heritage*, vol. 10, no. 2, pp. 248–257, Apr. 2009, doi: 10.1016/j.culher.2008.07.011.

[97] J. Höferová, ‘Historie skleněného obrazu a jeho proměna v průběhu staletí’, *Zprávy památkové péče*, vol. 77, no. 3, pp. 230–234, 2017.

[98] M. Kracík Štorkánová and D. Rohanová, ‘Materiálové rozdělení skleněných mozaik, jejich degradace a metody průzkumu’, *Zprávy památkové péče*, vol. 77, no. 3, pp. 235–243, 2017.

[99] V. Říhová and Z. Křenková, ‘History of Glass Mosaic’, in *Česká skleněná mozaika: historie, technologie, katalog exteriérových děl = Czech glass mozaic: history, technology, catalogue of exterior works*, Z. Křenková, I. Kučerová, and V. Říhová, Eds., Vydání: první.Praha: Vysoká škola chemicko-technologická v Praze, 2022, pp. 183–234.

[100] Z. Křenková and V. Říhová, ‘Evropská tradice a počátek novodobé mozaiky v Čechách a na Moravě’, *Theatrum historiae*, no. 20, pp. 193–222, 2017.

[101] S. Barr, *Venetian glass mosaics: 1860-1917*. Woodbridge (GB): Antique collectors' club, 2008.

[102] I. Seidlerová and J. Dohnálek, *Dějiny betonového stavitelství*. in Betonové stavitelství. Česká komora autorizovaných inženýrů a techniků činných ve výstavbě, 1999. [Online]. Available: https://books.google.cz/books?id=oK5iAAAACAAJ

[103] A. Sejková, M. Kracík Štorkánová, J. Sklenářová Teichmanová, and J. Štěpánek, *Atlas funeral: hřbitov Malvazinky*, 1. Únětice, Ústí nad Labem: Art & Craft Mozaika, UJEP, 2015.

[104] M. Kracík Štorkánová and T. Hájek, *Muzivní umění: Mozaika v českém výtvarném umění*. Prague: Národohospodářský ústav Josefa Hlávky, 2014.

[105] B. M. Kürtösi, 'Reštaurovanie nástenných mozaik zo začiatku 20. storočia', in *Zborník prednášok XIII. medzinárodného seminára o reštaurovaní, Tatranská Lomnica 2014*, Tatranská Lomnica: Obec reštaurátorov Slovensk, 2015, pp. 76–81.

[106] I. Perná, T. Hanzlíček, and M. Kracík Štorkánová, 'Characterization of historic mosaic at Pfeiffer-Kral sepulcher, Jablonec nad Nisou: A study of the mortar and tesserae origin', *Ceramics – Silikáty*, vol. 58, no. 4, pp. 308–313, 2014.

[107] B. M. Kürtösi, 'Bedding mortars of the late 19th and beginning of 20th century in Hungary and Bohemia', presented at the Restaurování mozaik ze skla a kamene, Litomyšl, Apr. 28, 2022.

[108] M. Novák, 'Mortars for Mosaic Installation and Restoration', in *Česká skleněná mozaika: historie, technologie, katalog exteriérových děl = Czech glass mozaic: history, technology, catalogue of exterior works*, Z. Křenková, I. Kučerová, and V. Říhová, Eds., Vydání: první.Praha: Vysoká škola chemicko-technologická v Praze, 2022, pp. 289–299.

[109] V. Říhová and Z. Křenková, 'Pražská mozaikářská dílna Viktora Foerstera. Přehled monumentálních zakázek', *Staletá Praha*, vol. 33, no. 1, pp. 31–59, 2017.

[110] Archive of the Czech Academy of Sciences, 'fond Svatobor (1896-1967)', box 89.

[111] *Učebnice výroby umělých kamenů pro práce hřbitovní a stavební*. Bzenec: Triplex.

[112] V. Ettler, O. Legendre, F. Bodénan, and J.-C. Touray, 'Primary Phases and Natural Weathering of Old Lead-Zinc Pyrometallurgical Slag from Příbram, Czech Republic', *The Canadian Mineralogist*, vol. 39, pp. 873–888, 2001.

[113] V. Vicherková and V. Kracík Štorkánová, 'Z dějin českého mozaikářství', *Zprávy památkové péče*, vol. 77, no. 3, pp. 197–206, 2017.

[114] V. Heidingsfeld, 'personal communication', Feb. 11, 2021.

[115] S. Pacovský, 'personal communication', Jan. 31, 2021.

[116] K. Koch and A. Galstyan, *Mosaiki: Bruchstücke einer Utopie: Mosaiken im postsowjetischen Raum = Fragments of an utopia:mosaics in post Soviet areas*, Erstausgabe, 1. Auflage. Berlin: Lukas Verlag, 2019.

[117] Z. Křenková, V. Říhová, and I. Kučerová, 'Katalog', in *Česká skleněná mozaika: historie, technologie, katalog exteriérových děl = Czech glass mozaic: history,*

technology, catalogue of exterior works, Z. Křenková, I. Kučerová, and V. Říhová, Eds., Vydání: první.Praha: Vysoká škola chemicko-technologická v Praze, 2022, pp. 301–544.

[118] D. Svoboda, 'Restaurování skleněné mozaiky s motivem racka z dolní stanice lanovky na Pastýřskou stěnu v Děčíně. Restaurování kamenné mozaiky Ptačí rodina v ulici Lidická v Litomyšli. Technická fotografie v UV, IR záření a falešných barvách.', diploma thesis (MgA.), Univerzita Pardubice, Fakulta restaurování, Pardubice, 2020.

[119] M. Kracík Štorkánová, 'Mozaiky v památkové péči z pohledu restaurátora v 21. století se zaměřením na problematiku transferů muzívních děl', *Zprávy památkové péče*, vol. 77, no. 3, pp. 265–274, 2017.

[120] Y. Doganis and A. Galanos, 'Conservation and Display of a Twentieth-Century Large Wall Mosaic', in *The conservation and presentation of mosaics: at what cost? proceedings of the 12th ICCM conference, Sardinia, October 27-31, 2014*, Sardinia, October 27-31, 2014: The Getty Conservation institute, 2017, p. 372. [Online]. Available: https://d2aohiyo3d3idm.cloudfront.net/publications/virtuallibrary/9781606065334.pdf

[121] M. Kracík Štorkánová, Ed., *Opus musivum: mozaika ve výtvarném umění*. Praha: Art & Craft Mozaika, 2016.

[122] M. Storch and E. Maireth, 'Mozaiky z Neuhauseroy dílny a Tyrolské sklomalířské a mozaikářské dílny v 19. a 20. století', *Zprávy památkové péče*, vol. 77, no. 3, pp. 321–323, 2017.

[123] R. Rampold, '140 Jahre Tiroler Glasmalerei- und Mosaikanstalt 1861-2001', 2001. Accessed: Jun. 26, 2023. [Online]. Available: https://mosaik-tirol.at/Literatur/TGM-Rampold

[124] Z. Křenková and V. Říhová, 'Mosaic Imports for Sepulcral Architecture in Bohemia and Moravia (Albert Neuhauser, Tiroler Malerei- und Mosaikanstalt, Bayerische Mosaikanstalt, Puhl and Wagner, Leopold Forstner)', in *Epigraphica et Sepulcralia*, J. Roháček, Ed., Prague: Ústav dějin umění AV ČR, 2021, pp. 255–278.

[125] Z. Křenková and V. Říhová, 'Viktor Foerster a mozaiková tvorba pro náhrobky / Viktor Foerster and mosaic production for tombstones', in *Epigraphica et Sepulcralia*, J. Roháček, Ed., Prague: Ústav dějin umění AV ČR, 2020, pp. 255–278. Accessed: Jun. 25, 2023. [Online]. Available: https://www.academia.edu/45090306/Viktor_Foerster_a_mozaikov%C3%A1_tvorba_pro_n%C3%A1hrobky_Viktor_Foerster_and_mosaic_production_for_tombstones

[126] V. Říhová, Z. Křenková, and J. Klazar, 'Mozaika pro kostel Panny Marie Růžencové v Českých Budějovicích', in *Památky jižních Čech*, České Budějovice: NPÚ ÚOP České Budějovice, 2017, pp. 135–149.

[127] M. Hemelík, *Nemám již snad žádného, s kým bych o věcech nebeských mluvil...Životní příběh a dílo zakladatele novodobého čského mozaikového umění Viktora Foerstera*, 1st ed. Světice: M. Hemelík, 2015.

[128] M. Kracík Štorkánová and M. Hemelík, *'Tvá práce svítí, Marie, modlitbou k Viktorovi' : prolínání životních a uměleckých osudů Viktora a Marie Viktorie*

Foersterových, 1. in Studie Národohospodářského ústavu Josefa Hlávky, no. 9/2017. Prague: Nadání Josefa a Marie Hlávkových, AVU v Praze, 2017.

[129] Z. Křenková and V. Říhová, 'Skleněné mozaiky od konce 19. do poloviny 20. století - příspěvek k umělecké topografii Moravy', *Zprávy památkové péče*, vol. 77, no. 3, pp. 207–218, 2017.

[130] V. Pařík and A. Paříková, 'Kamenná řezaná mozaika RAKO - znovuobjevení zaniklé technologie', *Zprávy památkové péče*, vol. 77, no. 3, pp. 244–253, 2017.

[131] Z. Křenková, 'Jan Tumpach a cesta k českému mozaikovému materiálu', *Zprávy památkové péče*, vol. 77, no. 3, pp. 254–259, 2017.

[132] P. Bauerová, M. Kracík Štorkánová, and V. Vicherková, 'Kamenná mozaika - muzívní technika s nejdelší tradicí', *Zprávy památkové péče*, vol. 77, no. 3, pp. 219–229, 2017.

[133] A. Ballardini and L. Ballardini, 'Dílo italského mozaikáře Saura Ballardiniho v Praze', *Zprávy památkové péče*, vol. 77, no. 3, pp. 314–320, 2017.

[134] M. Kracík Štorkánová, V. Vicherková, P. Bauerová, M. Hemelík, and D. Rohanová, 'Vesmírné i pozemské poselství mozaik Saura Ballardiniho. Záchrana a restaurování mozaiky ‚Člověk dobývající nové horizonty vesmíru' a hledání nových perspektiv pro historické mozaiky v ČR', *Staletá Praha*, vol. 38, no. 1, pp. 76–115, 2022, doi: 10.56112/sp.2022.1.04.

[135] Mětská část Praha 10, 'Mozaiky', *Veřejné prostory Prahy 10*. https://verejneprostory.cz/aktivity-a-verejne-prostory/menime-verejne-prostory/mozaiky (accessed Jun. 27, 2023).

[136] obec Únětice, 'Mozaikové lavičky - mapka', *Únětice - oficiální stránky obce*, May 03, 2023. https://www.unetice.cz/mozaikove-lavicky-mapka/d-3822 (accessed Jun. 27, 2023).

[137] ART & CRAFT Mozaika, 'ART & CRAFT Mozaika'. https://cs-cz.facebook.com/artacraftmozaika (accessed Jun. 27, 2023).

[138] *Současná česká mozaika*, Vydání první. Most: Oblastní muzeum a galerie v Mostě, 2019.

[139] M. Storch and M. Kracík Štorkánová, 'Mosaike in un aus Tirol', *Mosaic Connection*, 2018. https://mosaik-tirol.at/karte.html

[140] Izolyatsia - platform for Cultural Initiatives, 'Soviet Mosaics in Ukraine', *Soviet Mosaics in Ukraine*, 2013. https://sovietmosaicsinukraine.org (accessed Jun. 27, 2023).

[141] P. Karous, 'Plastic art in public areas in the period "Normalization"', *Vetřelci a volavky*. https://www.vetrelciavolavky.cz/en (accessed Jun. 27, 2023).

[142] P. Karous and S. Jankovičová, Eds., *Vetřelci a volavky: atlas výtvarného umění ve veřejném prostoru v Československu v období normalizace (1968-1989) = Aliens and herons: a guide to fine art in the public space in the era of normalisation in Czechoslovakia (1968-1989)*, Second revised edition. Praha: Pavel Karous, 2015.

[143] B. Kostuch, *Kolor i blask: ceramika architektoniczna oraz mozaiki w Krakowie i Małopolsce po 1945 roku*. Kraków: Muzeum Narodowe, 2015.

[144] M. Maleschka, *DDR: Kunst im öffentlichen Raum 1950 bis 1990*. in Baubezogene Kunst. Berlin: DOM Publishers, 2019.

[145] B. Stępień, *Łódzkie mozaiki i inne monumentalne akcenty plastyczne czasów PRL*, Wydanie 1. Łódź: Księży Młyn Dom Wydawniczy Michał Koliński, 2021.

[146] M. Kněžů Knížová *et al.*, 'Přehled skleněných exteriérových mozaik na území ČR - Seznam mozaik', 2015. http://mozaika.vscht.cz/data/kraje.html (accessed Jun. 27, 2023).

[147] Z. Křenková, I. Kučerová, and V. Říhová, Eds., *Česká skleněná mozaika: historie, technologie, katalog exteriérových děl = Czech glass mozaic: history, technology, catalogue of exterior works*, Vydání: první. Praha: Vysoká škola chemicko-technologická v Praze, 2022.

[148] I. Kučerová and J. Vojtěchovský, 'České mozaiky', *České mozaiky*. https://ceskemozaiky.cz/ (accessed Jun. 29, 2023).

[149] I. Kučerová, 'Ukončený projekt NAKI „Mozaika I" věnovaný středověkým mozaikám', *e-Monumentica*, vol. 4, no. 1, pp. 82–83, 2016, [Online]. Available: https://fr.upce.cz/fr/veda-vyzkum/e-monumentica.html

[150] V. Říhová and Z. Křenková, 'Decoration of Dittrich family tomb in Krásná Lípa with mosaic production from Berlin', in *Epigraphica et Sepulcralia*, J. Roháček, Ed., Prague: Ústav dějin umění AV ČR, 2022, pp. 207–230.

[151] V. Říhová and Z. Křenková, 'Mozaikářská produkce zahraničních firem pro sepulkrální památky v Sudetech', in *Paměť hřbitovů: sepulkrální památky někdejších Sudet : katalog výstavy*, J. Bílková and P. Hečková, Eds., 1st ed.Pardubice: Univerzita Pardubice, 2022, pp. 149–165.

[152] 'Osinkocement Olbrama Zoubka', *Beton-technologie, konstrukce, sanace*, no. 5, p. 24, 2016, [Online]. Available: https://www.ebeton.cz/wp-content/uploads/2016-5-24_0.pdf

[153] B. Middendorf, J. J. Hughes, K. Callebaut, G. Baronio, and I. Papayianni, 'Investigative methods for the characterisation of historic mortars—Part 1: Mineralogical characterisation', *Mat. Struct.*, vol. 38, no. 8, pp. 761–769, Oct. 2005, doi: 10.1007/BF02479289.

[154] B. Middendorf, J. J. Hughes, K. Callebaut, G. Baronio, and I. Papayianni, 'Investigative methods for the characterisation of historic mortars—Part 2: Chemical characterisation', *Mat. Struct.*, vol. 38, no. 8, pp. 771–780, Oct. 2005, doi: 10.1007/BF02479290.

[155] N. Doebelin and R. Kleeberg, 'Profex: a graphical user interface for the Rietveld refinement program BGMN', *J Appl Crystallogr*, vol. 48, no. Pt 5, pp. 1573–1580, Oct. 2015, doi: 10.1107/S1600576715014685.

[156] 'DIN 19539 - Investigation of solids - Temperature-dependent differentiation of total carbon (TOC400, ROC, TIC900).' Deutsches Institut fur Normung E.V., 2016.

[157] R. D. Terry and G. V. Chilingar, 'Summary of "Concerning some additional aids in studying sedimentary formations," by M. S. Shvetsov', *Journal of Sedimentary Research*, vol. 25, no. 3, pp. 229–234, Sep. 1955, doi: 10.1306/74D70466-2B21-11D7-8648000102C1865D.

[158] M. Thiery, G. Villain, P. Dangla, and G. Platret, ‘Investigation of the carbonation front shape on cementitious materials: Effects of the chemical kinetics’, *Cement and Concrete Research*, vol. 37, no. 7, pp. 1047–1058, Jul. 2007, doi: 10.1016/j.cemconres.2007.04.002.

[159] M. Singh, S. Vinodh Kumar, S. A. Waghmare, and P. D. Sabale, ‘Aragonite–vaterite–calcite: Polymorphs of CaCO3 in 7th century CE lime plasters of Alampur group of temples, India’, *Construction and Building Materials*, vol. 112, pp. 386–397, Jun. 2016, doi: 10.1016/j.conbuildmat.2016.02.191.

[160] J. Adams, D. Dollimore, and D. L. Griffiths, ‘Thermal analytical investigation of unaltered Ca(OH)2 in dated mortars and plasters’, *Thermochimica Acta*, vol. 324, no. 1, pp. 67–76, Dec. 1998, doi: 10.1016/S0040-6031(98)00524-3.

[161] D. Cígler Žofková, J. Frankl, and D. Frankeová, ‘Use of thermal analysis for the detection of calcium oxalate in selected forms of plastering exposed to the effects of Serpula lacrymans’, *Acta Polytechnica*, vol. 61, no. 4, pp. 511–515, 2021, doi: 10.14311/AP.2021.61.0511.

[162] T. Rosado, M. Gil, J. Mirão, A. Candeias, and A. T. Caldeira, ‘Oxalate biofilm formation in mural paintings due to microorganisms – A comprehensive study’, *International Biodeterioration & Biodegradation*, vol. 85, pp. 1–7, Nov. 2013, doi: 10.1016/j.ibiod.2013.06.013.

[163] J. Russ, W. D. Kaluarachchi, L. Drummond, and H. G. M. Edwards, ‘The Nature of a Whewellite-Rich Rock Crust Associated with Pictographs in Southwestern Texas’, *Studies in Conservation*, vol. 44, no. 2, pp. 91–103, 1999, doi: 10.2307/1506721.

[164] M. Lazzari and O. Chiantore, ‘Drying and oxidative degradation of linseed oil’, *Polymer Degradation and Stability*, vol. 65, no. 2, pp. 303–313, Aug. 1999, doi: 10.1016/S0141-3910(99)00020-8.

[165] P. Bauerová, M. Kracík-Štorkánová, P. Mácová, P. Reiterman, E. Vejmelková, and M. Keppert, ‘Estimation of the linseed oil content in historic lime mortar’, *J Therm Anal Calorim*, vol. 148, no. 3, pp. 697–709, Feb. 2023, doi: 10.1007/s10973-022-11792-9.

[166] A. Moropoulou, A. Bakolas, and K. Bisbikou, ‘Characterization of ancient, byzantine and later historic mortars by thermal and X-ray diffraction techniques’, *Thermochimica Acta*, vol. 269–270, pp. 779–795, Dec. 1995, doi: 10.1016/0040-6031(95)02571-5.

[167] A. Zhao, B. Xiong, Y. Han, and H. Tong, ‘Thermal decomposition paths of calcium nitrate tetrahydrate and calcium nitrite’, *Thermochimica Acta*, vol. 714, p. 179264, Aug. 2022, doi: 10.1016/j.tca.2022.179264.

[168] V. Nežerka, Z. Slížková, P. Tesárek, T. Plachý, D. Frankeová, and V. Petráňová, ‘Comprehensive study on mechanical properties of lime-based pastes with additions of metakaolin and brick dust’, *Cement and Concrete Research*, vol. 64, pp. 17–29, Oct. 2014, doi: 10.1016/j.cemconres.2014.06.006.

[169] K. Scrivener, R. Snellings, and B. Lothenbach, Eds., *A practical guide to microstructural analysis of cementitious materials*, First issued in paperback. Boca Raton London New York: CRC Press, 2017.

[170] G. Artioli, M. Secco, A. Addis, and M. Bellotto, ‘5. Role of hydrotalcite-type layered double hydroxides in delayed pozzolanic reactions and their bearing on

mortar dating', in *Cementitious Materials*, H. Pöllmann, Ed., De Gruyter, 2017, pp. 147–158. doi: 10.1515/9783110473728-006.

[171] G. Ponce-Antón, L. A. Ortega, M. C. Zuluaga, A. Alonso-Olazabal, and J. L. Solaun, 'Hydrotalcite and Hydrocalumite in Mortar Binders from the Medieval Castle of Portilla (Álava, North Spain): Accurate Mineralogical Control to Achieve More Reliable Chronological Ages', *Minerals*, vol. 8, no. 8, Art. no. 8, Aug. 2018, doi: 10.3390/min8080326.

[172] M. D. Jackson *et al.*, 'Mechanical resilience and cementitious processes in Imperial Roman architectural mortar', *Proc. Natl. Acad. Sci. U.S.A.*, vol. 111, no. 52, pp. 18484–18489, Dec. 2014, doi: 10.1073/pnas.1417456111.

[173] C. J. Brandon, R. L. Hohlfelder, M. D. Jackson, J. P. Oleson, and L. Bottalico, *Building for eternity: the history and technology of Roman concrete engineering in the sea*. Oxford ; Philadelphia: Oxbow Books, 2014.

[174] G. Vola, E. Gotti, C. Brandon, J. P. Oleson, and R. obert L. Hohlfelder, 'Chemical, mineralogical and petrographic characterization of Roman ancient hydraulic concretes cores from Santa Liberata, Italy, and Caesarea Palestinae, Israel', *Periodico di Mineralogia*, vol. 80, no. 2, pp. 317–338, Sep. 2011, doi: 10.2451/2011PM0023.

[175] E. Ruh, 'Refractory Materials, Metallurgical', in *Concise Encyclopedia of Advanced Ceramic Materials*, Elsevier, 1991, pp. 394–402. doi: 10.1016/B978-0-08-034720-2.50109-X.

[176] M. P. Riccardi, B. Messiga, and P. Duminuco, 'An approach to the dynamics of clay firing', *Applied Clay Science*, vol. 15, no. 3, pp. 393–409, Oct. 1999, doi: 10.1016/S0169-1317(99)00032-0.

[177] F. Chargui, M. Hamidouche, H. Belhouchet, Y. Jorand, R. Doufnoune, and G. Fantozzi, 'Mullite fabrication from natural kaolin and aluminium slag', *Boletín de la Sociedad Española de Cerámica y Vidrio*, vol. 57, no. 4, pp. 169–177, Jul. 2018, doi: 10.1016/j.bsecv.2018.01.001.

[178] E. Laita and B. Bauluz, 'Mineral and textural transformations in aluminium-rich clays during ceramic firing', *Applied Clay Science*, vol. 152, pp. 284–294, Feb. 2018, doi: 10.1016/j.clay.2017.11.025.

[179] C. N. Djangang *et al.*, 'Sintering of clay-chamotte ceramic composites for refractory bricks', *Ceramics International*, vol. 34, no. 5, pp. 1207–1213, Jul. 2008, doi: 10.1016/j.ceramint.2007.02.012.

[180] B. C. Mendes *et al.*, 'Evaluation of eco-efficient geopolymer using chamotte and waste glass-based alkaline solutions', *Case Studies in Construction Materials*, vol. 16, p. e00847, Jun. 2022, doi: 10.1016/j.cscm.2021.e00847.

[181] S. S. Musil and W. M. Kriven, 'In Situ Mechanical Properties of Chamotte Particulate Reinforced, Potassium Geopolymer', *Journal of the American Ceramic Society*, vol. 97, no. 3, pp. 907–915, 2014, doi: 10.1111/jace.12736.

[182] M. Gelnar, 'Technická keramika ze zaniklých sklářských hutí v Čechách'.

[183] F. Engström, D. Adolfsson, C. Samuelsson, Å. Sandström, and B. Björkman, 'A study of the solubility of pure slag minerals', *Minerals Engineering*, vol. 41, pp. 46–52, Feb. 2013, doi: 10.1016/j.mineng.2012.10.004.

[184] M. Tossavainen, F. Engstrom, Q. Yang, N. Menad, M. Lidstrom Larsson, and B. Bjorkman, ‘Characteristics of steel slag under different cooling conditions’, *Waste Management*, vol. 27, no. 10, pp. 1335–1344, Jan. 2007, doi: 10.1016/j.wasman.2006.08.002.

[185] A. Çelik *et al.*, ‘The effect of high temperature minerals and microstructure on the compressive strength of bricks’, *Applied Clay Science*, vol. 169, pp. 91–101, Mar. 2019, doi: 10.1016/j.clay.2018.11.020.

[186] J. Ou *et al.*, ‘Preparation and in vitro bioactivity of novel merwinite ceramic’, *Biomed. Mater.*, vol. 3, no. 1, p. 015015, Mar. 2008, doi: 10.1088/1748-6041/3/1/015015.

[187] V. Říhová and Z. Křenková, ‘The earliest tomb mosaics from the production of Innsbruck-based companies in Bohemia and Moravia’, *Opuscula historiae artium*, vol. 69, pp. 36–57, 2020.

[188] C. Nunes, P. Mácová, D. Frankeová, R. Ševčík, and A. Viani, ‘Influence of linseed oil on the microstructure and composition of lime and lime-metakaolin pastes after a long curing time’, *Construction and Building Materials*, vol. 189, pp. 787–796, Nov. 2018, doi: 10.1016/j.conbuildmat.2018.09.054.

[189] D. Erhardt, C. S. Tumosa, and M. F. Mecklenburg, ‘Long-Term Chemical and Physical Processes in Oil Paint Films’, *Studies in Conservation*, vol. 50, no. 2, pp. 143–150, Jun. 2005, doi: 10.1179/sic.2005.50.2.143.

[190] L. Robinet and M.-C. Corbeil-a2, ‘The Characterization of Metal Soaps’, *Studies in Conservation*, vol. 48, no. 1, pp. 23–40, Jan. 2003, doi: 10.1179/sic.2003.48.1.23.

[191] M. R. Derrick, D. Stulik, and J. M. Landry, *Infrared Spectroscopy in Conservation Science*. Getty Publications, 2000.

[192] E. Čechová, I. Papayianni, and M. Stefanidou, ‘Properties of Lime-Based Restoration Mortars Modified by the Addition of Linseed Oil’, in *Proceedings of the 2nd Historic Mortars Conference HMC2010 and RILEM TC 203-RHM Final Workshop*, J. Válek, C. J. W. P. Groot, and J. J. Hughes, Eds., Prague, Czech Republic, Sep. 2010, pp. 937–945. [Online]. Available: https://www.rilem.net/publication/publication/82

[193] C. Nunes and Z. Slížková, ‘Hydrophobic lime based mortars with linseed oil: Characterization and durability assessment’, *Cement and Concrete Research*, vol. 61–62, pp. 28–39, Jul. 2014, doi: 10.1016/j.cemconres.2014.03.011.

[194] P. Bauerová, P. Reiterman, V. Davidová, E. Vejmelková, M. K. Štorkánová, and M. Keppert, ‘Lime mortars with liseed oil: engineering properties and durability’, *Romanian Journal of Materials*, vol. 51, no. 2, pp. 239–246, 2021.

[195] I. Papayianni, V. Pachta, and M. Stefanidou, ‘Analysis of ancient mortars and design of compatible repair mortars: The case study of Odeion of the archaeological site of Dion’, *Construction and Building Materials*, vol. 40, pp. 84–92, Mar. 2013, doi: 10.1016/j.conbuildmat.2012.09.086.

[196] A. M. Gadalla and T. W. Livingston, ‘Thermal behavior of oxides and hydroxides of iron and nickel’, *Thermochimica Acta*, vol. 145, pp. 1–9, Jun. 1989, doi: 10.1016/0040-6031(89)85121-4.

[197] A. B. Pole and I. Sims, *Concrete petrography. A handbook of investigative techniques*, 2nd ed. Boca Raton: CRC Press, 2020.

[198] D. H. Campbell, *Microscopical Examination and Interpretation of Portland Cement and Clinker*, 2nd ed. Construction Technology Laboratories, 1999.

[199] M. Sekyra, 'Historie obce Tolštejn (Tollenstein) v letech 1935 - 1950', Bachelor thesis, Hradecc Králové University, Faculty of Arts, Hradec Králové, 2015.

[200] O. Meluzín, *Technologie betonu*. Brno: VUT Brno, 1977.

[201] R. Froněk, Ed., *Cement-vápno-azbestocement*. Výzkumný a vývojový ústav maltovin a osinkocementu, 1977.

[202] J. Zelinger, V. Heidingsfeld, P. Kotlík, and E. Šimůnková, *Chemie v práci konzervátora a restaurátora*. Prague: Academia, 1987.

[203] N. H. Sissener, R. Ørnsrud, M. Sanden, L. Frøyland, S. Remø, and A.-K. Lundebye, 'Erucic Acid (22:1n-9) in Fish Feed, Farmed, and Wild Fish and Seafood Products', *Nutrients*, vol. 10, no. 10, p. 1443, Oct. 2018, doi: 10.3390/nu10101443.

[204] E. Mareš, M. Pleva, A. Přikryl, and V. Jančík, 'Czechoslovak Patent No. 121244', 121244

[205] F. Vavřín and K. Retzl, *Ochrana stavebního díla proti korozi*. Prague: SNTL, 1987.

[206] S. A. Mjøs, 'The prediction of fatty acid structure from selected ions in electron impact mass spectra of fatty acid methyl esters', *European Journal of Lipid Science and Technology*, vol. 106, no. 8, pp. 550–560, 2004, doi: 10.1002/ejlt.200401013.

[207] S. Orsini, F. Parlanti, and I. Bonaduce, 'Analytical pyrolysis of proteins in samples from artistic and archaeological objects', *Journal of Analytical and Applied Pyrolysis*, vol. 124, pp. 643–657, Mar. 2017, doi: 10.1016/j.jaap.2016.12.017.

[208] L. De Viguerie, P. A. Payard, E. Portero, Ph. Walter, and M. Cotte, 'The drying of linseed oil investigated by Fourier transform infrared spectroscopy: Historical recipes and influence of lead compounds', *Progress in Organic Coatings*, vol. 93, pp. 46–60, Apr. 2016, doi: 10.1016/j.porgcoat.2015.12.010.

[209] S. Švarcová, E. Kočí, J. Plocek, A. Zhankina, J. Hradilová, and P. Bezdička, 'Saponification in egg yolk-based tempera paintings with lead-tin yellow type I', *Journal of Cultural Heritage*, vol. 38, pp. 8–19, Jul. 2019, doi: 10.1016/j.culher.2018.12.004.

[210] G. Poulenat, S. Sentenac, and Z. Mouloungui, 'Fourier-transform infrared spectra of fatty acid salts—Kinetics of high-oleic sunflower oil saponification', *J Surfact Deterg*, vol. 6, no. 4, pp. 305–310, Oct. 2003, doi: 10.1007/s11743-003-0274-1.

[211] J. Honzíček, 'Curing of Air-Drying Paints: A Critical Review', *Industrial & Engineering Chemistry Research*, Jun. 2019, doi: 10.1021/acs.iecr.9b02567.

[212] A. Schönemann and H. G. M. Edwards, 'Raman and FTIR microspectroscopic study of the alteration of Chinese tung oil and related drying oils during ageing', *Anal Bioanal Chem*, vol. 400, no. 4, pp. 1173–1180, May 2011, doi: 10.1007/s00216-011-4855-0.

[213] J. Van der Weerd, A. van Loon, and J. Boon, 'FTIR Studies of the Effects of Pigments on the Aging of Oil', *Studies in Conservation*, vol. 50, pp. 3–22, Jan. 2005, doi: 10.1179/sic.2005.50.1.3.

[214] F. Seniha Güner, Y. Yağcı, and A. Tuncer Erciyes, ‘Polymers from triglyceride oils’, *Progress in Polymer Science*, vol. 31, no. 7, pp. 633–670, Jul. 2006, doi: 10.1016/j.progpolymsci.2006.07.001.

[215] G. Falzone, I. Mehdipour, N. Neithalath, M. Bauchy, D. Simonetti, and G. Sant, ‘New insights into the mechanisms of carbon dioxide mineralization by portlandite’, *AIChE Journal*, vol. 67, no. 5, p. e17160, 2021, doi: 10.1002/aic.17160.

[216] E. Kočí, J. Rohlíček, L. Kobera, J. Plocek, S. Švarcová, and P. Bezdička, ‘Mixed lead carboxylates relevant to soap formation in oil and tempera paintings: the study of the crystal structure by complementary XRPD and ssNMR’, *Dalton Trans.*, vol. 48, no. 33, pp. 12531–12540, 2019, doi: 10.1039/C9DT02040C.

[217] S. Garrappa *et al.*, ‘Non-invasive identification of lead soaps in painted miniatures’, *Anal Bioanal Chem*, vol. 413, no. 1, pp. 263–278, Jan. 2021, doi: 10.1007/s00216-020-02998-7.

[218] A. Lagazzo, S. Vicini, C. Cattaneo, and R. Botter, ‘Effect of fatty acid soap on microstructure of lime-cement mortar’, *Construction and Building Materials*, vol. 116, pp. 384–390, Jul. 2016, doi: 10.1016/j.conbuildmat.2016.04.122.

[219] A. Izaguirre, J. Lanas, and J. I. Álvarez, ‘Effect of water-repellent admixtures on the behaviour of aerial lime-based mortars’, *Cement and Concrete Research*, vol. 39, no. 11, pp. 1095–1104, Nov. 2009, doi: 10.1016/j.cemconres.2009.07.026.

MOSAIC CATALOGUE

Appendix I – MOSAIC CATALOGUE

Appendix I – MOSAIC CATALOGUE

PB1702 – Sladkovský

The tomb of Czech politician Karel Sladkovský

Motif: Greek cross with laurel twigs

Location: Olšany Cemetery, Part IV, Prague 3

Date: 1884

Author/ Workshop: Albert Neuhauser

Karel Sladkovský (1823-1880) was an outstanding Czech politician. His tomb was completed in 1884. The mosaic is located in the pediment of the tomb. According to a newspaper report of the time, the mosaic was commissioned in Italy [1]. However, today's scholars attribute the work to the Neuhauser Company [2], [3]. Over the years, most of the tesserae fell off and the ornamental motif had to be renewed only according to preserved archive photos [4].

After renovation, 2020.

Before restoration. Photo:- M. K. Štorkánová

Restored Karel Sladkovský´s tomb.
Statues by J. V. Myslbek

Appendix I – MOSAIC CATALOGUE

PB1704 – Bittnerová

The tomb of Czech actress Marie (Maruška) Bittnerová

Motif: unclear, the mosaic is in a dilapidated state, most of the tesserae fell off

Location: Olšany Cemetery, Part IV, Prague 3

Date: 1899

Author/ Workshop: Albert Neuhauser

The architecture of the tomb is the work of Antonín Viktor Barvitius. The mosaic, the torso of which is in the tympanum, was made by Albert Neuhauser. This is evidenced by other tombstones with mosaic decoration designed by A. V. Barvitius as well as by the cooperation of A. V. Barvitius and A. Neuhauser in the decoration of the church of St. Wenceslas in Smíchov. Marie Bittnerová (1854 -1898) became famous as a theatre actress, among others in the newly established National Theatre. In 1896, at the age of 42, Marie gave birth to a stillborn child, which increased her desire for a child, and so she became pregnant at the end of 1897, but she did not carry the fetus to term and died in January 1898 [2].

Marie Bittnerová´s and her family tomb.

Detail of the mosaic torso.

Detail of the mosaic torso.

Appendix I – MOSAIC CATALOGUE

PB1706 – Beneš

Beneš Family Sepulchre

Motif: plant wreath

Location: Olšany Cemetery, Part IV, Prague 3

Date: 1890s

Author/ Workshop: Albert Neuhauser

A floral mosaic (Fig. 1b) in the triangular pediment of the tomb was probably made between 1896 (the death of hotel keeper Václav Beneš) and 1899 (the completion of the tomb). The mosaic has been recently renovated (2016).

7

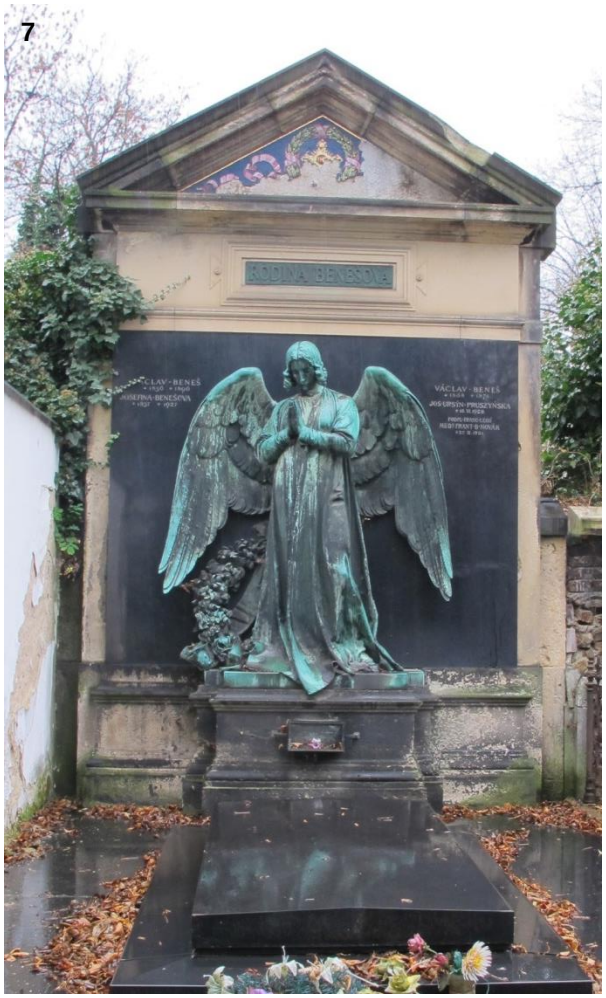

8

Beneš Family sepulchre, the mosaic before and after restoration. Photo 7 by M. K. Štorkánová

Appendix I – MOSAIC CATALOGUE

PB1707 – Peluněk

Peluněk Family sepulchre

Motif: Resurrected Christ

Location: Malvazinky Cemetery, Prague 5

Date: late 19th century

Author/ Workshop: Albert Neuhauser

A floral mosaic (Fig. 1b) in the triangular pediment of the tomb was probably made between 1896 (the death of hotel keeper Václav Beneš) and 1899 (the completion of the tomb). The mosaic was renovated in 2015.

9

Peluněk Family sepulchre before restoration.
Photo: M. K. Štorkánová

10

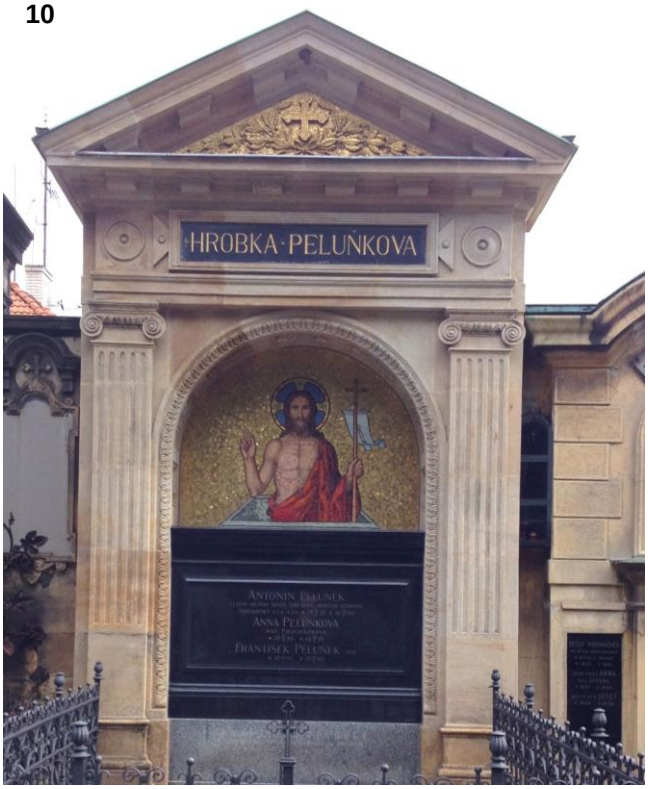

Peluněk Family sepulchre after restoration.

Appendix I – MOSAIC CATALOGUE

PB2003 – Mašek

František Mašek´s tomb

Motif: Christ with a Lamb

Location: Malvazinky Cemetery, Prague 5

Date: late 1890s

Author/ Workshop: Albert Neuhauser

The circular medallion with the half-length figure of Christ as the Good Shepherd was made according to the design of Professor František Sequens. The mosaic has almost completely disappeared, the glass tesserae have gradually fallen out, and only the mortar bed of the tesserae provides a clear record of the mosaic´s *andamentum* - the composition of the tesserae [2].

Mašek´s tomb, 2018.

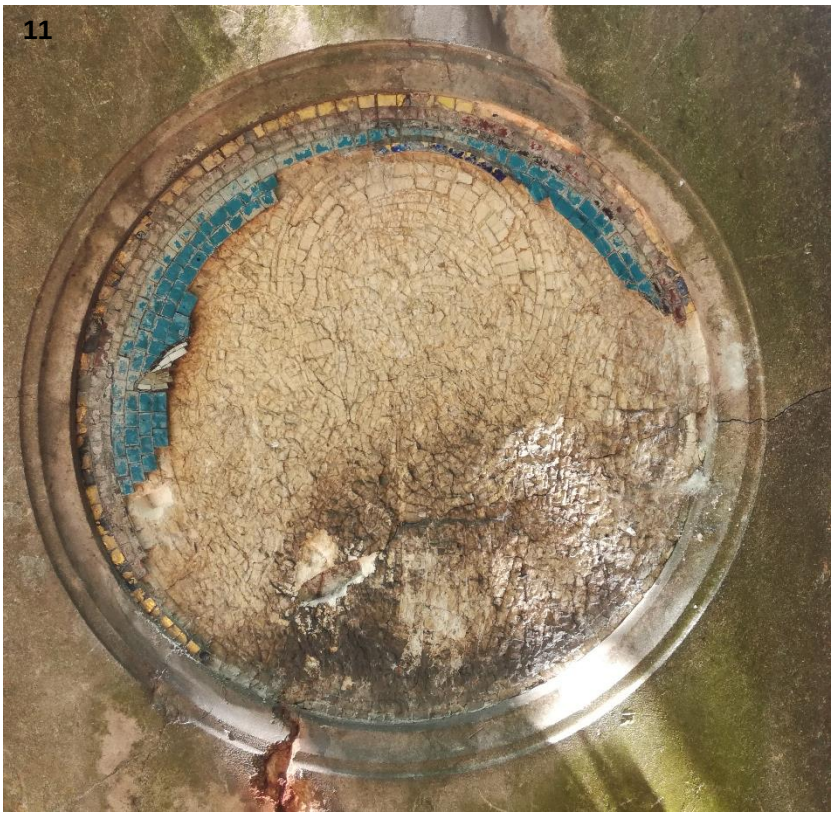

Detail of the mosaic torso, Mašek ´s tomb.

Detail of the andamento.

Appendix I – MOSAIC CATALOGUE

PB2106 – Pfannerer

Tomb of ThDr. Maur Pfannerer (1818 -1892)

Motif: probably a Beuron cross or symbols, the mosaic almost disappeared

Location: Olšany Cemetery, part VII, Prague 3

Date: 1890s

Author/ Workshop: Albert Neuhauser

The tombstone was supplied by the Prague stone company of the Italian stonemason Giovanni Ciani (1847-?), a C.C. court master stonemason who settled in Prague's Vinohrady district and began to supply mainly Neo-Renaissance works at the end of the 19th century. In the lunette of the tomb there is a mosaic with a small motif of the head of Christ measuring 30 cm H, 50 cm W. The mosaic was attributed to the Neuhauser Company [2], [3]. Above the lunette there is a torso of a mosaic decoration in the triangular gable of the tombstone. It has a golden bordure and a blue background of the few surviving tesserae. We assume that the torso is of the same provenance as the underlying undestroyed mosaic.

Canon´s Pfannerer tomb. Photo: M. Müller.

Detail of the mosaic torso studied. Photo: M. Müller.

Appendix I – MOSAIC CATALOGUE

PB2204 – Getzner and PB2205 - Krip

Getzner coat of Arms and Krip coat of arms on the façade of Hall Town hall

Motif: coats of arms

Location: eastern and southern wall, façade of the town hall in Hall, Austria

Date: 1897

Author/ Workshop: Albert Neuhauser

The samples were provided by Austrian restorer Malu Storch who renovated the mosaic decoration of the town hall. The mosaics had no frame, they were installed directly on the wall (at some spots an iron mesh reinforcement was found).

The town hall of Hall, Tirol, Austria. Photo: M. Storch.

Getzner mosaic. Photo: M. Storch.

Krip mosaic. Photo: M. Storch.

Appendix I – MOSAIC CATALOGUE

PB1709 – Reith

Madonna with a Child from Reith bei Seefeld, Austria

Motif: Madonna with a Child

Location: cemetery, Reith bei Seefeld, Tirol, Austria

Date: before 1906

Author/ Workshop: Josef Pfefferle

The mosaic Madonna with Child was made by Josef Pfefferle after he left the Neuhauser workshop. It was recently placed on a covered stair landing in a village cemetery in Reith bei Seefeld. According to the restorer Maria Luisa Storch, Pfefferle's great-granddaughter (oral information), the mosaic was made in 1906 at the latest and was designed as an interior piece. The mosaic was later transferred to the façade of a parish office. Exposure to the outside environment left the mosaic in a dilapidated state. After restoration (in 2016), the mosaic was installed in a covered staircase in the cemetery of Reith. The mosaic was fixed in a circular iron frame (64 cm in diameter) [5].

The mosaic during restoration works. Photos 18 and 19: Courtesy of Storch Family.

Mosaic after restoration.

Appendix I – MOSAIC CATALOGUE

PB2206 – Oberhofen

St. Michael the Archangel

Motif: St. Michael the Archangel

Location: church façade, Oberhofen, Austria

Date: 1903-1904

Author/ Workshop: Josef Pfefferle

The sample was provided by Austrian restorer Malu Storch who restored the mosaic. The mosaics had no frame, it was installed directly on the wall (at some spots an iron mesh reinforcement was found).

St. Nicolaus Church in Oberhofen with the mosaic on the façade. Photo: Malu Storch.

St. Michael the Archangel on the façade. Photo: Malu Storch.

Appendix I – MOSAIC CATALOGUE

PB2207 – Hopfgarten

Madonna with a Child

Motif: Madonna with a Child

Location: façade, St. Jacob and Leonhard Church, Hopfgarten im Brixental, Austria

Date: 1905

Author/ Workshop: Tiroler Glasmalerei- und Mosaikanstalt

The sample was provided by Austrian restorer Malu Storch who restored the mosaic. The mosaics had no frame, it was installed directly on the wall.

Madonna with a Child. Photo: Malu Storch

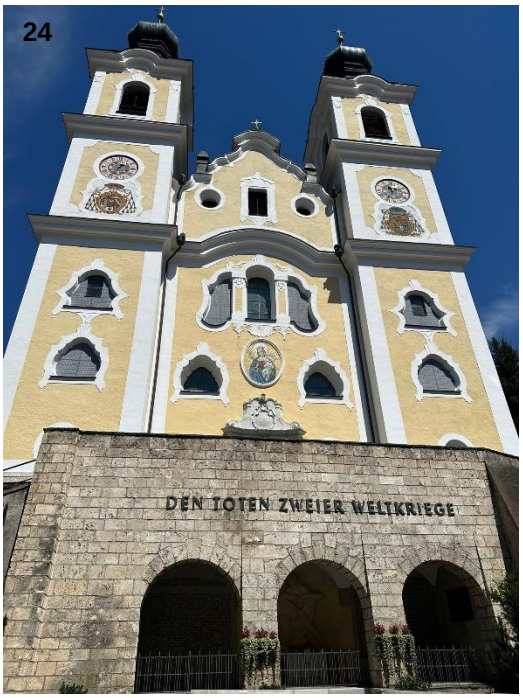

The church in Hopfgarten. Photo: Dita Frankeová

Appendix I – MOSAIC CATALOGUE

PB1705 – Lauschmann

Lauschmann Family sepulchre

Motif: Christ and wall decor

Location: Vyšehrad Cemetery, Prague 2

Date: 1908

Author/ Workshop: Viktor Foerster

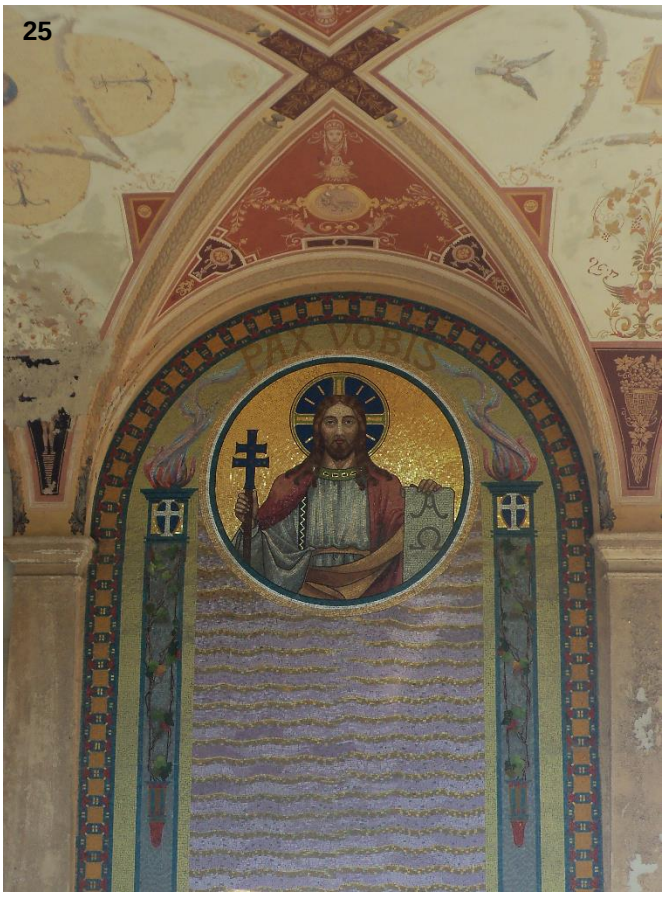

Appendix I – MOSAIC CATALOGUE

PB1802 – Dolín

Ornamental bordure of the portal

Motif: ornamental decor

Location: façade of St. Simon and St. Jude Church, Dolín u Slaného

Date: 1908

Author/ Workshop: Viktor Foerster

The mosaic decoration was made during the neo-Gothic renovation of the church in 1907-1908, initiated by the dean and parish priest of Zlonice, František Kraus, to whose parish the Dolín church belonged [6].


28


29


30

Appendix I – MOSAIC CATALOGUE

PB1802-2 – Dolín

Christ the Good Shepherd

Motif: Christ the Good Shepher

Location: façade of St. Simon and St. Jude Church, Dolín u Slaného

Date: 1908

Author/ Workshop: Viktor Foerster

A mosaic in the tympanum above the portal representing Christ the Good Shepherd. The mosaic´s restoration was finished two years ago. The mosaic decoration was made during the neo-Gothic renovation of the church in 1907-1908, initiated by the dean and parish priest of Zlonice, František Kraus, to whose parish the Dolín church belonged [6]..

Appendix I – MOSAIC CATALOGUE

PB1902 – Pelhřimov

Mosaic panel

Motif: Mascron

Location: originally a part of Pelhřimov cemetery gate, now stored in the Highlands Museum in Pelhřimov

Date: 1906

Author/ Workshop: Viktor Foerster

The panel is part of a set of two almost identical mosaic panels originally intended to be displayed at the gate of the Pelhřimov cemetery. Foerster participated in the decoration of the gate together with his friend and famous sculptor František Bílek [7]. However, the decoration was removed only two years after its installation. Both mosaic panels now stored in the depository of the Highlands Museum, Pelhřimov


32


33

Appendix I – MOSAIC CATALOGUE

PB1903 – Evropa hotel

Monumental mosaic in the gable of the present-day Evropa hotel

Motif: Mosaic sign and floral motifs in the gable of the former hotel “Archduke Stephen´s Hotel (today the Evropa hotel).

Location: façade of the Evropa hotel, Wenceslas Square 826/25, Prague 1

Date: 1906

Author/ Workshop: Viktor Foerster

Semi-circular monumental Art Nouveau mosaic with a golden inscription "hotel" and ornamental floral motifs. The mosaic was restored two years ago. The photo shows the mosaic´s condition before renovation.

34

Appendix I – MOSAIC CATALOGUE

PB1904 – Barrandov

Motif: Mosaic décor with Christian symbols

Location: façade of the Chapel of Marry of Sorrows, Hlubočepy, Prague 5

Date: 1906

Author/ Workshop: Viktor Foerster

This mosaic decoration is regarded to be the first Foerster´s completed mosaic work in the Czech Lands.

35

36

37

Appendix I – MOSAIC CATALOGUE

PB2007 – Slavín

Vault mosaic in the Slavín crypt

Motif: Starry sky

Location: Slavín crypt, Vyšehrad Cemetery, Prague 2

Date: 1929

Author/ Workshop: Marie Viktorie Foersterová

The vault mosaic in the crypt of Slavín is inspired by the mosaics in the Mausoleum of Galla Placidia in Ravenna (Fig. 6 in the thesis).

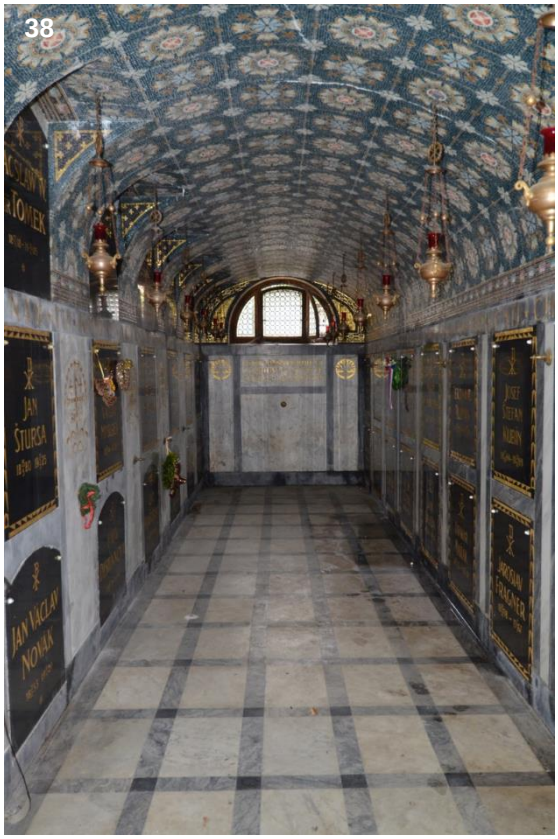

38 – Photo by M. K. Štorkánová.

Appendix I – MOSAIC CATALOGUE

PB1708 – Pfeiffer-Kral

Plant ornament

Motif: plant Art Nouveau ornament

Location: Pfeiffer-Kral Family sepulchre, Jablonec nad Nisou cemetery

Date: 1902

Author/ Workshop: Königlich Bayerische Mosaik- Hofkunstanstalt

The photos show the mosaic before and after restoration.

40

41

40 – Photo by M. K. Štorkánová

Appendix I – MOSAIC CATALOGUE

PB1803 – Dittrich

Mosaic decoration inside the crypt of Dittrich Family sepulchre

Motif: Funeral motifs on a golden background

Location: Dittrich Family sepulchre, Krásná Lípa

Date: 1920

Author/ Workshop: Pull & Wagner

The tomb was built in the 1880s in connection with the death of the important textile industrialist Carl Dittrich (1819-1886). However, the unique mosaic decoration of the crypt was created more than 30 years later [8]. The mosaic is in very poor condition.

Appendix I – MOSAIC CATALOGUE

PB2005 – Holy Family

Portable mosaic panel depicting Holy Family

Motif: Holy Family

Location: Liberec Muzeum

Date: 1910

Author/ Workshop: ?

Photo 47 by M. K. Štorkánová.

Appendix I – MOSAIC CATALOGUE

PB2108 – Schicht

Mosaic decor

Motif: golden background

Location: Schicht Family sepulchre, Střekov cemetery, Ústí nad Labem

Date: around 1912

Author/ Workshop: ?

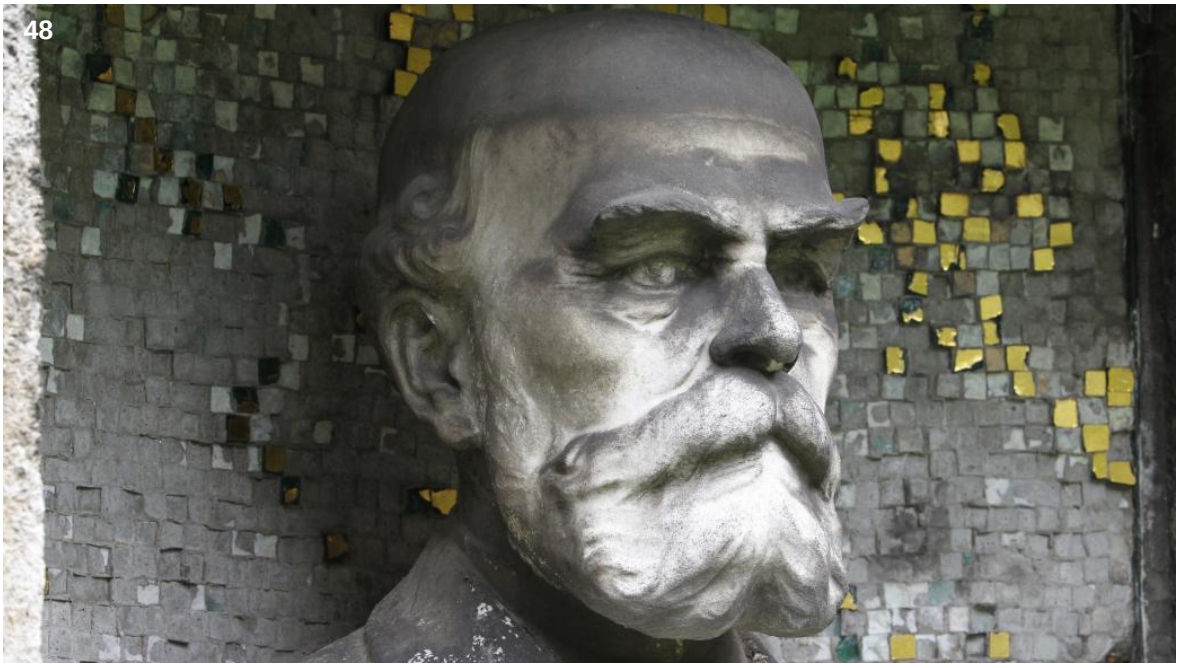

48 - Photo by Iveta Lhotská, Mafra, Profimedia.

Appendix I – MOSAIC CATALOGUE

PB1901 – Ballardini

Mankind Conquering New Space Horizons

Location: originally at the Central Telecommunication Building (ÚTB), now fixed on portable panels

Date: 1980

Author/ Workshop: Sauro Ballardini/ Academy of Fine Arts in Prague

The mosaic was originally located insidde the Central Telecommunication Building in Žižkov, Prague 3. It was fixed on concrete panels with preserved underdrawings (Fig. 52). However, the building was demolished. The mosaic was saved from destruction by its transfer to portable panels [9].

Appendix I – MOSAIC CATALOGUE

PB2006 – Sladký

Architect´s Reason and Sense

Location: façade of the Faculty of Civil Engineering in Prague, CTU, Prague 6

Date: 1977

Author/ Workshop: Martin Sladký/ Central Art & Craft studio (ÚUŘ)

According to archival documents the façade of the two auditoriums was originally intended to be decorated with prefabricated glass mosaic cubes but the author came up with the idea to install an original mosaic made of stone. He designed a wall made of 288 prefabricated reinforced concrete panels, some of which would be decorated with a mosaic [10].

Appendix I – MOSAIC CATALOGUE

PB2009 – Pardubice

Map of Czechoslovakia

Location: façade of the Faculty of Civil Engineering in Prague, CTU, Prague 6

Date: 1957

Author/ Workshop: Richard Lander/ Česká mosaika/ Central Art & Craft studio (ÚUŘ)

Appendix I – MOSAIC CATALOGUE

PB2103 – Milovice

Fighting Friendship with Soviet Troops

Location: hall of the Municipal Administration Building in Milovice (former Officer´s House)

Date: 1980-82

Author/ Workshop: Radomír Kolář/ Central Art & Craft studio (ÚUŘ)

In 1968-1991, the town of Milovice served as a central military base for the Soviet occupational troops. In the former Officer´s House cultural events for Soviet officers were organised. The mosaic was restored last year (photos after renovation).

57

58

Appendix I – MOSAIC CATALOGUE

PB2201 – Kmentová

Listening Woman

Date: 1957

Description: a mosaic sculpture

Author: Eva Kmentová

When Eva Kmentová completed the sculpture, she seemed not so happy about it. She found the mosaic mantle quite difficult to make and the result was “too decorative” in her opinion [11]. The statue was restored last year, the photos were taken before restoration.


59


60

Appendix I – MOSAIC CATALOGUE

REFERENCES:

[1] ‘Odhalení pomníku dra. K. Sladkovského’, *Národní listy*, Prague, p. 2, March 16, 1884.

[2] M. Kracík Štorkánová, P. Bauerová, V. Vicherková, M. Hemelík, and V. Holzapfelová, ‘Mozaiky firmy Neuhauser Innsbruck na pražských hřbitovech’, in *Epigraphica et Sepulcralia*, J. Roháček, Ed., Prague: Ústav dějin umění AV ČR, 2021, pp. 363–413. Accessed: Jun. 25, 2023. [Online]. Available: https://www.academia.edu/45090306/Viktor_Foerster_a_mozaikov%C3%A1_tvorba_pro_n%C3%A1hrobky_Viktor_Foerster_and_mosaic_production_for_tombstones

[3] Z. Křenková, V. Říhová, and I. Kučerová, ‘Katalog’, in *Česká skleněná mozaika: historie, technologie, katalog exteriérových děl = Czech glass mozaic: history, technology, catalogue of exterior works*, Z. Křenková, I. Kučerová, and V. Říhová, Eds., Vydání: první.Praha: Vysoká škola chemicko-technologická v Praze, 2022, pp. 301–544.

[4] M. Kracík Štorkánová, ‘Mozaika v segmentovém štítu hrobky Karla Sladkovského’, Prague, Restoration report, 2017.

[5] Bauerová, M. Kracík Štorkánová, P. Mácová, M. Pavlíková, L. Scheinherrová, and M. Keppert, ‘Searching for common technological features of 19th–20th-century mosaic mortars ascribed to the Neuhauser company’, *Archaeometry*, vol. 63, no. 6, pp. 1216–1235, 2021, doi: 10.1111/arcm.12678.

[6] M. Kracík Štorkánová and M. Hemelík, *‘Tvá práce svítí, Marie, modlitbou k Viktorovi’ : prolínání životních a uměleckých osudů Viktora a Marie Viktorie Foersterových*, 1. in Studie Národohospodářského ústavu Josefa Hlávky, no. 9/2017. Prague: Nadání Josefa a Marie Hlávkových, AVU v Praze, 2017.

[7] M. Kracík Štorkánová, Ed., *Opus musivum: mozaika ve výtvarném umění*. Praha: Art & Craft Mozaika, 2016.

[8] V. Říhová and Z. Křenková, ‘Decoration of Dittrich family tomb in Krásná Lípa with mosaic production from Berlin’, in *Epigraphica et Sepulcralia*, J. Roháček, Ed., Prague: Ústav dějin umění AV ČR, 2022, pp. 207–230.

[9] M. Kracík Štorkánová, V. Vicherková, P. Bauerová, M. Hemelík, and D. Rohanová, ‘Vesmírné i pozemské poselství mozaik Saura Ballardiniho. Záchrana a restaurování mozaiky ‚Člověk dobývající nové horizonty vesmíru‘ a hledání nových perspektiv pro historické mozaiky v ČR’, *Staletá Praha*, vol. 38, no. 1, pp. 76–115, 2022, doi: 10.56112/sp.2022.1.04.

[10] Bauerová *et al.*, ‘What fixes architect’s reason and sense? Materials study of CTU façade mosaic mortar’, *AIP Conference Proceedings*, no. 1, p. 020024, Feb. 2021, doi: 10.1063/5.0041947.

[11] A. Němcová, ‘Sochy Evy Kmentové v letech 1958–1968’, Bachelor thesis, Charles University in Prague, Catholic Theological Faculty, Praha, 2011.

PHOTOS: Unless otherwise stated, the photos were taken by author of the thesis.